LIQUID-LIQUID AND LIQUID-SOLID DISTRIBUTION STUDIES OF 8-HYDROXYQUINOLINIUM-ANION PAIR SYSTEMS: APPLICATION TO THE CHROMATOGRAPHIC SEPARATION OF ALIPHATIC AND AROMATIC SULFONATES

By

MAO-SUNG KUO

Bachelor of Science
Tunghai University
Taichung, Taiwan
Republic of China
1969

Master of Science
Ohio State University
Columbus, Ohio
1975

Submitted to the Faculty of the Graduate College
of the Oklahoma State University
in partial fulfillment of the requirements
for the Degree of
DOCTOR OF PHILOSOPHY
December, 1979

LIQUID-LIQUID AND LIQUID-SOLID DISTRIBUTION STUDIES OF 8-HYDROXYQUINOLINIUM-ANION PAIR SYSTEMS: APPLICATION TO THE CHROMATOGRAPHIC SEPARATION OF ALIPHATIC AND AROMATIC SULFONATES

Thesis Approved:

Horacio A. Mottola
Thesis Adviser

E. Eisenbraun

A. L. Gearhart

H. Olin Spivey

Norman N. Durham
Dean of the Graduate College

ACKNOWLEDGEMENTS

I wish to express my gratitude to Dr. H. A. Mottola for his help, patient guidance, and deep understanding throughout the course of this investigation. I am also thankful to the members of my committee, Dr. E. J. Eisenbraun, Dr. H. L. Gearhart, and Dr. H. O. Spivey for their help, encouragement, and valuable suggestions.

I am also grateful to Dr. O. C. Dermer, who has read this manuscript and has contributed to its form. I am also thankful to Mr. A. E. Goodwin for his help in many ways during my study at this University and also for the electron scan micrographs taken at CONOCO, Ponca City, Oklahoma. I am also thankful to my colleagues and members of my research group for their help and friendship. Thanks are also to Mr. Hall and his co-workers for modifying the shaker, taking the pictures for the instrumental set-up in this thesis, and for their help. I also thank Mr. Adkins and Mr. Friedle for their aid.

The financial support and experience gained by way of a teaching assistantship in the Department of Chemistry since August, 1975 until now is also gratefully acknowledged. I also thank the Sun Oil Company for partial financial support during the Summer of 1976; Arts and Sciences Research for the partial financial support in the form of research assistantship during the summer of 1977; Halliburton for a scholarship in the form of industrial fellowship during the summer of 1978; Arts and Sciences Research for a research assistantship and Alumni and Friends Fellowship during the summer of 1979. I am indebted

to Mrs. Janet Sallee for the excellent typing of this manuscript.

Finally, I am deeply grateful to my family for their encouragement all the time.

TABLE OF CONTENTS

Chapter Page

LIST OF TABLES

LIST OF FIGURES

Figure Page

CHAPTER I

INTRODUCTION

Solvent extraction of ion pairs and liquid-liquid and liquid-solid chromatographic separations involving ion-pair formations are well recognized tools in analytical chemistry. For some chemical species (e.g. drugs and some other organic species) the efficiency of extraction and selectivity are improved with respect to other extraction systems involving the partition of molecular (uncharged) species (1). Inorganic anions (2,3) and hydrophilic organic compounds (4) have been successfully extracted and separated after ion-pair formation. Ion-pair formation and distribution between two immiscible phases has particular advantages for aprotic ions (e.g., quaternary ammonium ions, organic sulfonates) and for compounds that are difficult to extract in uncharged form (e.g., amino acids and aminophenols) (5). A variety of ion-selective electrode membranes show responses based on ion-pair formation (6,7).

The purpose of the work reported in this thesis was the evaluation of 8-hydroxyquinoline (in the form of hydroxyquinolinium ion) as an ion-pair extractant of anionic species and its use in the liquid-solid chromatographic separation of such anions. A brief incursion in the area of ion-selective electrodes is also part (Appendix D) of the reported work.

8-Hydroxyquinoline and some of its derivatives were first intro-

duced in analytical chemistry by Berg (8) in 1926. Since then 8-hydroxyquinoline has become one of the most commonly used reagents in chemical analysis (9,10).

8-Hydroxyquinoline is also known as 8-quinolinol or as oxine (an abbreviation for oxyquinoline), structurally represented as 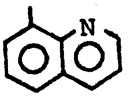

. A symbol of HO_x is commonly used for simplicity. Its protonated form is called 8-hydroxyquinolinium ion (11), 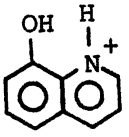

, and is simply symbolized as $H_2O_x^+$. At sufficiently high pH, 8-hydroxyquinoline exists as the 8-hydroxyquinolinate or oxinate anion, 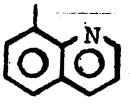

, symbolized as O_x^-. It follows then that 8-hydroxyquinoline is an amphoteric species in aqueous solution as a result of the weak acid character of the phenolic group and weak basic characteristics of the pyridinic nitrogen. Several workers have studied the acid-base properties of 8-hydroxyquinoline and a selection of reported values for the two acid dissociation constants is presented in Table I. 8-Hydroxyquinoline is only slightly soluble in water (3.56×10^{-3} M at $18^{\circ}C$) (15), but as a result of base properties, is readily soluble in aqueous solutions of mineral acids (e.g., normal solutions of HCl or $HClO_4$)(22) as well as in a variety of organic solvents of a broad polarity spectrum (butanols and higher molecular weight organic alcohols, benzene, chloroform, carbon tetrachloride, etc.).

The light-absorbing characteristics of the three species of 8-quinolinol in ethanolic solutions are shown in Figure 1. It is of

TABLE I

DISSOCIATION CONSTANTS OF 8-HYDROXYQUINOLINIUM ION

Authors	pKa_1	pKa_2	Method	Reference
Fox	4.8	10.36	Solvent Extraction	(12)
Kilthoff	4.5	9.7	Colorimetry	(13)
Stone and Friedman	----	10.38	Solubility in alkaline buffer	(14)
	----	10.37	Spectrophotometry	
Lacroix	5.23	9.70	Potentiometric Titration	(15)
Irving, Ewart, and Wilson	4.88	9.89	Spectrophotometry	(16)
	5.13	9.82	Solubility Measurement	
Phillips, Elbinger, and Merritt	4.91	-----	Spectrophotometry	(17)
Sandell and Spindler	4.92	-----	Potentiometry	(18)
Nasanen, Lumme, and Mukula	5.02	9.81	Potentiometry	(19)
	----	9.81	Spectrophotometry	
Dyrssen	5.00	9.62	Potentiometry	(20)
Mottola and Freiser	4.85	9.95	Solvent Extraction	(21)

interest to note that the 8-quinolinium ion shows significant absorption around 360 nm, a wavelength at which 8-hydroxyquinoline itself shows negligible absorption.

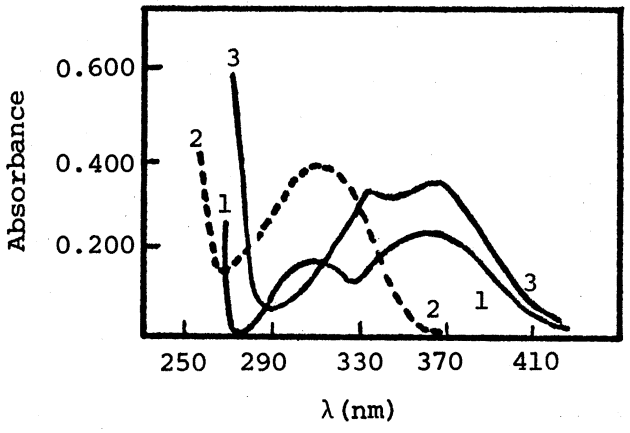

Figure 1. Absorption Spectra of 8-Hydroxyquinoline in 95% Ethanol

1. 0.01 M HCl
2. Neutral
3. 0.01 M NaOH

This permits the determination of the protonated form in presence of the neutral species in acidic solutions. These light-absorbing characteristics are paralleled in aqueous solutions.

8-Hydroxyquinoline is widely used in metal ion separation and determination as a result of its chelate-forming properties. By adjustment of the pH of aqueous solutions (23-26), 8-hydroxyquinoline is capable of reacting with sixty metal ions (27(a)). This reactivity has led to a large number of methods for separation and also gravimetric, titrimetric, and colorimetric (photometric) determination of metal ions in solution. More recent analytical applications of 8-quinolinol record

its use as a functional group in chelating ion-exchange resins (28-33), or as separation agent chemically bonded to controlled-pore glass beads (34,35) and porous silica (36). From this brief overview, it is manifest that 8-hydroxyquinoline is one of the most useful reagents in chemical analysis.

As early as 1952, Dyrssen (20) investigated the distribution of 8-hydroxyquinoline between acidic aqueous solutions and oxygen-containing organic solvents. His work was focused on the use of methyl isobutyl ketone as organic phase and constitutes the first report that the hydroxyquinolinium ion can pair with anions (perchlorate in this particular case) and permit their extraction into highly polar organic solvents. Dyrssen proposed a simplified model to account for such behavior and with the aid of Equation (1), derived from the model, estimated the distribution constant for the ion-pair species:

$$D = K_{D(H_2O_x^+,A^-)} + \frac{Ka_1 K_{D(HO_x)}}{[H^+]} \qquad (1)$$

in which D is the distribution ratio for 8-hydroxyquinoline; $K_{D(H_2O_x^+,A^-)}$ is the distribution constant for the $(H_2O_x^+,A^-)$ ion-pair; Ka_1 is the first dissociation constant of 8-hydroxyquinolinium ion; $K_{D(HO_x)}$ is the distribution constant of 8-hydroxyquinoline; and $[H^+]$ is the equilibrium concentration of hydronium ion. Since D and $[H^+]$ can be determined experimentally, a plot of D versus $\frac{1}{[H^+]}$ will give a straight line with $Ka_1 \cdot K_{D(HO_x)}$ as slope and $K_{D(H_2O_x^+,A^-)}$ as intercept. (For details on the model and derivation of Equation (1), see Appendix A).

Dyrssen's model and approach was later applied by Mottola and Freiser (21) to the extraction of the same ion pair into isopentyl alcohol. Their value for the distribution constant of the ion pair, 0.8 against 0.11 in methyl isobutyl ketone, shows the expected increase in solubility as the basic (polar) characteristics of the solvent are increased and pointed to the potential use of 8-hydroxyquinolinium ion in anion separation in chromatographic systems. These earlier works by Dyrssen and Mottola and Freiser motivated the studies reported in this thesis. These studies were initiated with a systematic determination of distribution constants for a variety of anionic species between aqueous acidic solutions and isopentyl alcohol or 1-butanol. Organic and inorganic anions were included in these batch extraction studies. From the results of such studies, aliphatic and aromatic sulfonates of industrial interest were selected for further work involving 8-hydroxyquinoline immobilized (by chemical attachment) on controlled-pore glass. Both batch equilibration experiments and chromatographic separations were performed to explore the potential of immobilized 8-hydroxyquinolinium ion for the separation of aliphatic and aromatic sulfonates. The rationale to pursue these studies was based on the encouraging results collected in batch experiments, the industrial and environmental importance of sulfonates, and the fact that the inorganic (silicate) backbone of controlled-pore glass bearing immobilized 8-hydroxyquinoline should offer excellent mechanical properties for its use in liquid-liquid (liquid-solid) chromatography.

As a result of the batch equilibration studies, which have shown a larger distribution constant for aliphatic sulfonates than for aromatic ones, a brief excursion on the potential use of immobilized 8-hydroxy-

quinolinium ion in membranes for ion-selective detection of ethanesulfonate was performed.

CHAPTER II

SOME OBSERVATIONS ON PARAMETERS THAT AFFECT ION PAIR FORMATION

This chapter deals with some theoretical considerations about parameters that affect ion pair formation.

A. Liquid-Liquid Systems

The ion pair extraction technique may be applied to all compounds that can appear in an ionized form (1). In liquid-liquid systems, all ionic compounds may be extracted with different extent into an organic phase as ion pairs. The value of the extraction constant (which quantitatively describes the process) depends on the solvation in the organic phase and in the aqueous phase (4).

1. Two Postulated Models

Usually, there are two models (37) which are proposed to describe the extraction of an ion pair. They may be depicted as shown in Figure 2.

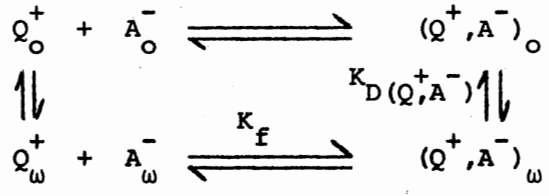

Figure 2. Ion-Pair (Q^+,A^-) Formation and Extraction

Here Q^+ is a cation; A^- is a counterion; (Q^+,A^-) is the ion-pair; o refers to species in the organic phase; ω refers to species in the aqueous phase; K_f is the formation constant for $(Q^+,A^-)_\omega$; and $K_{D(Q^+,A^-)}$ is the partition constant for (Q^+,A^-) between the organic and aqueous phases. The first model assumes that the ion-pair, $(Q^+,A^-)_\omega$, is formed first in the aqueous phase and then partitions between the organic and the aqueous phases, as represented by Equation (2).

$$Q^+_\omega + A^-_\omega \underset{}{\overset{K_f}{\rightleftharpoons}} (Q^+,A^-)_\omega \overset{K_{D(Q^+,A^-)}}{\rightleftharpoons} (Q^+,A^-)_o \qquad (2)$$

where

$$K_f = \frac{[(Q^+,A^-)_\omega]}{[Q^+]_\omega[A^-]_\omega} \qquad (3)$$

and

$$K_{D(Q^+,A^-)} = \frac{[(Q^+,A^-)_o]}{[(Q^+,A^-)_\omega]} \qquad (4)$$

While the second model assumes that the cation, Q^+_ω, and the counterion, A^-_ω, are first transferred from the aqueous into the organic phase, simultaneously and then associate in the organic phase, as represented by Equations (5), (6), and (7).

$$Q^+_\omega \rightleftharpoons Q^+_o \qquad (5)$$

$$A^-_\omega \rightleftharpoons A^-_o \qquad (6)$$

$$Q^+_o + A^-_o \rightleftharpoons (Q^+,A^-)_o \qquad (7)$$

Since neither of the two models alone satisfactorily describes real extraction systems, the true mechanism may involve both models. Hence, only the first model (Equation (2)) is considered here.

If an overall net reaction is used, Equation (2) can be expressed as follows:

$$Q^+_\omega + A^-_\omega \underset{}{\overset{E_{(Q^+,A^-)}}{\rightleftharpoons}} (Q^+,A^-)_o \tag{8}$$

where $E_{(Q^+,A^-)}$ is the extraction constant defined as

$$E_{(Q^+,A^-)} = \frac{[(Q^+,A^-)_o]}{[Q^+]_\omega [A^-]_\omega} \tag{9}$$

Incorporating Equations (3) and (4) into (9) yields

$$E_{(Q^+,A^-)} = K_f \cdot K_{D(Q^+,A^-)} \tag{10}$$

When no reactions except that of Equation (8) occur, the distribution ratio of Q^+, D_{Q^+}, between organic and aqueous phases may be expressed as follows:

$$D_{Q^+} = \frac{\Sigma[Q^+]_o}{\Sigma[Q^+]_\omega} = \frac{[(Q^+,A^-)_o]}{[Q^+]_\omega} \tag{11}$$

Incorporating Equation (9) into (11):

$$D_{Q^+} = E_{(Q^+,A^-)} [A^-]_\omega \tag{12}$$

Hence, the distribution ratio, D_{Q^+}, varies not only with the nature and

the concentration of the counterion, A^-, but also with the extraction constant, $E_{(Q^+,A^-)}$, which depends on the solvation interaction in both phases.

2. Parameters That Affect the Extraction Constant ($E_{(Q^+,A^-)}$)

a. Nature of the Anion (A^-)

Ion hydration depends not only on the charge and radius (38) of an anion but also on the attractability (39) of the anion toward water. Generally speaking, an anion with a small charge, large radius, and poorly hydrated characteristics tends to form ion pairs which are more soluble in organic phases than in aqueous phases (27(a)). Hence, a large extraction constant will be obtained. Anions which contain hydrophilic (such as hydroxyl, carboxyl, and amino) groups will give low extraction constants (4,40) because these hydrophilic ions will be preferably bonded to water through hydrogen bonding decreasing the possibility of ion-pairing. Anions containing alkyl or aryl groups show more hydrophobic characteristics (4); hence, their extraction constants are comparatively larger. Generally, the extraction constant increases linearly with increasing number of carbon atoms in the alkyl group or benzene rings in the aryl group.

b. Nature of the Organic Solvent

Since all ion pairs have a more or less pronounced polar character (5), the polarity of the organic solvent has a very strong influence on the value of the extraction constant. Generally, the more polar the

solvent, the larger the ion-pair extraction. The relative polarity of an organic solvent may be expressed in terms of the solubility parameter, δ, as defined by Hildebrand and coworkers (41,42) in their regular solution theory for nonpolar solvents. Later, the solubility parameter was modified by Hansen (43) and expressed as in Equation (13).

$$\delta = (\delta_d^2 + \delta_p^2 + \delta_h^2)^{\frac{1}{2}} \tag{13}$$

where δ_d is a contribution due to dispersion interactions; δ_p is due to permanent and induced dipole orientations; and δ_h is due to hydrogen bonding contribution. Hydrophilic organic anions are difficult to extract into an organic phase of low polarity, and only very hydrophobic counterions (such as, large quaternary ammonium ions) are sufficiently extracted to be useful.

c. Side Reactions

Since side reactions (e.g., dimerization, protolysis, etc.) will affect the concentrations of free anions and/or cations in the aqueous phase, or that of the ion pair in the organic phase, the extraction constant of the ion pair will vary. The tendency to dimerization increases with decreasing polarity and solvating ability of the organic phase, but this will not be included in this thesis because the extent of dimerization is expected to be very low because of the high polarity of the solvents used in this work. While protolysis in the aqueous phase for some ions does often occur during ion-pair formation, these cases will be discussed as follows.

(i) Case a. If protolysis of A^- is represented as follows:

$$H^+ + A^-_\omega \underset{K_{a(HA)}}{\rightleftharpoons} (HA)_\omega \xrightarrow[}{K_{D(HA)}} (HA)_o \quad (14)$$

where $K_{a(HA)}$ is the acid dissociation constant of HA and $K_{D(HA)}$ is the partition constant of HA. They are expressed as

$$K_{a(HA)} = \frac{[H^+][A^-]_\omega}{[HA]_\omega} \quad (15)$$

$$K_{D(HA)} = \frac{[HA]_o}{[HA]_\omega} \quad (16)$$

The distribution ratio of Q^+ has the same expression as that of Equation (12). However, the $[A^-]_\omega$ may be expressed in terms of total analytical concentration, C_{A^-}, as follows:

$$C_{A^-} = [A^-]_\omega + [HA]_\omega + [HA]_o + [Q^+,A^-]_o \quad (17)$$

or rearranging Equation (17):

$$C_{A^-} - [Q^+,A^-]_o = C'_A = [A^-]_\omega + [HA]_\omega + [HA]_o \quad (18)$$

where C'_A is the total concentration of A^- which has not been extracted as ion pairs. Incorporating Equations (15) and (16) into (18), one obtains

$$C'_A = [A^-]_\omega \left\{1 + \frac{[H^+]}{K_{a(HA)}} (1 + K_{D(HA)})\right\} \quad (19)$$

Hence, Equation (12) can be expressed as

$$D_{Q^+} = \frac{E_{(Q^+,A^-)}\ C'_A}{1 + \frac{[H^+]}{K_{a(HA)}}\ (1 + K_{D(HA)})} = E'_{(Q^+,A^-)}\ C'_A \qquad (20)$$

where $E'_{(Q^+,A^-)}$ is the conditional (44) extraction constant. Equation (20) shows that when $K_{a(HA)} >> [H^+]$, or HA is a strong acid, the distribution ratio (or the conditional extraction constant) is the same as if there were no side reaction. However, when the $K_{a(HA)} << [H^+]$, or HA is a weak acid, then the conditional extraction constant is lowered owing to the competitive reaction of $H^+ + A^- \rightleftharpoons HA^-$ as shown in Equation (14).

(ii) Case b. If Q^+ is a protonated species and is symbolized as HX^+, and besides the protolysis of A^-, a dissociation of HX^+ in the aqueous phase and a partition of X between the organic phase and the aqueous phase can occur, the condition may be expressed as follows:

$$(HX^+)_\omega + (A^-)_\omega \overset{E_{(HX^+,A^-)}}{\rightleftharpoons} (HX^+,A^-)_o \qquad (21)$$

$$(HX^+)_\omega \overset{Ka_1}{\rightleftharpoons} H^+ + (X)_\omega \qquad (22)$$

$$(X)_\omega \overset{K_{D(X)}}{\rightleftharpoons} (X)_o \qquad (23)$$

$$H^+ + (A^-)_\omega \underset{K_{a(HA)}}{\rightleftharpoons} (HA)_\omega \qquad (24)$$

where

$$E_{(HX^+,A^-)} = \frac{[(HX^+,A^-)_o]}{[HX^+]_\omega [A^-]_\omega} = \text{extraction constant of the } (HX^+,A^-) \text{ ion-pair} \qquad (25)$$

$$K_{a1} = \frac{[H^+][X]_\omega}{[HX^+]_\omega} = \text{acid dissociation constant of } HX^+ \quad (26)$$

$$K_{D(X)} = \frac{[X]_o}{[X]_\omega} = \text{partition constant of } X \quad (27)$$

The distribution ratio of X, D_X, can be expressed as

$$D_X = \frac{\Sigma[X]_o}{\Sigma[X]_\omega} = \frac{[(HX^+,A^-)_o] + [X]_o}{[HX^+]_\omega + [X]_\omega} \quad (28)$$

Incorporating Equations (25), (26), and (27) into (28) gives:

$$D_X = \frac{E_{(HX^+,A^-)} \frac{[H^+][X]_\omega}{Ka_1} [A^-]_\omega + K_{D(X)} [X]_\omega}{\frac{[H^+][X]_\omega}{Ka_1} + [X]_\omega} \quad (29)$$

or

$$D_X = \frac{E_{(HX^+,A^-)} [H^+][A^-]_\omega + K_{D(X)} Ka_1}{[H^+] + Ka_1} \quad (30)$$

On the assumption that $Ka_1 << [H^+]$ by a factor of $\sim 10^3$, Equation (30) can be simplified as follows:

$$D_X = E_{(HX^+,A^-)} [A^-]_\omega + \frac{K_{D(X)} Ka_1}{[H^+]} \quad (31)$$

If $E_{(HX^+,A^-)}$ is expressed in terms of $K_{D(HX^+,A^-)}$ and K_f as in Equation (10), then Equation (31) can be rewritten as:

$$D_{\chi} = K_{D(HX^{+},A^{-})} K_f [A^{-}]_{\omega} + \frac{K_{D(\chi)} K_{a1}}{[H^{+}]} \quad (32)$$

where

$$K_{D(HX^{+},A^{-})} = \frac{[(HX^{+},A^{-})_o]}{[(HX^{+},A^{-})_{\omega}]} \quad (33)$$

$$K_f = \frac{[(HX^{+},A^{-})_{\omega}]}{[HX]_{\omega}[A^{-}]_{\omega}} \quad (34)$$

or,

$$K_f [A^{-}]_{\omega} = \frac{[(HX^{+},A^{-})_{\omega}]}{[HX]_{\omega}} \quad (35)$$

For the case that $K_f[A^{-}]_{\omega}$ is close to 1, then, Equation (32) can be simplified further:

$$D_{\chi} = K_{D(HX^{+},A^{-})} + \frac{K_{D(\chi)} Ka_1}{[H^{+}]} \quad (36)$$

Equation (36) corresponds to the Dyrssen's model which has been derived in Appendix A, where $HO_x = \chi$.

If a more general term of $K_f[A^{-}]_{\omega}$ is used instead of assuming a value of 1, Equation (32) can be rewritten incorporating the total analytical concentration of A^{-}, $C_{A^{-}}$, as follows:

The mass balance equation for A^{-} can be expressed as in Equation (37).

$$C_{A^-} = [A^-]_\omega + [HA]_\omega + [(HX^+,A^-)_o] \quad (37)$$

or,

$$C_{A^-} = [A^-]_\omega \left(1 + \frac{[H^+]}{Ka_{(HA)}} + K_{D(HX^+,A^-)}\ K_f[HX^+]_\omega\right) \quad (38)$$

Incorporating Equation (38) into (32) gives

$$D_X = \frac{K_{D(HX^+,A^-)}\ C_{A^-}\ K_f}{1 + \frac{[H^+]}{K_{a(HA)}} + K_{D(HX^+,A^-)}\ K_f[HX^+]_\omega} + \frac{K_{D(X)}\ Ka_1}{[H^+]} \quad (39)$$

or,

$$D_X = \frac{[H^+]\left\{K_{D(HX^+,A^-)}\ K_f\ C_{A^-} + \frac{K_{D(X)}\ Ka_1}{Ka_{(HX)}}\right\} + K_{D(X)}Ka_1(1+K_{D(HX^+,A^-)}K_f[HX^+]_\omega)}{[H^+]\ (1+\frac{[H^+]}{K_{a(HA)}} + K_{D(HX^+,A^-)}\ K_f[HX^+]_\omega)} \quad (40)$$

If $Ka_{(HA)} >> [H^+]$ by a factor of $\sim 10^3$ for a strong acid, Equation (40) can be simplified as

$$D_X = \frac{K_{D(HX^+,A^-)}\ C_{A^-}\ K_f}{1 + K_{D(HX^+,A^-)}\ K_f[HX^+]_\omega} + \frac{K_{D(X)}\ Ka_1}{[H^+]} \quad (41)$$

A plot of D_X versus $\frac{1}{[H^+]}$, in Equation (41), will give a straight line with $K_{D(X)} \cdot Ka_1$ as slope and

$$\frac{K_{D(HX^+,A^-)}\ C_{A^-}\ K_f}{1 + K_{D(HX^+,A^-)}\ K_f[HX^+]_\omega}$$

as intercept. For weak acids, Equation (40) is complicated to solve for $K_{D(X)}$ and $K_{D(HX^+,A^-)}$.

(iii) Case c. Another modified model can be considered as follows: In addition to case b above, the term of $[HX^+,A^-]_\omega$ is also included in $\Sigma[X]_\omega$ of Equation (28). Then the distribution ratio of X, D_X, is expressed as

$$D_X = \frac{[(HX^+,A^-)_o] + [X]_o}{[(HX^+,A^-)_\omega] + [HX^+]_\omega + [X]_\omega} \qquad (42)$$

Assuming that $[X]_\omega$ is much smaller than those of $[(HX^+,A^-)_\omega]$ or $[HX^+]_\omega$ and incorporating Equations (25), (26), and (27) into (42) yields

$$D_X = \frac{K_{D(HX^+,A^-)}\ K_f[A^-]_\omega}{K_f[A^-]_\omega + 1} + \frac{Ka_1\ K_{D(X)}}{K_f[A^-]_\omega + 1}\ \frac{1}{[H^+]} \qquad (43)$$

Equation (43) indicates that a plot of D_X versus $\frac{1}{[H^+]}$ will give a straight line with $\frac{Ka_1\ K_{D(X)}}{K_f[A^-]_\omega+1}$ as slope and $\frac{K_{D(HX^+,A^-)}\ K_f[A^-]_\omega}{K_f[A^-]_\omega + 1}$ as intercept. Hence, theoretically $K_{D(HX^+,A^-)}$ and $K_{D(X)}$ can be calculated using the mass balance equations for X and for A, respectively, and the charge balance equation.

Equation (43) may also be considered as follows:

Case (i). If $K_f[A^-]_\omega >> 1$, or $[HX^+,A^-]_\omega >> [HX^+]_\omega$, Equation (43) can be simplified as

$$D_X = K_{D(HX^+,A^-)} + \frac{Ka_1\ K_{D(X)}}{K_f[A^-]_\omega}\ \frac{1}{[H^+]} \qquad (44)$$

Comparing Equations (44) with (1), a plot of D_χ versus $\frac{1}{[H^+]}$ will give a straight line with the same intercept of $K_{D(HX^+,A^-)}$ but a different slope of $\frac{Ka_1 \; K_{D(X)}}{K_f[A^-]_\omega}$. Hence, the intercept should correspond to the distribution constant for the ion pair but the slope should correspond to $Ka_1 \; K_{D(X)}$ divided by $K_f[A^-]_\omega$, a factor greater than 1.

Case (ii). If $K_f[A^-]_\omega << 1$, or $[HX^+,A^-]_\omega << [HX^+]_\omega$, Equation (43) can be simplified as

$$D_\chi = K_{D(HX^+,A^-)} \; K_f[A^-]_\omega + Ka_1 \; K_{D(X)} \; \frac{1}{[H^+]} \qquad (45)$$

Comparing Equations (45) with (1), a plot of D_χ versus $\frac{1}{[H^+]}$ will yield a straight line with the same slope but different intercept. That is the slope should correspond to $Ka_1 \; K_{D(X)}$ and the intercept should correspond to $K_{D(HX^+,A^-)}$ multiplied by $K_f[A^-]_\omega$, a factor smaller than 1.

Case (iii). If neither $K_f[A^-]_\omega$ is not much greater than 1, nor much smaller than 1, but close to 1. Then Equation (43) can be rewritten as

$$D \cong \frac{K_{D(HX^+,A^-)}}{2} + \frac{Ka_1 \; K_{D(X)}}{2} \; \frac{1}{[H^+]} \qquad (46)$$

By comparing Equations (46) with (1), a plot of D versus $\frac{1}{[H^+]}$ will give a straight line with twice the values for both intercept and slope as those obtained from Equation (1).

B. Liquid-Solid Systems

In liquid-solid systems, two types are considered. They are batch system and chromatographic system.

1. Batch System

If one considers that an ion pair is formed on a resin, R, in an acidic solution with a sample of X^- and a competing species Y^-, then ion-pair formation may be expressed as follows:

$$R_r + H^+_\omega + X^-_\omega \underset{}{\overset{K_1}{\rightleftharpoons}} (RH^+,X^-)_r \qquad (47)$$

$$R_r + H^+_\omega + Y^-_\omega \underset{}{\overset{K_2}{\rightleftharpoons}} (RH^+,Y^-)_r \qquad (48)$$

where r refers to the resin, ω refers to the aqueous solution,

$$K_1 = \frac{[(RH^+,X^-)]_r}{[H^+]_\omega [X^-]_\omega} = \text{formation constant of the species of interest} \qquad (49)$$

$$K_2 = \frac{[(RH^+,Y^-)]_r}{[H^+]_\omega [Y^-]_\omega} = \text{formation constant of the interferent species} \qquad (50)$$

Equations (47) and (49) indicate that the $(RH^+,X^-)_r$ ion-pair formation increases with increasing $[H^+]$ and $[X^-]_\omega$ if an excess of sites are available in the resin. This is related to the surface area as well as the "acidity" of the resin. Equation (48) shows that competition for ion-pair formation of $(RH^+,Y^-)_r$ will consume H^+_ω. That should lower the formation of $(RH^+,X^-)_r$, especially, when $[Y^-]_\omega$ becomes large.

2. Chromatographic System (45-47)

In a chromatographic system, the stationary phase is first conditioned with the mobile phase as expressed in Equation (51).

$$R_r + H_m^+ + A_m^- \rightleftharpoons (RH^+,A^-)_r \qquad (51)$$

where r refers to the resin; m refers to the mobile phase; and A_m^- is the anion component of the mobile phase. After the sample (Y^-) is introduced to the column, the adsorption of Y^- requires displacement of the anion A^- from the resin as shown in Equation (52).

$$(RH^+,A^-)_r + Y_m^- \rightleftharpoons (RH^+,Y^-)_r + A_m^- \qquad (52)$$

Since the sample is eluted by the mobile phase, the sample goes through the column with sorption-desorption steps and the reverse step in Equation (52) occurs. The whole process is a combination of ion-pair formation, liquid-solid adsorption, and anion-exchange chromatography. The following parameters are generally considered to affect the ion-pair formation on the resin.

a. Affinity of Anions for the Resin

If the packing material (resin) has a greater affinity for the sample (Y^-) than that for A^- in the mobile phase, then the sample will replace the A^- which adsorbed on the resin, and Y^- will be retained on the resin. With two mobile phases, the stronger the affinity for the resin, the faster the sample is displaced and thus eluted from the sample. Among sample anions, the larger the affinity for the resin, the longer the retention on the column. The affinity of an anion for

the resin may be expressed in terms of the molar distribution coefficient, K_d, which is defined (48) in batch experiment as

$$K_d = \frac{\text{millimoles of anion on the resin per gram of resin}}{\text{millimoles of anion remaining in solution per ml of solution}} \quad (53)$$

where the anion is the species studied. The larger the affinity of an anion for the resin, the larger the value of K_d.

b. Type of Adsorbent

(i) Polarity. Since separations by liquid-solid chromatography are usually carried out on polar adsorbents, relative adsorption increases as the polarity increases because the total interaction between the molecule and the polar adsorbent surface is increased.

(ii) Surface Area. The sample retention volumes and adsorbent linear capacity are proportional to the specific area of the adsorbent. Hence, the surface area of the adsorbent has an important effect on the chromatographic properties. The surface area is a function of pore diameter and pore volume (35). As pore volume increases, so does surface area, but as pore diameter increases, surface area decreases.

(iii) Particle Size and Geometry. Generally, smaller particle size gives a smaller height equivalent to a theoretical plate (HETP), according to the relationship: HETP $\sim d_p^{1.4-1.8}$ (49). Hence the column efficiency, N, will be improved by a factor of $(\frac{d_{p2}}{d_{p1}})^{1.4-1.8}$, where d_{p2} and d_{p1} are diameters of the larger and the smaller particles, respectively. Since the rigid adsorbent fixes the positions of the

reactive groups or adsorption sites on its surface, the interaction of the functional group in a sample varies with the geometry of the adsorbent, being stronger when the positions of groups and sites are matched.

(iv) Acidity of the Adsorbent. Since the hydronium ion is involved in ion-pair formation (Equation (51)), the acidity of the adsorbent will have large effect on adsorption. The more acidic the adsorbent, the more favored is the ion-pair formation.

c. Solvent Composition

For ion-exchange systems, the degree of retention of a sample depends on the pH of the mobile phase. For gradient elution, the separation (or selectivity) is improved by varying the concentration of the mobile phase because the optimum retention times will be obtained.

d. Net Adsorption Energy

The net adsorption energy, ΔE_a, for Equation (52) can be expressed as

$$\Delta E_a = E_{(RH^+,Y^-)_r} + E_{(A^-)_m} - E_{(RH^+,A^-)_r} - E_{(Y^-)_m} \quad (54)$$

Assuming that

$$E_{(A^-)_m} \cong E_{(Y^-)_m} \quad (55)$$

then Equation (54) is simplied as

$$\Delta E_a = E_{(RH^+,Y^-)_r} - E_{(RH^+,A^-)_r} \quad (56)$$

The interaction energies are determined by the interaction of either Y^- or A^- with the adsorbent surface. If the same solvent (mobile phase) is used, larger positive values of ΔE_a for Y^- favor adsorption on the resin.

CHAPTER III

LIQUID-LIQUID DISTRIBUTION STUDIES OF 8-HYDROXYQUINOLINIUM-ANION PAIR SYSTEMS

This chapter reports some studies of liquid-liquid extraction of 8-quinolinium cation by batch extraction. 8-Hydroxyquinoline was used in solutions with isopentyl alcohol or 1-butanol as solvents. Salts of the anions to be studied were dissolved in aqueous solutions at pH's between 1 and 2.

The perchlorate anion was studied in isopentyl alcohol/H_2O system. A partition constant value of 0.76 was obtained. This value is comparable with the 0.80 reported by Mottola and Freiser (21). Several other inorganic anions containing hydroxyl group (such as HSO_4^-, $H_2PO_4^-$, and $HSeO_3^-$), halogens (such as Cl^- and I^-), and oxygen (such as AsO_2^- and IO_4^-) were also included in the study. Organic anions containing carboxylate group (such as benzoate and acetate) and some of interest in pharmacology (such as penicillinate) or in industry (such as p-toluenesulfonate) were also studied.

This part of the work was concentrated on the estimation of the 8-hydroxyquinolinium-anion pair partition constant for each system and on the pH profile of distribution ratios. The data collected was later used in the design of separation schemes.

A. Partition Constants of 8-Hydroxyquinolinium-Anion Pairs Between Isopentyl Alcohol and Aqueous Phases in Low-pH Region

1. Experimental

a. Reagents

Isopentyl alcohol, $CH_3-\underset{\displaystyle CH_3}{\underset{|}{CH}}-CH_2-CH_2OH$, (Baker Analyzed Reagent) was purified by shaking 250 ml of isopentyl alcohol with 100 ml of 0.01 M sodium hydroxide solution and then rinsing four times with 125 ml of deionized-distilled water in order to remove oxidants from the solvent (22).

The following chemicals of analytical-reagent grade were used without further purification.

- 8-Hydroxyquinoline, 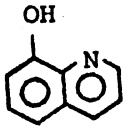 , Eastman Organic Chemicals.
- Sodium hydrogen sulfate, $NaHSO_4$, 'Baker Analyzed' Reagent.
- Sodium iodide, NaI, 'Baker Analyzed' Reagent.
- Sodium dihydrogen phosphate, NaH_2PO_4, 'Baker Analyzed' Reagent.
- Glacial acetic acid, CH_3COOH, DuPont Reagent.
- Sulfuric acid, H_2SO_4, DuPont Reagent.
- Hydrochloric acid, HCl, DuPont Reagent.
- Sodium arsenite, $NaAsO_2$, General Chemical Company.
- Sodium selenite, Na_2SeO_3, Pfaltz Bauer, Inc.
- Benzoic acid, C_6H_5COOH, 'Baker Analyzed' Reagent.
- Sodium hydroxide, NaOH, 'Baker Analyzed' Reagent.
- Sodium meta-periodate, $NaIO_4$, 'Baker Analyzed' Reagent.

- Sodium perchlorate, $NaClO_4$, G. Frederick Smith Chemical Co.

- Perchloric acid, $HClO_4$, DuPont Reagent.

All aqueous solutions were prepared using deionized-distilled water which was obtained by distilling laboratory deionized water, through a Corning AG1a boiler.

b. Apparatus

A Corning Model 7 pH meter, equipped with a Sargent miniature combination electrode (S-30070-10), was used for all pH measurements. The pH readings were estimated to ±0.01 units. When measuring pH, solutions were maintained at a constant temperature (25 ± 0.2 ^{o}C) by use of a water bath equipped with a temperature regulator (Brinkmann IC-2).

Spectrophotometric measurements were recorded on a Bausch and Lomb Spectronic 505 spectrophotometer. A pair of matched quartz cells (1 cm) were used and the absorbance readings were estimated to ± 0.001 units. A modified shaker with 31 strokes/min was used for shaking in all of the batch experiments. The shaker is based on an air-driven mechanism provided by a vacuum motor for a windshield wiper of the type commonly used in cars before the advent of electric motors for the same purpose. A picture of the shaker is shown in Figure 3.

c. Procedure

(i) Calibration Curve for 8-Hydroxyquinolinium Ion in Acidic Solutions. A stock solution containing 6.50 x 10^{-4} M of 8-hydroxyquinolinium ion was prepared by dissolving a suitable amount of 8-hydroxyquinoline in an acidic solution (such as: 0.10 M hydrochloric acid or 0.10 M perchloric acid) at pH about 1.0. A series of solutions in the range

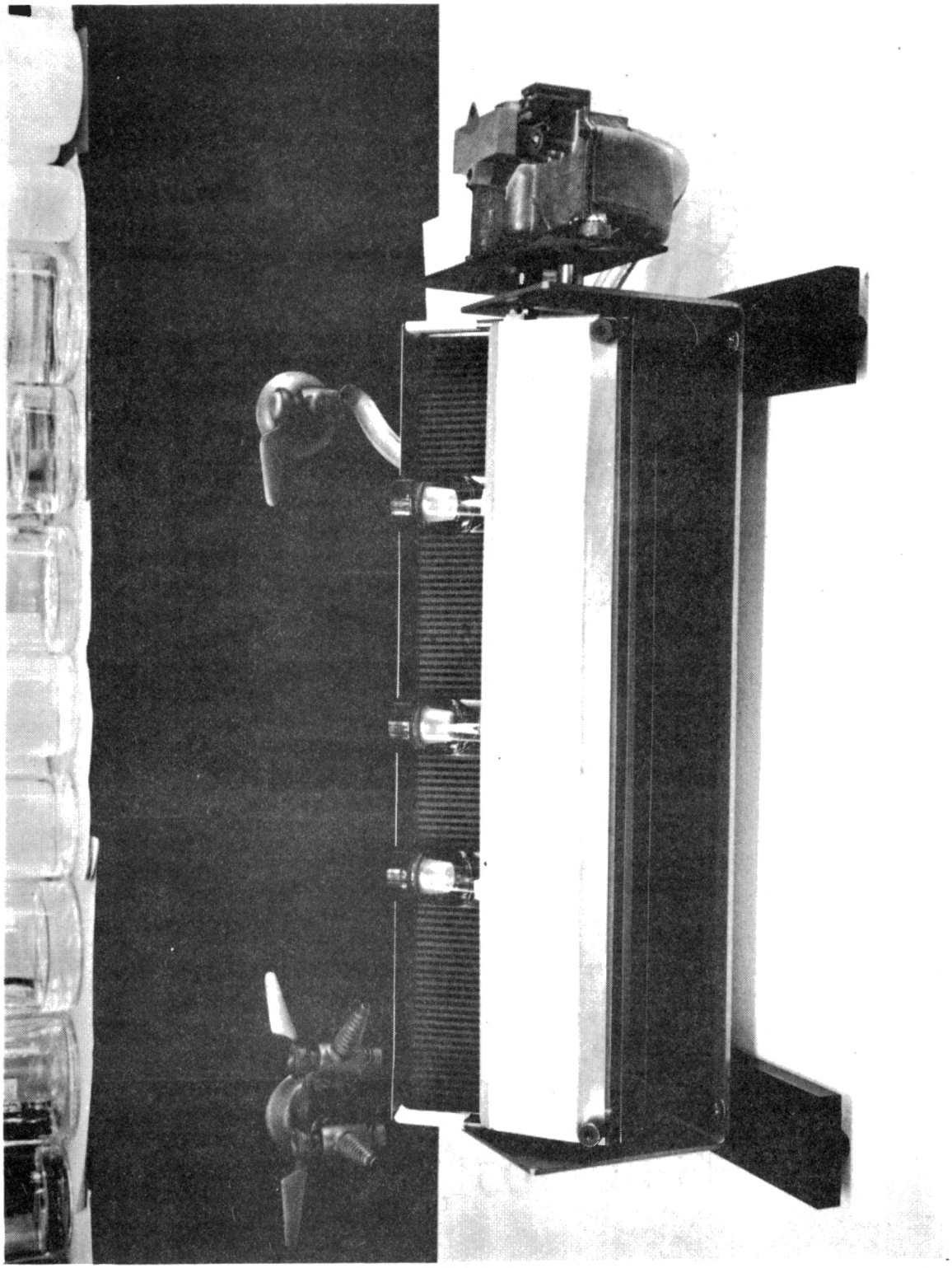

Figure 3. Custom-Made Shaker

of (0.50 - 5.0) x 10^{-4} M were prepared by diluting the stock solution with the corresponding acidic solution. Since the color of 8-hydroxyquinolinium ion is yellow, the absorption spectrum (Figure 1) shows that 8-hydroxyquinolinium ion has a maximum absorbance around 360 nm; this wavelength was chosen for measuring the 8-hydroxyquinolinium species. Readings of absorbance were obtained spectrophotometrically using the corresponding blank solution as reference. A calibration curve was made by plotting absorbance versus concentration and by least-square fitting, the molar absorptivity of the 8-hydroxyquinolinium species was calculated.

(ii) Distribution Studies of 8-Hydroxyquinolinium-Anion Pairs Between Isopentyl Alcohol and Aqueous Phases (21). A suitable amount of 8-hydroxyquinoline dissolved in isopentyl alcohol (in the range of (1-3) x 10^{-3} M) was used as organic phase. Anions being studied were prepared in aqueous solutions. Ionic strengths were adjusted to 0.1 M by the addition of salts (such as $NaHSO_4$, NaCl, $NaClO_4$, and Na_2SO_4) and pH was adjusted to 1-2 by addition of H_2SO_4.

Distribution studies were performed at room temperature (~25 °C) by pipetting equal volumes (10-15 ml) of the organic phase and aqueous solution into 35-ml vials, which were stoppered with plastic caps. The mixture was shaken for 15 minutes in the shaker. Beyond 15 minutes of shaking, no sufficient difference in the values of distribution ratios was observed (21). After equilibrium, the solutions were placed in the thermostat at 25 °C for one hour to ensure phase separation.

After that, an aliquot (~7 ml) of the aqueous phase was removed. Some portion of the aliquot (~2 ml) was used for pH measurement at 25 °C

in the thermostat; the reading was taken as the equilibrium pH value. The other portion of the aliquot (5.00 ml) was pipetted and transferred to a 20-ml beaker. The pH of the aliquot was adjusted to 1.0 as close as possible by adding 1.0 M HCl (or other suitable acidic solutions) dropwise. The solution was then transferred to a 25-ml volumetric flask, with rinsing and diluting to the mark with 0.10 M HCl (or another corresponding acidic solutions). The same procedure was used for preparing the blank in order to minimize errors that might be possible because of molar absorptivity dependence on the ratio of water to organic solvent. Absorbance readings for the sample solutions were measured spectrophotometrically at 360 nm against the blank.

The concentration of 8-hydroxyquinolinium ion in the aqueous phase was calculated from the calibration curve. According to Beer's law,

$$A = \varepsilon b c \tag{57}$$

where

A = absorbance; ε = molar absorptivity in M^{-1} cm^{-1}; b = cell length in cm; and c = molar concentration in M, a plot of absorbance versus concentration gives a straight line with εb as the slope. Since b is 1.00 cm, the molar absorptivity has the same value as the slope. Since the total concentration of 8-hydroxyquinoline, C_{HO_x}, introduced was known, the distribution ratio can be easily calculated from Equation (58).

$$D = \frac{C_{HO_x} - \Sigma[HO_x]_\omega}{\Sigma[HO_x]_\omega} \tag{58}$$

Assuming that $\Sigma[HO_x]_\omega \cong [H_2O_x^+]_\omega$ at pH of 1-2, Equation (58) can be

rewritten as follows:

$$D = \frac{C_{HO_x} - [H_2O_x^+]_\omega}{[H_2O_x^+]_\omega} \qquad (59)$$

2. Theory and Formula Used

a. Dyrssen's Model

Equation (1), which was used by Dyrssen and derived in Appendix A, was used to estimate values of $K_{D(H_2O_x^+,A^-)}$ which are intercepts from plots of D versus $\frac{1}{[H^+]}$.

b. Modified Model

In deriving Equation (1), assumptions of large $[A^-]_\omega$ and large K_a were made so that the side reaction of forming HA was neglected. If the side reaction (Equation (24)):

$$H^+ + A^-_\omega \underset{Ka_{(HA)}}{\rightleftharpoons} (HA)_\omega \qquad (24)$$

in aqueous phase is considered, $K_{D(HX^+A^-)}$ and $K_{D(X)}$ can be calculated from Equations (41) for a strong acid; and from Equation (43) for a general case (i.e., when K_a is relative small and/or C_{A^-} is only slightly in excess of C_χ; where X represents HO_x) by incorporating with the mass balance equation of A^- (Equation (38) or (60), the mass balance equation of X (Equation (61)), and the charge-balance equation (Equation (62)).

$$C_{A^-} = [A^-]_\omega \{1 + \frac{[H^+]}{Ka_{(HA)}} + (1 + K_{D(HX^+A^-)}) K_f [HX^+]_\omega\} \qquad (60)$$

$$C_{\chi} = [H\chi^{+}] \{\frac{Ka_1 K_{D(\chi)}}{[H^{+}]} + K_f [A^{-}]_{\omega} (1 + K_{D(H\chi^{+}A^{-})}) + 1\} \quad (61)$$

$$[H^{+}] + [H\chi^{+}] + [Na^{+}] = [A^{-}]_{\omega} + [HSO_4^{-}] + 2[SO_4^{2-}] + [OH^{-}] \quad (62)$$

However, the results obtained from Equation (43) were not satisfactory because $K_{D(HO_x)}$ values calculated were negative. Hence, two simplified equations (44) and (45) were also tested.

3. Results

a. Calibration curves for 8-hydroxyquinolinium ion at 360 nm in 0.10 M HCl and in 0.10 M $HClO_4$ are shown in Figures 4 and 5, respectively. Molar absorptivities for 8-hydroxyquinolinium ion at 360 nm obtained from calibration curves are 1.70×10^3 M^{-1} cm^{-1} and 1.72×10^3 M^{-1} cm^{-1}, respectively. These values are comparable with the value $(1.65 \pm 0.03) \times 10^3$ M^{-1} cm^{-1}, as reported by Mottola and Freiser (21).

b. Using Dyrssen's equation, plots of D versus $\frac{1}{[H^{+}]}$ for several inorganic (ClO_4^{-}, HSO_4^{-}, Cl^{-}, I^{-}, $H_2PO_4^{-}$, AsO_2^{-}, $HSeO_3^{-}$, and IO_4^{-}) and organic ($C_6H_5COO^{-}$ and CH_3COO^{-}) anions are shown in Figures 6-15, respectively. Slopes, $Ka_1 \cdot K_{D(HO_x)}$, and partition constants for 8-hydroxyquinolinium-anion pairs, $K_{D(H_2O_x^{+},A^{-})}$, obtained between isopentyl alcohol and aqueous solutions are tabulated in Table II. The $K_{D(H_2O_x^{+},A^{-})}$ values calculated from the modified equations (44) and (45) are also listed in Table II using the values of $Ka_1 = 1.41 \times 10^{-5}$ and $K_{D(HO_x)} = 62.2$ (21).

c. Since periodate anion, IO_4^{-}, is a strong oxidizing agent and decomposes (or is unstable) in an acidic medium, the D values obtained

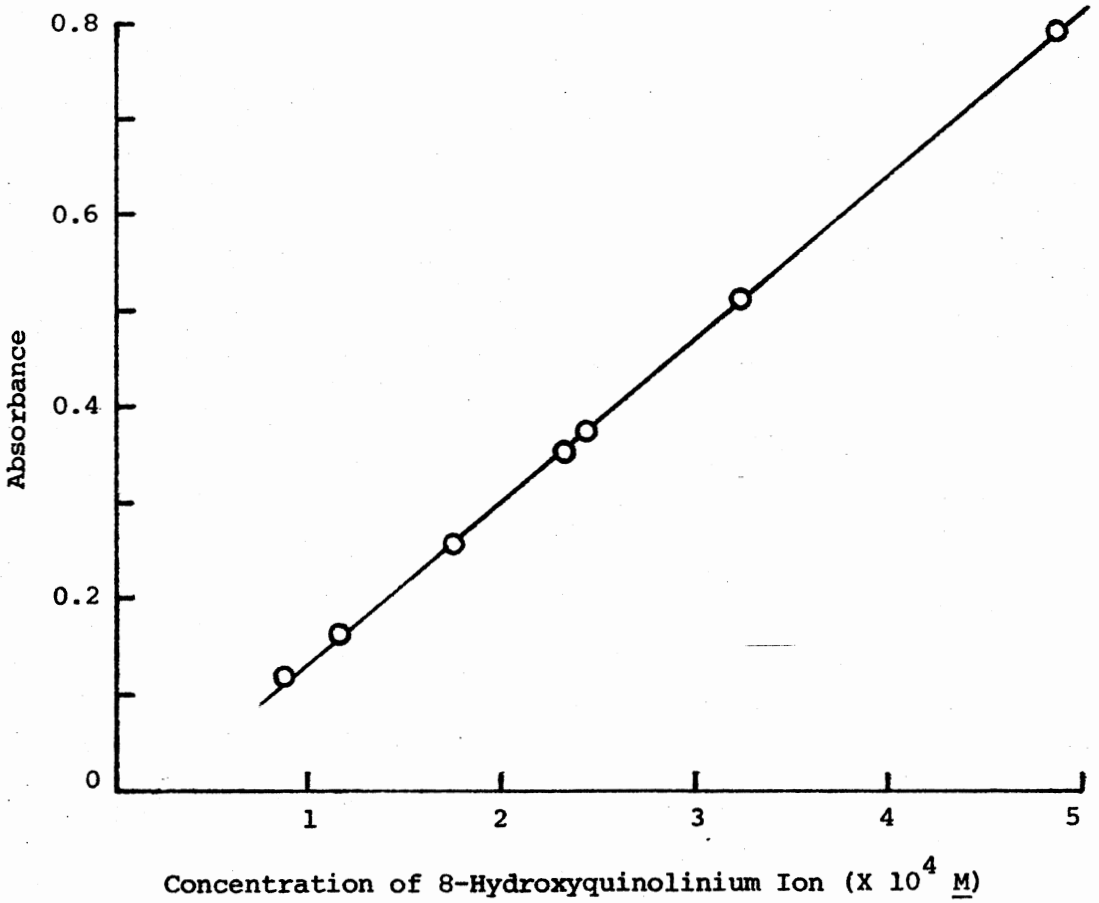

Figure 4. Calibration Curve for 8-Hydroxyquinoline in 0.10 M HCl at 360 nm

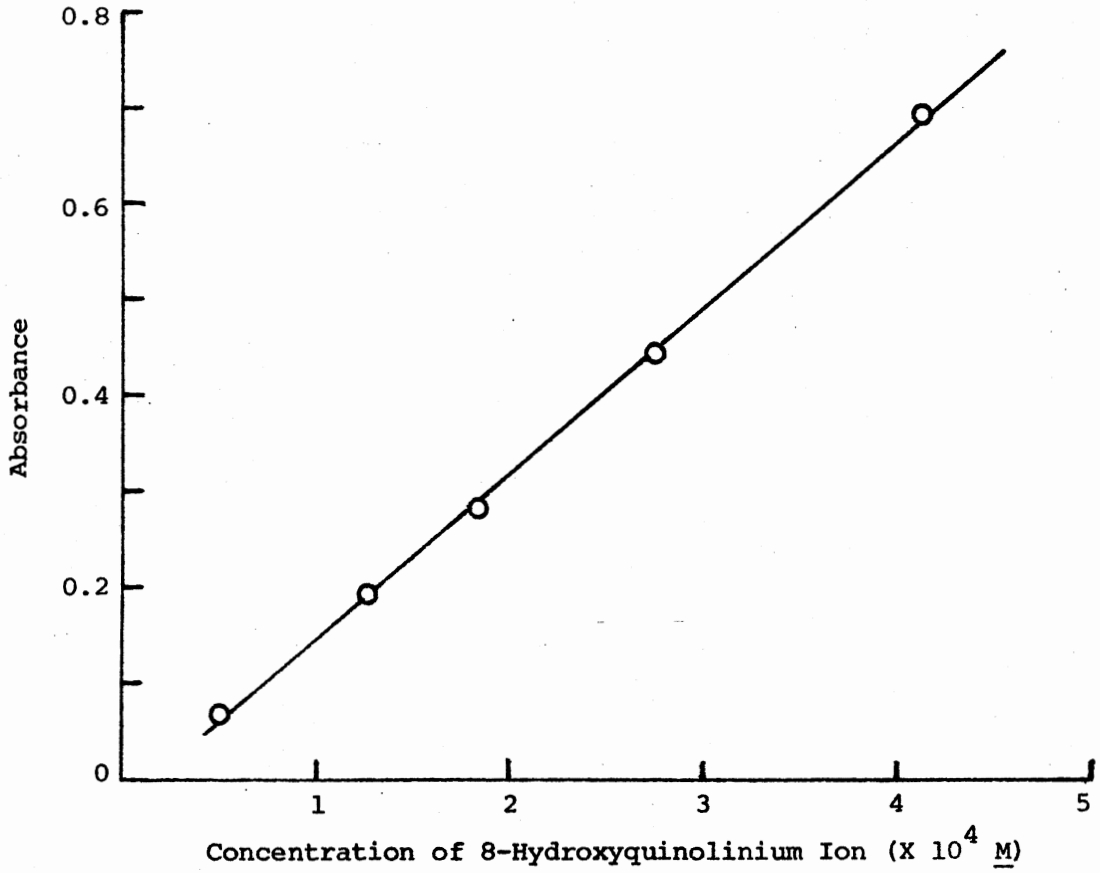

Figure 5. Calibration Curve for 8-Hydroxyquinoline in 0.10 M $HClO_4$ at 360 nm

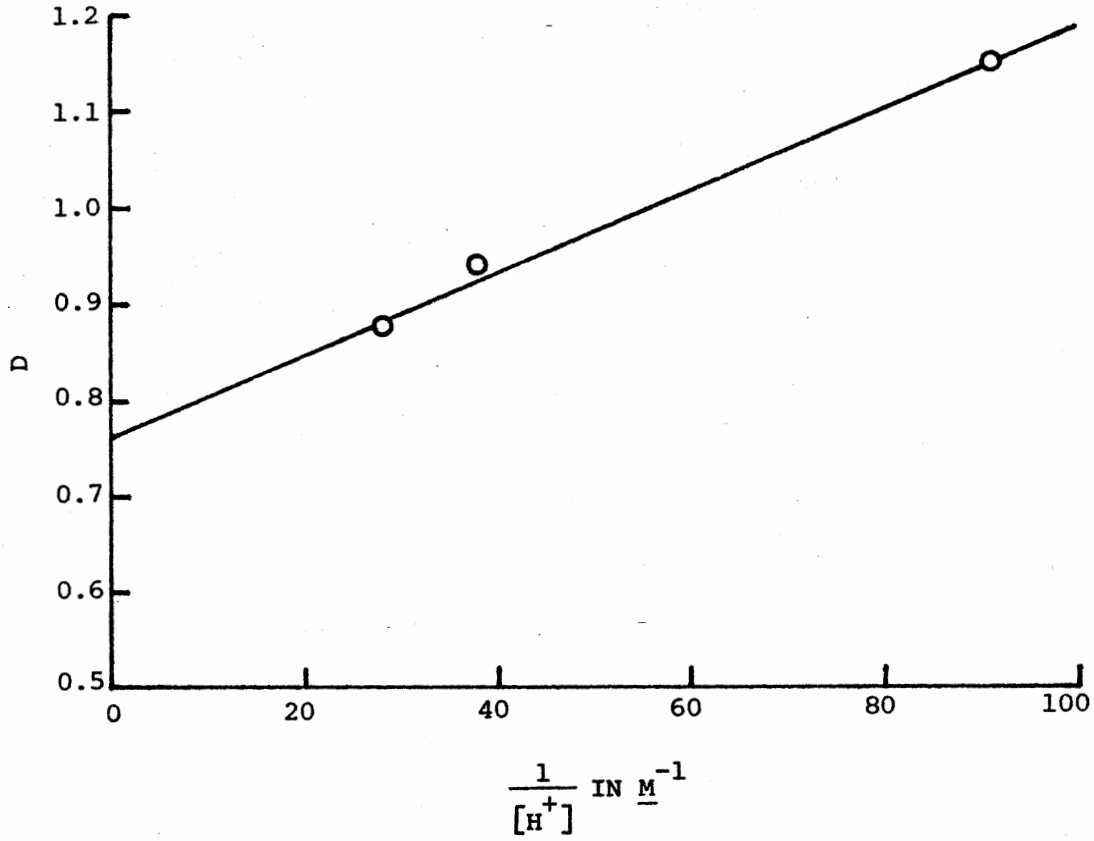

Figure 6. Plot to Determine $K_{D(H_2O_x^+, ClO_4^-)}$ in Isopentyl Alcohol System

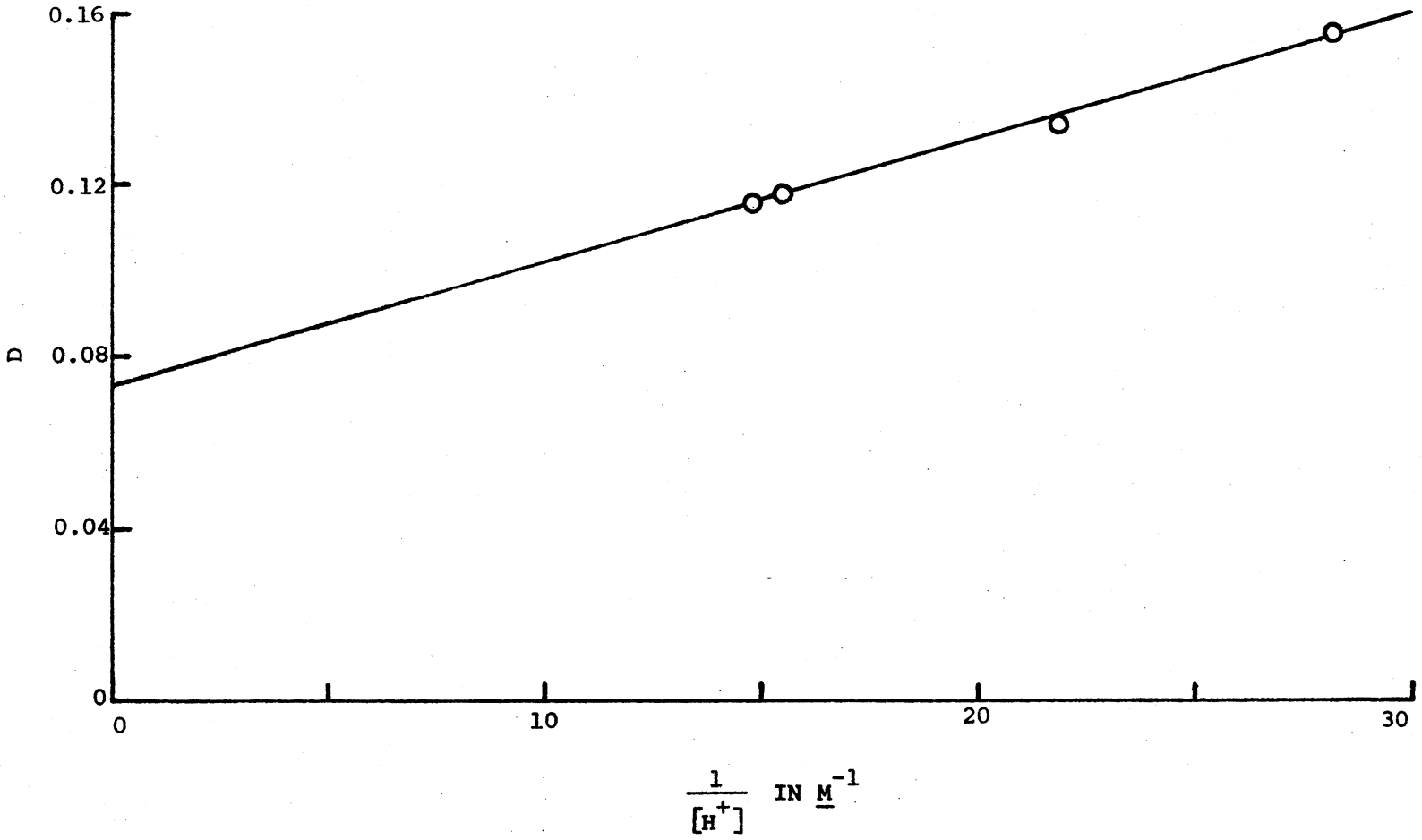

Figure 7. Plot to Determine $K_{D(H_2O_x^+,\ HSO_4^-)}$ in Isopentyl Alcohol System

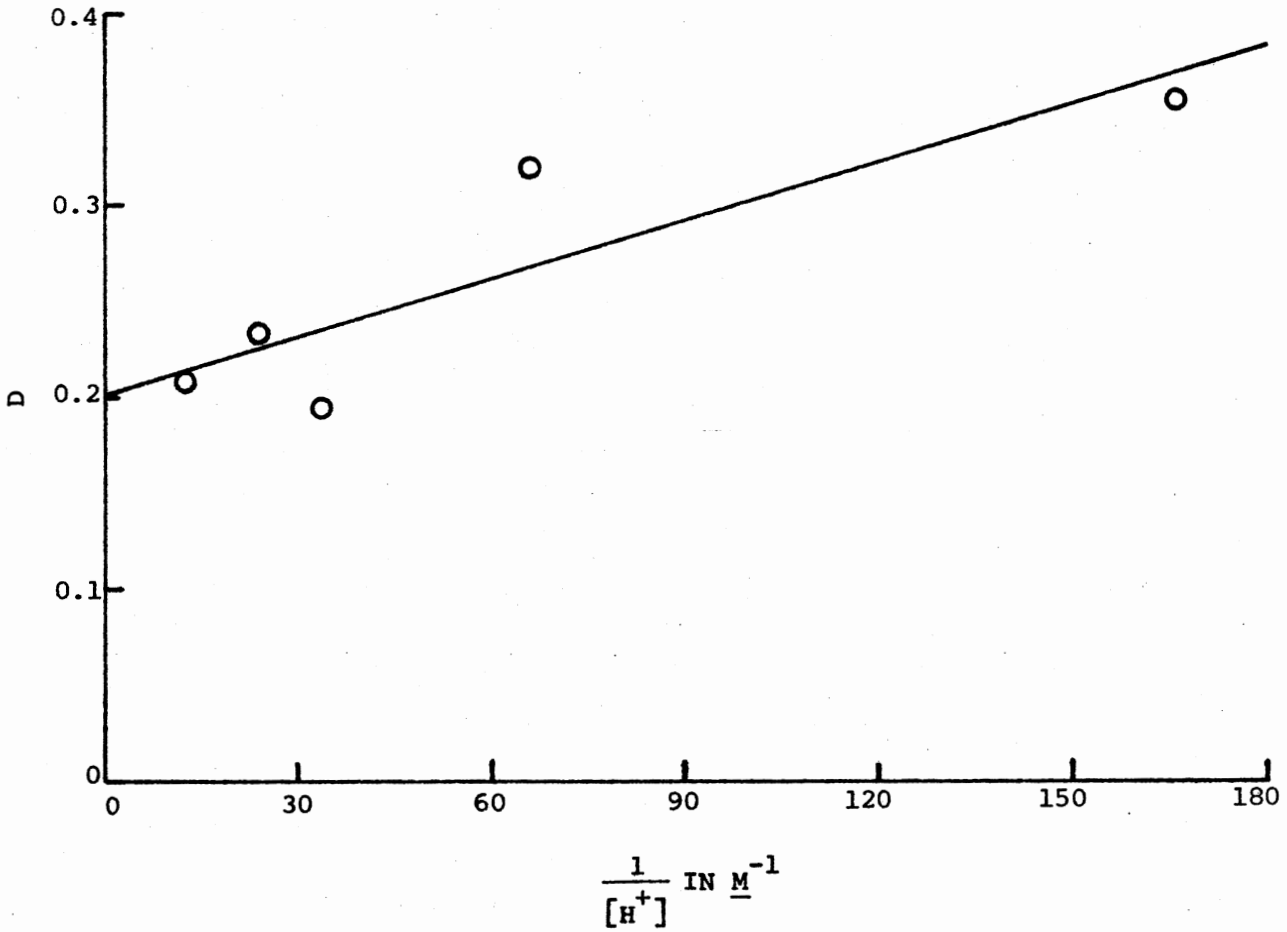

Figure 8. Plot to Determine $K_{D(H_2O_x^+,\ Cl^-)}$ in Isopentyl Alcohol System

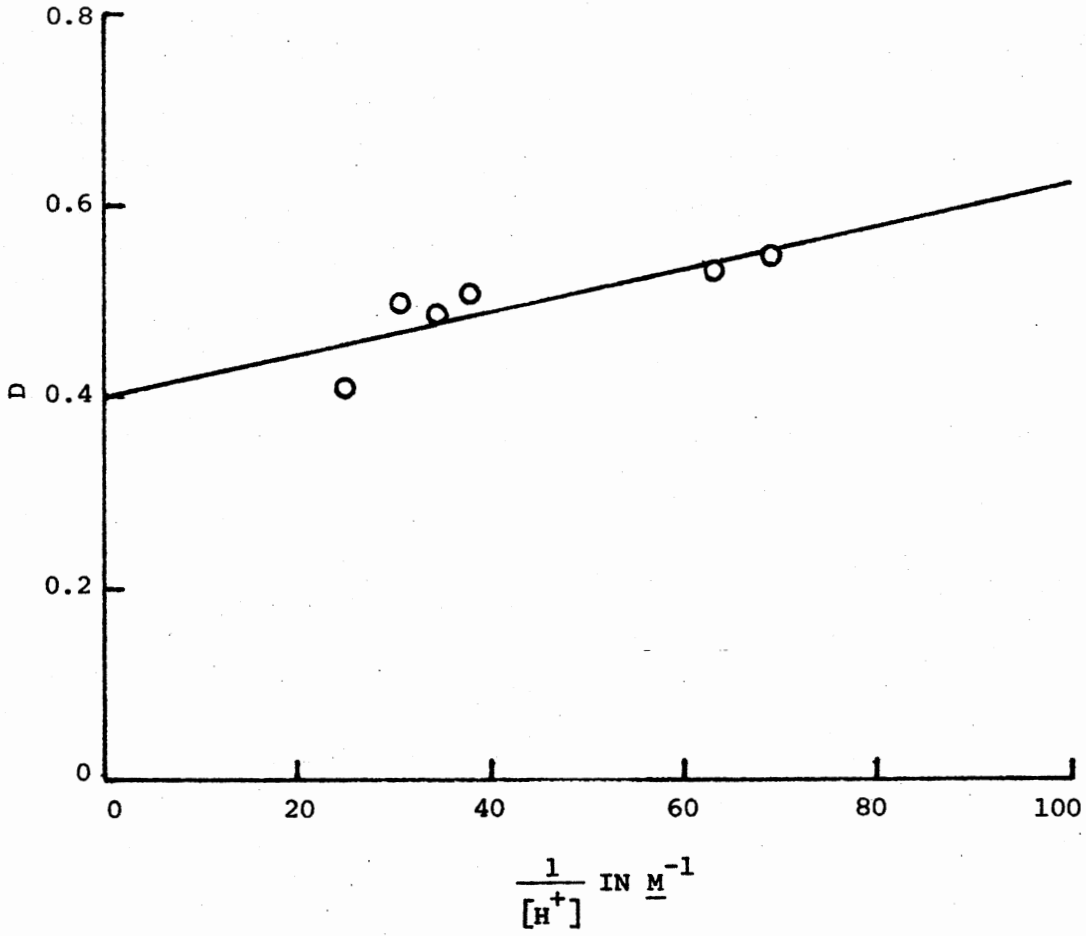

Figure 9. Plot to Determine $K_{D(H_2O_x^+,\ I^-)}$ in Isopentyl Alcohol System

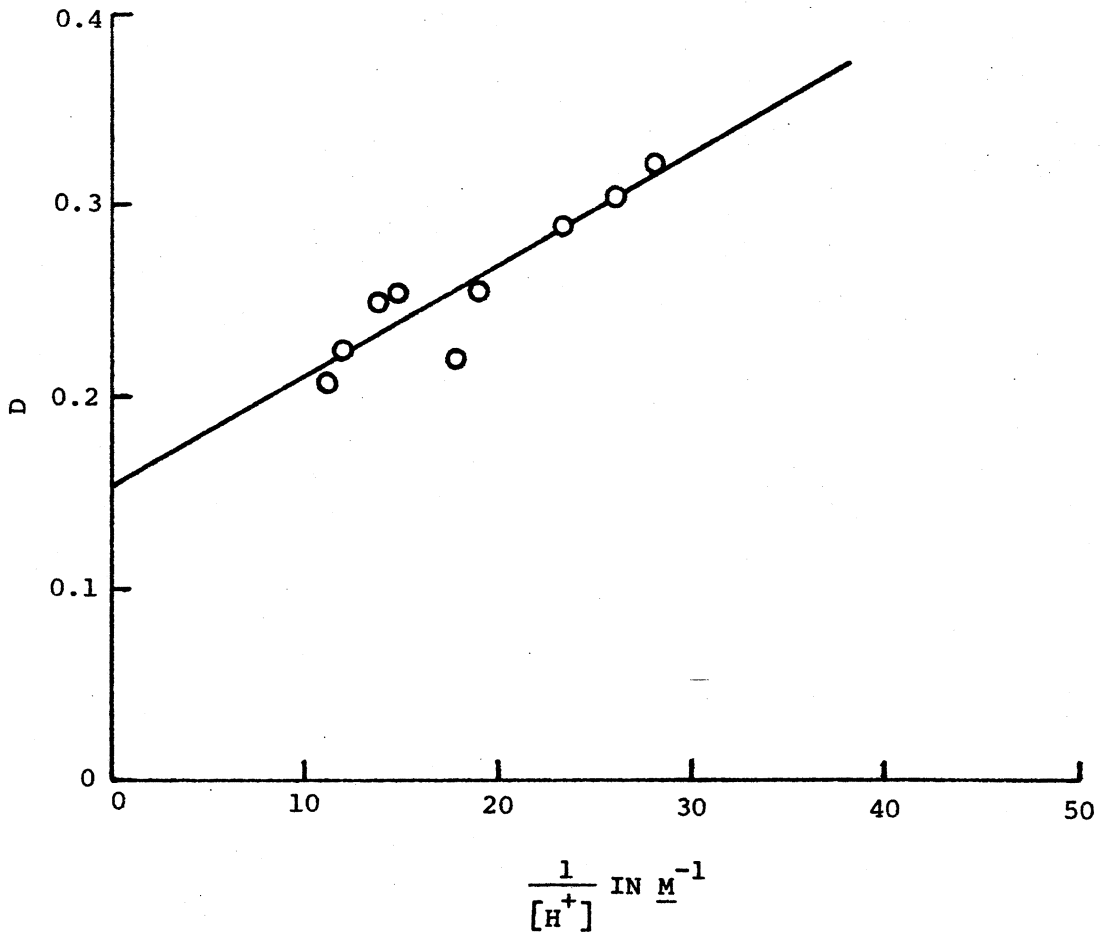

Figure 10. Plot to Determine $K_{D(H_2O_x^+,\ H_2PO_4^-)}$ in Isopentyl Alcohol System

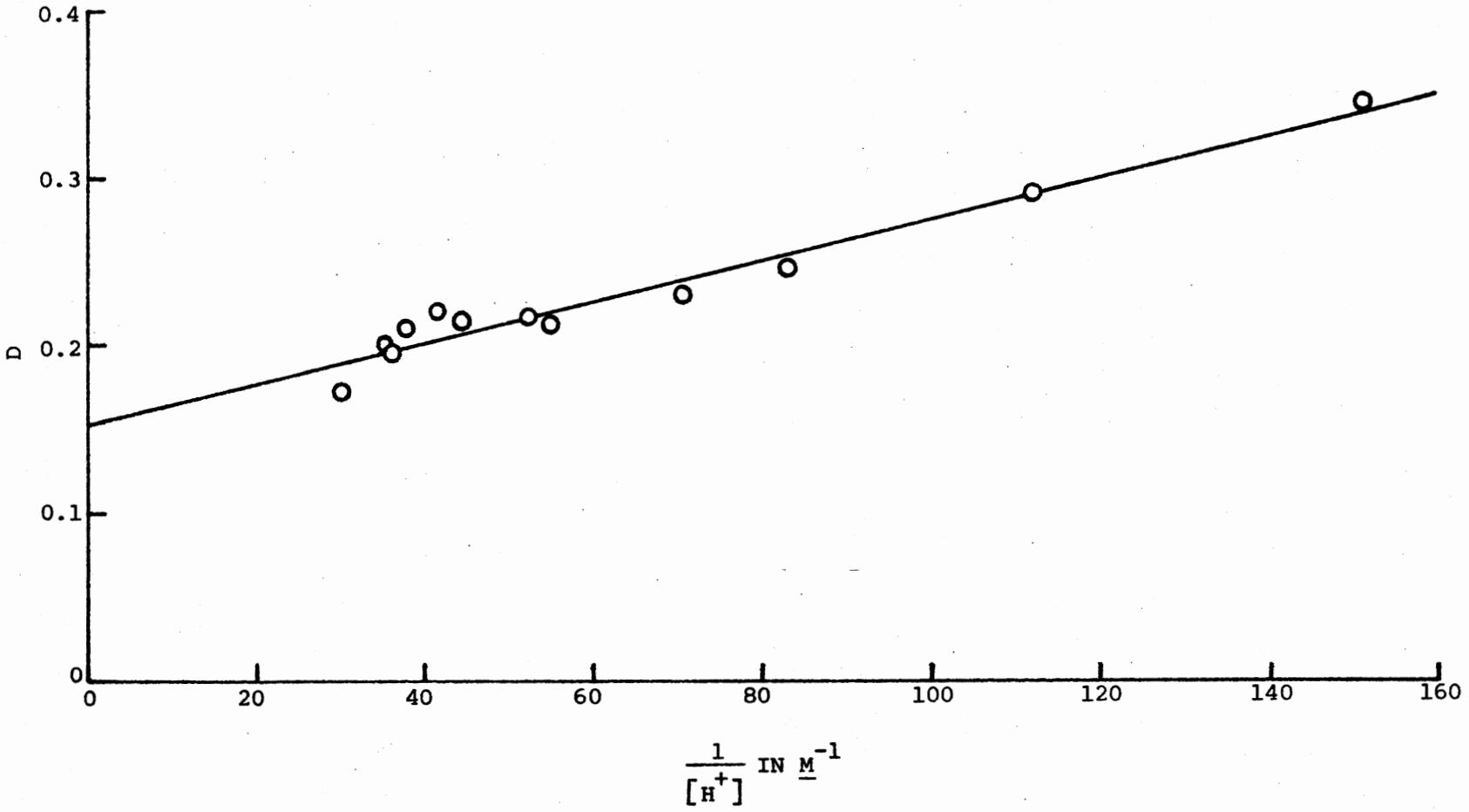

Figure 11. Plot to Determine $K_{D(H_2O_x^+,\ AsO_2^-)}$ in Isopentyl Alcohol System

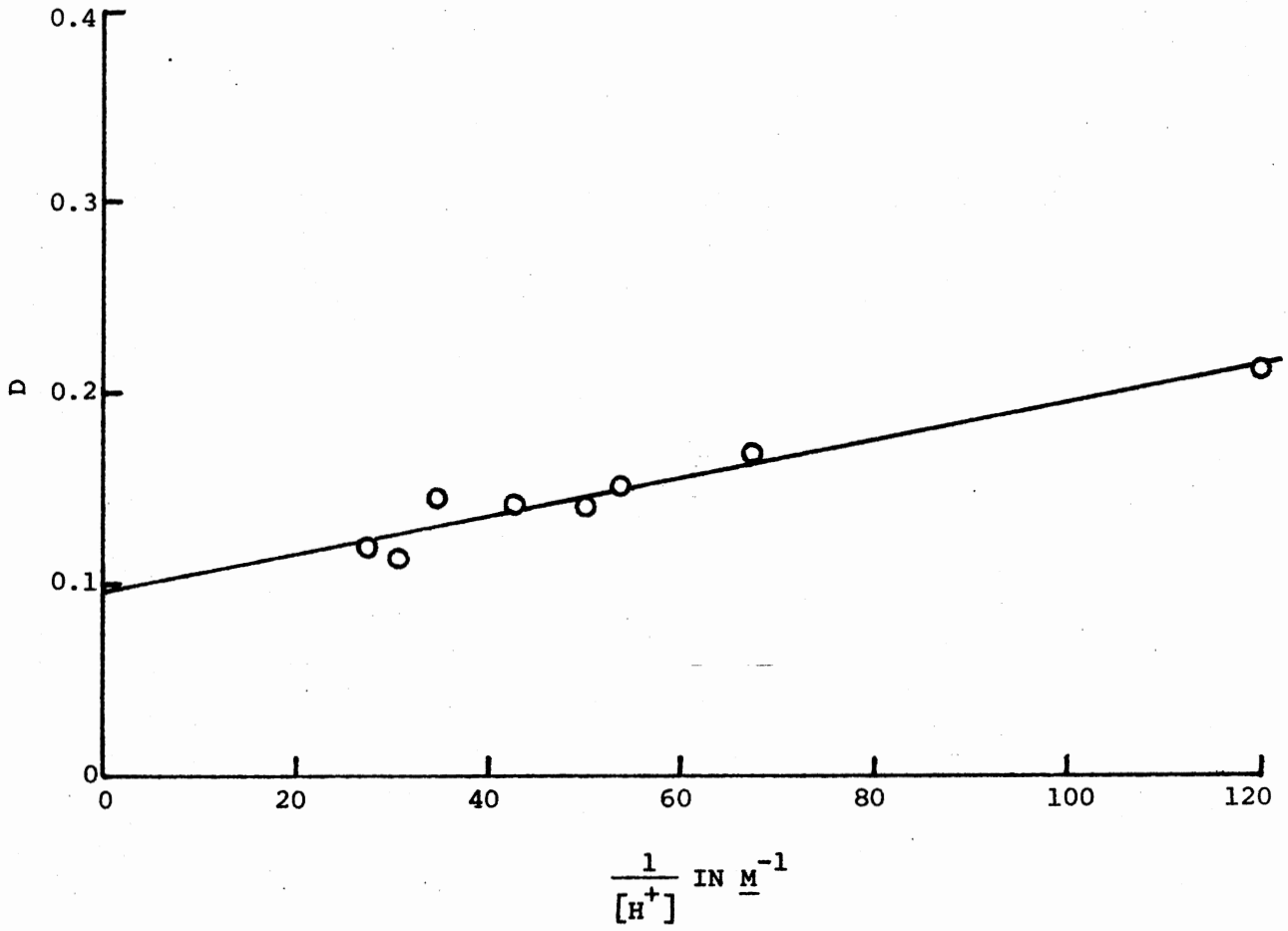

Figure 12. Plot to Determine $K_{D(H_2O_x^+,\ HSeO_3^-)}$ in Isopentyl Alcohol System

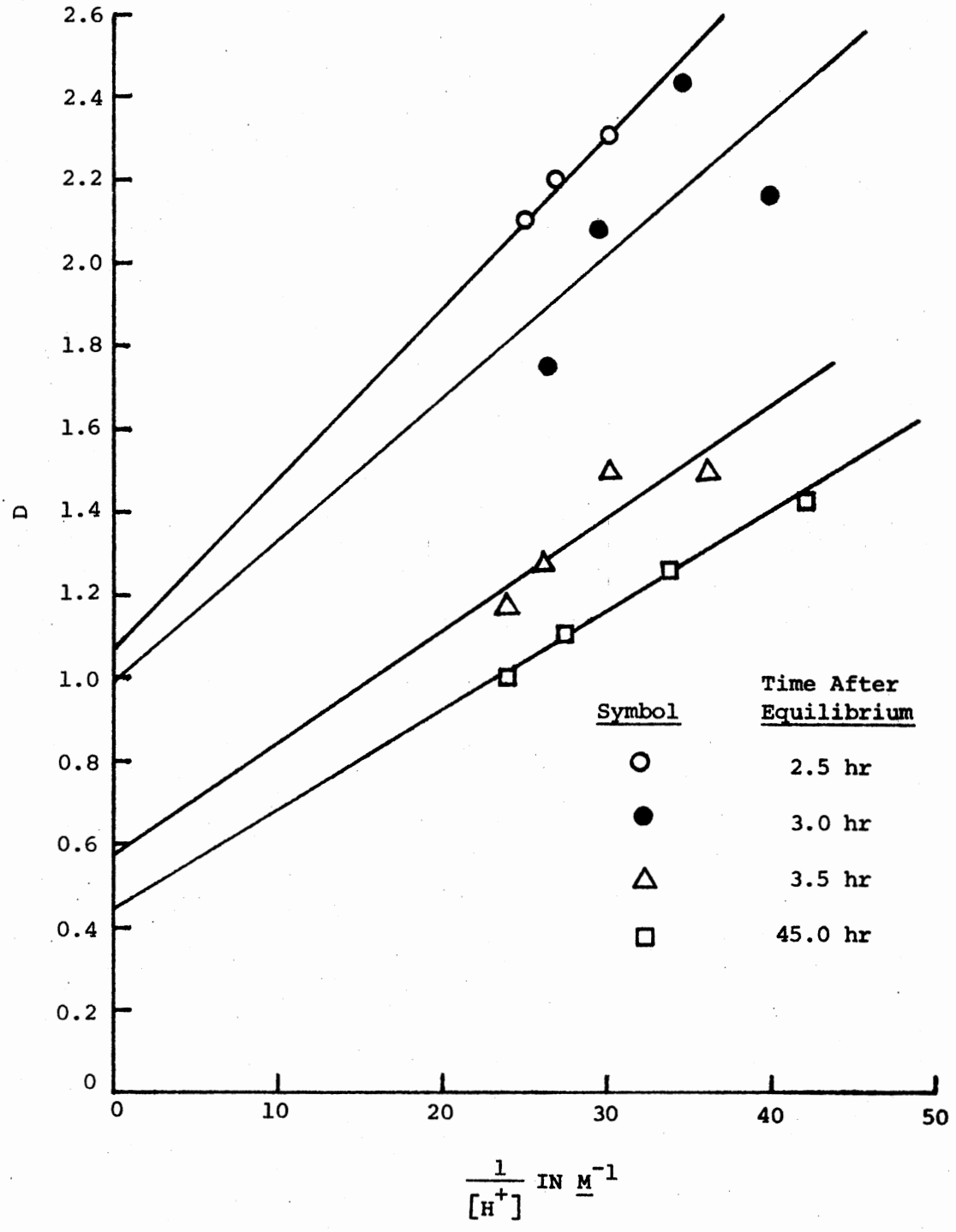

Figure 13. Plot to Estimate $K_{D(H_2O_x^+,\ IO_4^-)}$ in Isopentyl Alcohol System

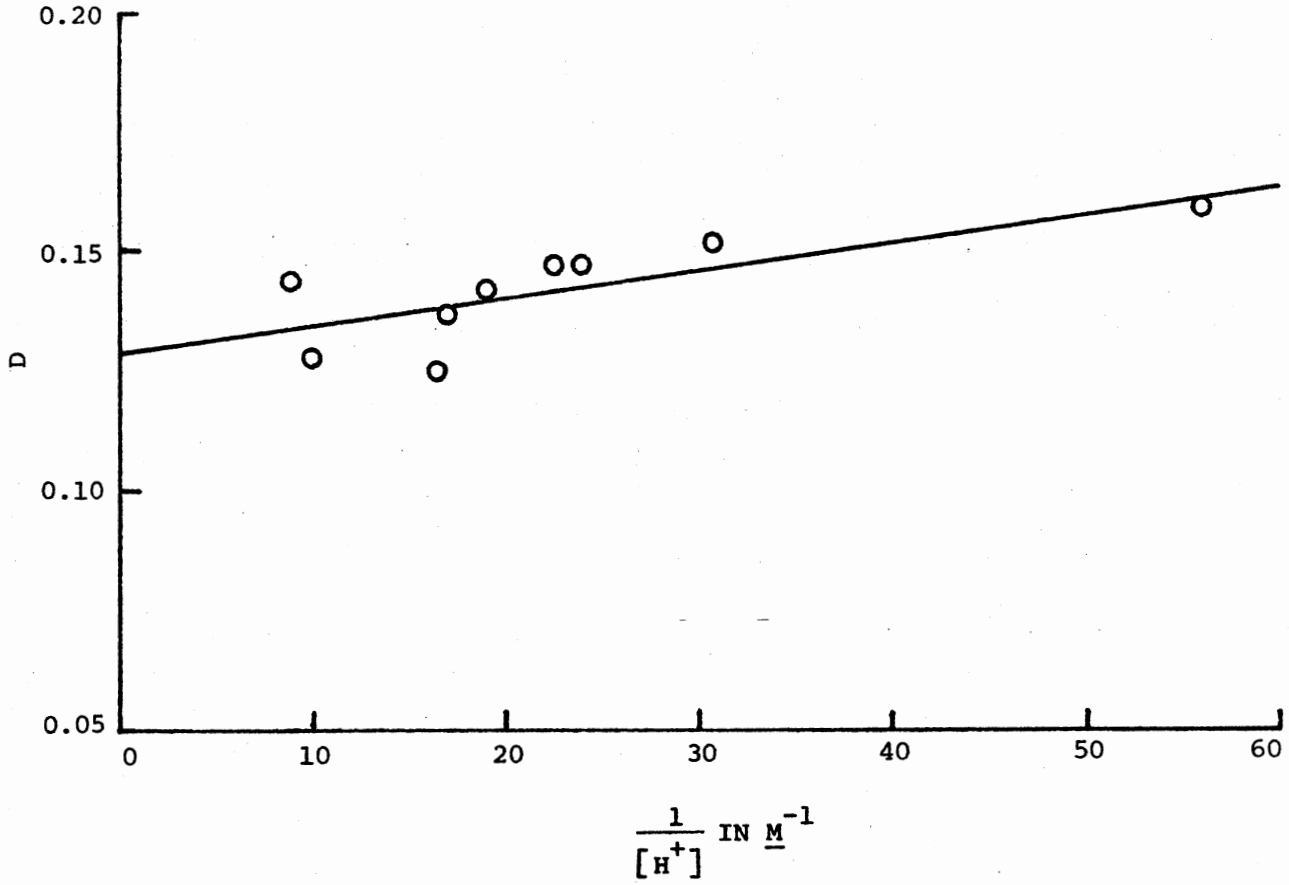

Figure 14. Plot to Determine $K_{D(H_2O_x^+,\ C_6H_5COO^-)}$ in Isopentyl Alcohol System

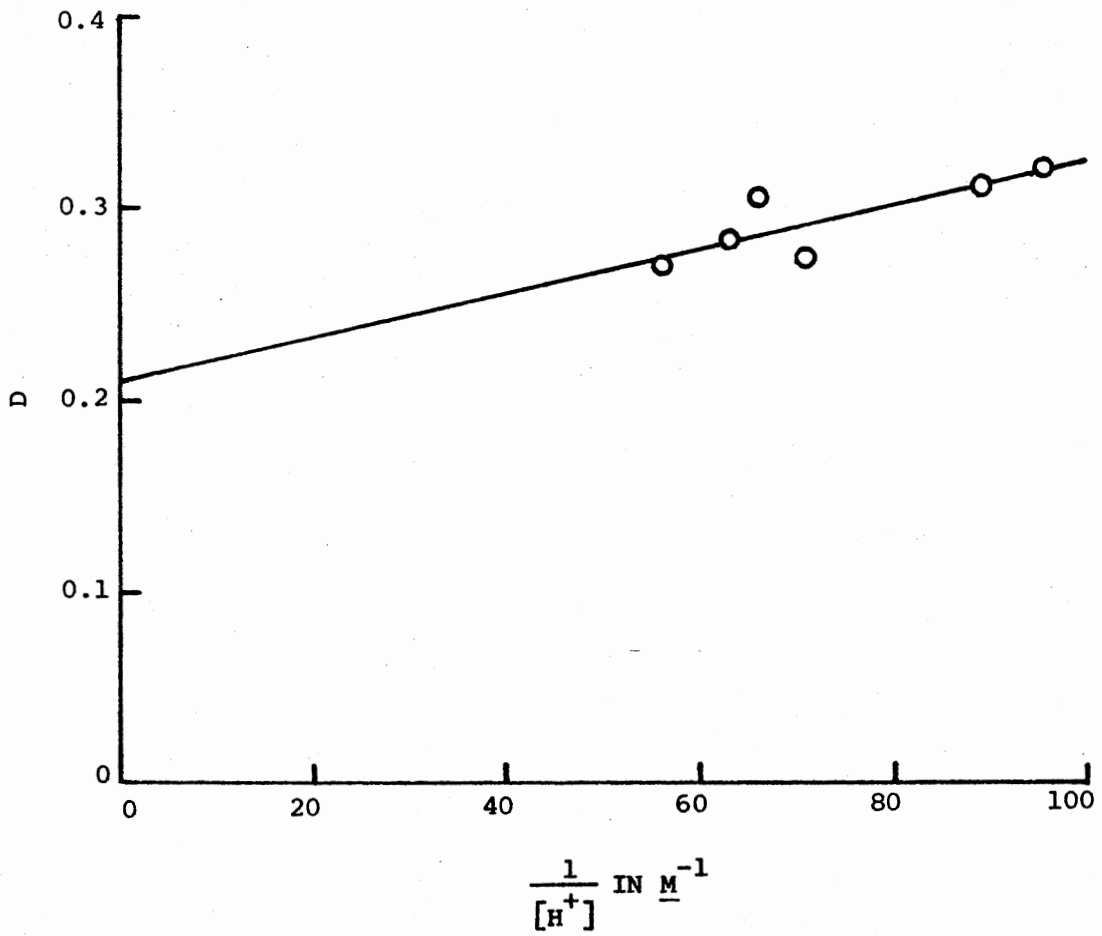

Figure 15. Plot to Determine $K_{D(H_2O_x^+,\ CH_3COO^-)}$ in Isopentyl Alcohol System

TABLE II

SUMMARY OF $K_{D(H_2O_x^+,A^-)}$ AND SLOPE OF $Ka_1 \cdot K_{D(HO_x)}$ IN ISOPENTYL ALCOHOL SYSTEM USING DYRSSEN'S EQUATION; $K_f[A^-]_\omega$ AND $K_{D(H_2O_x^+,A^-)}$ FROM MODIFIED EQUATIONS; AND SOME PROPERTIES OF ANIONS

Anion	(Ka)[a] for HA	C_{A^-} X 10^3 (M)	C_{HO_x} X 10^3 (M)	Dyrssen's Equation: Intercept $K_{D(H_2O_x^+,A^-)}$	Dyrssen's Equation: Slope $Ka_1 \cdot K_{D(HO_x)}$ (X 10^3)	Modified Equation: Eq. (44)[b] $K_f[A^-]_\omega$	Modified Equation: Eq. (45)[c] $K_{D(H_2O_x^+,A^-)}$	Crystal Radii (Å) (50)	Hydrated Radii (Å) (50)
HSO_4^-	100	74	1.60	0.073	2.86	0.307	0.24		
$HSeO_3^-$	3.47×10^{-3}	20	2.38	0.097	0.996	0.880	0.11		
$H_2PO_4^-$	7.08×10^{-3}	53.7	2.03	0.15	5.82	0.151	0.99		
AsO_4^-	6.03×10^{-3}	16.2	2.38	0.15	1.01	0.868	0.17		
Cl^-	100	100	2.38	0.20	1.01	0.868	0.23	1.81	2.55
I^-	100	50.8	2.41	0.40	1.86	0.472	0.85	2.16	
ClO_4^-	100	100	1.38	0.76	4.30	0.204	3.73	2.36	2.43
$C_6H_5COO^-$	0.0631×10^{-3}	2.28	1.61	0.13	0.572	1.53	0.085		
CH_3COO^-	0.0174×10^{-3}	105	1.94	0.21	1.27	0.690	0.30	1.59	2.96

a. Ka is estimated as 100 for strong acids; others are obtained from Reference (51).

b. $K_f[A^-]_\omega = Ka_1 \cdot K_{D(HO_x)}$/slope of Dyrssen's Eq.; where $Ka_1 = 1.41 \times 10^{-5}$ and $K_{D(HO_x)} = 62.2$ (21) were used.

c. $K_{D(H_2O_x^+,A^-)}$ = Intercept of Equation (45)/the value of $K_f[A^-]_\omega$.

are not reproducible at the same pH if measured at different times after equilibrium is attained. The $K_{D(H_2O_x^+,\ IO_4^-)}$ value varies from 1.07 to 0.44 as shown in Figure 13. Hence, IO_4^- is not listed in Table II.

4. Discussion

a. The partition constants of the 8-hydroxyquinolinium-anion pair, $K_{D(H_2O_x^+,A^-)}$, obtained from Dyrssen's model can be qualitatively explained from the viewpoint of the nature of anion and the side reactions (protolysis) that have been described in Chapter II. A. 2. a and c. The $K_{D(H_2O_x^+,A^-)}$ value increases in the order of $Cl^- < I^- < ClO_4^-$. This is not only because Cl^- has the smallest crystal radius and the largest hydrated radius (Table II) among the three anions but also because the nature of solvent affects. Hence, Cl^- is the most strongly solvated (or attracted) by water and the $K_{D(H_2O_x^+,A^-)}$ value is the lowest one. A plot of $K_{D(H_2O_x^+,A^-)}$ versus anionic radius is shown in Figure 16. This proves that, as expected, large and poorly hydrated anions tend to form ion pairs that are more soluble in the organic phase than in the aqueous phase (27(a)). The $K_{D(H_2O_x^+,A^-)}$ values for HSO_4^-, $HSeO_3^-$, $H_2PO_4^-$, $C_6H_5COO^-$, and CH_3COO^- are also small compared to that of ClO_4^- because they contain either a hydroxyl or a carboxylic group, a highly hydrophilic component. Hence, these anions are strongly hydrated by water, especially HSO_4^-, and have only little tendency to be extracted into the organic phase. The $K_{D(H_2O_x^+,A^-)}$ value for AsO_2^- is smaller than that of ClO_4^- probably because of the trend of the radius. The side reaction of protolysis may also affect and lower the $K_{D(H_2O_x^+,A^-)}$ values as indicated in Table II for those acids of moderate or low strength.

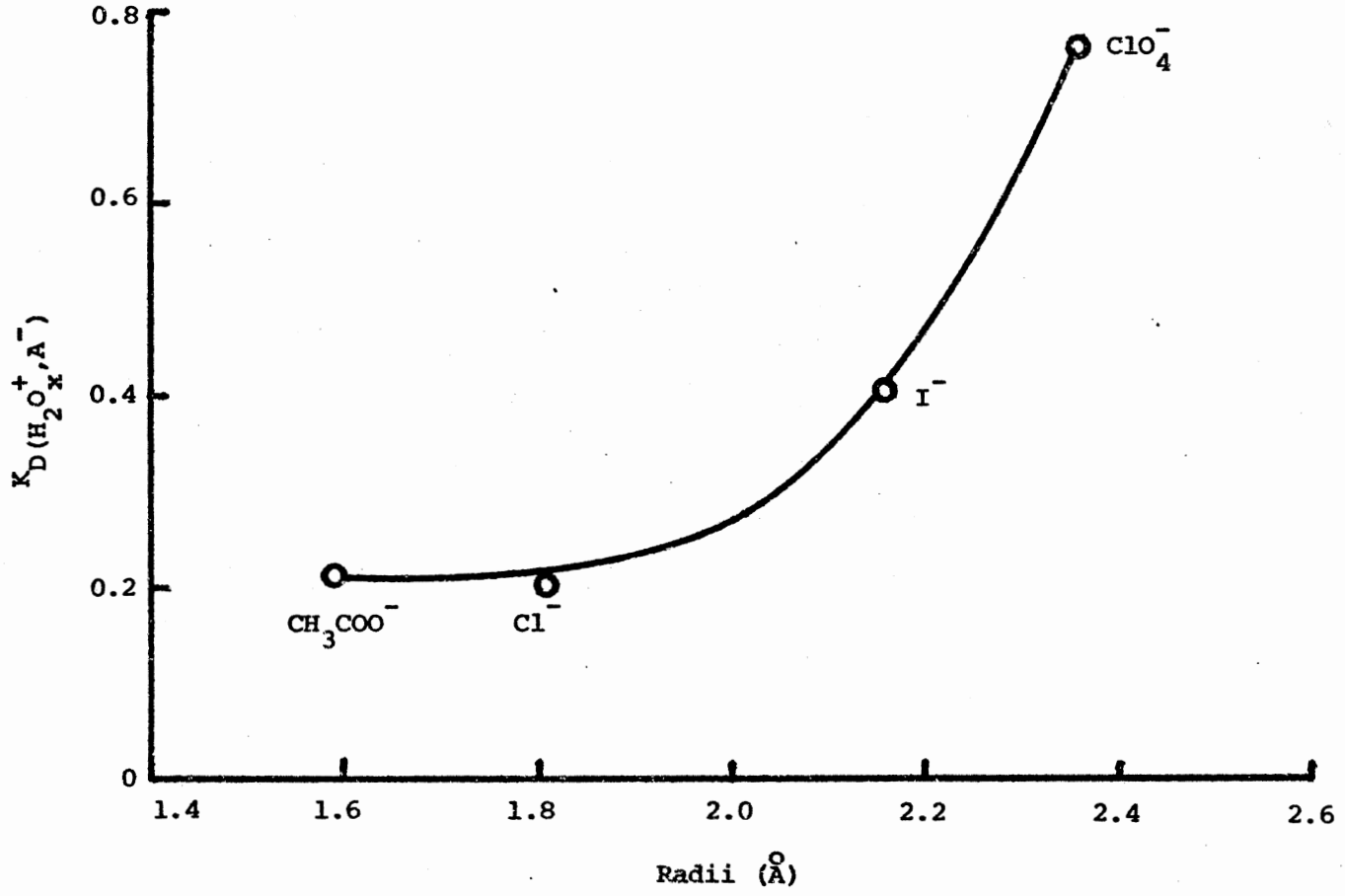

Figure 16. $K_{D(H_2O_x^+,A^-)}$ Versus Crystal Radii of Anion in Isopentyl Alcohol System Using Dyrssen's Model

b. The slopes obtained from Dyrssen's equation are the product of Ka_1 and $K_{D(HO_x)}$. Since Ka_1 is a constant, as shown in Table I, the partition constant of 8-hydroxyquinoline, $K_{D(HO_x)}$, between isopentyl alcohol and aqueous phase is calculated and tabulated in Table III.

The distribution ratio for 8-hydroxyquinoline in neutral aqueous solutions can be expressed as follows:

$$D = \frac{[HO_x]_o}{[H_2O_x^+]_\omega + [HO_x]_\omega + [O_x^-]_\omega} \tag{63}$$

Since $[H_2O_x^+]_\omega$ and $[O_x^-]_\omega$ are smaller than $[HO_x]_\omega$ at neutral solutions, Equation (63) can be rewritten as

$$D \cong \frac{[HO_x]_o}{[HO_x]_\omega} = K_{D(HO_x)} \tag{64}$$

Equation (64) shows that, in a given organic solvent, $K_{D(HO_x)}$ will be a constant at neutral aqueous solutions. The $K_{D(HO_x)}$ value between isopentyl alcohol and aqueous phase was reported as 62.2 ± 0.03 by Mottola and Freiser (21). However, the $K_{D(HO_x)}$ values (Table III) obtained from the slope of Dyrssen's equation show that only the values for $HSeO_3^-$, AsO_2^-, and Cl^- are close to this constant. Others are either too large or too small. This is because Equation (1) proposed by Dyrssen corresponds to a too simplified model.

c. When the modified equation (Eq. (44)) was used, the $K_f[A^-]_\omega$ values were calculated from the slope and the values of $Ka_1 = 1.41 \times 10^{-3}$ and $K_{D(HO_x)} = 62.2$ (21) were used. The $K_f[A^-]_\omega$ values listed in Table

TABLE III

$K_{D(HO_x)}$ VALUES CALCULATED FROM THE SLOPES OF DYRSSEN'S EQUATION IN ISOPENTYL ALCOHOL SYSTEM

Anion	$K_{D(HO_x)} = \frac{Slope}{Ka_1}$	Relative % Error of $K_{D(HO_x)}$
HSO_4^-	203	226
$HSeO_3^-$	70.5	13
$H_2PO_4^-$	412	562
AsO_2^-	71.1	14
Cl^-	71.1	14
I^-	132	112
ClO_4^-	304	388
$C_6H_5COO^-$	40.6	-35
CH_3COO^-	90.1	45

where $Ka_1 = 1.41 \times 10^{-5}$ (21) is used and the relative % error is based on $K_{D(HO_x)} = 62.2$ (21).

II are all smaller than 1 except that for benzoate; these results contradict the assumption ($K_f[A^-]_\omega >> 1$) made. Since $K_f[A^-]$ values obtained from Eq. (44) are smaller than 1, they are used to estimate $K_{D(H_2O_x^+,A^-)}$ values from the intercept of Equation (45). The $K_{D(H_2O_x^+,A^-)}$ values obtained are comparable with those obtained from Dyrssen's equation but are larger. However, the values for HSO_4^- and $H_2PO_4^-$ are really too large.

d. Since the $K_{D(H_2O_x^+,A^-)}$ values obtained have a good qualitative correlation using either Dyrssen's model or a modified model, the ion-pair partition constants fit the model well and the estimate of $K_{D(H_2O_x^+,A^-)}$ from the intercept is applicable. While the $K_{D(HO_x)}$ values obtained from the slope change from one anion to another, this may be because the slope term also depends on the concentration of anions as indicated in Equation (43) or on some more complicated terms besides the $[H^+]$.

B. Partition Constants of 8-Hydroxyquinolinium-Anion Pairs Between 1-Butanol and Aqueous Phases in Low-pH Region

1. Experimental

a. Reagents

1-Butanol, $CH_3CH_2CH_2CH_2OH$, (Baker Analyzed Reagent) was purified by shaking with 0.01 M sodium hydroxide solution and then rinsing with deionized-distilled water as described in Chapter III.A.1.a.

A. R. chemicals of 8-hydroxyquinoline, sodium hydrogen sulfate,

sodium iodide, sulfuric acid, hydrochloric acid, sodium hydroxide, sodium perchlorate, and perchloric acid were used as described in Chapter III.A. 1.a. Besides of these, potassium penicillin G,

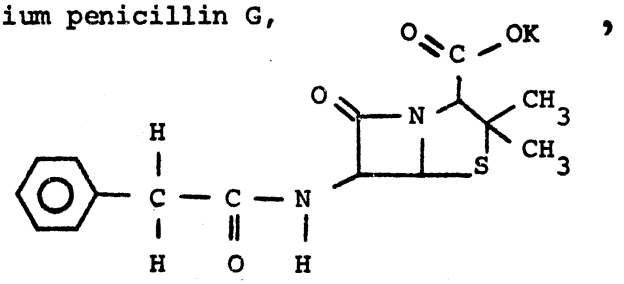

(E. R. Squibb and Sons, Inc., U.S.P.) and p-toluenesulfonic acid,

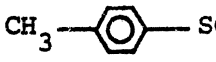

(Baker Analyzed Reagent) were used without further purification. All aqueous solutions were prepared using deionized-distilled water.

b. Apparatus

Same as described in Chapter III.A.1.b.

c. Procedure

The calibration curve of 8-hydroxyquinolinium ion in 0.10 M HCl at 360 nm was used. The procedure for the distribution studies was the same as that described in Chapter III.A.1.c. except that 1-butanol was used instead of isopentyl alcohol. Ionic strengths of aqueous phases were adjusted to 0.1 M with addition of salts (for example, $NaHSO_4$, Na_2SO_4, NaCl, NaI, or $NaClO_4$) and the pH was adjusted to 1-2 with H_2SO_4.

2. Theory and Formula Used

Same as described in Chapter III.A.2.

3. Results

a. A molar absorptivity of 1.70×10^3 $\underline{M}^{-1}$ cm^{-1} for 8-hydroxyquinolinium ion at 360 nm was used as described in Chapter III.A.3.a.

b. By using Dyrssen's equation, plots of D versus $\frac{1}{[H^+]}$ for several inorganic (HSO_4^-, Cl^-, I^-, and ClO_4^-) and organic (penicillinate and p-toluenesulfonate) anions are shown in Figures 17-22, respectively. Slopes, $Ka_1 \cdot K_{D(HO_x)}$, and partition constants for 8-hydroxyquinolinium-anion pairs, $K_{D(H_2O_x^+,A^-)}$, between 1-butanol and aqueous phase are tabulated in Table IV. The $K_{D(H_2O_x^+,A^-)}$ values calculated from the modified equations (44, 45) are also listed in Table IV using the values of $Ka_1 = 1.41 \times 10^{-5}$ and $K_{D(HO_x)} = 45.4$ (21).

4. Discussion

a. The partition constants, $K_{D(H_2O_x^+,A^-)}$, obtained from Dyrssen's model are explained as follows:

The $K_{D(H_2O_x^+,A^-)}$ value for penicillinate is as small as that of bisulfate. It is considered that the side reaction of protolysis (Eq. (24)) may occur and lower the $K_{D(H_2O_x^+,A^-)}$ value. Table IV also indicates that C_{A^-} for penicillinate used is about 1.5 times as large as that of C_{HO_x} instead of about 30 times for other anions studied. In fact, the benzylpenicillinate is unstable in an acidic solution (52). This may be the reason why the $K_{D(H_2O_x^+,A^-)}$ value for penicillinate is low in the pH region of 1-2.

The $K_{D(H_2O_x^+,A^-)}$ value increases in the orfer of $HSO_4^- < Cl^- < I^- < ClO_4^-$ < p-toluenesulfonate. This is because HSO_4^- contains the hydroxyl

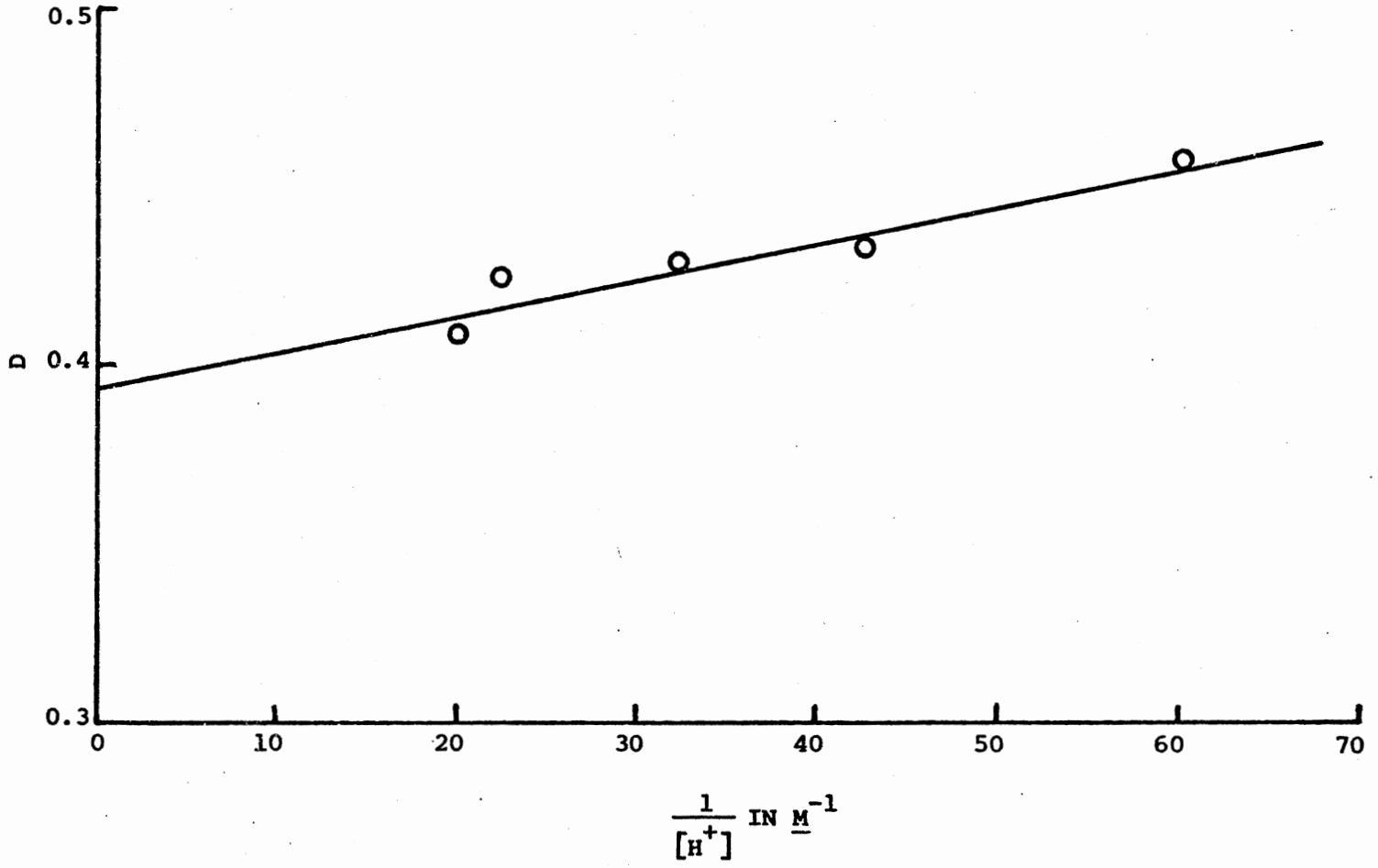

Figure 17. Plot to Determine $K_{D(H_2O_x^+, HSO_4^-)}$ in 1-Butanol System

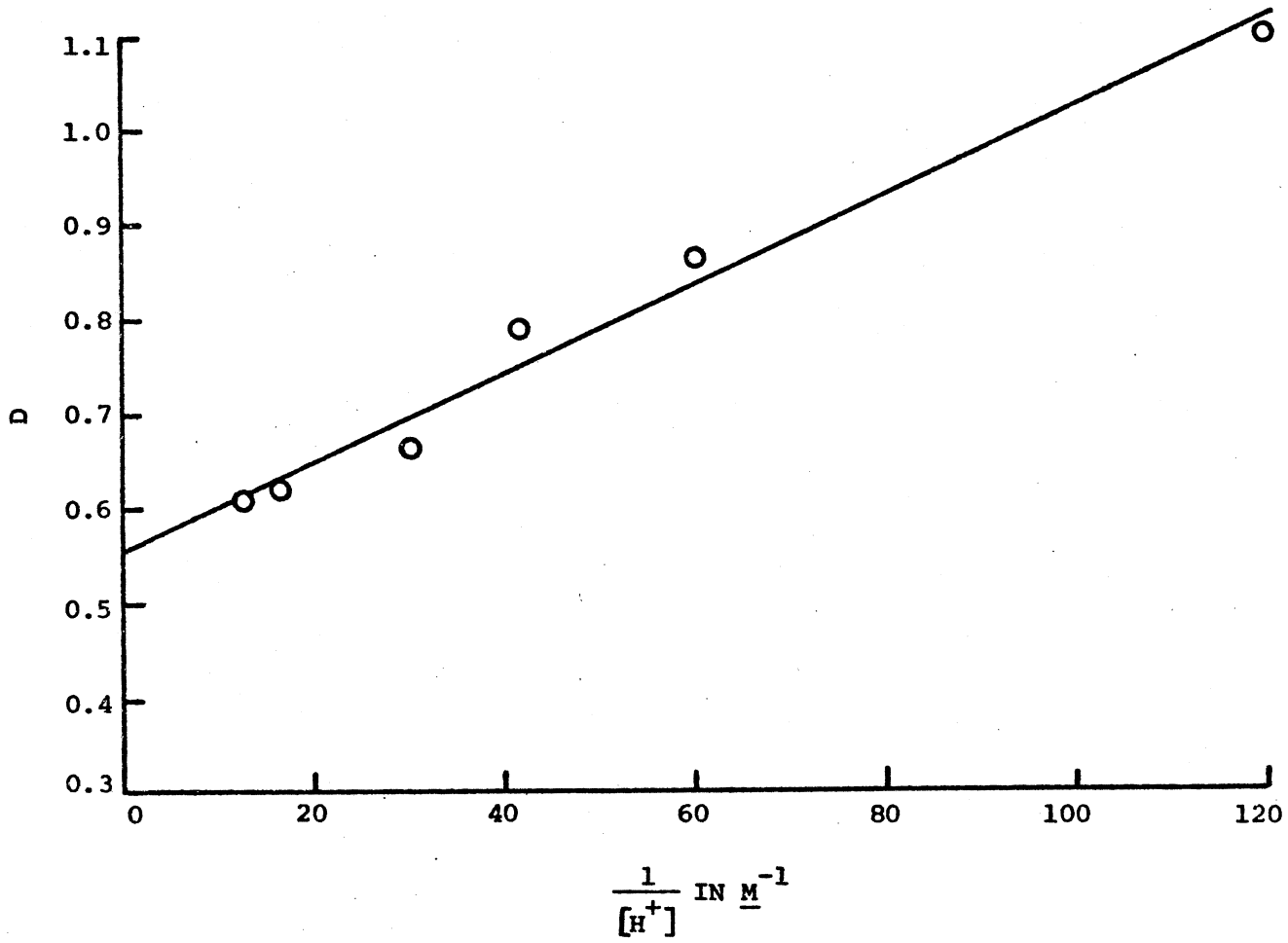

Figure 18. Plot to Determine $K_{D(H_2O_x^+,Cl^-)}$ in 1-Butanol System

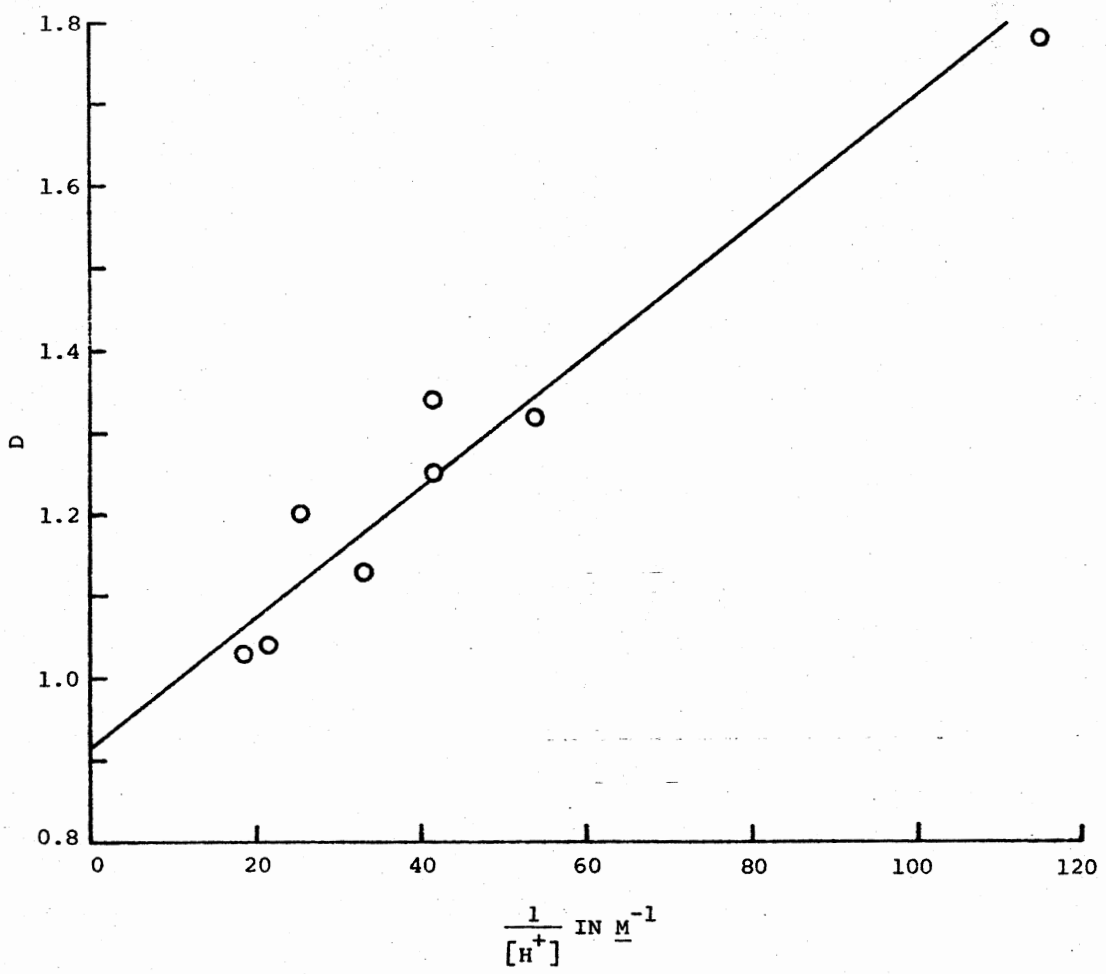

Figure 19. Plot to Determine $K_{D(H_2O_x^+, I^-)}$ in 1-Butanol System

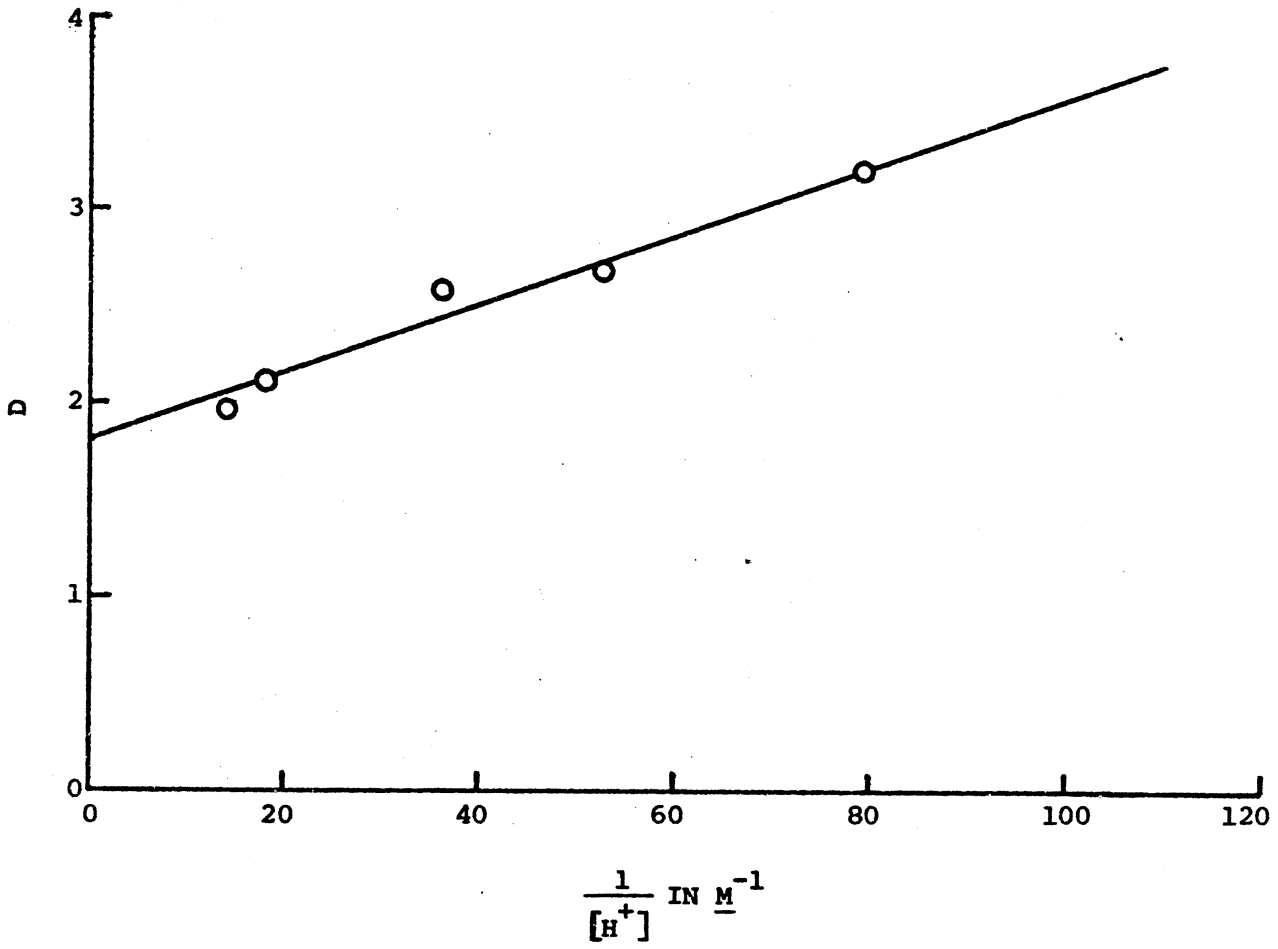

Figure 20. Plot to Determine $K_{D(H_2O_x^+, ClO_4^-)}$ in 1-Butanol System

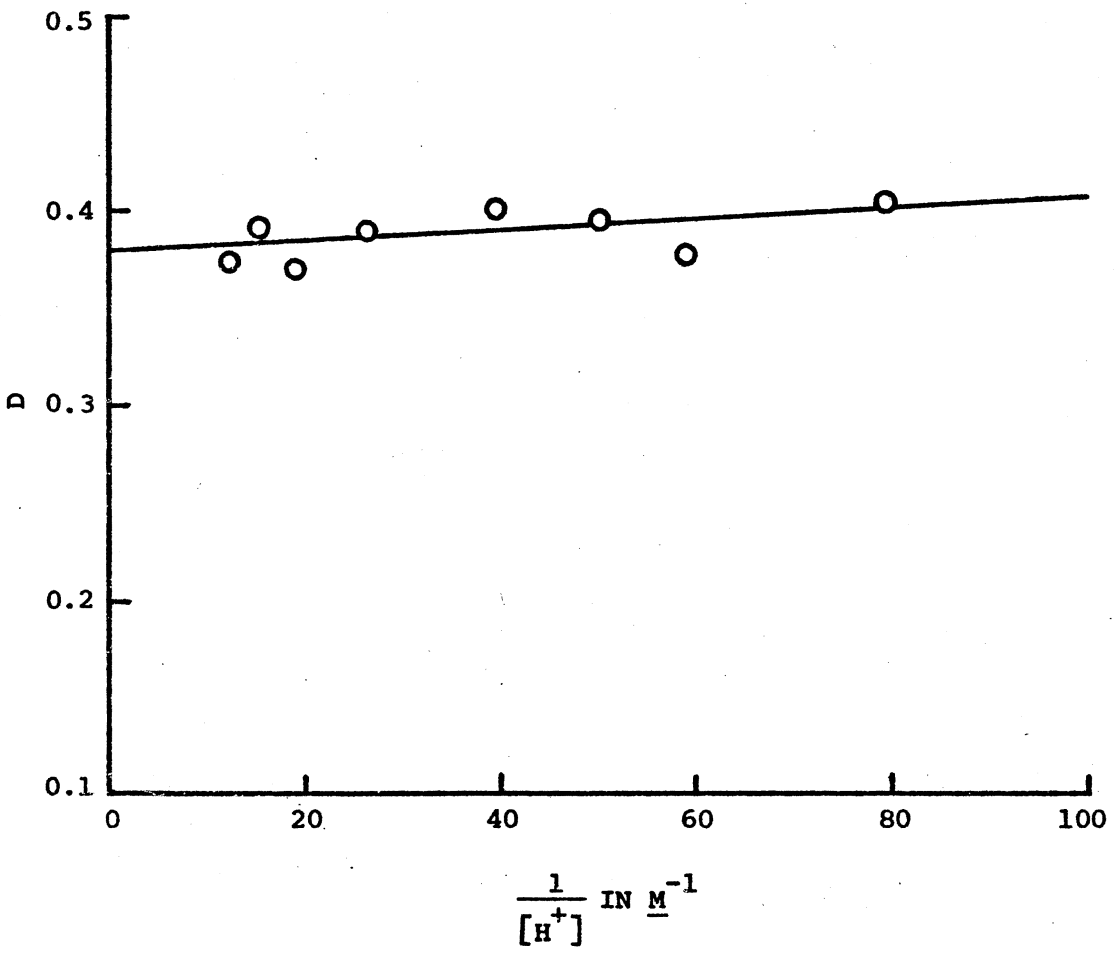

Figure 21. Plot to Determine $K_{D(H_2O_x^+,\text{penicillinate})}$ in 1-Butanol System

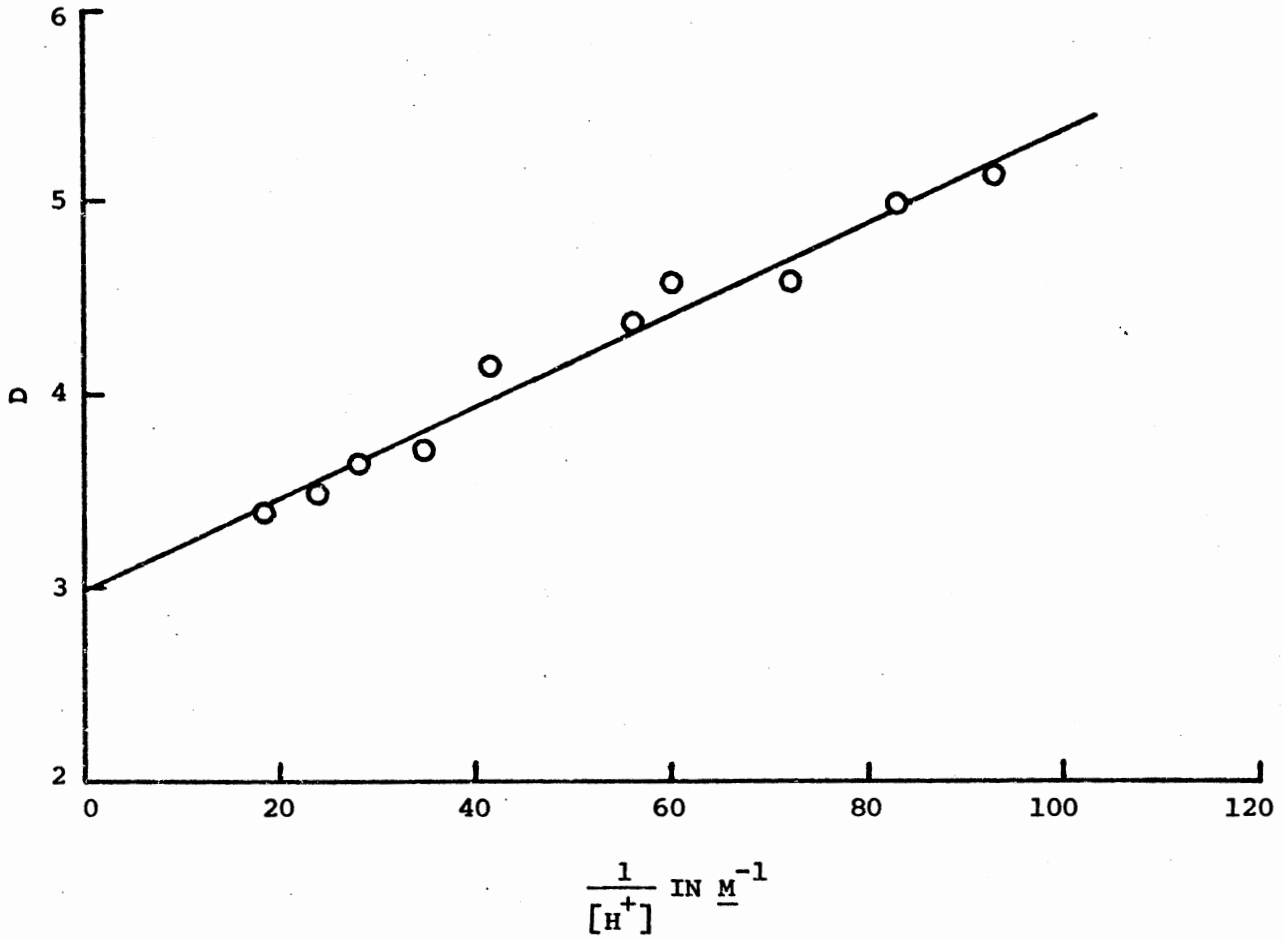

Figure 22. Plot to Determine $K_{D(H_2O_x^+, \underline{p}\text{-toluenesulfonate})}$ in 1-Butanol System

TABLE IV

SUMMARY OF $K_{D(H_2O_x^+,A^-)}$ AND SLOPE OF $Ka_1 \cdot K_{D(HO_x)}$ IN 1-BUTANOL SYSTEM USING DYRSSEN'S EQUATION; $K_f[A^-]_\omega$ AND $K_{D(H_2O_x^+,A^-)}$ FROM MODIFIED EQUATIONS: AND SOME PROPERTIES OF ANIONS

Anion	(Ka)[a] for HA	C_{A^-} X 10^3 (M)	C_{HO_x} X 10^3 (M)	Dyrssen's Equation		Modified Equation		Crystal Radii (Å) (50)	Hydrated Radii (Å) (50)
				Intercept $K_{D(H_2O_x^+,A^-)}$	Slope $Ka_1 \cdot K_{D(HO_x)}$ (X 10^3)	Eq. (44)[b] $K_f[A^-]_\omega$	Eq. (45)[c] $K_{D(H_2O_x^+,A^-)}$		
HSO_4^-	100	74	1.51	0.39	1.02	0.628	0.57		
Cl^-	100	100	1.50	0.55	4.69	0.136	4.04	1.81	2.55
I^-	100	50.8	1.50	0.92	7.95	0.0805	11.4	2.16	
ClO_4^-	100	100	1.50	1.80	17.8	0.0360	50.	2.36	2.43
Penicillinate	1.74×10^{-3}	2.76	1.50	0.38	0.434	1.47	0.26		
p-toluene-sulfonate	100	100	1.51	3.0	23.7	0.0270	111.	6.8[d]	

a. Ka is estimated as 100 for strong acids; the other is from Reference (52).

b. $K_f[A^-]_\omega = Ka_1 \cdot K_{D(HO_x)}$/slope of Dyrssen's Eq.; where $Ka_1 = 1.41 \times 10^{-5}$ and $K_{D(HO_x)} = 45.4$ (21) were used.

c. $K_{D(H_2O_x^+,A^-)}$ = Intercept of Equation (45)/the value of $K_f[A^-]_\omega$.

d. Estimated from the molecular model (Godfrey Molecular Models).

(-OH) group, which is more hydrophilic than other anions used. Since the crystal radius increases in the order of Cl^- < I^- < ClO_4^- < p-toluenesulfonate and the hydrophobicity also increases in this order, the hydration of the anion in the aqueous phase decreases in the order of Cl^- > I^- > ClO_4^- > p-toluenesulfonate. Moreover, the p-toluenesulfonate is a highly polar species (53) which is largely extracted into a polar organic solvent after forming the ($H_2O_x^+$, p-toluenesulfonate) ion-pair. A plot of $K_{D(H_2O_x^+,A^-)}$ versus crystal radius is shown in Figure 23.

b. A comparison of the polarity of organic solvents as mentioned in Chapter II.A.b. for the same ion-pair extraction shows that the $K_{D(H_2O_x^+,A^-)}$ values for HSO_4^-, Cl^-, I^-, or ClO_4^- in 1-butanol are about twice as large as those in isopentyl alcohol. This is because 1-butanol has a larger solubility parameter (or polarity) than that of isopentyl alcohol due to both larger polar interaction (δ_p) and greater hydrogen bonding (δ_h) as described in Equation (13) and shown in Table V. The mutual hydrogen bonding between 1-butanol and an ion pair of ($H_2O_x^+$,A^-) occurs as depicted in Figure 24.

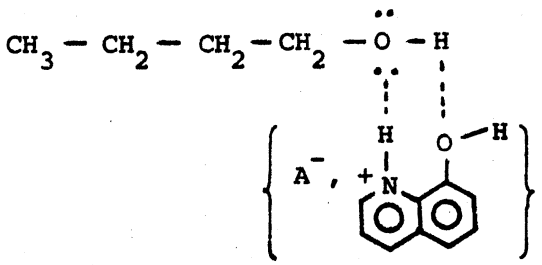

Figure 24. Hydrogen Bonding Between 1-Butanol and an ($H_2O_x^+$,A^-) Ion Pair

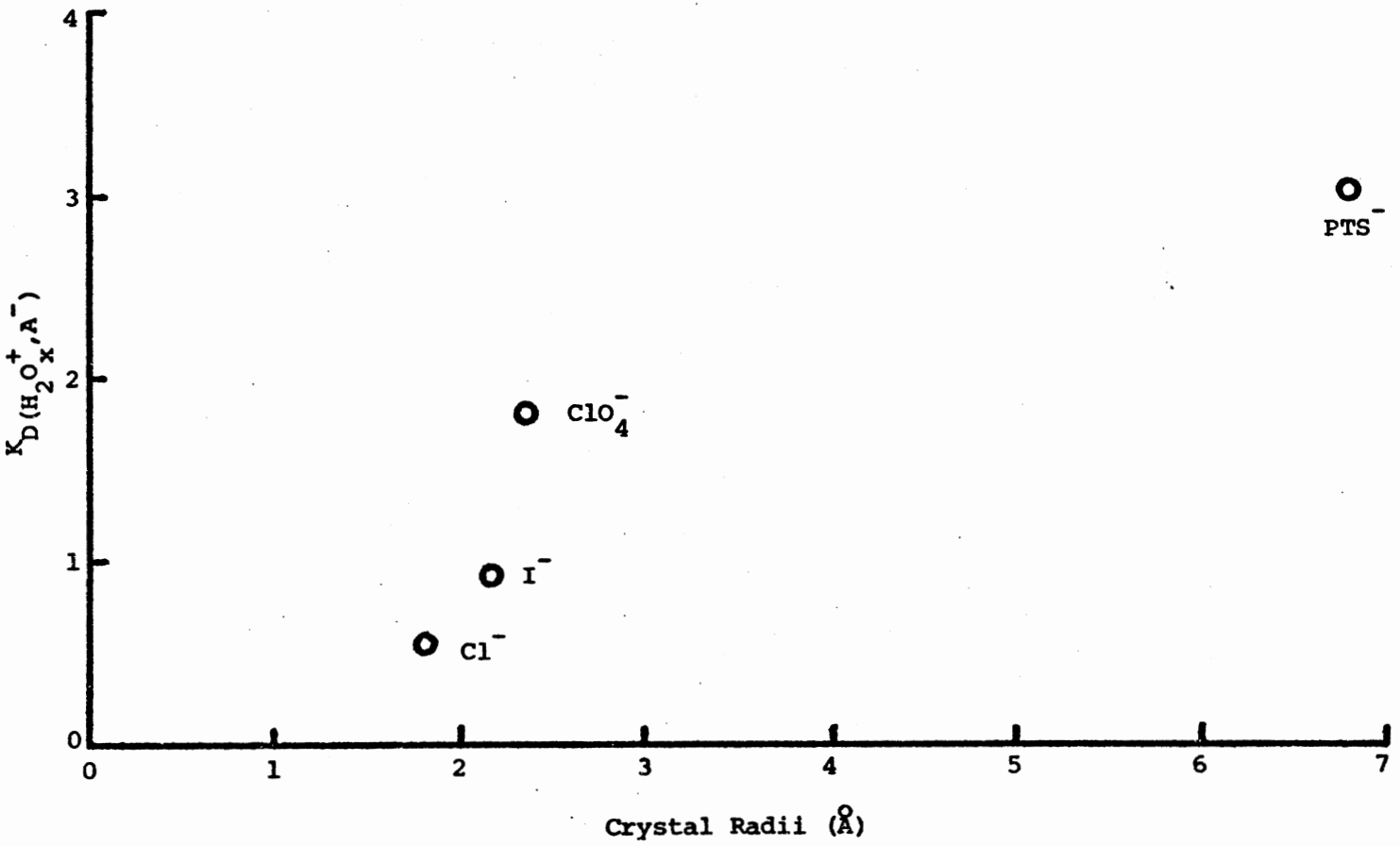

Figure 23. $K_{D(H_2O_x^+,A^-)}$ Versus Crystal Radii of Anion in 1-Butanol System

TABLE V

SOLUBILITY PARAMETERS OF ISOPENTYL ALCOHOL AND 1-BUTANOL

Organic Solvent	Isopentyl Alcohol	1-Butanol
Solubility Parameter $\delta\,(\frac{cal}{ml})^{\frac{1}{2}}$	10.9[a]	11.4[a,b]
δ_d	7.8[c]	7.8[b]
δ_p	2.2[c]	2.8[b]
δ_h	6.8[c]	7.7[b]

a. From Reference (21).

b. From Reference (54).

c. Estimated from 1-pentanol in Reference (54).

c. As before, the slopes obtained from Dyrssen's equation are $Ka_1 \cdot K_{D(HO_x)}$. Since Ka_1 is known, the partition constant of 8-hydroxyquinoline, $K_{D(HO_x)}$, between 1-butanol and aqueous phase is calculated; values are listed in Table VI. The $K_{D(HO_x)}$ value was reported as 45.4 (21) in 1-butanol. However, the values of $K_{D(HO_x)}$ in Table VI calculated from the Dyrssen's equation show that all are larger than this constant except that for penicillinate, which is lower. Again, this occurs because Equation (1) proposed by Dyrssen is too simplified.

d. When the modified equation (Eq. (44)) was used, the $K_f[A^-]_\omega$ values were calculated from the slope and the values of $Ka_1 = 1.41 \times 10^{-5}$ and $K_{D(HO_x)} = 45.4$ (21) were used. The $K_f[A^-]_\omega$ values tabulated in Table IV are smaller than 1 except that for penicillinate; these results contradict the assumption ($K_f[A^-]_\omega >> 1$) made. Again, the $K_f[A^-]_\omega$ values obtained were used to estimate the $K_{D(H_2O_x^+,A^-)}$ values from the intercept of Equation (45). The $K_{D(H_2O_x^+,A^-)}$ values obtained are comparable with those obtained from Dyrssen's equation but are larger. Again, it is concluded that both Dyrssen's model and the modified model are good for estimating $K_{D(H_2O_x^+,A^-)}$ values. However, the slope term must contain some more complicated terms besides the $[H^+]$.

TABLE VI

$K_{D(HO_x)}$ VALUES CALCULATED FROM THE SLOPES OF DYRSSEN'S EQUATION IN 1-BUTANOL SYSTEM

Anion	$K_{D(HO_x)} = \frac{Slope}{Ka_1}$	Relative % Error of $K_{D(HO_x)}$
HSO_4^-	72.3	59.3
Cl^-	332	631
I^-	563	1140
ClO_4^-	1260	2675
penicillinate	30.7	-32.4
p-toluenesulfonate	1677	3594

where $Ka_1 = 1.41 \times 10^{-5}$ (21) is used and the relative % error is based on $K_{D(HO_x)} = 45.4$ (21).

CHAPTER IV

LIQUID-SOLID DISTRIBUTION STUDIES OF 8-HYDROXY-QUINOLINIUM-ANION PAIR SYSTEMS

Controlled-pore glass is manufactured specifically as a support material for use in liquid chromatography (35) because it is made from borosilicate base material which possesses a high mechanical strength; it is suitable for high-pressure operation. Moreover, controlled-pore glass offers several additional advantages: it is convenient to handle; it is thermally stable; and it does not swell with changing environments. Hence, 8-hydroxyquinoline immobilized (chemically bonded) on controlled-pore glass (CPG-$8HO_x$) was chosen for study. Results of these studies are reported in this chapter.

Distribution studies using CPG-$8HO_x$ resin, manufactured by Corning Chemical Company, were performed as batch experiments. p-Toluenesulfonate ion was selected as counterion since it showed the largest $K_{D(H_2O_x^+,A^-)}$ among anions studied in liquid-liquid systems. Chloride ion was also used as a counterion and the results were compared with those for p-toluenesulfonate ion. Distribution studies with CPG-$8HO_x$ paralleled the observations in liquid-liquid systems. The studies were extended to include several other sulfonates, such as, aromatic sulfonates (benzenesulfonate, 2-mesitylenesulfonate, and 1-naphthalenesulfonate) and aliphatic sulfonates (methanesulfonate and ethanesulfonate). Part C of this chapter was concentrated on the distribution studies of

aliphatic and aromatic sulfonates using CPG-8HO$_x$ resin in batch experiments. The experiments were designed with the idea of collecting information useful for the application of CPG-8HO$_x$ as a chromatographic support for the separation of industrially relevant sulfonates.

Since the Corning Chemical Company discontinued the manufacture of CPG-8HO$_x$ resin in April 1978, synthesis of this resin was performed in our laboratory, and is described in Part D of this chapter. Starting material was aminopropyl controlled-pore glass. Some characteristics (such as capacity for 8-hydroxyquinoline binding and pKa_1 of 8-hydroxyquinolinium ion from CPG-8HO$_x$ resin) were also determined and are reported in Part D. Distribution studies for aromatic and aliphatic sulfonates using the synthesized CPG-8HO$_x$ resin were also carried out and are summarized in Part E. The results of distribution coefficients using the synthesized CPG-8HO$_x$ and Corning CPG-8HO$_x$ are also compared in this chapter.

A. Distribution Studies Using Immobilized 8-Hydroxyquinoline on Controlled-Pore Glass (CPG-8HO$_x$) Manufactured by Corning Chemical Company: p-Toluenesulfonate Ion as Counterion

1. Experimental

a. Reagents

The Corning CPG-8HO$_x$ resin, 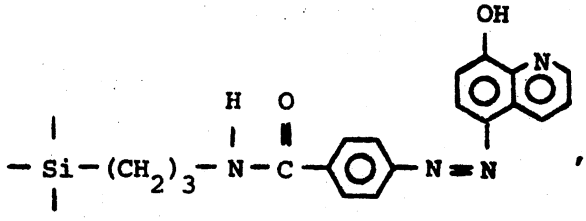

,

was purchased from the Pierce Chemical Company. The resin has particle diamater of 177 - 840 microns, an average pore size of 550 Å, a surface area of 70 m^2/g, and a reported capacity of 0.03 mmoles of bonded 8-hydroxyquinoline per gram of resin. The Corning CPG plain glass beads (-Si-) were also purchased from the Pierce Chemical Company. The plain glass beads have the same pore size and surface area as that of Corning CPG-$8HO_x$ resin, but a smaller particle diameter (37 - 74 microns).

p-Toluenesulfonic acid, sodium hydroxide, sodium chloride, and hydrochloric acid were described previously and used without further purification. Deionized-distilled water was used to prepare all aqueous solutions.

b. Apparatus

A Beckman Zeromatic pH meter and a Sargent miniature combination electrode (S-300700-10) were used for all pH measurements. The Spectrophotometer and the quartz cells, described in Chapter III.A.1.b., were used for absorbance measurements in the UV region. A modified shaker (Figure 3), described previously, was used for shaking the CPG-$8HO_x$ resin and aqueous solutions to reach equilibrium.

c. Procedure

A small amount (~0.600 g) of CPG-$8HO_x$ resin was weighed in a 20-ml beaker and transferred to a 35-ml vial by using deionized-distilled water. The resin was washed four more times with deionized-distilled water and then the water in the vial was removed as much as possible by inclining the vial and absorbing the water with "kimwipes".

Solutions containing p-toluenesulfonate ion in the range of (0.50 - 5.00) x 10^{-3} M were prepared in 50-ml volumetric flasks. Ionic strengths (0.025 - 0.775 M) were adjusted with NaCl solution and their pH (1.1 - 8.0) were adjusted with 0.10 M HCl or 0.10 M NaOH solutions. A volume (3.00 ml) of known concentration of p-toluenesulfonate solution was pipetted into each vial, which was stoppered with a plastic cap. The mixture was shaken in the shaker (31 strokes/min) for 30 minutes at room temperature (~25 ^{o}C). Beyond 20 minutes of shaking, no significant difference in the values of distribution ratio was observed. After equilibrium the mixture was allowed to stand in a thermostated bath (25.0 ± 0.2 ^{o}C) for another 30 minutes. Then a suitable aliquot (~1.0 ml) was transferred to a 5-ml beaker which was thermostated at 25.0 ± 0.2 ^{o}C. This was used for pH measurement; the reading taken as the equilibrium pH value. The p-toluenesulfonate solution remaining in the aqueous phase after equilibration was diluted and used for spectrophotometric measurements. Since p-toluenesulfonate solutions show maximum absorbance around 259 nm, the absorbance was measured at this wavelength and against deionized-distilled water as blank. A calibration curve was made by measuring absorbance with a series of known p-toluenesulfonate concentrations. From interpolation into the calibration curve, the concentration and then the amount of p-toluenesulfonate remaining in the solution were calculated. The resin was reused after washing with deionized-distilled water (100 ml/0.6 g resin) and drying at ~130 ^{o}C in an oven for 1 hour.

One set of experiments to ascertain the effect of pH on the molar distribution coefficient at constant ionic strength (0.10 M) and p-toluenesulfonate concentration (5.00 x 10^{-3} M) were run using Corning

plain CPG glass beads in order to compare the results with those obtained Corning CPG-8HO$_x$ resin.

2. Formula Used

The mass balance equation for p-toluenesulfonate (PTS^-) ion can be expressed as in Equation (65).

$$\begin{pmatrix}\text{total amount of}\\ PTS^- \text{ added}\end{pmatrix} = \begin{pmatrix}\text{amount of } PTS^-\\ \text{on the resin}\end{pmatrix} + \begin{pmatrix}\text{amount of } PTS^-\\ \text{remaining in solution}\end{pmatrix} \quad (65)$$

Since the total amount of PTS^- added is known and the amount of PTS^- remaining in solution can be calculated, the amount of PTS^- on the resin can be obtained from Equation (65).

The molar distribution coefficient, K_d, is then calculated from the definition (48) as:

$$K_d = \frac{\text{Millimoles of Anion on the Resin Per Gram of Resin}}{\text{Millimoles of Anion Remaining in Solution Per ml of Solution}} \quad (66)$$

where the anion is the species studied.

3. Results

a. Calibration Curve for p-Toluenesulfonate Ion Estimation

A plot of absorbance versus p-toluenesulfonate concentration is shown in Figure 25.

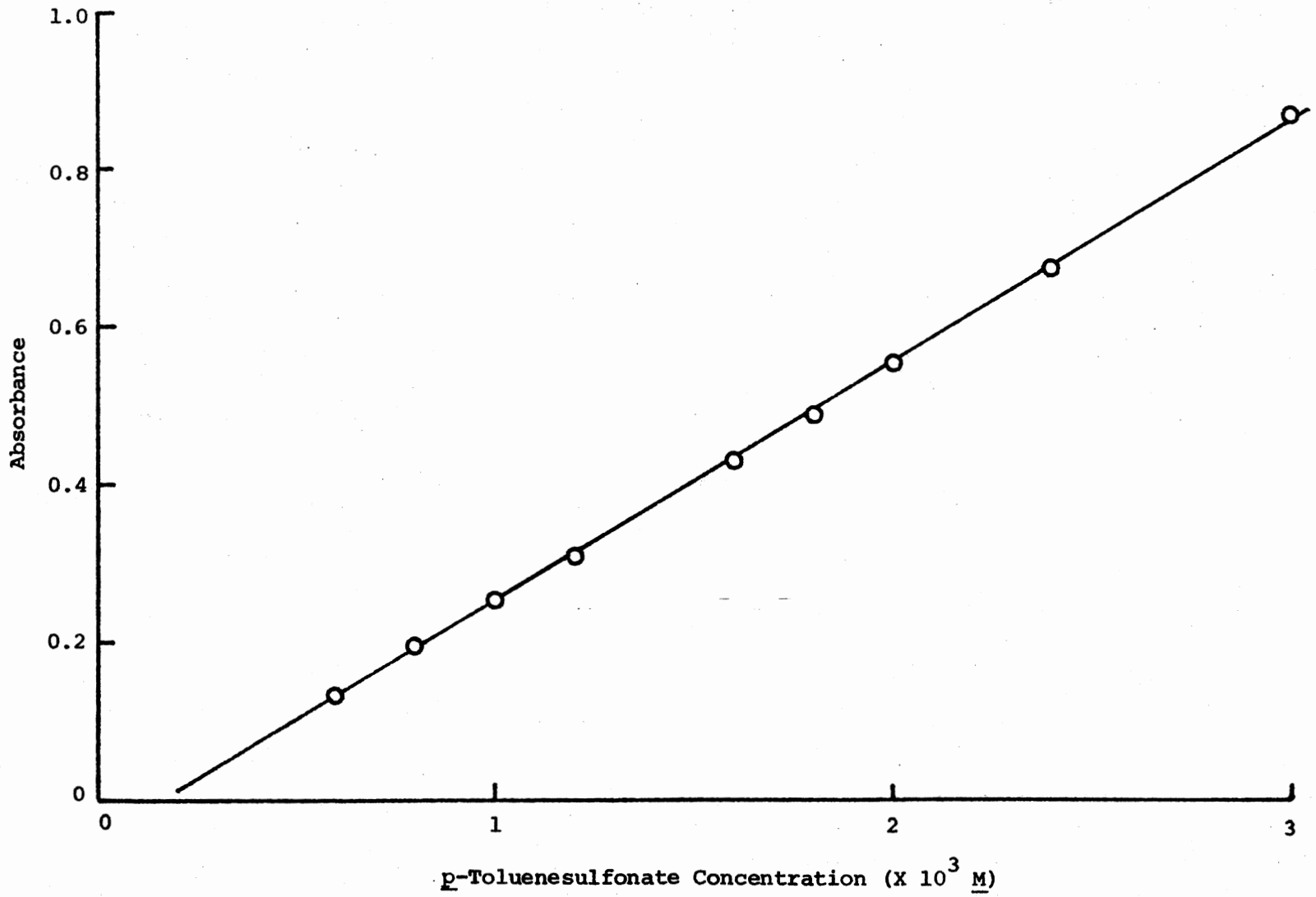

Figure 25. Calibration Curve for p-Toluenesulfonate Ion at 259 nm

b. Effect of pH on K_d at Constant Ionic Strength (0.10 M) and p-Toluenesulfonate Concentration (5.00×10^{-3} M)

A plot of K_d versus pH for both CPG-8HO$_x$ resin and CPG plain glass beads is shown in Figure 26.

c. Effect of p-Toluenesulfonate Concentration on K_d at Constant Ionic Strength (0.10 M) and pH (1.5)

A plot of K_d versus PTS^- concentration is shown in Figure 27.

d. Effect of Ionic Strength on K_d at Constant p-Toluenesulfonate Concentration (5.00×10^{-3} M) and pH (1.8)

A plot of K_d versus ionic strength is shown in Figure 28.

4. Discussion

When Corning CPG-8HO$_x$ resin is used, the results obtained in Figures 26 and 27 show that K_d values increase with increasing concentrations of hydronium ion and p-toluenesulfonate ion at a constant ionic strength. It may be concluded that the (CPG-8H$_2$O$_x^+$, PTS^-) complex is formed and favored in the low-pH region as expressed in Equation (66) or (67).

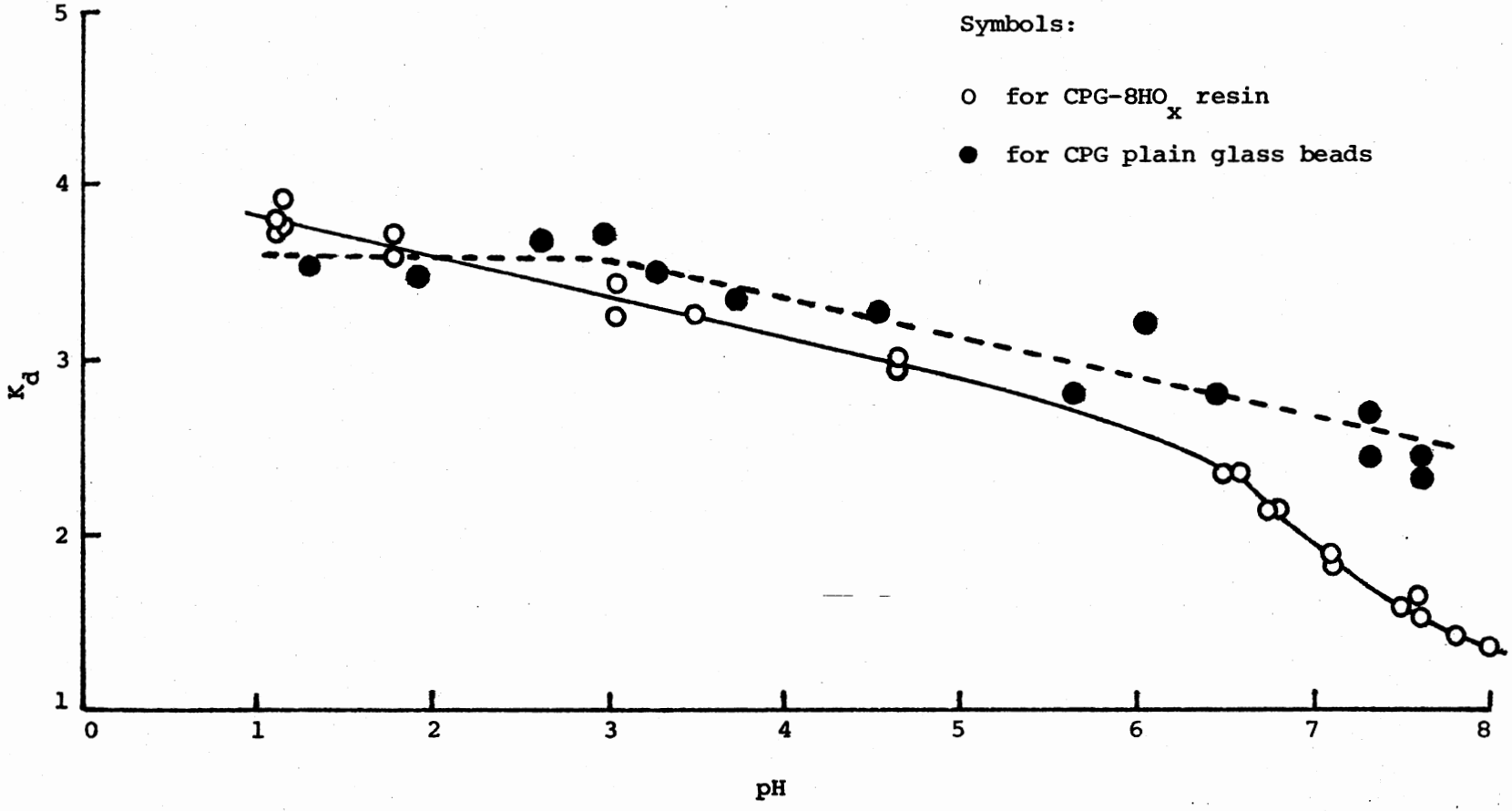

Figure 26. Effect of pH on K_d at Constant Ionic Strength (0.10 M) and p-Toluenesulfonate Concentration (5.00×10^{-3} M)

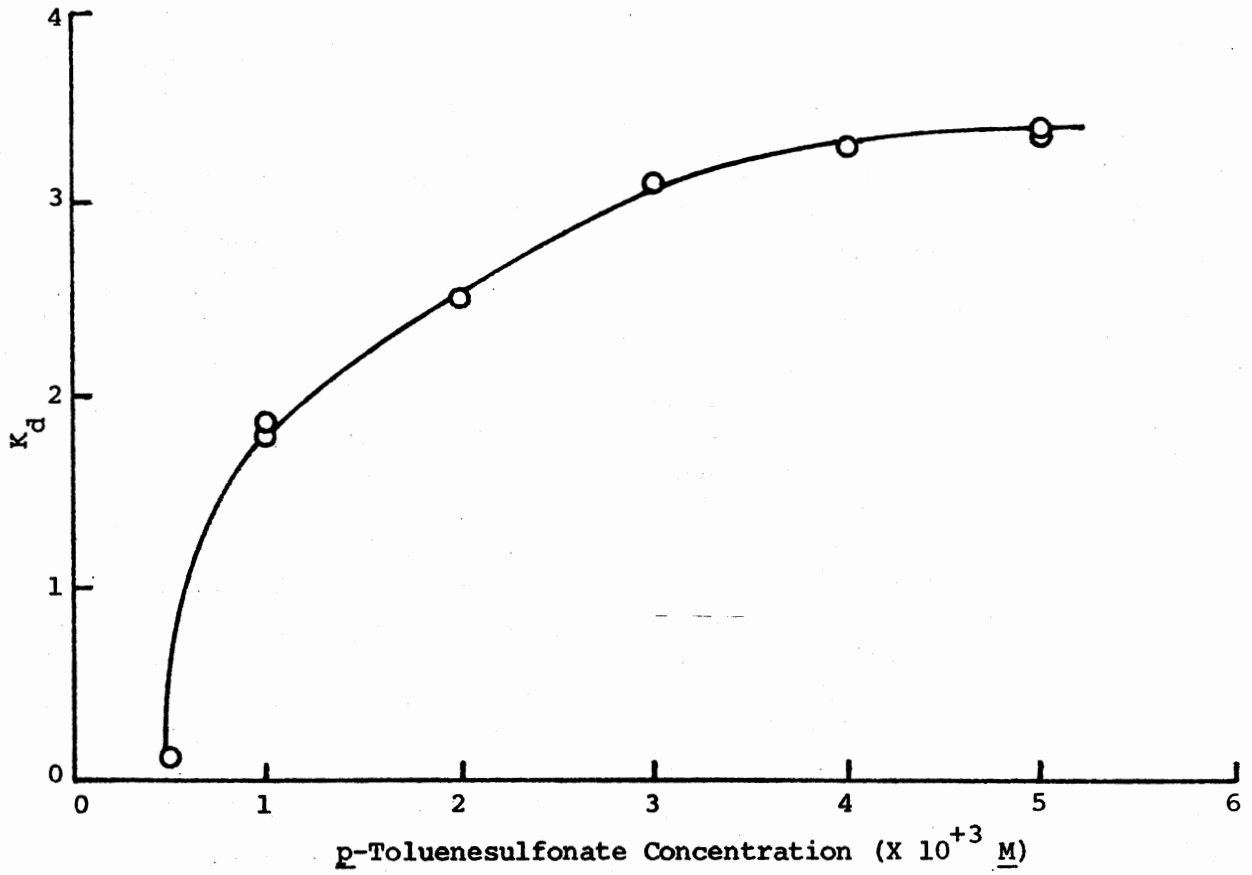

Figure 27. Effect of PTS^- Concentration on K_d at Constant Ionic Strength (0.10 M) and pH (1.5)

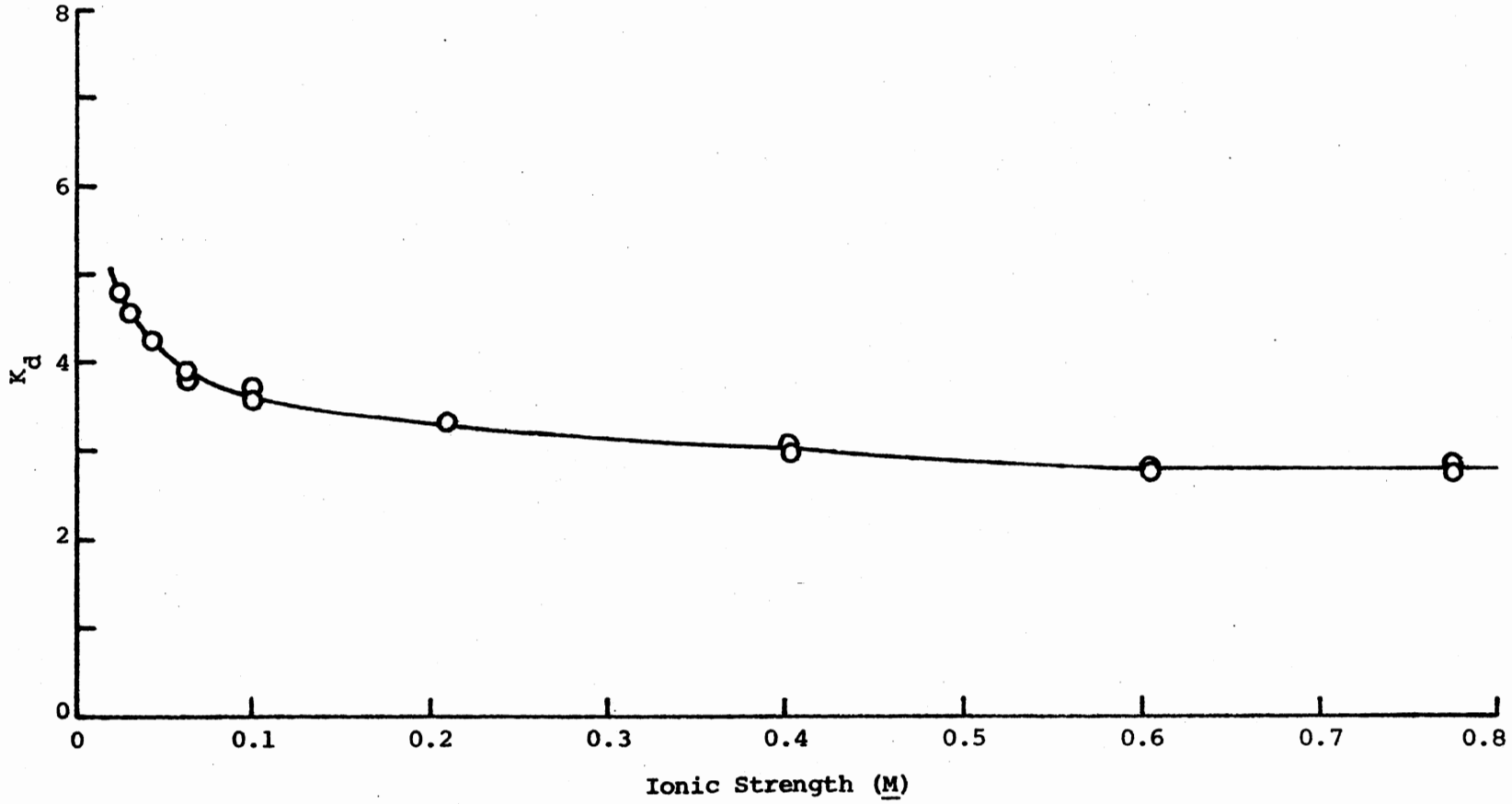

Figure 28. Effect of Ionic Strength on K_d at Constant PTS^- Concentration (5.00×10^{-3} M) and pH (1.8)

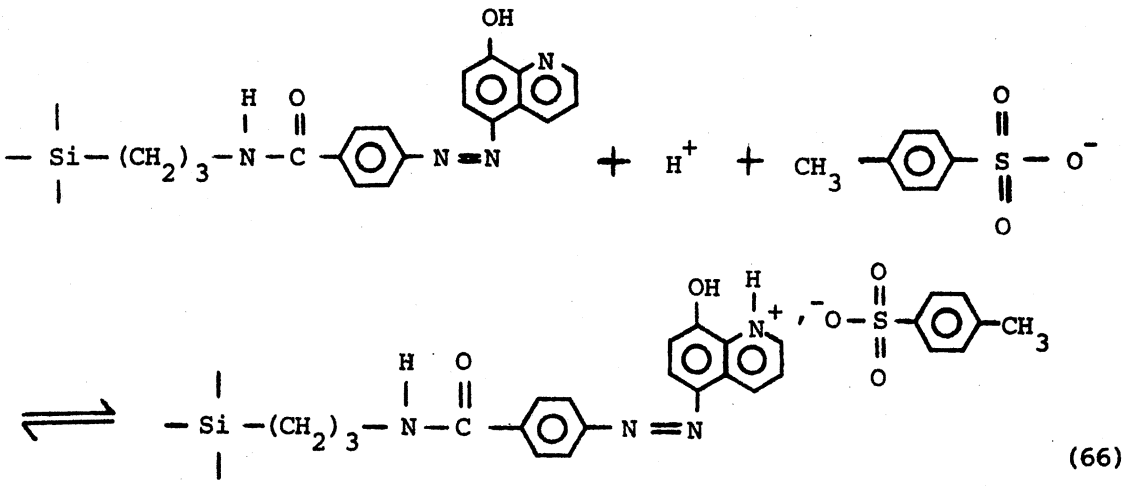

(66)

or,

$$(\text{CPG} - 8\text{HO}_x)_{\text{resin}} + \text{H}^+ + \text{PTS}^- \rightleftharpoons (\text{CPG} - 8\text{H}_2\text{O}_x^+, \text{PTS}^-) \qquad (67)$$

b. The K_d values obtained in Figure 26 using Corning CPG-$8HO_x$ resin and Corning CPG plain glass beads indicate that there is a competition between the (CPG-$8H_2O_x^+$, PTS^-) ion-pair association on the CPG-$8HO_x$ resin and the static attraction (or adsorption) of PTS^- on the plain CPG glass beads.

c. Figure 28 shows that K_d value decreases when the ionic strength increases. The K_d value also decreases rapidly when the ionic strength is smaller than 0.1 M and becomes constant when ionic strength is greater than 0.6 M. This may be due to competition of chloride ion to form the (CPG-$8H_2O_x^+$,A^-) as expressed in Equations (68) and (67).

$$(\text{CPG-}8\text{HO}_x)_{\text{resin}} + \text{H}^+ + \text{Cl}^- \rightleftharpoons (\text{CPG-}8\text{H}_2\text{O}_x^+, \text{Cl}^-) \qquad (68)$$

The K_d value becomes constant at 2.8. This may be because the available sites on the CPG-$8HO_x$ resin are saturated with chloride ion at ionic strength of 0.60 M.

B. Distribution Studies Using the Corning CPG-8HO$_x$ Resin : Chloride Ion as Counter Ion

Chloride ion was selected because of the following:

1. Sodium chloride is a neutral salt and it is easier to use for adjusting the ionic strength of aqueous solutions to a constant value (0.10 M) than sodium bisulfate.

2. The partition constant for ($H_2O_x^+$,Cl^-) is relatively small compared with that for ($H_2O_x^+$,PTS^-) as shown by liquid-liquid distribution studies in Chapter III. If the same trend is followed, the molar distribution coefficient for PTS^- should not be much lowered by competition with Cl^-.

3. Chloride concentrations can be easily measured using an ion-selective membrane electrode.

4. Hydrochloric acid is easy to handle and is a relatively cheap acid.

1. Experimental

a. Reagents

The Corning CPG-8HO$_x$ resin and the A. R. reagents sodium hydroxide and hydrochloric acid were described in Chapter IV.A.1.a. The following reagents of A. R. grade were used without further purification.

- Nitric acid, HNO_3, Mallinckrodt, Inc.
- Sodium Nitrate, $NaNO_3$, Fisher Scientific Company.
- Silver Nitrate, $AgNO_3$, Goldsmith Bros. Division.

Deionized-distilled water was used to prepare all aqueous solutions.

b. Apparatus

A Beckman Zeromatic pH meter and a Sargent miniature combination electrode as described in Chapter IV.A.1.b, were used for all pH measurements. An Orion Model 801A digital pH/MV meter which can be read to ± 0.1 MV, a Ag^{+}/S^{2-} ion-selective membrane electrode (Orion Model 94-16A), and a sleeve-type double-junction reference electrode (with Orion 90-00-02 as the inner filling solution and Orion 90-00-03, 10% KNO_3, as the outer filling solution) were used for the measurements of free silver ion concentration in the solution.

c. Procedure

A stock solution of 1.00×10^{-2} M $AgNO_3$ was prepared and stored in a brown-color glass bottle. A solution of 5.00×10^{-4} M $AgNO_3$ was freshly prepared by dilutions from stock solution. Ionic strengths of diluted silver nitrate solutions were adjusted to 0.10 M with 0.5 M $NaNO_3$. Beakers and flasks containing silver nitrate solution were covered with aluminum foil to minimize the light effect on silver ion during measurements.

A calibration curve for chloride at room temperature (24.2 °C) was made by relating the change of millivolts corresponding to free silver ion before and after adding a known amount of chloride solution (3.00 ml of 0.00 - 8.00×10^{-3} M) to a known excess amount of silver ion solution (50.0 ml of 5.00×10^{-4} M). Each trial was duplicated. The reported values were the average of these two separate determinations. Several points were located in each experiment at room temperature (~25 °C) and the results were observed to be very close to those of the calibration curve, within an error of 1%.

The procedure used for the determination of distribution of chloride ion using CPG-8HO$_x$ resin was as follows:

A small amount (0.6000 g) of CPG-8HO$_x$ resin was weighed in a 20-ml beaker. After transferring to a 35-ml vial, the resin was washed with deionized-distilled water and the water in the vial was removed as much as possible by inclining the vial and absorbing the water with "Kim-wipes". A series of chloride ion solutions were prepared in 50-ml volumetric flasks. Ionic strengths (0.025 - 0.775 M) were adjusted by the addition of $NaNO_3$ solution (0.10 - 1.0 M) and pH values (1.40 - 7.40) were adjusted by 0.10 M HNO_3 or 0.122 M NaOH solutions. A volume (3.00 ml) of chloride solution was pipetted into a vial, which was closed with a plastic cap. The solution and the resin in the vial were shaken in the shaker for 30 minutes at room temperature (~25 ^{o}C). The mixture was then allowed to stand in the thermostated bath (25.0 ± 0.2 ^{o}C) for another 30 minutes. After that, an aliquot was transferred to a 5-ml beaker and the readings of pH at 25.0 ± 0.2 ^{o}C were taken as the equilibrium pH values. The difference of millivolts corresponding to free silver ion were obtained by adding 3.00 ml of chloride solution (readings were made before addition and after equilibrium) to 50.0 ml of 5.00 x 10^{-4} M Ag^{+} solution in 100-ml beakers. The solution was stirred during the measurement of electrical potential values. The concentrations of chloride ion added and that remaining in solution after equilibrium were obtained from the calibration curve. The resin was reused after treatment as described in Chapter IV.A.1.c.

2. Formula Used

Formulae similar to those in Equations (65) and (53) were used ex-

cept that Cl^- was used instead of PTS^-.

3. Results

a. Calibration Curve for Chloride Ion

The change in millivolts (ΔmV) corresponding to free silver ion before and after adding 3.00 ml of the chloride solution to 50.0 ml of 5.00×10^{-4} M silver nitrate solution is plotted versus chloride concentration in Figure 29.

b. Effect of pH on K_d at Constant Ionic Strength (0.10 M) and Chloride Concentration (5.00×10^{-3} M)

A plot of K_d versus pH is shown in Figure 30.

c. Effect of Chloride Concentration on K_d at Constant Ionic Strength (0.10 M) and pH (3.0)

A plot of K_d versus chloride concentration is shown in Figure 31.

d. Effect of Ionic Strength on K_d at Constant Chloride Concentration (5.00×10^{-3} M) and pH (1.8)

A plot of K_d versus ionic strength is shown in Figure 32.

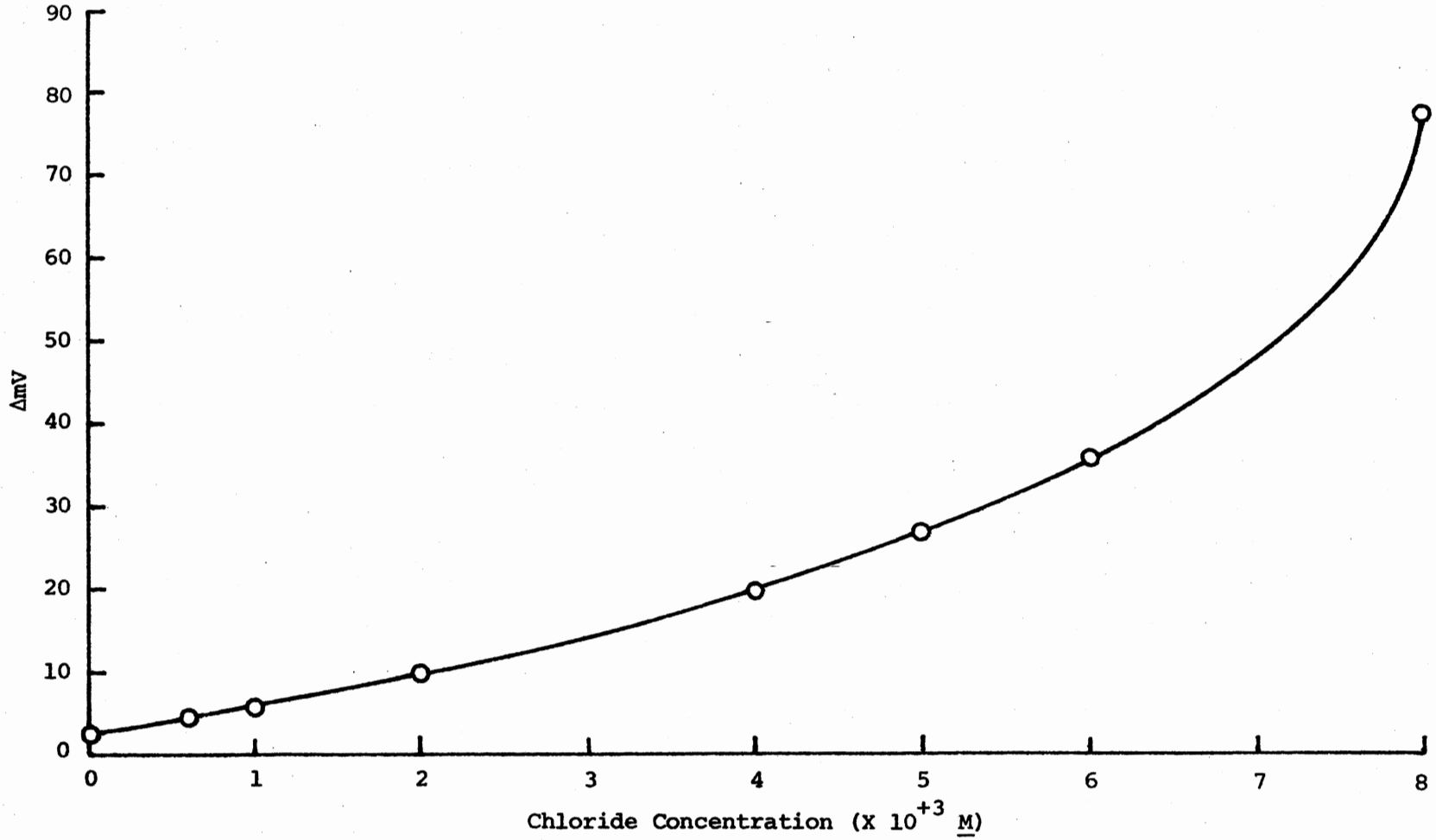

Figure 29. Calibration Curve for Chloride Ion

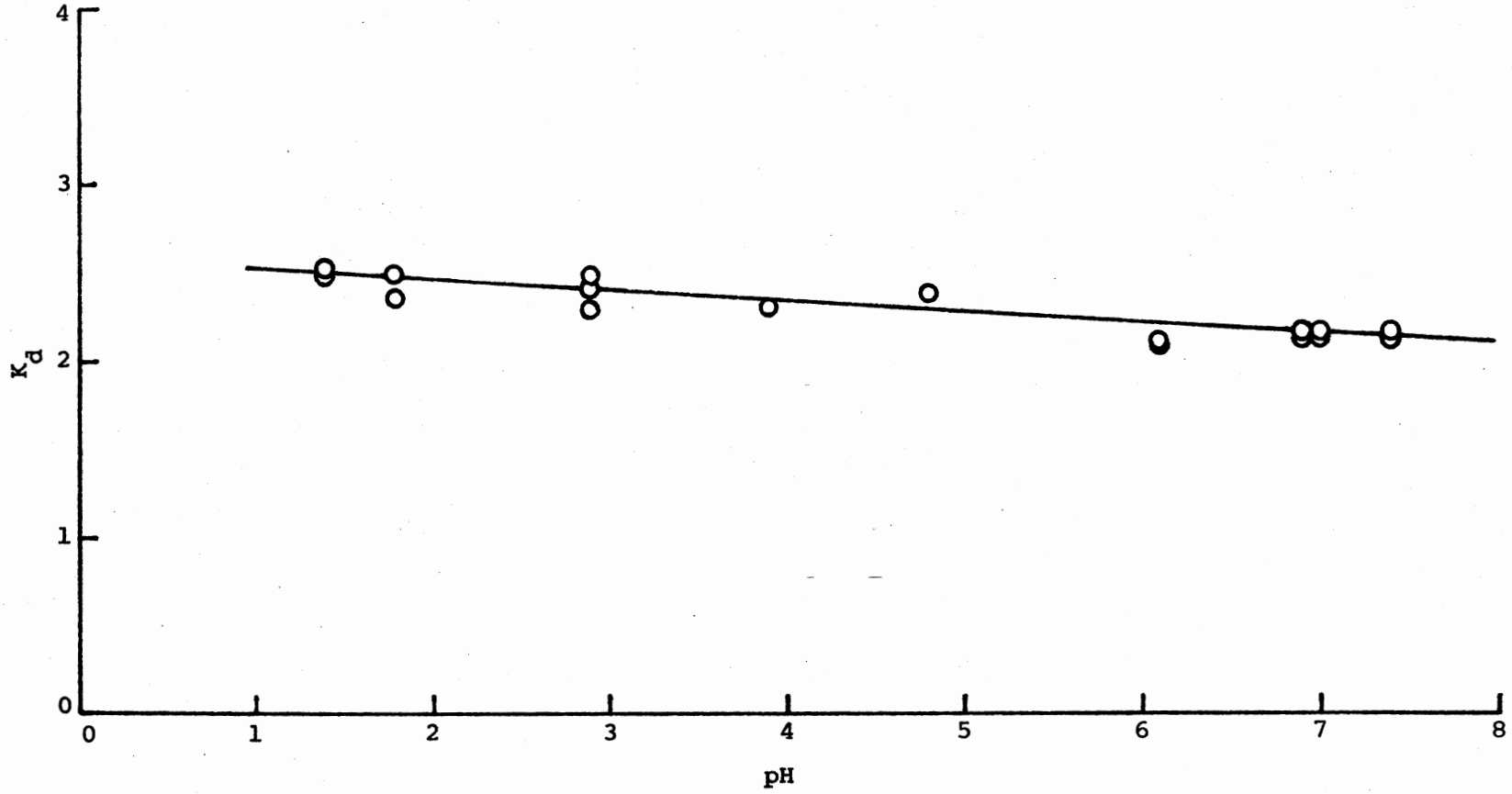

Figure 30. Effect of pH on K_d at Constant Ionic Strength (0.10 M) and Chloride Concentration (5.00×10^{-3} M)

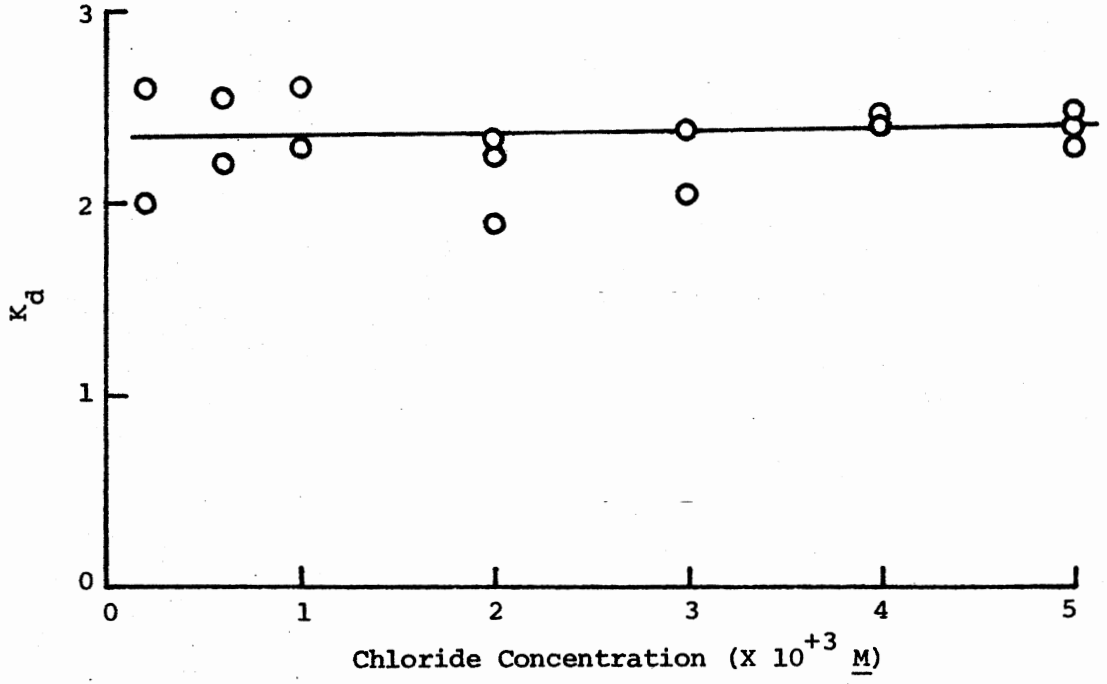

Figure 31. Effect of Chloride on K_d at Constant Ionic Strength (0.10 M) and pH (3.0)

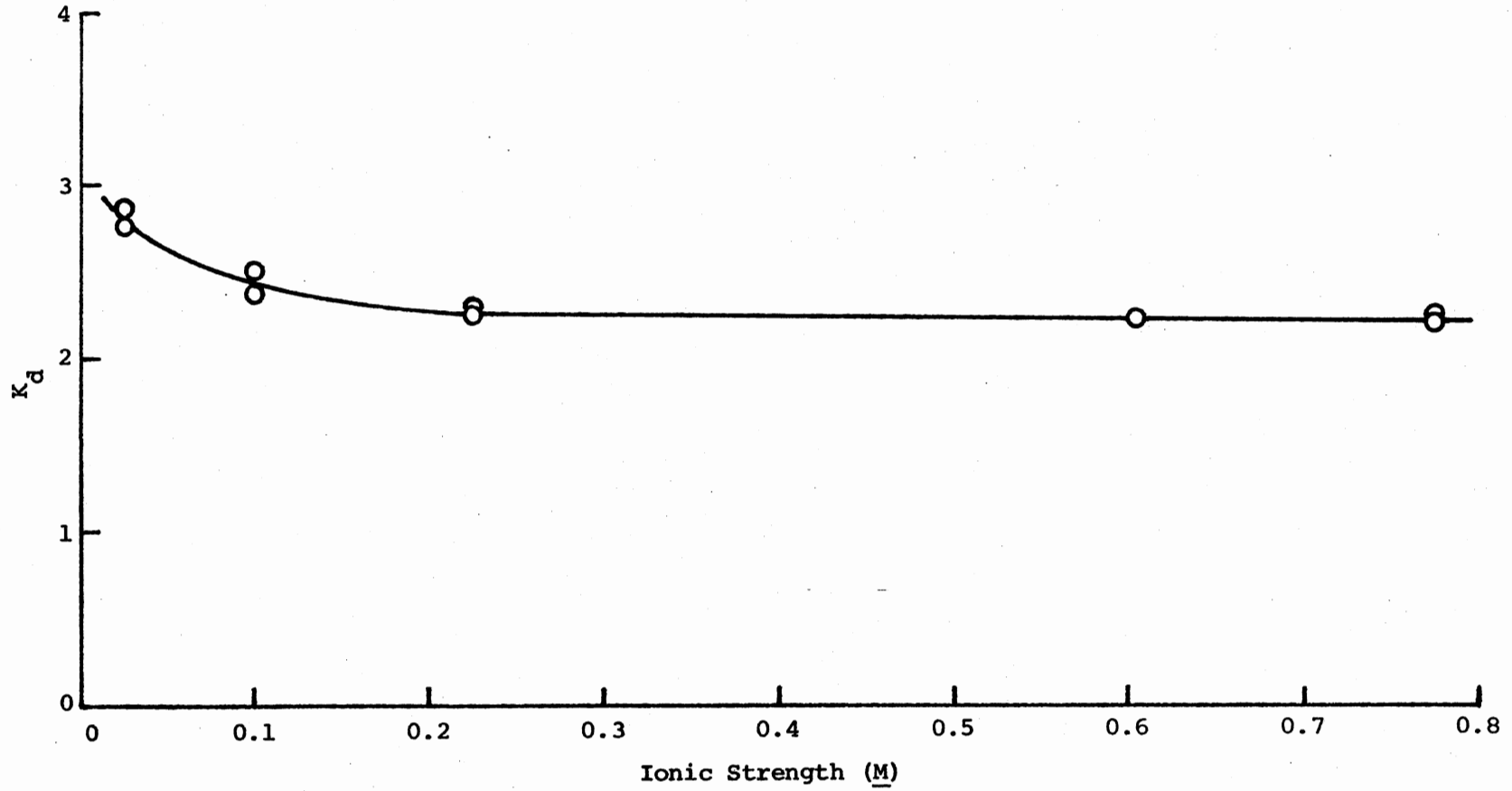

Figure 32. Effect of Ionic Strength on K_d at Constant Chloride Concentration (5.00×10^{-3} M) and pH (1.8)

4. Discussion

a. The K_d value obtained in Figure 30 increases slightly with decreasing pH, at constant chloride concentration and ionic strength. This trend is consistent with the association model of Equation (68). The results obtained in Figure 32 indicate the competition of NO_3^- with Cl^- to form $(CPG\text{-}8H_2O_x^+,A^-)$.

b. A comparison of Figures 26 and 30 shows that K_d values for PTS^- are about one unit larger than that for Cl^- in the low-pH region, pH = 1 to 2. This indicates that the ion-pair association model for PTS^- and Cl^- using $CPG\text{-}8HO_x$ resin parallels that of $8\text{-}HO_x$ in the liquid-liquid system.

c. Comparing results in Figures 28 and 32, it can be seen that K_d values become constant around 0.6 M when Cl^- is used to adjust the ionic strength in PTS^- solution while the same occurs at about 0.3 M when NO_3^- is used to adjust the ionic strength in Cl^- solution. This may indicate that the competition of NO_3^- for sites occupied by Cl^- to form the $(CPG\text{-}8H_2O_x^+,A^-)$ is more pronounced than the competition of Cl^- for sites occupied by PTS^-.

C. Effect of pH on the Distribution Coefficient of Several Aromatic and Aliphatic Sulfonates Using Corning $CPG\text{-}8HO_x$ Resin and CPG Plain Glass Beads

1. Experimental

a. Reagents

Both Corning $CPG\text{-}8HO_x$ resin and CPG plain glass beads, as described

in Chapter IV.A.1.a., were purchased from the Pierce Chemical Company. Besides the chemicals described in Chapter IV.A.1.a., the following chemicals of A. R. grade were used without further purification.

- Benzenesulfonic acid, 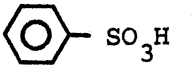 , Eastman Chemical Co.
- 2-Mesitylenesulfonic acid, 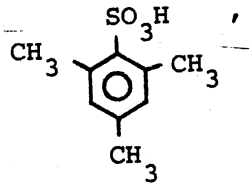 , Aldrich Chemical Co.
- 1-Naphthalenesulfonic acid, 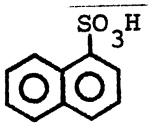 , Aldrich Chemical Co.
- Methanesulfonic acid, CH_3SO_3H, Aldrich Chemical Co.
- Ethanesulfonic acid, $C_2H_5SO_3H$, Aldrich Chemical Co.

Deionized-distilled water was used to prepare all aqueous solutions.

b. Apparatus

Same as described in Chapter IV.A.1.b.

c. Procedure

(i) For Aromatic Sulfonates. Same as described in Chapter IV.A.1.c., except that the concentration of each sulfonate solution was kept at 5.00×10^{-3} M and the ionic strength was kept at 0.10 M with NaCl solution. The same procedure was also used for the CPG plain glass beads in order to compare the distribution coefficient due to the attraction of sulfonates to the sodium ions which are a part of the glass beads. Since benzenesulfonate (BS^-), 2-mesitylenesulfonate ($2\text{-}MS^-$), and 1-naphthalenesulfonate ($1\text{-}NS^-$) have maximum absorbances at 260 nm, 271 nm, and 281 nm, respectively, these corresponding wavelengths were selected for

spectrophotometric determinations.

(ii) For Aliphatic Sulfonates. The same procedure as described in (i) was used except that a potentiometric acid-base titration method replaced the spectrophotometric determination. Ionic strengths were adjusted to 0.10 M with NaCl or $NaNO_3$ solutions. After attainment of equilibrium, the mixture in the vial was filtered and the filtrate containing the sulfonate was used for pH measurements and sulfonate determination.

A calibration curve was made by titrating a known amount (5.00 - 15.0 mmoles) of an aliphatic sulfonic acid solution with a standardized NaOH solution (1.219×10^{-3} M). The quantity of the NaOH required to reach the end point was obtained from a second derivative plot of $\frac{\Delta^2 pH}{\Delta V^2}$ versus milliliters of NaOH.

2. Formula Used

The same formulae as those expressed in Equations (65) and (53) were used except that the corresponding sulfonate was substituted for PTS^-.

3. Results

a. Calibration Curves for Aromatic and Aliphatic Sulfonates

Calibration curves of absorbances versus concentrations for benzenesulfonate (BS^-), 2-mesitylenesulfonate ($2\text{-}MS^-$), and 1-naphthalene sulfonate ($1\text{-}NS^-$) are shown in Figures 33, 34, and 35, respectively. Cali-

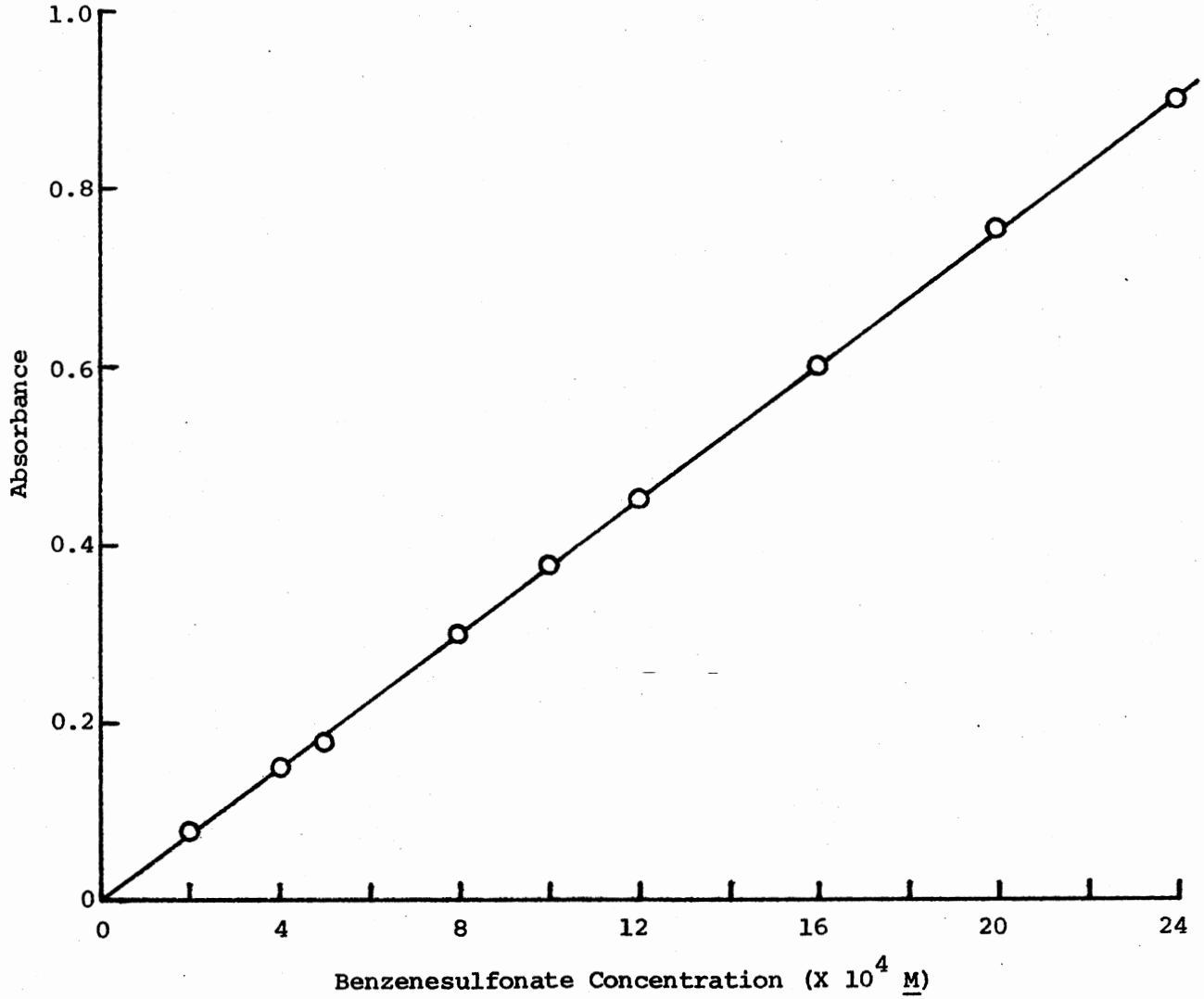

Figure 33. Calibration Curve for Benzenesulfonate Ion at 260 nm

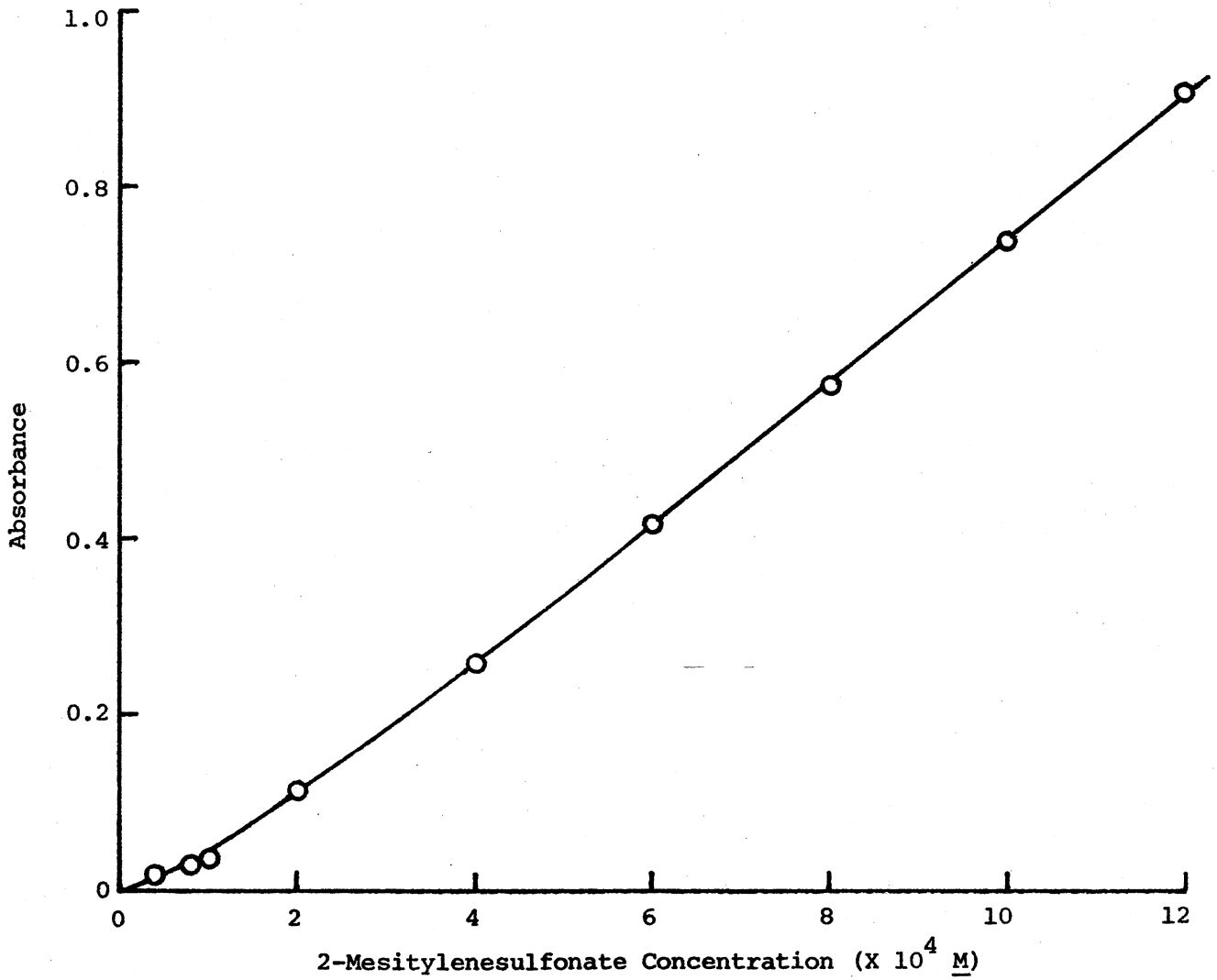

Figure 34. Calibration Curve for 2-Mesitylenesulfonate Ion at 271 nm

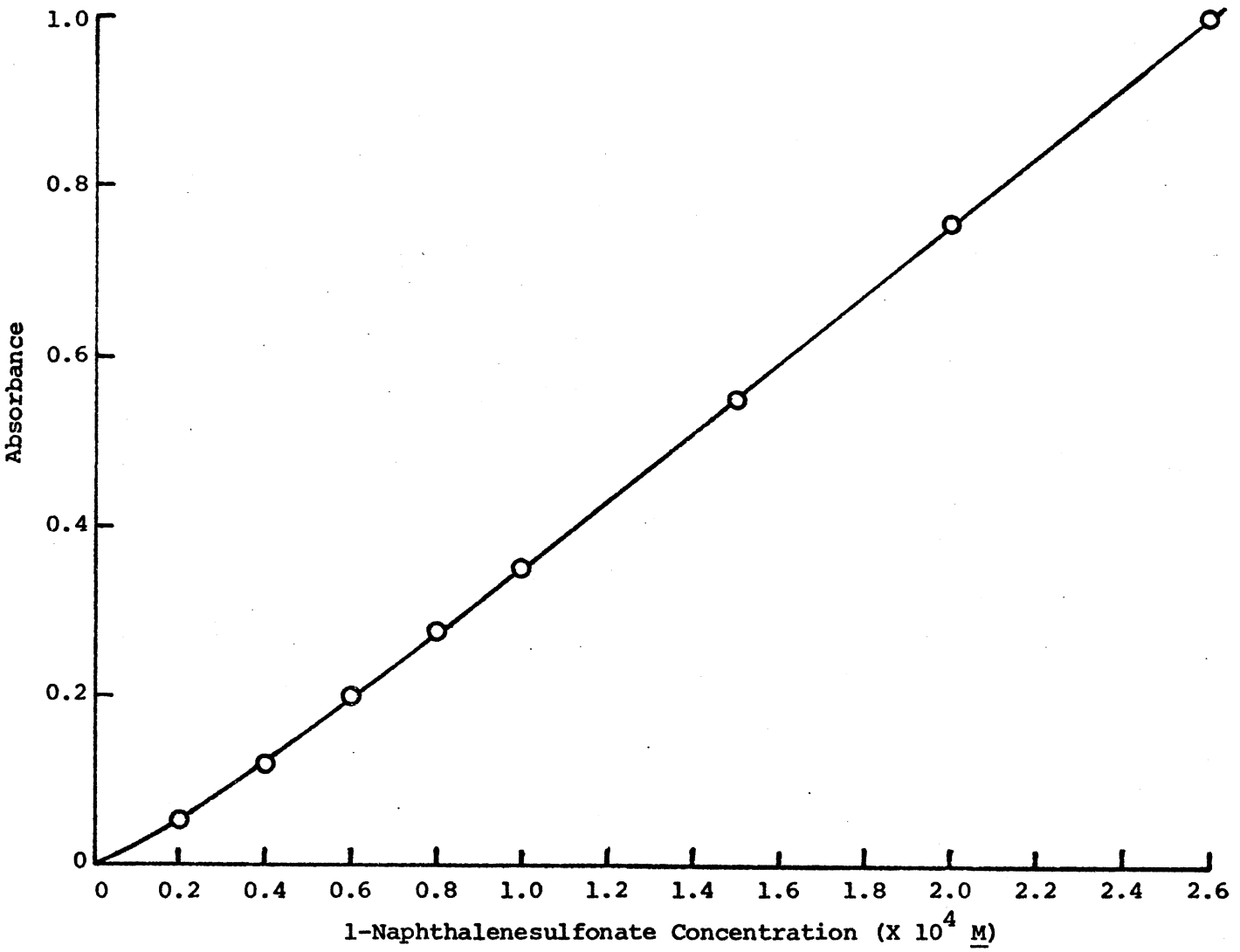

Figure 35. Calibration Curve for 1-Naphthalenesulfonate Ion at 281 nm

bration curves of millimoles of methanesulfonic acid and ethanesulfonic acid versus amount of NaOH used are shown in Figures 36 and 37, respectively.

b. Effect of pH on K_d at Constant Ionic Strength (0.10 M) and Sulfonate Concentration (5.00×10^{-3} M) Using Corning CPG-8HO$_x$ Resin

A plot of K_d versus pH for aromatic and aliphatic sulfonates studied is shown in Figure 38, where the results for PTS^- are obtained from Chapter IV.A.3.b.

c. Effect of pH on K_d at Constant Ionic Strength (0.10 M) and Sulfonate Concentration (5.00×10^{-3} M) Using Corning Plain Glass Beads

A plot of K_d versus pH for aromatic and aliphatic sulfonates is shown in Figure 39, where the results for PTS^- are also obtained from Chapter IV.A.3.b.

4. Discussion

a. Figure 38 shows that the K_d for aromatic sulfonates increases in the order of

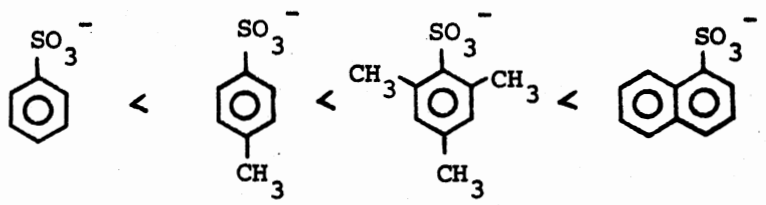

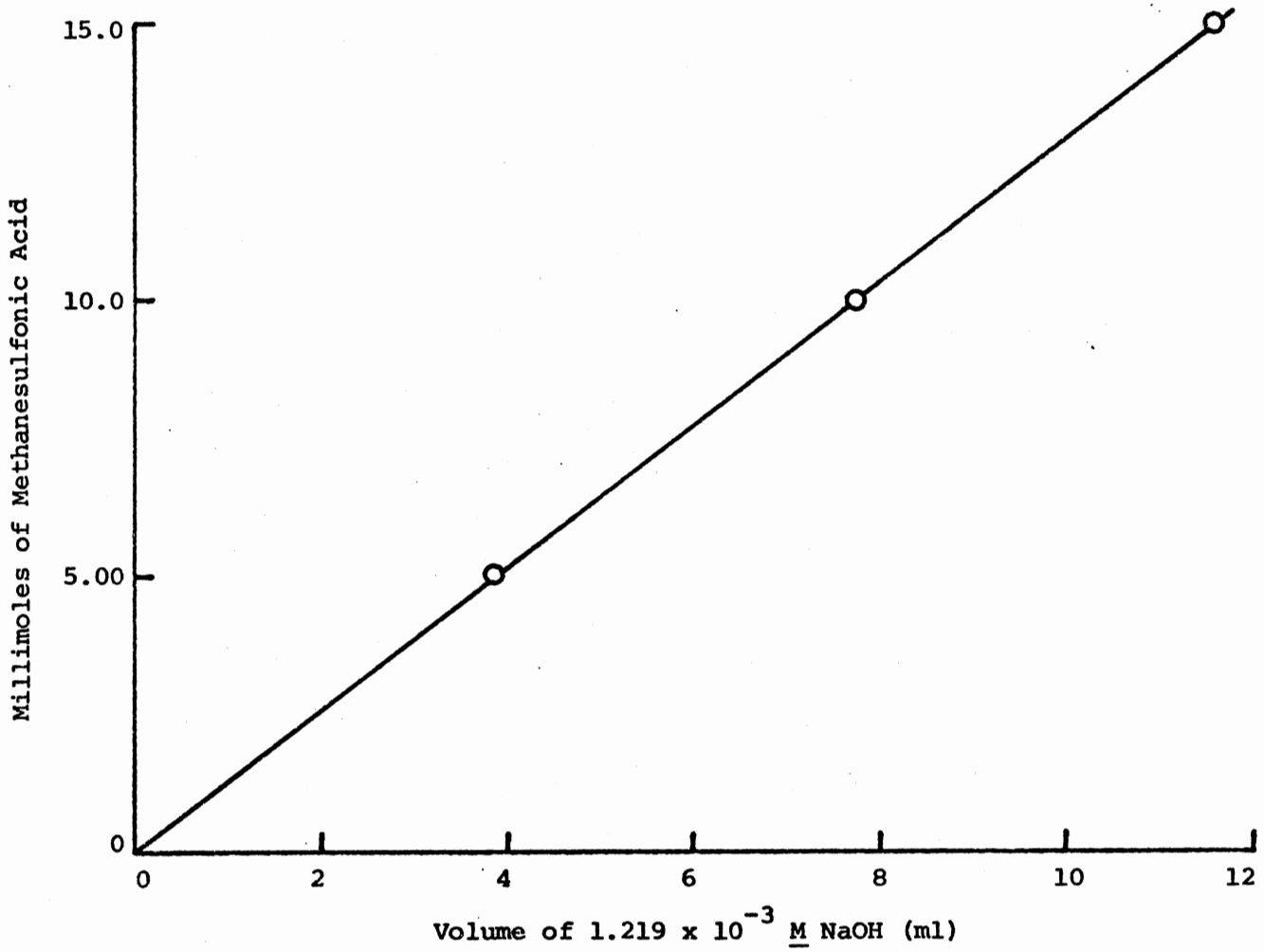

Figure 36. Calibration Curve for Methanesulfonic Acid

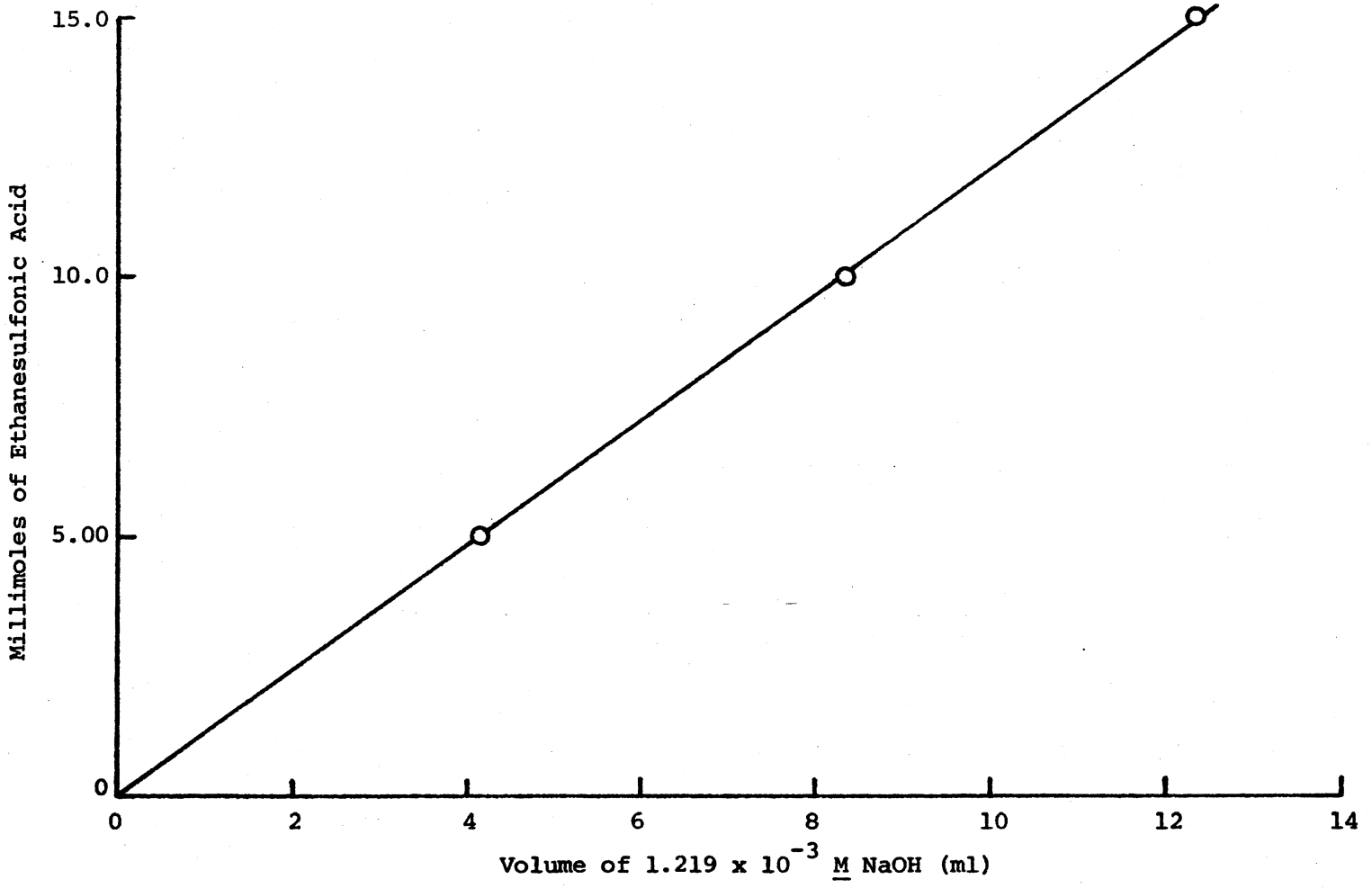

Figure 37. Calibration Curve for Ethanesulfonic Acid

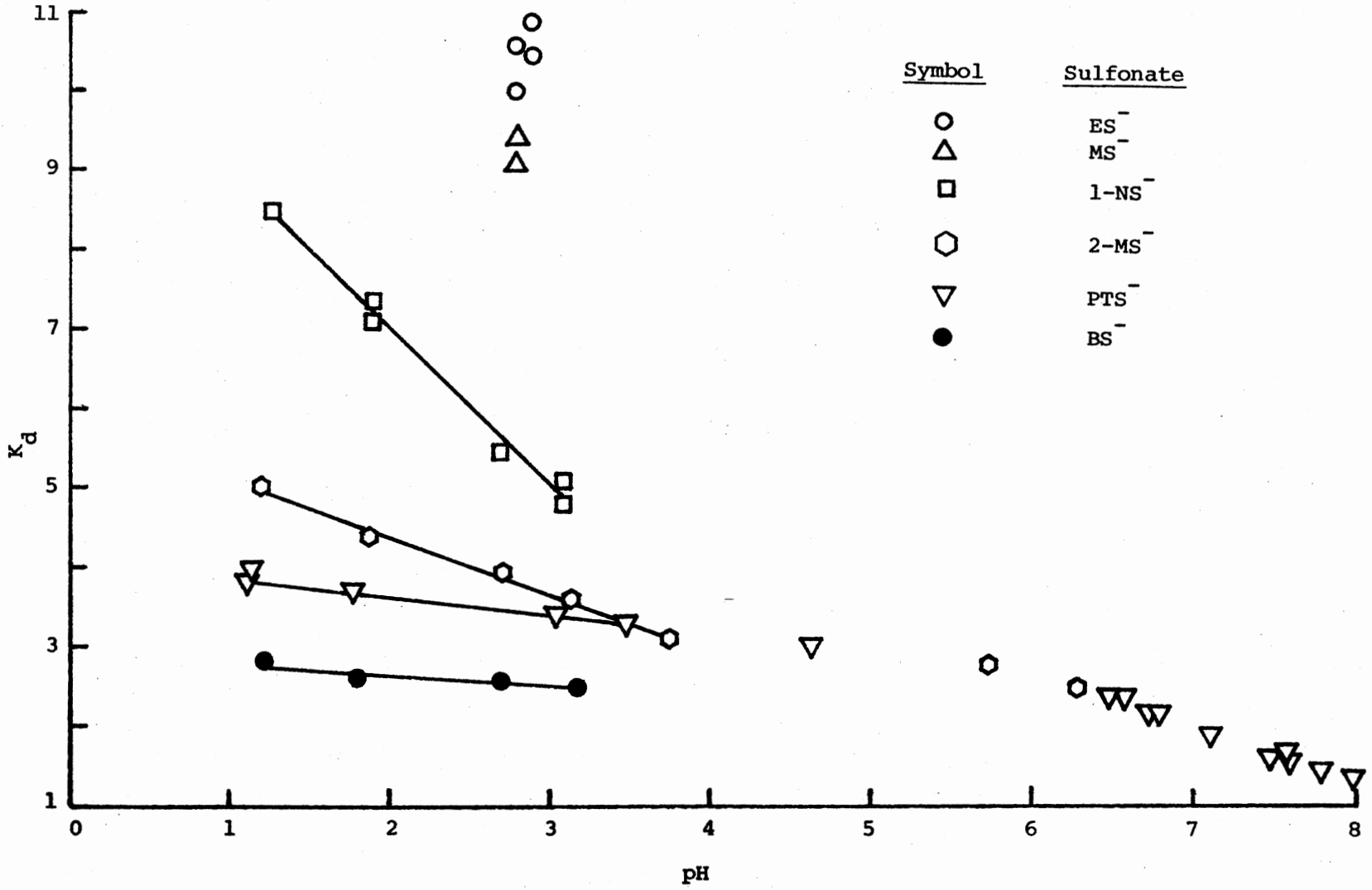

Figure 38. pH Effect on K_d for Several Sulfonates Using Corning CPG-8HO$_x$ Resin

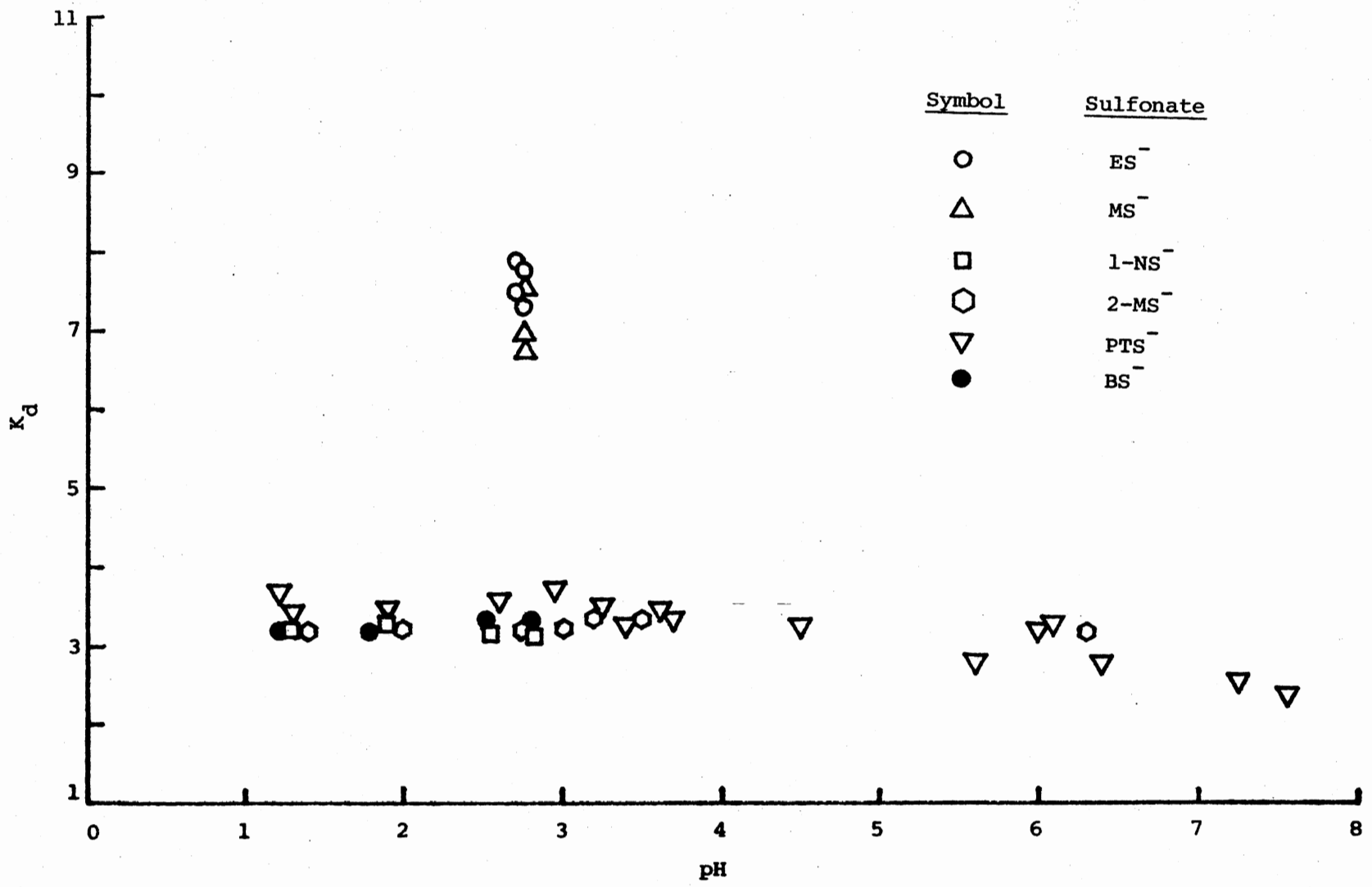

Figure 39. pH Effect on K_d for Several Sulfonates Using Corning Plain Glass Beads

in the low-pH region, 1-3. This is because the hydrophobicity increases with increasing numbers of methyl or aryl carbons (benzene ring in 1-naphthalenesulfonate) (1) (38) as mentioned in Chapter II.A.2.a. Hence, the relative hydrophobicity increases in the order BS^- < PTS^- < $2\text{-}MS^-$ < $1\text{-}NS^-$.

b. Comparing the K_d values for aromatic sulfonates obtained in Figures 38 and 39 at low pH (especially at pH around 1) shows that the differences of K_d between sulfonate species is relatively large when the CPG-8HO$_x$ resin is used, while it is very small when the plain CPG glass bead resin is used. This shows a high potential for the CPG-8HO$_x$ resin for use as a stationary phase to separate these four aromatic sulfonates by liquid chromatography. If suitable acidic solutions are used as mobile phases, an elution order of benzenesulfonate, p-toluene-sulfonate, 2-mesitylenesulfonate, and 1-naphthalene-sulfonate should be obtained because K_d values increase in the order BS^- < PTS^- < $2\text{-}MS^-$ < $1\text{-}NS^-$.

c. The K_d values obtained for ethanesulfonate are larger than those of methanesulfonate as shown in Figure 38. This is because the former has an additional $-CH_2-$ group which gives more hydrophobicity.

As Figures 38 and 39 show, the difference of K_d between ethane-sulfonate and methanesulfonate is larger when CPG-8HO$_x$ resin is used and smaller when CPG plain glass beads are used. This also indicates that CPG-8HO$_x$ resin possesses a higher potential to separate aliphatic sulfonates than that of CPG plain glass beads.

d. The K_d values for aromatic sulfonates are lower than for aliphatic ones in both Figures 38 and 39. This may be because aliphatic sulfonates are more hydrophobic than that of aromatic sulfonates. The

relative diameters of aliphatic and aromatic sulfonates estimated from a molecular model (Godfrey Molecular Models, Inc., New Jersey) are tabulated in Table VII for reference. The large difference in K_d (at pH ~2.8) between aliphatic and aromatic sulfonates indicates that a group separation for sulfonates is possible. Either CPG-8HO$_x$ resin or even CPG plain glass beads can be used as stationary phase and a suitable acidic solution (pH ~2.8) can be used as a mobile phase for liquid chromatography.

e. The K_d's for benzenesulfonate ion using the CPG-8HO$_x$ resin are slightly lower than those obtained from CPG plain glass beads. This may be either because the adsorption of BS^- on the plain CPG glass beads is more favored than the ion-pair association of (CPG-8H$_2$O$_x^+$,BS^-) on the CPG-8HO$_x$ resin as discussed in Chapter IV.A.4.b., or because of the experimental error.

D. Synthesis of CPG-8HO$_x$ Resin and Characteristics of the Synthesized CPG-8HO$_x$ Resin

1. Synthesis of CPG-8HO$_x$ Resin From Aminopropyl-CPG

a. Reagents

The aminopropyl controlled-pore glass (CPG-AMP), $-\overset{|}{\underset{|}{Si}}-(CH_2)_3-NH_2$, was purchased from Electro-Nucleonics, Inc. (New Jersey). The CPG-AMP has particle diameters of 125-177 microns, a mean pore size of 544 Å (Figure 40), a pore volume of 1.24 cc/g, and a surface area of 57 m^2/g.

A. R. reagents of 8-hydroxyquinoline, sodium chloride, and hydrochloric acid have been described previously. The following chemicals of

TABLE VII

THE RELATIVE VOLUME AND DIAMETER OF SULFONATES ESTIMATED FROM GODFREY MOLECULAR MODELS

Sulfonate	Length (Å)	Width (Å)	Height (Å)	Volume (Å)^3	Diameter (Å)
Methanesulfonate	7.03	6.18	4.00	174	10.1
Ethanesulfonate	8.91	6.18	4.24	233	11.6
Benzenesulfonate	10.6_7	6.18	3.63	239	12.8
p-Toluenesulfonate	11.6_4	6.18	3.76	270	13.7
2-Mesitylenesulfonate	12.0_o	8.79	3.76	397	15.3
1-Naphthalenesulfonate	11.7_6	9.76	3.52	404	15.7

(The scale of the model is 2.54 cm $\rightleftharpoons$ 1.54 Å).

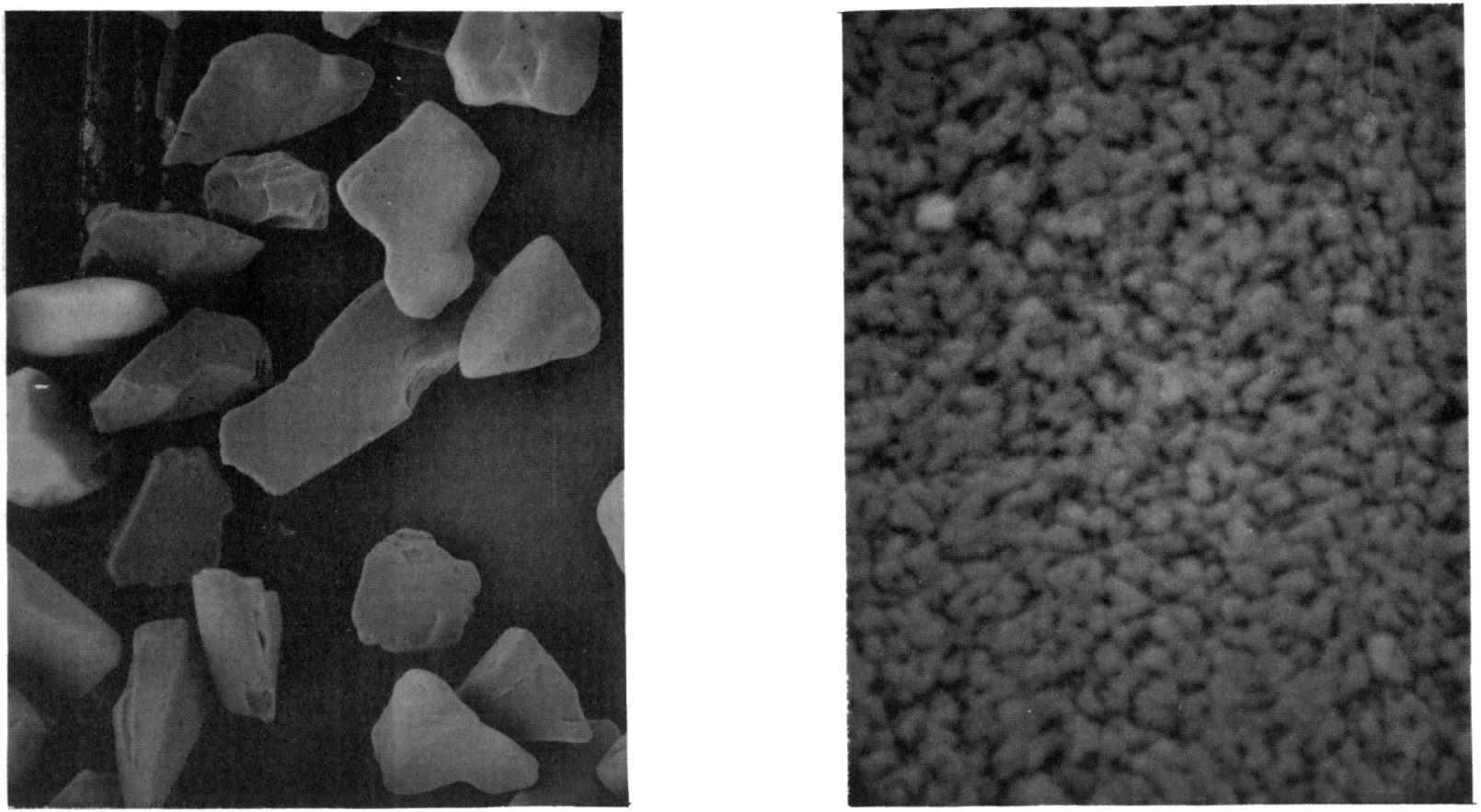

Figure 40. Electron Scan Micrograph for CPG-AMP With Particle Diameter of 125-177 μ and Pore Size of 544 Å. The Magnification is 100X (Left) and is 30000X (Right)

A. R. grade were used without further purification.

- p-Nitrobenzoyl chloride, 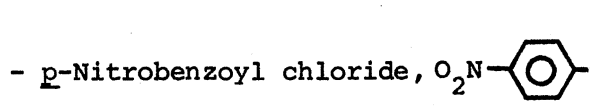 Aldrich Chemical Co.
- Triethylamine, $N(C_2H_5)_3$, Eastman Organic Chemicals.
- Sodium dithionite, $Na_2S_2O_4$, Eastman Organic Chemicals.
- Sulfamic acid, NH_2SO_3H, Brothers Chemical Co. (Orange, New Jersey).
- Sodium nitrite, $NaNO_2$, Baker Analyzed Reagent.
- Sodium carbonate, Na_2CO_3, Mallinckrodt Analytical Reagent.

Deionized-distilled water was used to prepare all aqueous solutions.

b. Procedure

The scheme for the synthesis of CPG-8HO$_x$ from CPG-AMP is shown in Figure 41. The procedure for step 1 is from reference (55) and steps 2 and 3 are adapted from references (35) and (56).

A 2-g portion of CPG-AMP was weighed out in a 50-ml beaker. After introducing a solution of p-nitrobenzoyl chloride (2.84 g) in chloroform (25 ml) containing 5% triethylamine (1.94 g), the mixture was covered with aluminum foil and allowed to react overnight. The glass beads were then separated from the solution by filtering the mixture through filter paper (Whatman No. 42). The treated glass beads were transferred to a 400-ml beaker by using 100 ml of 0.30 M sodium dithionite solution. The solution in the beaker was heated on a hot plate with a constant stirring for about 1.5 hours. Some gases (HCl and SO_2) were expelled.

After cooling the mixture down to room temperature, it was filtered as described above. The glass beads were transferred to another 400-ml beaker by use of 48 ml of 2 N HCl and the beaker was kept in an ice bath

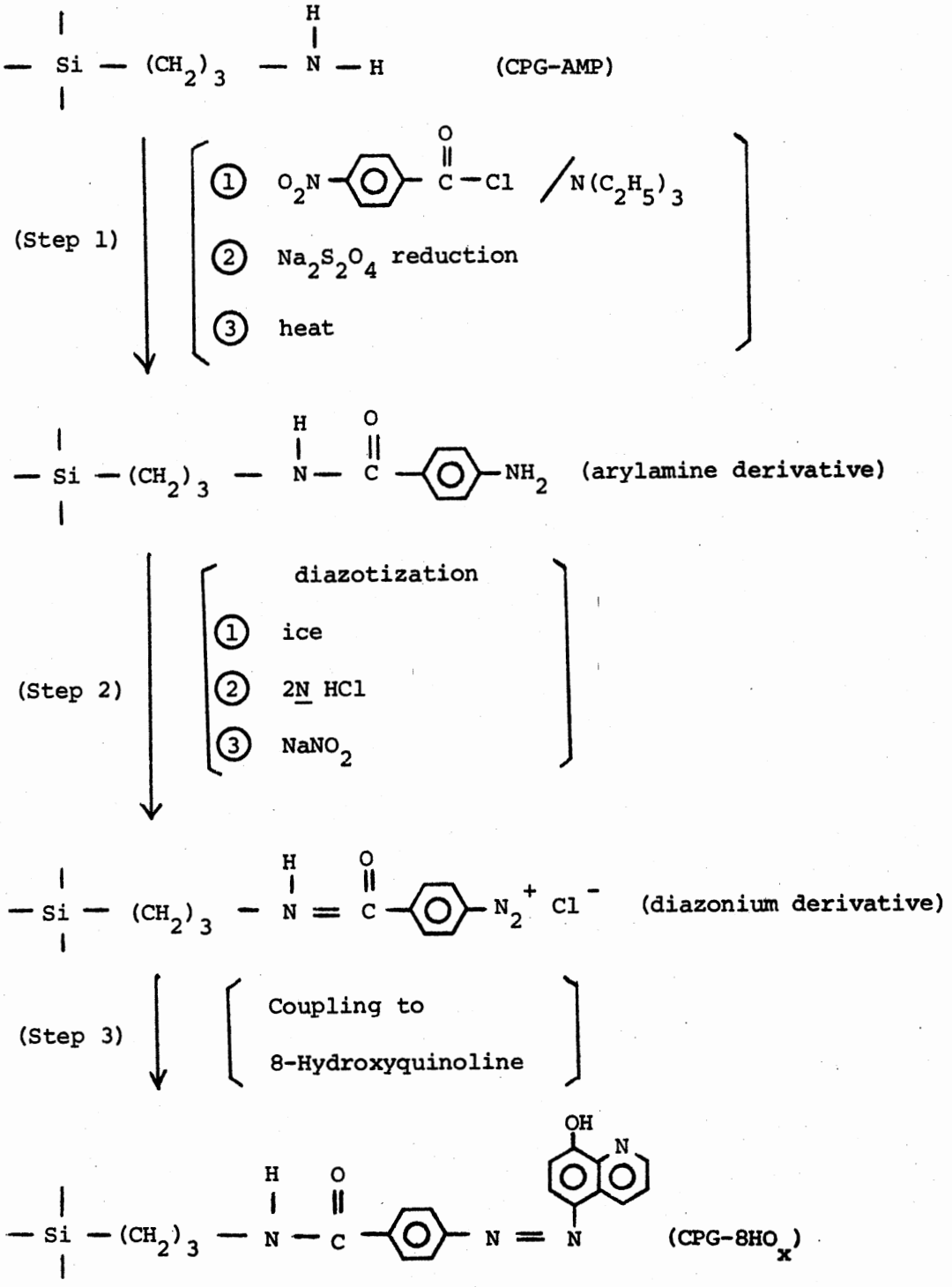

Figure 41. Scheme for the Synthesis of CPG-8HO$_x$ From CPG-AMP

(ice + NaCl) at ~0°C to -10°C. 1.2 g of sodium nitrite was then added slowly with stirring for about 30 minutes. Foam was formed and the solution turned to a brownish yellow color. The obtained mixture was placed in a vacuum desiccator and gases were evacuated for another 30 minutes using a water pump.

The mixture was then decanted and washed with 100 ml of cold deionized-distilled water, 100 ml of cold 1% sulfamic acid solution, and two more times with 100 ml cold deionized-distilled water. The diazotized glass was coupled to 8-hydroxyquinoline by adding 50 ml of saturated 8-hydroxyquinoline solution in 0.05 M Na_2CO_3 and stirring for about 40 minutes. A deep dark red color appeared. After filtering, the CPG-8HO$_x$ resin was washed with deionized-distilled water until the filtrate was colorless. The product was finally air dried.

2. Characteristics of the Synthesized CPG-8HO$_x$ Resin

The Corning CPG-8HO$_x$ resin was also used in this part because some characteristics of it were known or could be determined for comparing it with the synthesized one. In part a, Cu^{2+} solution was selected to determine the capacity of the CPG-8HO$_x$ resin because the Cu^{2+} was 100% extracted (35) by CPG-8HO$_x$ resin in the pH range of 4-5. The metal complex formed is $Cu(Ox)_2$ with a Cu^{2+}:Ox^- ratio of 1:2. The Cu^{2+} concentrations can be easily determined using an atomic absorption spectrophotometer.

a. Determination of the Capacity of 8-Hydroxyquinoline in Batch Experiments in Terms of Cu^{2+} Complexed

(i) Materials. The Corning CPG-8HO$_x$ resin and the synthesized CPG-8HO$_x$ resin (Figure 42) were used. A. R. reagents of cupric sulfate, $CuSO_4 \cdot 5H_2O$, (Baker Analyzed Reagent), glacial acetic acid, and sodium hydroxide were used without further purification.

(ii) Apparatus. An atomic absorption spectrophotometer (Perkin Elmer Model 290B), a copper hollow cathode lamp (Perkin Elmer Intensitron TM Lamp, No. 2252), and acetylene and air (1:1) were used.

(iii) Procedure (35). A portion (0.2000 g) of the synthesized CPG-8HO$_x$ resin was weighed out in a 35-ml vial. A stock solution of Cu^{2+} (8.411×10^{-4} M) was prepared by dissolving 0.0525 g $CuSO_4 \cdot 5H_2O$ in 250 ml of 0.20 M acetate buffer at a pH of about 5.0. After pipetting 20.0 ml of the Cu^{2+} solution into the vial, the mixture was shaken for 30 minutes by use of the shaker. After equilibrium, the mixture was filtered and the filtrate was collected. The Cu^{2+} in the filtrate was determined by atomic absorption spectrophotometry at a wavelength of 324.7 nm. Dilutions were performed with deionized-distilled water as necessary. The corresponding concentrations of Cu^{2+} in the filtrate were determined by interpolation into a calibration curve prepared in the range of 0 to 20 ppm. The amount of Cu^{2+} unextracted by the resin was then calculated and that extracted to the resin was determined by difference. The same procedure was used for the Corning CPG-8HO$_x$ resin.

(iv) Results. A calibration curve for Cu^{2+} estimation at 324.7 nm

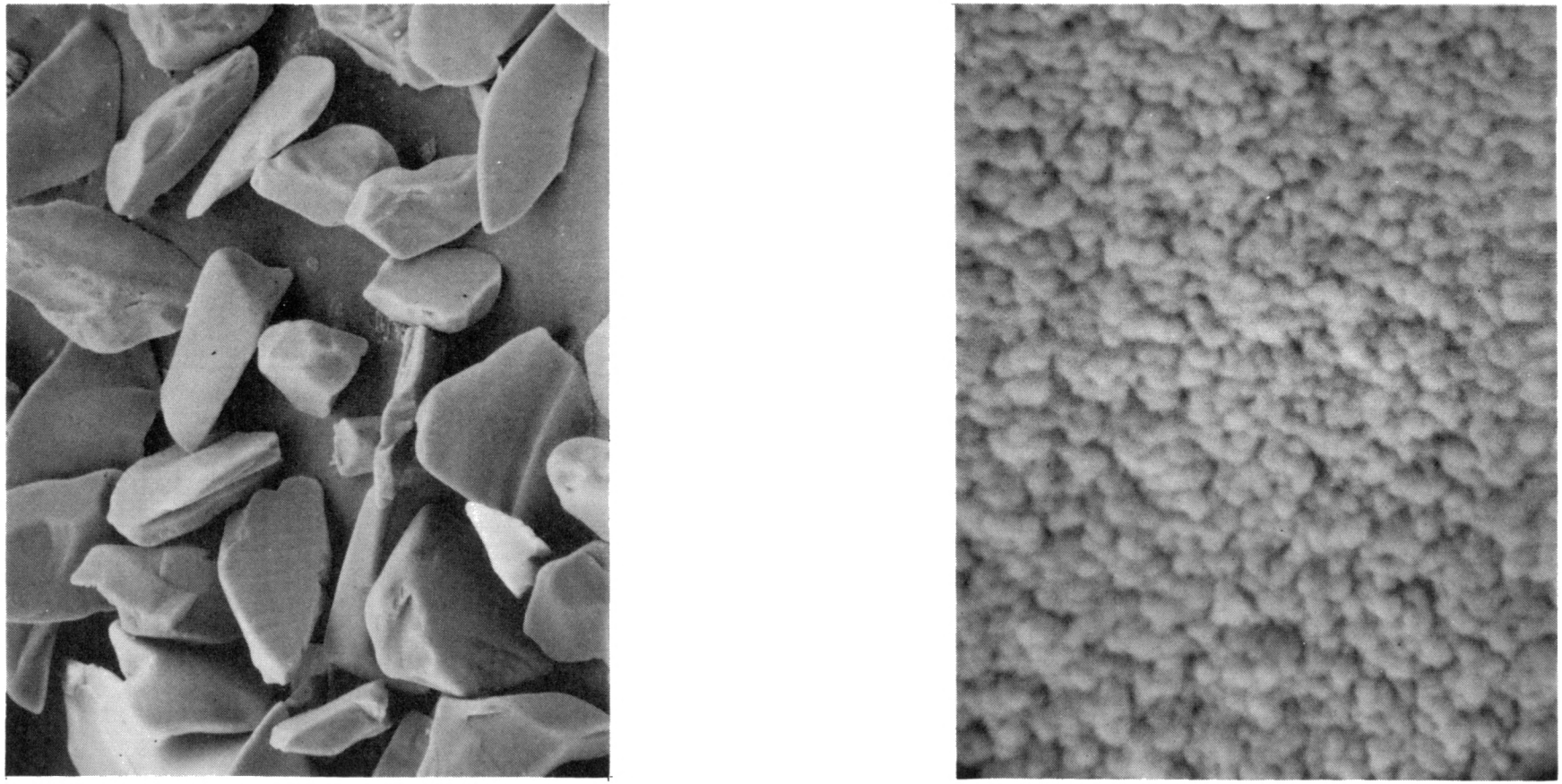

Figure 42. Electron Scan Micrograph for Synthesized CPG-8HO$_x$ Resin With Particle Diameter of 125-177 μ and Pore Size of 544 Å. The Magnification is 100X (Left) and is 30000X (Right)

in the range of 0-20 ppm is shown in Figure 43. Data for the determination of the capacity of 8-hydroxyquinoline on CPG-8HO$_x$ resin in terms of Cu^{2+} extracted per gram of resin are tabulated in Table VIII. Since the complex of $Cu(O_x)_2$ is formed and this table shows that the amount of Cu^{2+} extracted per gram of resin is 0.184 mmole for Corning CPG-8HO$_x$ resin, the capacity of 8-hydroxyquinoline should be 0.184 $\frac{\text{mmole}}{\text{g}}$ x $\frac{1}{2}$, or 0.0920 mmole per g of Corning CPG-8HO$_x$ resin. This capacity is about three times that of the manufacture's value which is given by label on the bottle. Since the synthesized CPG-8HO$_x$ resin has a capacity about 2.11 times as large as that of Corning's, the capacity is 0.0920 $\frac{\text{mmole}}{\text{g}}$ x 2.11, or 0.194 mmole 8-hydroxyquinoline per gram of the synthesized resin according to batch experiments. The synthesized resin shows a larger capacity than that of Corning's, probably because of differences in particle size.

b. Determination of the Acid Characteristics (pKa_1) of the Synthesized CPG-8HO$_x$ Resin by Potentiometric Titration

(i) Materials. Both Corning and the synthesized CPG-8HO$_x$ resins were used. A. R. reagents of sodium dihydrogen phosphate, sodium hydroxide, hydrochloric acid, disodium hydrogen phosphate, Na_2HPO_4, and potassium acid phthalate, $C_8H_5O_4K$ (Mallinckrodt Reagent) were used. 8-Hydroxyquinoline (Eastman Organic Chemicals) was recrystallized once from ethanol : deionized-distilled water (1:1). Nitrogen gas (high-purity dry grade supplied by Union Carbide Corporation) in a cylinder tank was used.

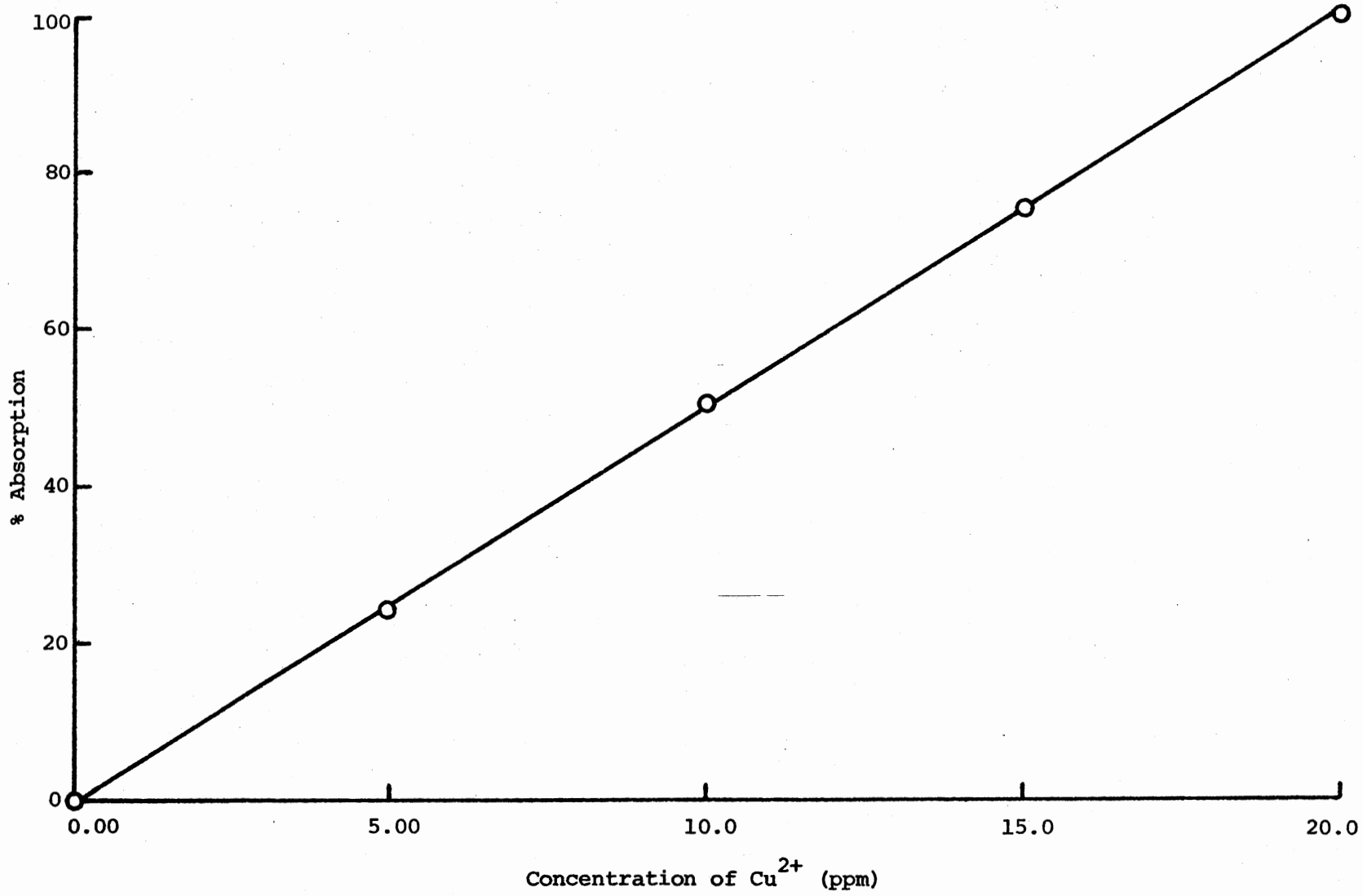

Figure 43. Calibration Curve for Cu^{2+} at 324.7 nm

TABLE VIII

DATA FOR THE DETERMINATION OF THE CAPACITY OF 8-HYDROXYQUINOLINE ON CPG-8HO$_x$ RESIN IN TERMS OF AMOUNT OF Cu^{2+} EXTRACTED PER GRAM OF RESIN

Type of CPG-8HO$_x$ Resin	Amount of Resin Used (g)	Dilution of Filtrate Containing Cu^{2+} With d.d. Water	Average[a] % Absorption of Cu^{2+} After Dilution	$[Cu^{2+}]$ After Dilution (ppm)	$[Cu^{2+}]$ Before Dilution (ppm)	Amount of Cu^{2+} Unextracted by the Resin ($\times 10^3$ mmole)	Amount[b] of Cu^{2+} Extracted into the Resin ($\times 10^3$ mmole)	Amount of Cu^{2+} Extracted Per Gram of Resin ($\frac{mmole}{g}$)	Capacity Ratio of Synthesized to Corning
Synthe-sized	0.2000	1→3	48.2	9.58	28.7	9.05	7.77	0.389	2.11
Corning	0.2000	1→3	69.9	13.9_2	41.8	13.1_5	3.67	0.184	1.00

a. The results were average of two individual determinations.

b. The total amount of Cu^{2+} introduced was $16.8_2 \times 10^{-3}$ mmole.

(ii) Apparatus. All pH measurements were made using a Beckman Zeromatic pH meter and a Sargent miniature combination electrode as described in Chapter IV.A.1.b. A recorder (Heath Model EU-20B) was connected to the pH meter to check pH readings at equilibrium. The results were plotted using a X-Y plotter (Hewlett-Packard 9862A) which was interfaced to a desk-top programmable calculator (Hewlett-Packard 9825A). A 50-ml buret which could be read to ± 0.01 ml was used for the titration.

(iii) Procedure. A sample of 3 g of CPG-8HO$_x$ resin was weighed out in a 100-ml beaker. After washing three times with 0.001 M phosphate buffer (pH ~7.0), the resin was immersed in the buffer for two hours. The treated CPG-8HO$_x$ resin was filtered and dried in the air. A 0.5 - 1.0 g portion of the dried CPG-8HO$_x$ resin was accurately weighed out in a 250-ml beaker and 100 ml of deionized-distilled water was added. The resin in the solution was titrated with a standardized hydrochloric acid solution ($1.98_3 \times 10^{-3}$ M). The pH was measured from the pH meter and the volume of acid used (at increments of 1.00 ml or 0.50 ml) was read from the buret. Nitrogen gas was bubbled through the solution to stir it. The synthesized CPG-8HO$_x$ resin without treatment with the phosphate buffer, and Corning CPG-8HO$_x$ resin with and without treatment with the buffer were also used for comparison purposes. The pure 8-hydroxyquinoline chemical was also used in order to test the validity of the approach used.

(iv) Formula Used. A typical titration curve for the synthesized CPG-8HO$_x$ resin with HCl is represented in Figure 44, where point A is assumed to be the first end point, point O is the end of the level off,

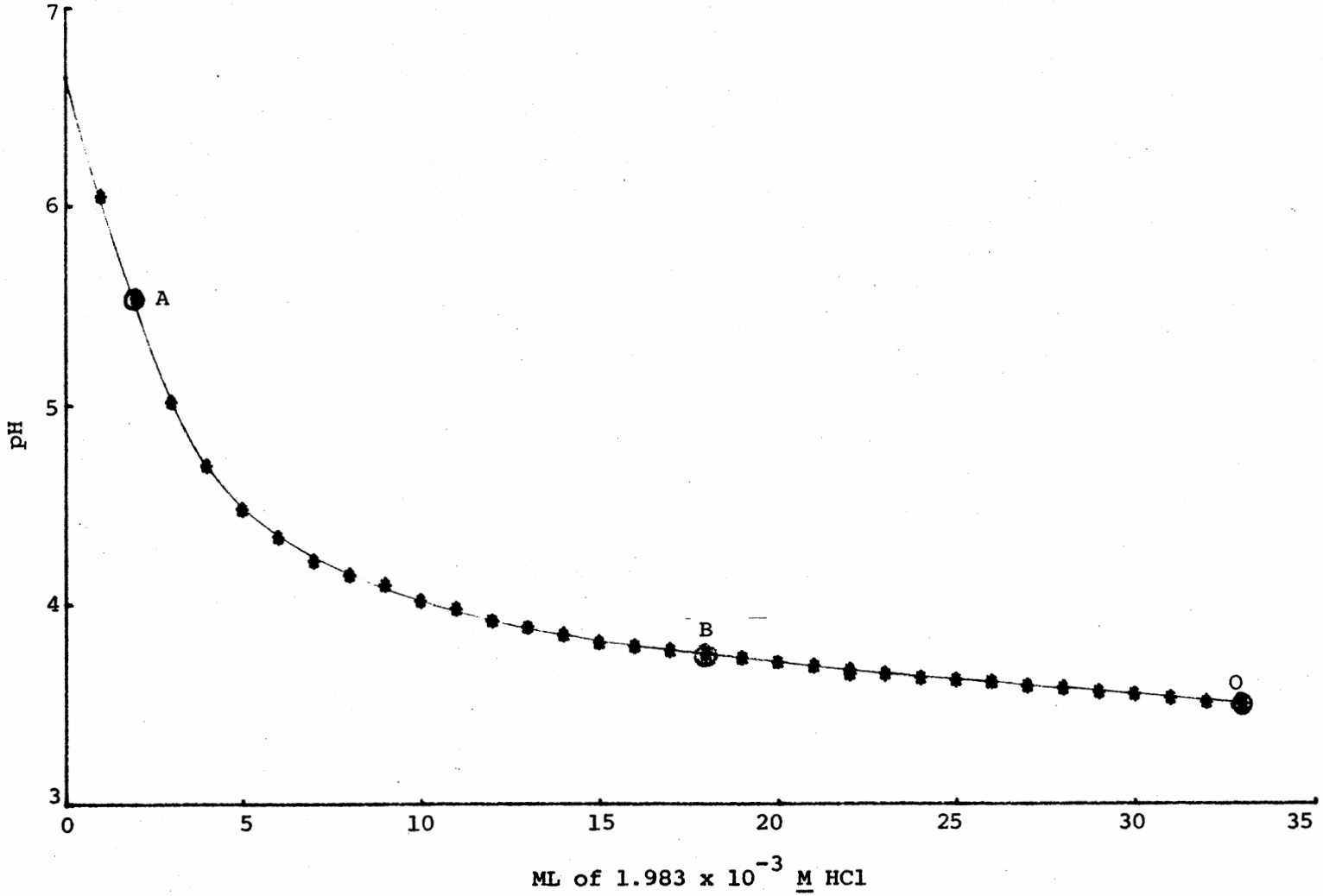

Figure 44. Titration Curve for 0.5000 g of Synthesized CPG-8HO$_x$ Resin (Treated With Buffer pH 7) With HCl

and point B is the midpoint between A and O. If points around B are chosen, a simplified equation for the determination of pKa_1 may be derived as follows:

Let the first acid dissociation constant of 8-hydroxyquinolinium ion be Ka_1 as described in Equations (69) and (70).

$$H_2O_x^+ \underset{}{\overset{Ka_1}{\rightleftharpoons}} H^+ + HO_x \tag{69}$$

$$Ka_1 = \frac{[H^+][HO_x]}{[H_2O_x^+]} \tag{70}$$

The mass- and charge-balance equations are expressed by Equations (71) and (72), respectively.

$$C_{HO_x} = [H_2O_x^+] + [HO_x] + [O_x^-] \tag{71}$$

$$[H^+] + [H_2O_x^+] + [Na^+] = [Cl^-] + [OH^-] + [H_2PO_4^-] + 2[HPO_4^{2-}] \tag{72}$$

Since $[O_x^-]$ is negligible compared with $[H_2O_x^+]$ or $[HO_x]$ at pH below 4, $[Na^+]$ is small compared with $[H^+]$, and $[OH^-]$, $[H_2PO_4^-]$, and $[HPO_4^{2-}]$ are negligible compared with $[Cl^-]$, Equations (71) and (72) can be simplified and rewritten as Equations (73) and (74), respectively.

$$C_{HO_x} = [HO_x]\left(\frac{[H^+]}{Ka_1} + 1\right) \tag{73}$$

$$[Cl^-] - [H^+] = [HO_x]\left(\frac{[H^+]}{Ka_1}\right) \tag{74}$$

Dividing Equation (73) by Equation (74) gives

$$\frac{C_{HO_x}}{[Cl^-] - [H^+]} = 1 + \frac{Ka_1}{[H^+]} \tag{75}$$

Let

$$S = \frac{C_{HO_x}}{[Cl^-] - [H^+]} \tag{76}$$

where S can be determined experimentally. Substituting Equation (76) into Equation (75) and rearranging yields

$$S - 1 = \frac{Ka_1}{[H^+]} \tag{77}$$

Taking logarithms of both sides of Equation (77) and rearranging results in

$$pH = pKa_1 + \log(S-1) \tag{78}$$

Since pH and log(S-1) can be calculated, a plot of pH versus log(S-1) will give a straight line with pKa_1 as the intercept at log(S-1) = 0.

(v) Results. Plots of pH versus log(S-1) for the synthesized CPG-$8HO_x$ resin, Corning CPG-$8HO_x$ resin, and pure 8-hydroxyquinoline are shown in Figures 45-49. The values of pKa_1 for 8-hydroxyquinolinium ion determined from the pH intercept at log(S-1) = 0 are summarized in Table IX. The pKa_1 obtained from the pure 8-hydroxyquinoline is 4.76, which is comparable with reported values (Table I) and is within a relative error of 5% based on pKa_1 of 5.0.

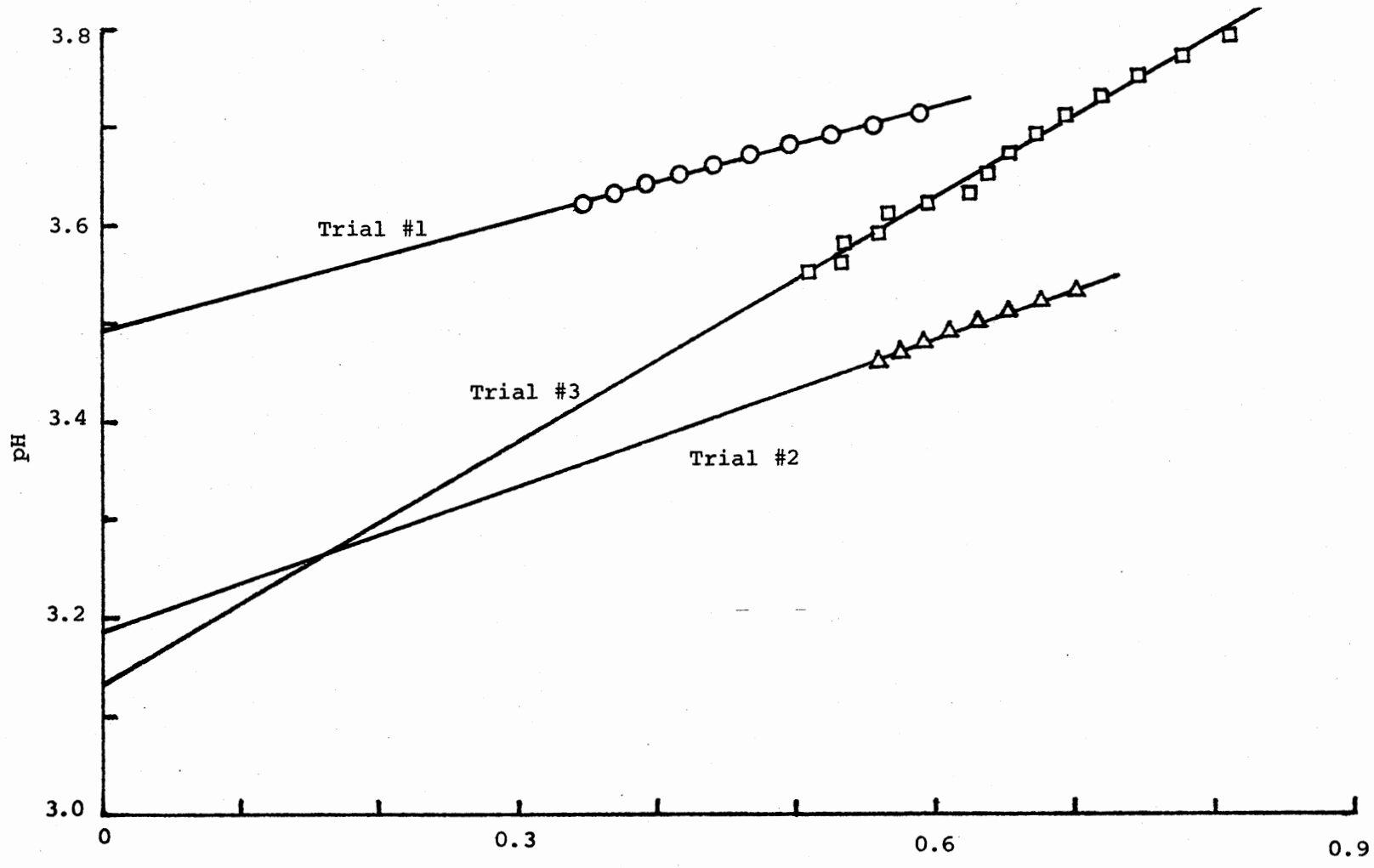

Figure 45. Estimation of pKa_1 for 8-$H_2O_x^+$ Using Synthesized CPG-8HO_x Resin Pretreated With Buffer

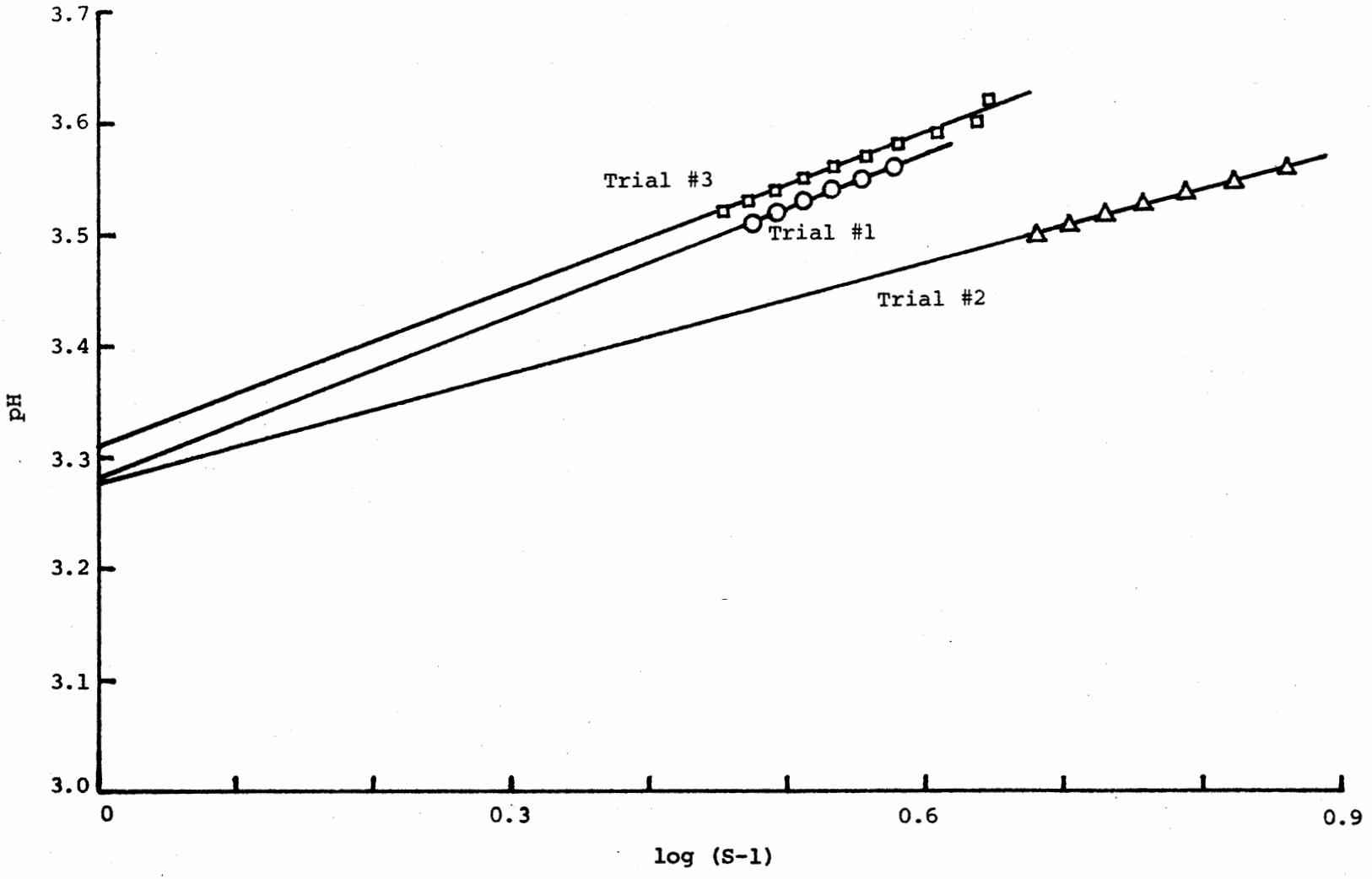

Figure 46. Estimation of pKa_1 for 8-$H_2O^+_x$ Using Synthesized CPG-8HO_x Resin

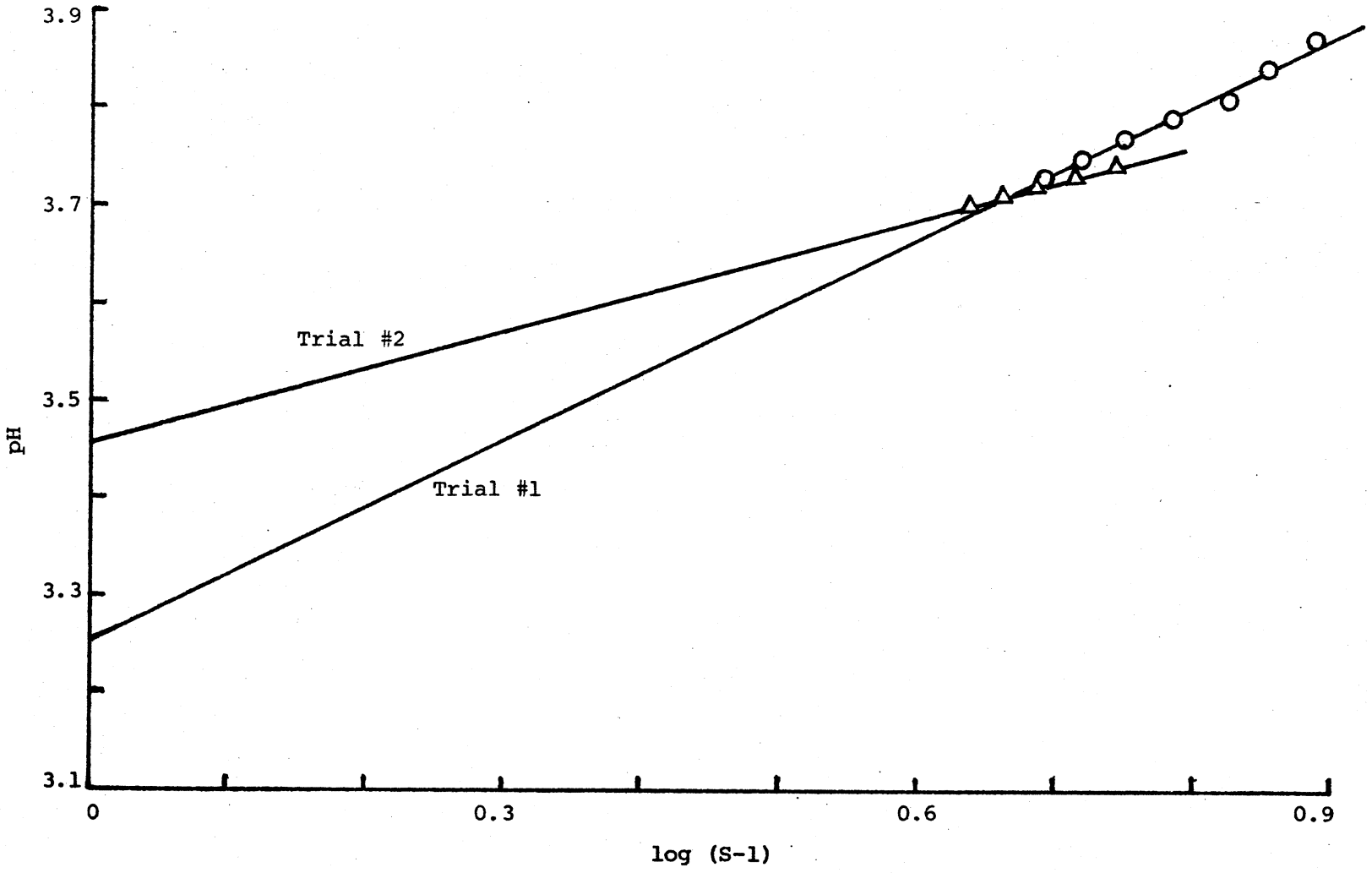

Figure 47. Estimation of pKa_1 for $8\text{-}H_2O_x^+$ Using Corning $CPG\text{-}8HO_x$ Resin Pretreated With Buffer

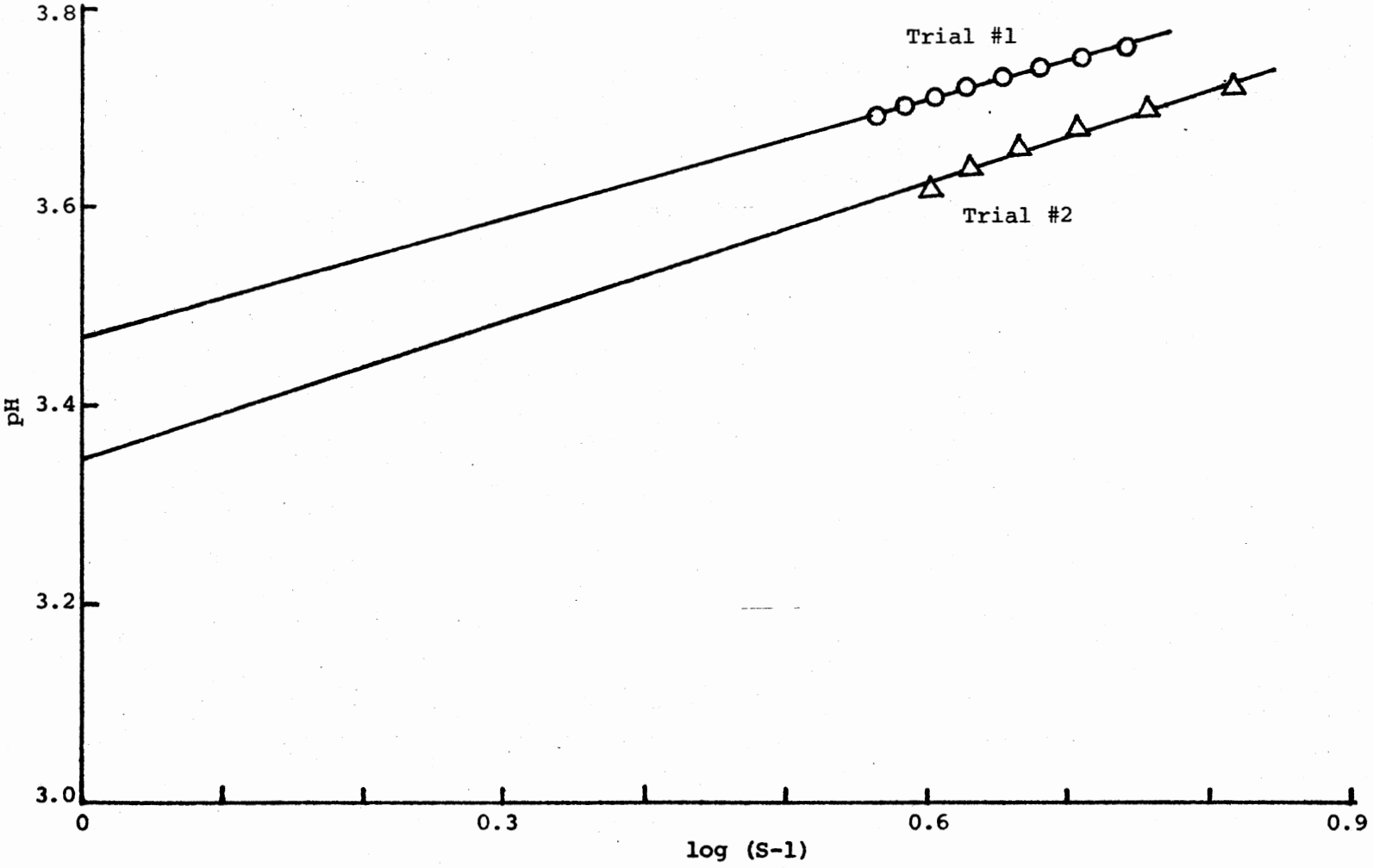

Figure 48. Estimation of pKa_1 for $8\text{-}H_2O^+_x$ Ion Using Corning $CPG\text{-}8HO_x$ Resin

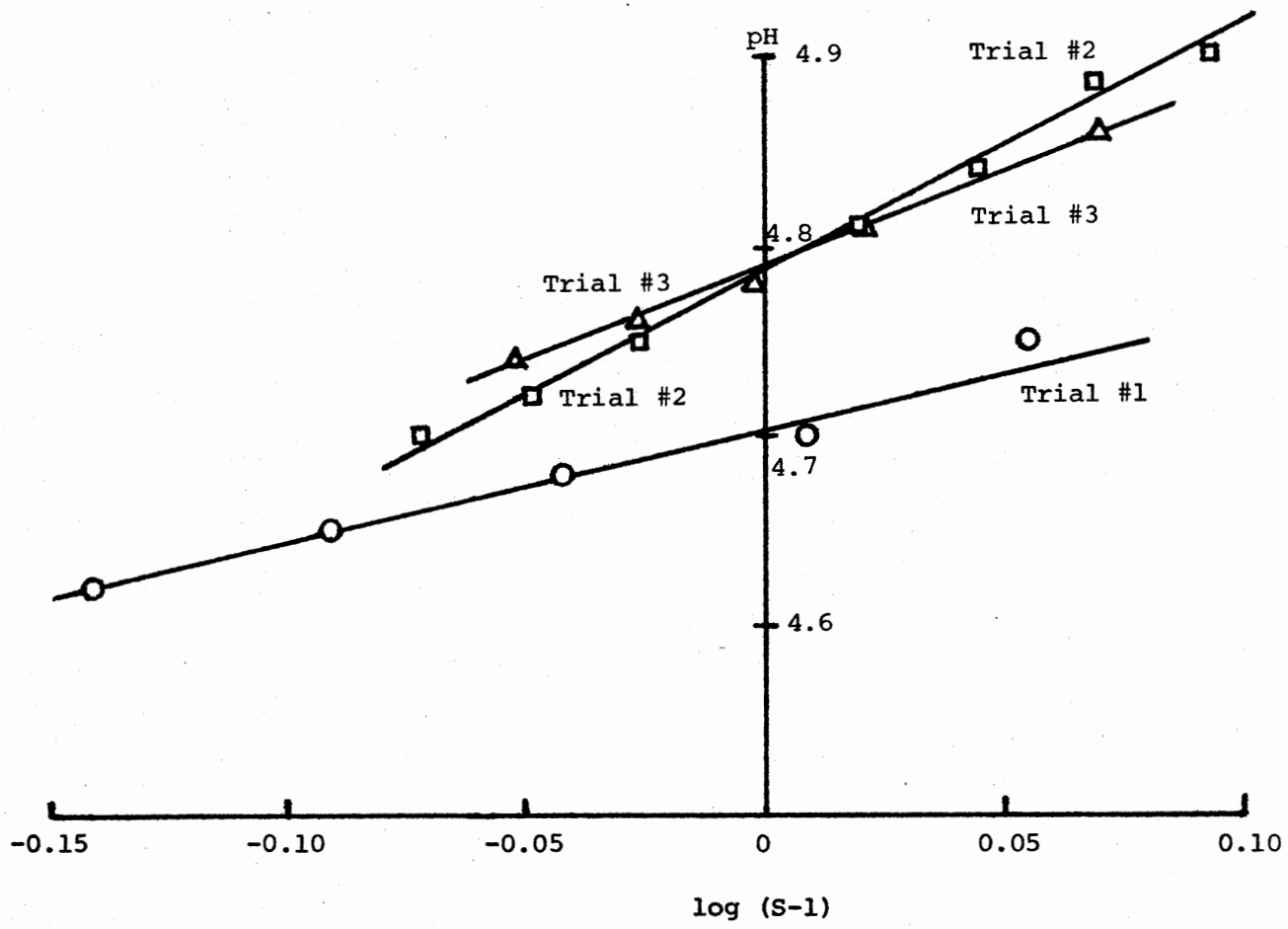

Figure 49. Estimation of pKa_1 Value for Pure 8-Hydroxyquinoline

The average value of pKa_1 for the synthesized CPG-$8HO_x$ is comparable and slightly lower (0.1 - 0.15 units) than that of Corning's. The CPG-$8HO_x$ resins with and without treatment with phosphate buffer have very close values of pKa_1, as shown in Table IX. The pKa_1 obtained from CPG-$8HO_x$ resin is comparable with that of Porasil - $8HO_x$ resin, which was reported as 3.3 by Jezorek and Freiser (36). However, the pKa_1 obtained from the pure 8-hydroxyquinoline is about 1.4 units higher than that obtained from the CPG-$8HO_x$ resin. This may be because the controlled-pore glass is composed of some material (such as silica) which has acidic properties.

E. Distribution Studies for Aromatic and Aliphatic Sulfonates Using the Synthesized CPG-$8HO_x$ Resin

1. Experimental

a. Reagents

The synthesized CPG-$8HO_x$ resin was obtained as described in Chapter IV.D.1. The plain CPG glass beads with a particle size of 37-74 microns, the same pore size (544 Å) (Figure 50), the same pore volume (1.24 cc/g), and the same surface area (57 m^2/g) as those of CPG-AMP, described in part D.1.a, were purchased from Electro-Nucleonics, Inc., (ENI). Aromatic and aliphatic sulfonates have been described previously.

b. Apparatus and Procedure

Same as described in Chapter IV.A.1.b. and IV.C.1.c., respectively.

TABLE IX

pKa_1 of 8-HYDROXYQUINOLINIUM ION OBTAINED FROM CPG-$8HO_x$ RESIN AND PURE 8-HYDROXYQUINOLINE BY POTENTIOMETRIC TITRATION

Source of 8-Hydroxyquinoline	Amount (g)	Amount (mmole)[a]	pKa_1 Value Determined	Average pKa_1	Figures
Synthesized CpG-$8HO_x$ Buffered	0.5000	0.0970	3.49; 3.19; 3.13	3.27	45
Synthesized CPG-$8HO_x$ Without Buffer	0.5000	0.0970	3.28; 3.27_5; 3.31	3.29	46
Corning CPG-$8HO_x$ Buffered	1.000 0.5000	0.0920 0.0460	3.25 3.46	3.36	47
Corning CPG-$8HO_x$ Without Buffer	0.5000	0.0460	3.47; 3.35	3.41	48
Pure $8\text{-}HO_x$	0.0092	0.063_4	4.70; 4.79; 4.79	4.76	49

a. The capacities are 0.092 mmole $8\text{-}HO_x$ per g of Corning CPG-$8HO_x$ resin and 0.194 mmole $8\text{-}HO_x$ per g of the synthesized CPG-$8HO_x$ resin.

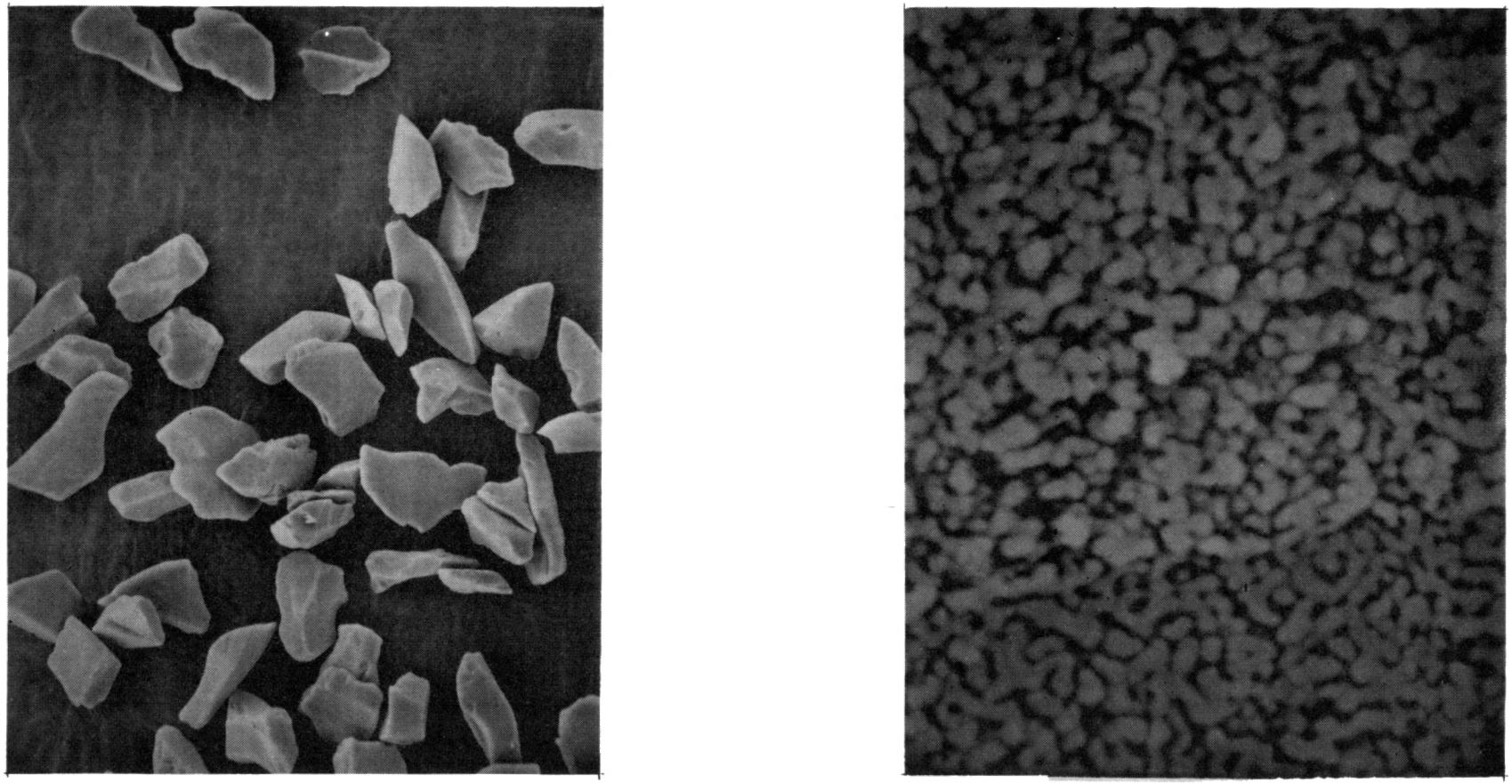

Figure 50. Electron Scan Micrograph for CPG Plain Glass Beads With Particle Diameter of 37-74 μ and Pore Size of 544 Å. The magnification is 100X (Left) and is 30000X (Right)

2. Results

Calibration curves of absorbance versus concentration at 260 nm, 259 nm, 271 nm, and 281 nm for benzenesulfonate, p-toluesulfonate, 2-mesitylenesulfonate, and 1-naphthalenesulfonate, respectively, are similar to Figures 33, 25, 34, and 35, respectively. Calibration curves for methanesulfonate and ethanesulfonate, as shown in Figures 36 and 37, respectively, are directly used. The effect of pH on K_d for aromatic and aliphatic sulfonates using the synthesized CPG-8HO$_x$ resin are shown in Figures 51 and 52, respectively. The effect of pH on K_d for aromatic sulfonates using ENI plain glass beads is also shown in Figure 51 in solid symbols.

3. Discussion

a. The values of K_d obtained in Figure 51 for aromatic sulfonates with the synthesized CPG-8HO$_x$ resin gave a trend of distribution like that of Corning CPG-8HO$_x$ resin (Figure 38). That is, the K_d values increase in the order $BS^- < PTS^- < 2\text{-}MS^- < 1\text{-}NS^-$ in the low-pH region (1-3). The reasons for this have been discussed previously in Chapter IV.C.4.a. and should apply here. The K_d at a given pH (in the low-pH region) is larger for the synthesized CPG-8HO$_x$ resin than for Corning's as a result of the larger capacity, which permits accommodation of more sulfonate per gram of resin. Hence, for $1\text{-}NS^-$ and $2\text{-}MS^-$, the K_d values obtained using the synthesized CPG-8HO$_x$ resin are about 1.5 times as large as those obtained from Corning's. However, the K_d for p-toluene-sulfonate and benzenesulfonate are close and about the same as those obtained from Corning's. This may be because BS^- and PTS^- are not hydrophobic enough to be largely extracted to the resin as those of

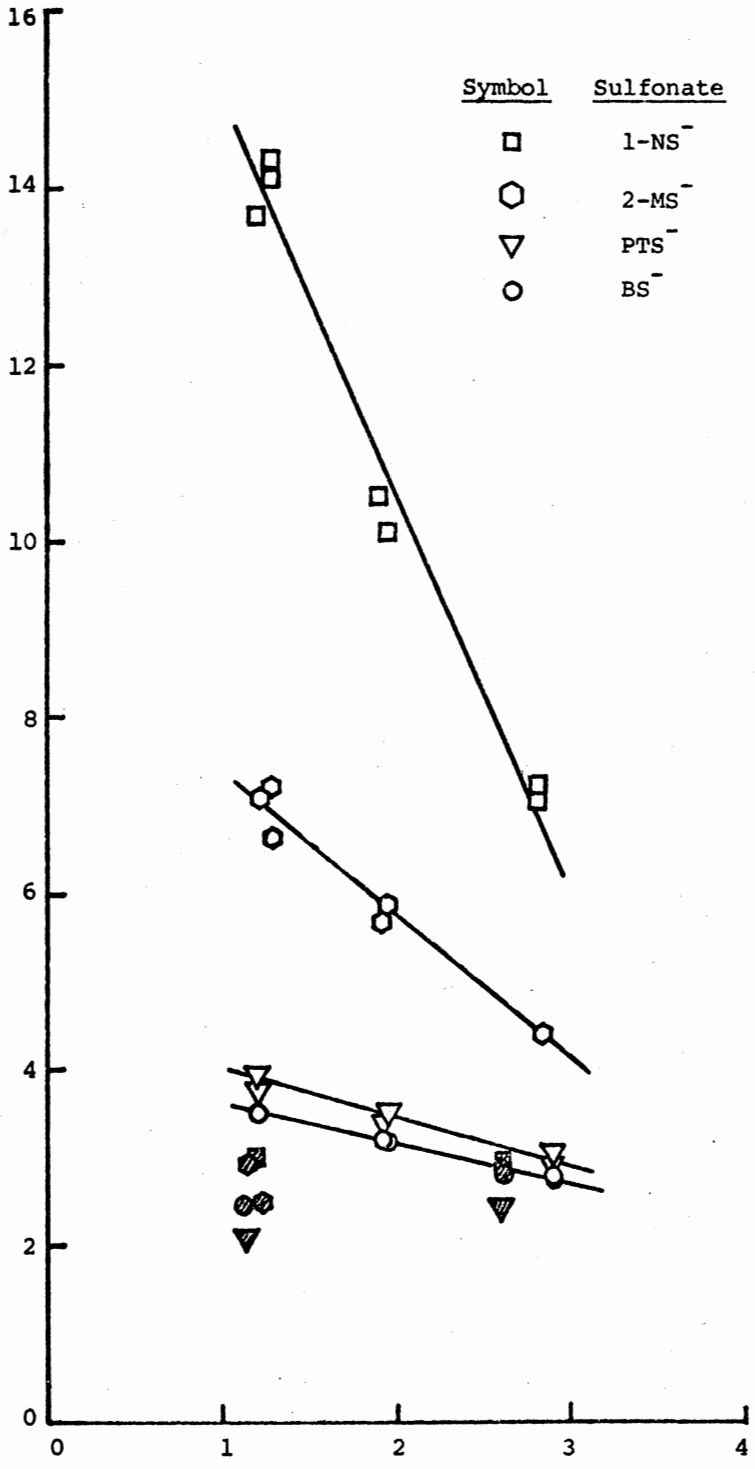

Figure 51. Effect of pH on K_d for Aromatic Sulfonates Using the Synthesized CPG-8HO$_x$ Resin in Open Symbols and the ENI Plain CPG Glass Beads in Solid Symbols

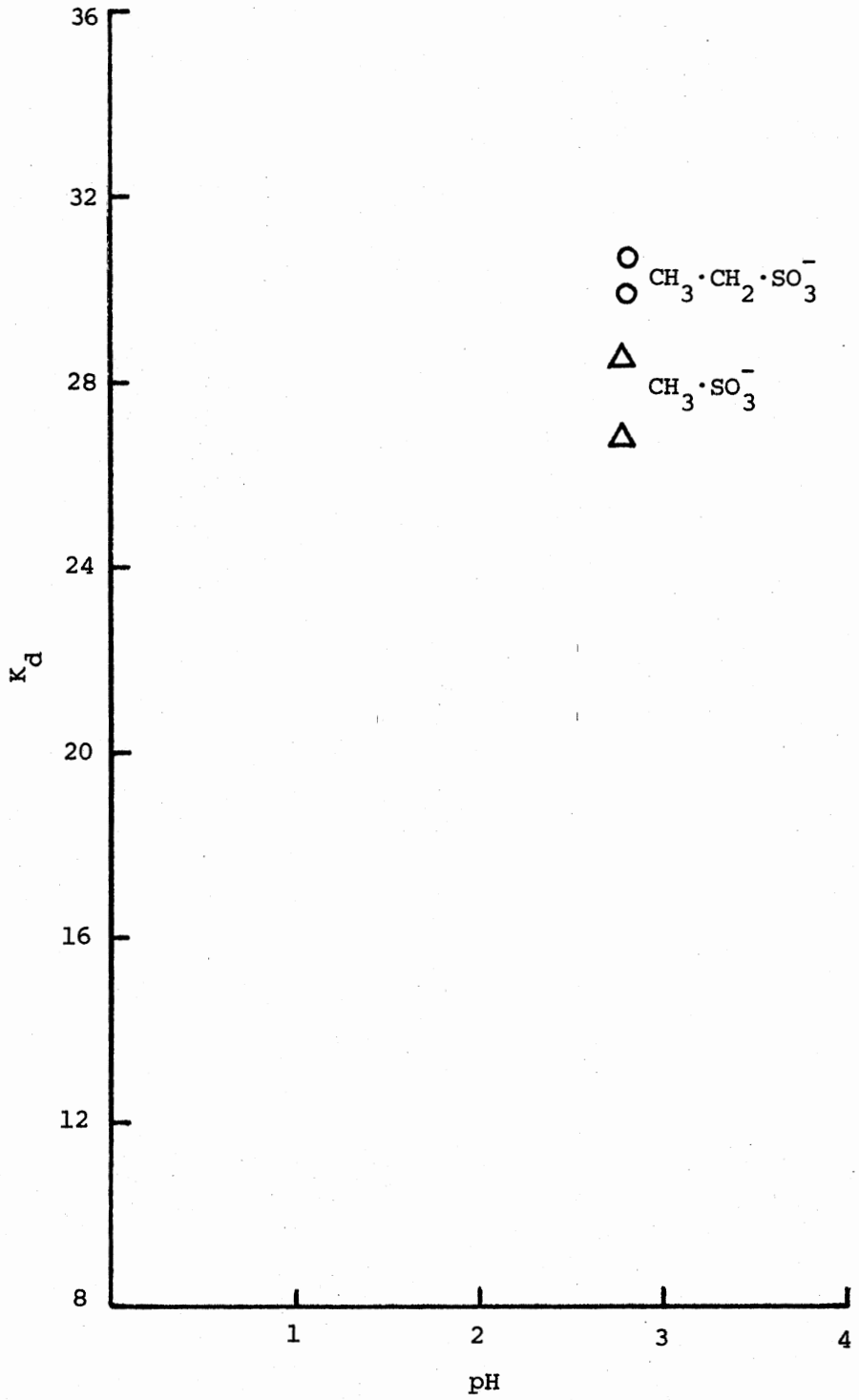

Figure 52. K_d Values for Aliphatic Sulfonates at pH ≅ 2.8 Using the Synthesized CPG-8HO$_x$ Resin

2-MS^- and 1-NS^-. From the results obtained in Figure 51, the predicted elution order for these aromatic sulfonates in a chromatographic separation at low pH is the same as for the Corning resin (Chapter IV.C.4.b). However, the retention for 2-MS^- and 1-NS^- on the resin will be longer because of the larger K_d values.

b. When the ENI plain CPG glass beads are used, the K_d values obtained for aromatic sulfonates in Figure 51 are almost constant (~2.5) and comparable with those obtained from Corning CPG plain glass beads, about 3.2 (Figure 39). This is because both plain glass beads have the same particle size and pore diameter, except that the Corning CPG plain glass beads have a slightly larger surface area (70 m^2/g) than those of ENI's (57 m^2/g).

CHAPTER V

A LITERATURE REVIEW OF ANALYTICAL METHODS FOR SEPARATION AND DETERMINATION OF ALIPHATIC AND AROMATIC SULFONATES

Among the anions tested in liquid-liquid systems (Chapter III), p-toluenesulfonate ion gave the largest $K_{D(H_2O_x^+,A^-)}$ value. This restricted the distribution studies to sulfonates. The results of molar distribution coefficients obtained using the CPG-8HO$_x$ resin in batch experiments (Chapter IV) show that a chromatographic separation of aromatic sulfonates or a group separation of aromatic from aliphatic sulfonates is possible. Hence, a literature review on the analytical methods for separation and determination of sulfonates was made in this chapter.

A. Preface

Sulfonates are extensively used in the petroleum industry (57) as flotation agents, emulsifiers, corrosion inhibitors, lubricants, etc. Sulfonates are also important because of their use in synthetic detergents which can lead to water pollution and become relevant to sewage treatment (58). As such, a review of methods which have been used in the determination and separation of aliphatic and aromatic sulfonates is of interest.

In this review, seven methods of separation and twelve methods of

determination for sulfonates, published during the past twenty years, are compared. Papers that are not included in this comparison are cited in the Appendix B.

B. Determination Methods

The methods reviewed involve titrimetry including two-phase titration, gravimetry, ultraviolet, visible, and infrared absorption spectrometry, gas chromatography, nuclear magnetic resonance, mass spectrometry, atomic absorption, radiometry, and the use of ion-selective membrane electrodes.

1. Titrimetric Methods

One phase titration methods are based on titration of the corresponding sulfonic acids with a standard base by using indicators, for example, phenolphthalein or neutral red. A determination of aromatic sulfonation mixtures containing sulfuric and sulfonic acids was analyzed by Houff, Christie, and Beaumont (59) in 1957. After precipitating sulfates by adding barium hydroxide, the mixture was filtered. The filtrate was converted to the corresponding sulfonic acids by passing through a cation exchanger in the (H^+) form and then titrated with 0.1 N NaOH using phenolphthalein indicator. Six commercial compounds containing aromatic sulfonates were determined in three replicates with accuracy and precision of ± 0.3% and ± 1%, respectively. In this review, accuracy is reported as relative % error and precision is reported as relative % average deviation from the mean. This method determines the total amount of sulfonate in a smaple provided that the barium sulfonates are soluble in the presence of barium hydroxide solution.

Using neutral red and thymolphthalein indicators, Gribova (60) determined 1-naphthalenesulfonic acid in sulfuric acid by titrating with tetraethylammonium hydroxide in a benzene-ethanol (2:1) mixture. The first equivalent point, at which the color changes from red to yellow, indicates the complete neutralization of the sulfonic acid and conversion of the sulfuric acid to hydrogen sulfate, HSO_4^-; the second equivalent point, at which the color changes from yellow to blue-green, indicates that the hydrogen sulfate is completely neutralized. The results of the 1-naphthalenesulfonic acid analysis were comparable with those obtained from the potentiometric titration, with accuracy and precision of ± 0.074% and ± 0.46%, respectively. The titrimetric methods are simple and need only simple equipment, but they are ususally slow.

2. Two-Phase Titration Methods

The determination of anionic surfactants by forming a complex with methylene blue, extracting into chloroform, and titrating with cationic surfactants until the color in the two phases is identical was introduced by Epton (61) in 1948. Using this technique, Fenwick (62) in 1971 determined the content of sulfonate in an oil-soluble petroleum sulfonate by titrating with Hyamine 1622 [(p-(tert-octylphenoxy)ethoxy)ethyldimethylbenzylammonium chloride]. The complex of methylene blue with sulfonate in chloroform is replaced by that of Hyamine-sulfonate and the liberated methylene blue can be extracted out of the chloroform layer. The end point is obtained when the colors of both phases are identical. The results of ten determinations were obtained with a mean of 67.6%, a standard deviation of 0.029%, and a coefficient of variation of 0.25%.

Instead of methylene blue, a mixture of a cationic dye (dimidium

bromide: 2,7-diamino-10-methyl-9-phenylphenanthridinium bromide) and an anionic dye (disulphine blue, also known as Erioglaucine) was used by Brewer (63) in 1972 to determine the sulfonate content of oil-soluble sulfonates. After the dimidium-sulfonate complex was formed in chloroform layer, the two-phase mixture was titrated with Hyamine. The dimidium-sulfonate complex was replaced by Hyamine-sulfonate until an excess amount of Hyamine formed a chloroform soluble blue complex with disulphine blue. The color in the chloroform layer then changed from red through grey to blue. The grey color was taken as the end point. The amount of sulfonate was calculated from the amount of Hyamine used. The results for sodium and calcium petroleum sulfonates obtained by two-phase titration were comparable with those obtained from ASTM (The Standard of American Society for Testing and Materials) D 855-56 and D 1216-56 methods, respectively.

Determinations of linear alkylbenzenesulfonates (LAS) in fresh water and sea water by use of two-phase titration was reported in 1973 by Wang et al. (64). Wang et al. analyzed branched-chain alkylbenzene-sulfonates in commercial detergents (65).

The sulfonate sample in water was treated with a known excess of cetyldimethylbenzylammonium chloride to form a nondissociated complex of the quaternary ammonium sulfonate. After adding chloroform to the solution, the excess of quarternary ion was dissolved in chloroform, where it formed a yellow color. The two-phase mixture was then titrated with standard sodium tetraphenylborate until the excess ammonium ion was removed from the chloroform layer and the yellow color disappeared. The accuracy for LAS was ± 10% in sea water and ± 5.2% in fresh water; the precision was ± 0.4%. This titration is simple, fast, and free from

interference by inorganic salts in water samples, except for relatively high concentrations of potassium ion, which forms a precipitate with tetraphenylborate anion. Another limitation is that the technique determines only the total content of anionic surfactant in water sample. The two-phase titration methods are reliable for determining the sulfonates in oil-soluble petroleum sulfonates.

3. Gravimetric Methods

An alkylarenesulfonate forms a precipitate with benzidine dihydrochloride as follows:

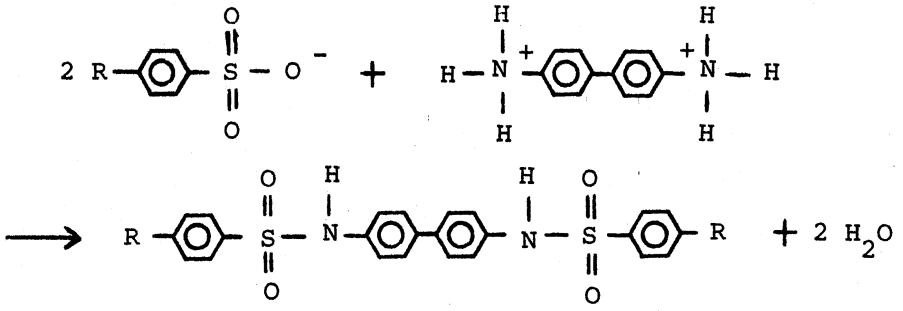

(79)

The amount of the alkylarenesulfonate is proportional to that of the corresponding precipitate and can be determined from a calibration curve. Maurmeyer and Rafalowitz (66) used this technique in 1964 to analyze sodium salts of dodecylbenzenesulfonates and nonylbenzenesulfonates in commercial materials. The accuracy was within ± 3% for 15 mg of C_{12}-SO_3^- and 22 mg of C_{11}-SO_3^-, and the precision was within ± 0.8% for both.

The composition of petroleum sulfonic acids in acid sludges, which were obtained by sulfonation of various petroleum hydrocarbon oils, was investigated by Chhibber, Anand, and Malik (67) in 1976. After neutralizing the sulfuric acid and petroleum sulfonic acids by titration with 0.5 N NaOH using thymol blue and phenolphthalein indicators, re-

spectively, the oil part was removed by extraction with petroleum ether and the aqueous part was evaporated to dryness for analysis for petroleum sulfonic acids. Six acid sludges (10-15 g) were analyzed in three replicates; the results were comparable to those obtained with the modified ASTM D-855 with an accuracy of ± 5.5%. In the same year, the determination of content of petroleum sulfonates by titrating the sample in a mixture of water and 2-propanol with a base using phenolphthalein indicator was reported by Parmar and Sahukar (68). After removing the oil part by extraction with solvent naphtha, excess sodium carbonate was slowly added to the aqueous alcohol solution, which formed two layers. The clear alcohol layer was evaporated to dryness for determination of the petroleum sulfonates. The results were also comparable with those obtained with the ASTM D-855 method with an accuracy of ± 2.6%.

4. Ultraviolet Absorption Methods

Since the UV spectrum of benzene having various alkyl substituents on the ring gives different maximum absorption peaks in the region of 210-290 nm, the concentration of an arenesulfonate in a solution can be determined by measuring the absorbance at a suitable wavelength and using Beer's Law. For a mixture of arenesulfonates, absorbances are measured at several wavelengths and the concentration of each sulfonate is calculated by solving a set of linear equations.

Using this technique, the composition of alkylarenesulfonates in several commercial detergents was determined in the region of 210-230 nm by Kelly, Blank, Thompson, and Fine (69). The maximum absorbance at 224 nm was used for studies of the alkylarenesulfonates. The accuracy and precision were within ± 1% for the three detergents tested.

Later, an improved automatic procedure for preparing liquid samples of detergents containing alkylarenesulfonate by using a Technicon Preparative Sampler and instrumentally recording the peak height of absorbance at 224 nm was reported by Brandli and Kelley (70) in 1970. The peak height measured at 224 nm is proportional to the amount of alkylarenesulfonate. In the twelve random samples of detergents studied, the accuracy and precision were within ± 4.8% and ± 3.5%, respectively. The speed of analysis is about 10 min/sample. This can be used as a routine check for the determination of alkylarenesulfonate in detergent manufacturing.

A multicomponent analysis of mixtures of ortho-, meta-, and para-toluenesulfonic acids in sulfuric acid solution was reported by Cerfontain, Duin, and Vollbracht (71). From the spectrum of each component, represented in Figure 53, the absorbances of both standard and unknown mixtures were measured manually at 39 equidistant points between 243 and 281 nm with a Zeiss PMQ II spectrophotometer. The concentration of each sulfonate in the unknown was computer-calculated using a curve-fitting program to minimize the mean square residual,

$$r^2 = \frac{\sum_{i=1}^{k} (A_{i,calc} - A_{i,obs})^2}{k-n} \qquad (80)$$

where $A_{i,calc} = \sum_{j=1}^{n} \varepsilon_{ij}(b)C_j$ = absorbance calculated at wavelength i

ε_{ij} = molar absorptivity of component j at wavelength i

C_j = the concentration of component j

b = the cell path length

k = number of data points

n = number of constituents in the unknown mixture

r = the mean square residual

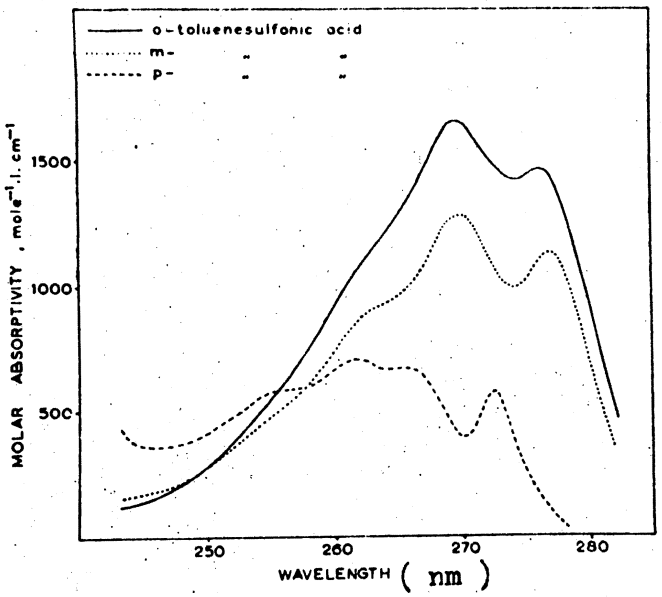

Figure 53. UV Absorption Spectra of Three Isomeric Toluenesulfonic Acids in 82.4 Weight % Sulfuric Acid

Using the same technique (71) in the region of 240-300 nm, Cerfontain et al. (72) analyzed several more isomeric mixtures of arenesulfonic acids. The applicability of this method depends on the differences in shape of the absorption spectra of the components. The accuracy ranges from ± 0.8 to ± 20%.

5. Colorimetric Methods

Determination by colorimetric methods is based on the formation of a colored dye-sulfonate complex, of which the color intensity is propor-

tional to the amount of sulfonate and can be measured by a colorimeter or a spectrophotometer in the visible region.

a. Methylene Blue Method

A determination of anionic detergent, mainly sodium alkylbenzenesulfonates, in sewage effluents by use of a basic methylene blue solution in chloroform was reported by Longwell and Maniece (73). The absorbance of methylene blue-sulfonate complex in chloroform was measured with a photoelectric absorptiometer at 650 nm. The results showed about 97% recovery of added detergent in effluent in the range of 10-20 ppm. The colorimetric method with methylene blue involving formation of the dye-sulfonate complex and extracting it into chloroform is time-consuming. Since thiocyanates (at 30 ppm) largely interfere with the extraction, they should be removed by oxidation with hydrogen peroxide before extracting with chloroform.

Another determination of trace amounts (ppm) of alkylbenzenesulfonates in river waters by forming methylene blue sulfonate complex and adsorbing on polyurethane foam was reported by Tanaka, Hiiro, and Kawahara (74) in 1973. The color intensity of the foam is proportional to the concentration of alkylbenzenesulfonate and may be estimated by visual comparison with a series of standards. The accuracy of determination of alkylbenzenesulfonate found in the Ikeda City River (Japan) was ± 12% at 11 ppm and ± 8% at 16 ppm; the limit of detection was 0.5 ppm.

b. Azure A Method

In 1976, Wang (75) and Ross (76) used Azure A to determine trace amounts (0-10 ppm) of linear and branched-chain alkylbenzenesulfonates

in water. The Azure A sulfonate complex was soluble in chloroform and the absorbance of that was measured in a spectrophotometer at 623 nm. The concentration of alkylbenzenesulfonate is determined by comparing with a calibration curve of absorbance versus concentration. The colorimetric method with Azure A has several advantages over that with methylene blue (73): (i) The color of the complex is more intense; (ii) the dye reagent is more stable under light exposure; (iii) the chloroform extraction time is less.

c. Diazosulfanilic Acid Method

A detemination of aromatic sulfonates by alkali fusion and subsequent formation of azo dyes by coupling with diazosulfanilic acid was studied by Whitlock, Siggia, and Smola (77) in 1972. Six sodium salts (3-10 mg) of benzenesulfonates and naphthalenesulfonates were analyzed and the azo dyes were measured at 461 nm by visible spectrophotometry with precision of ± 2.2%. This is a complementary method for gas chromatography (84) in the determination of sulfonates which have low volatility after converting to the corresponding phenols. The process, however, has the same limitations of gas chromatography (84) and is not suitable for the determination of sulfonates containing free halogen groups.

6. Infrared Spectrometric Methods

In general, if the position and intensity of a stretching band, arising from vibrations of a sulfonate group, are not affected significantly by changes in alkyl substituion on a benzene ring, a variety of homologs and isomers of alkylbenzenesulfonates can be determined by

infrared spectrometric methods by appropriate selection of wavelengths. As early as 1949, the IR spectrum of ammonium xylenesulfonates in KBr pellet was studied by Schreiber (78) and by Koch et al. (79); it is shown in Figure 54.

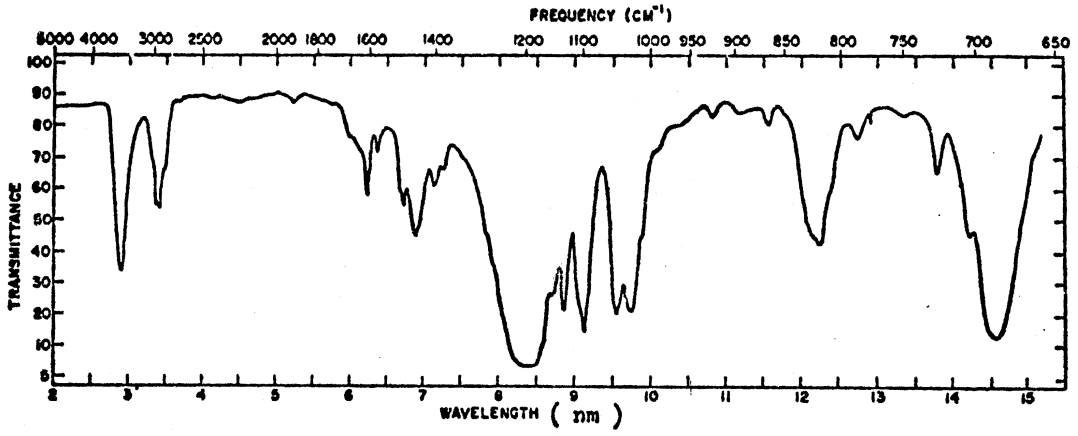

Figure 54. IR Spectrum for Ammonium Xylenesulfonates in KBr Pellet [Taken From Reference (81)]

The band representing S-O asymmetric stretching vibration, centered at 1175 cm^{-1} (80), was used for the analysis of toluene- and xylenesulfonate solutions by Kullbom and Smith (81) in 1963. Thirteen samples of ammonium and sodium xylenesulfonates were analyzed and the results were comparable with those obtained with a gravimetric method with a relative error of ± 1%.

7. Gas Chromatographic Methods

Mixtures of alkanesulfonates, mixture of arenesulfonates, and mixtures of alkane- and arenesulfonates can be analyzed by gas chroma-

tography provided that sulfonates are converted to volatile, thermally stable derivatives. Kirkland (82) thus analyzed several systems of sodium sulfonates by converting them to the corresponding sulfonyl chlorides. A column (2 ft. x 6 mm) packed with Chromosorb (40/50 mesh) coated with 20% silicone grease and a helium carrier gas were used. The following mixtures were studied:

- 1-butanesulfonate and 3-methyl-1-butanesulfonate;
- benzenesulfonate, p-toluenesulfonate, and 2,5-dimethylbenzenesulfonate;
- benzenesulfonate, p-toluenesulfonate, and 2-naphthalenesulfonate;
- p-n-butylbenzenesulfonate and 1-dodecanesulfonate.

The accuracy in systems 1, 2, and 4 was within ± 2.8%, ± 5.1%, and ± 2%, respectively, and ± 21% for system 3. Although the time of analysis for each system by GC is less than 12 minutes, it takes several minutes to two hours to prepare a sulfonyl chloride sample. This method is not applicable to sulfonates containing substituents that react with thionyl chloride, such as -OH or $-NH_2$ groups.

Another analysis of long-chain α-alkenesulfonates (C_{14}-C_{18}) and hydroxyalkanesulfonates by hydrogenation with H_2/Pd and conversion to sulfonyl chlorides was reported by Nagai, Hashimoto, Yamane, and Mori (83) in 1970. A glass column (2.5 m x 4 mm) packed with 3% Silicone SE-30 on Chromosorb W (60/80 mesh) was used. The qualitative and quantitative analyses of unknown mixtures were determined by comparing the retention times and peak areas with those of standards. Mixtures of C_{16}- and C_{18}-α-alkenesulfonates/hydroxyalkanesulfonates were analyzed with accuracy of ± 2.8% and ± 2.2%, and precision of ± 7.0% and ± 5.9%, respectively.

A determination of arenesulfonates involving alkali fusion was

reported by Siggia, Whitlock and Tao (84) in 1969. The resultant phenol, which corresponds to the amount of arenesulfonate, is measured by gas chromatography. The accuracy obtained for five pure arenesulfonates was within ± 3% and for a mixture of three arenesulfonates, within ± 4%.

Later, pyrolysis-gas chromatography was used by Siggia and Whitlock (85) to determine SO_2 derived from nonvolatile arenesulfonic acids and their salts. The accuracy for ten arenesulfonates was within ± 2.8%.

8. Nuclear Magnetic Resonance

From the NMR spectra of a mixture of isomers, if the absorption regions are relatively separated and the areas are proportional to the number of nuclei involved, a quantitative analysis of the mixture is possible. In 1974, Cerfontain, Koeberg-Telder, Kruk, and Ris (86) determined the composition of a mixture of isomeric toluenedisulfonates by obtaining areas under different absorption regions from a NMR spectrum and solving a set of linear equations as in Equation (81).

$$ {}_jA = ({}_jp_1x_1 + {}_jp_2x_2 + ... + {}_jp_ix_i)\ S \qquad (81) $$

where ${}_jp_i$ = the number of magnetically equivalent nuclei of isomer i which absorbs in area j

x_i = the mole fraction of isomer component i

${}_jA$ = the area of region j

i = 1, 2, ..., m = components of isomer

j = 1, 2, ..., n = the well separated regions in the spectrum

S = a proportional constant

A mixture of toluene-2,5-, -3,4-, and -3,5-disulfonic acids in sulfuric acid was analyzed with accuracy and precision within ± 6%.

9. Mass Spectrometry

Since sulfonates and most sulfonic acids of commercial importance have low volatility, they may be converted to the corresponding volatile sulfonic esters by reaction with diazomethane or tetramethylammonium hydroxide and may be identified by mass spectrometry. In 1970, Heywood, Mathias, and Williams (87) analyzed five unknowns containing benzene-, naphthalene-, and anthraquinonesulfonates by comparing with the molecular ions and fragmentation patterns of nine reference compounds. This method is used only for qualitative analysis of unknown sulfonates.

10. Atomic Absorption Methods

Sulfonates extractable into a suitable organic solvent and forming an ion-association compound with a proper metal complex cation can be determined by atomic absorption methods (88). In 1976, Crisp, Eckert, Gibson, Kirkbright, and West (89) determined linear alkylate sulfonates (LAS) in water samples at a level below 50 ppb by use of atomic absorption. The LAS was extracted into chloroform and converted to compound with bis(ethylenediamine)copper(II). The copper compound in chloroform was measured at 324.7 nm with an atomic absorption spectrophotometer (Perkin-Elmer 300 S). The accuracy of the recovery of LAS in sea water was 92%, the precision was within ± 5% in the range of 10 ppb to 200 ppb, and the limit of detection was 2 ppb. Most anions (Cl^-, NO_3^-, SO_4^{2-} at 0.5 M; SCN^-, ClO_4^-, NO_2^-, CH_3COO^- at concentrations of 1 g/l) and metal cations (Cu^{2+}, Ni^{2+} at 100 mg/l; Al^{3+}, Cr^{3+}, Mn^{2-}, Zn^{2+}, Co^{2+} at 10 mg/l) do not seriously interfere with the determination of LAS, but sulfide (0.1 mg/l) and Fe^{3+} (1 mg/l) do. These interferences can be

suppressed by treating with 30% H_2O_2 and 2% EDTA, respectively, before adding bis(ethylenediamine)Cu(II). This method is reliable for determining trace amounts of sulfonates down to 10 ppb in fresh water or sea water.

11. Radiometric Methods

A determination of trace amounts of anionic surfactants by a radiometric method was reported by Taylor and Waters (90) in 1972. It is based on the fact that anionic surfactants form complexes with ^{59}Fe-labelled ferroin, $[^{59}Fe(II)(1,10\text{-phen})_3]^{2+}$, and these complexes are soluble in chloroform. The amount of labelled ferroin extracted into chloroform is proportional to the concentration of anionic surfactants and can be measured by a proportional counter. Using this technique, Clementz (91) reported the determination of alkylarenesulfonates in crude oils. The detection limit of petroleum sulfonate was 0.5 μg in crude oils. The results were comparable with those of the two-phase titration method (63). Although the radiometric method is slow, it has an advantage over the two-phase titration method in determining petroleum sulfonates in crude oils because the radiometric method is not limited by the dark color of crude oils and brines.

12. Use of Ion-Selective Membrane Electrodes

A liquid membrane, containing a suitable cation which has a larger ion-association constant or higher sensitivity response with sulfonates than with other anions, can be used as a sulfonate ion selective electrode membrane. In 1968, Coetzee and Freiser (92) reported a membrane composed of methyltricaprylyammonium ion in 1-decanol that had a linear

response to p-toluenesulfonate from 10^{-1} to 10^{-3} M with a response time within 1 minute and a useful life of one month. The crystal violet cation and its analogs in nitrobenzene or in 1,2-dichloroethane as an effective ion-exchange site in the membrane electrode were studied by Ishibashi and Kohara in 1972 (93) and 1973 (94). The assembled cell is represented in Figure 55 (95), where the salt bridge is saturated KCl in agar. The membrane potential of the cell was measured by use of an electrometer across the two saturated calomel electrodes. The results exhibited a linear response (56 mv/log[sulfonate]) for benzenesulfonate from 10^{-1} to 10^{-5} M, for p-toluenesulfonate from 10^{-1} to 10^{-5} M and for 1-naphthalenesulfonate from 10^{-2} to 2×10^{-4} M.

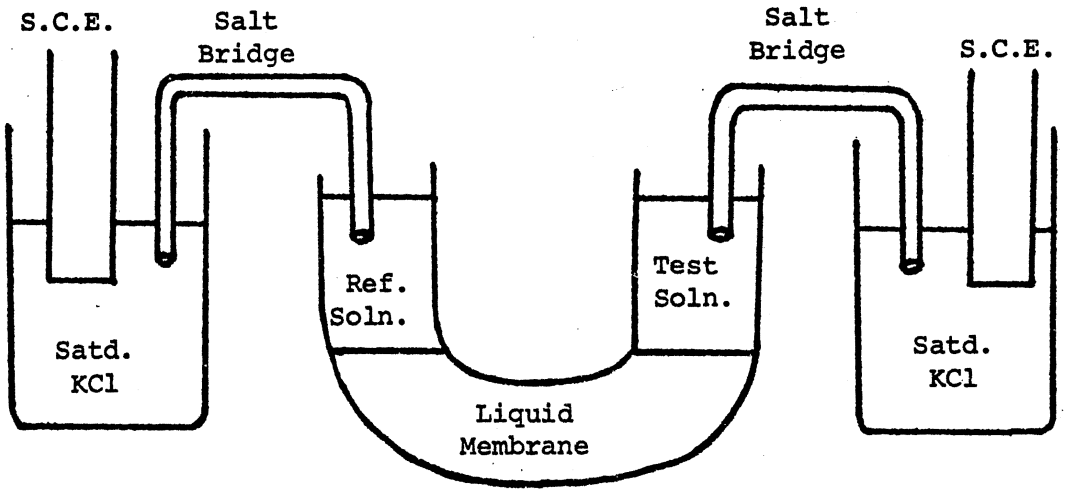

Figure 55. Assembled Cell for Ion-Selective Membrane Electrode

The interferences of nitrate and 1-naphthalenesulfonate ions are large at a benzenesulfonate electrode while those of nitrate and benzenesulfonate ions for a 1-naphthalenesulfonate electrode are small. The

selectivity coefficients $K_{i,j}$ for benzenesulfonate and 1-naphthalene-sulfonate electrodes calculated from Equation (82) are tabulated in Table X. The membrane potentials are stable in the pH range between 2.5 and 12.

$$E = \text{Constant} + \frac{2.303\ RT}{nF} \log \left(A_i + K_{i,j}\ A_j^{\frac{Z_i}{Z_j}} \right) \qquad (82)$$

where E = the membrane potential

i = the primary sulfonate ion

j = the interfering ions in the sample solution

A_i, A_j = activities of ions i and j, respectively

Z_i, Z_j = charges of ions i and j, respectively

The use of ion-selective membrane electrodes provides a rapid and convenient measurement of individual concentration of sulfonates in the range of 10^{-5} ~10^{-1} M.

C. Summary of Observations on Methods of Determination

1. Among the twelve methods of determination of sulfonates, the mass spectrometric method is used only for qualitative analysis; the other methods can be used for quantitative analysis.

2. The type of sulfonates determined, the accuracy, precision, amounts used, detection limit, and speed of the process are summarized in Table XI.

3. From Table XI, the most rapid methods are two-phase titration (62)(63)(64), UV (70), colorimetry with Azure A (76), IR (81), and use of ion-selective membrane electrode (94). Among these, the ion-selective

TABLE X

SELECTIVITY COEFFICIENTS ($K_{i,j}$) FOR BENZENESULFONATE AND 1-NAPHTHALENESULFONATE ELECTRODES

Benzenesulfonate Electrode			α-Naphthalenesulfonate Electrode		
Interferent, j	C_j (M)	$K_{BS,j}$	Interferent, j	C_j (M)	$K_{NS,j}$
Cl^-	0.5	0.003	Cl^-	0.5	0.0004
NO_3^-	0.005	0.76	NO_3^-	0.005	0.03
Phenol-4-sulfonate	0.005	0.016	Benzenesulfonate	0.005	0.07
Benzene-m-disulfonate	0.005	0.005	1,5-Naphthalenedisulfonate	0.005	0.0007
Benzoate	0.005	0.04	1,3,6-Naphthalenetrisulfonate	0.1	0.00006
1-Naphthalenesulfonate	0.00025	16	4-Hydroxy-2-naphthalenesulfonate	0.005	0.025
1,3,6-Naphthalenetrisulfonate	0.005	0.0008	2,3-Dihydroxynaphthalene-6-sulfonate	0.005	0.00045

TABLE XI

SUMMARY OF OBSERVATIONS ON METHODS OF DETERMINATION

Ref.	Method	Type of Sulfonates Determined	Accuracy (± %)	Precision (± %)	Amount of Sample Used (g)	Detection Limit (g)	Approximate Time Required for Process (hr)
(59)	titrimetric	aromatic	0.3	1.0	0.5-0.6	----	2
(60)	titrimetric	aromatic	0.074	0.46	0.2	----	2
(62)	two-phase titrn. (methylene blue)	aromatic	-----	0.25	8×10^{-2}	----	0.5
(63)	two-phase titrn. (two dyes)	aromatic	0.3	0.9	$(2-10) \times 10^{-2}$	----	0.5
(64)	two-phase titrn. (back titrn.)	aromatic	5.2-10	0.4	$(1-10) \times 10^{-4}$	----	0.5
(66)	gravimetric	aromatic	3	0.8	2×10^{-2}	----	1
(67)	gravimetric	aromatic	5.5	----	10-15	----	1
(68)	gravimetric	aromatic	2.6	----	10	----	3
(69)	UV	aromatic	1	1	0.9-1.1	----	1
(70)	UV	aromatic	4.8	3.5	$(1.8-2.3) \times 10^{-1}$	----	0.3
(71)	UV	aromatic	0.8-20	----	$(1-10) \times 10^{-4}$	----	1
(72)	(multicomponent)						

TABLE XI (Continued)

Ref.	Method	Type of Sulfonates Determined	Accuracy (± %)	Precision (± %)	Amount of Sample Used (g)	Detection Limit (g)	Approximate Time Required for Process (hr)
(73)	colorimetric (methylene blue)	aromatic	1-3	----	$(2\text{-}25)\times10^{-5}$	-----	4
(74)	colorimetric (M.B.+polyurethane foam)	aromatic	8-12	----	1×10^{-4}	1×10^{-5}*	1
(76)	colorimetric (Azure A)	aromatic	----	----	$(5\text{-}15)\times10^{-2}$	-----	0.5
(77)	colorimetric (diazosulfanilic acid)	aromatic	----	2.2	$(3\text{-}10)\times10^{-3}$	3×10^{-7}**	1
(81)	IR	aromatic	1.0	----	0.6-0.9	-----	0.5
(82)	GC (sulfonyl chloride)	aliphatic, aromatic, and mixtures of both	2-5	----	0.5	-----	3
(83)	CG (H_2+ sulfonylization)	aliphatic	2.2-2.8	5.9-7.0	3×10^{-5}	-----	4
(84)	GC (alkali fusion)	aromatic	3-4	----	$(1.7\text{-}8.6)\times10^{-3}$	-----	1.5

*The lowest detectable concentration of alkylbenzenesulfonate is 0.5 ppm in 20 ml of water.

**The minimum detectable amount for phenol with absorbance = 0.05, molar absorptivity = 5×10^4 $(cm)^{-1}(\underline{M})^{-1}$, cell length = 1 cm, and a cell volume = 3 ml.

TABLE XI (Continued)

Ref.	Method	Type of Sulfonates Determined	Accuracy (± %)	Precision (± %)	Amount of Sample Used (g)	Detection Limit (g)	Approximate Time Required for Process (hr)
(85)	GC (pyrolysis)	aromatic	2.8	----	$(8.6\text{-}43)\times10^{-3}$	-----	1.5
(86)	NMR	aromatic	6	6	8×10^{-2}	-----	1.5
(89)	atomic absorption	aromatic	8	5	$(5\text{-}20)\times10^{-10}$	1.0×10^{-10}*	1.5
(91)	radiometric	aromatic	comparable to (63)	----	$(5\text{-}100)\times10^{-6}$	5×10^{-7}**	3
(94)	use of ion-selective membrane electrode	aromatic	----	----	$(1.7\text{-}1700)\times10^{-4}$	1.7×10^{-5}***	5

*The concentration of LAS which gave an absorbance equal to twice the standard deviation of a set of 16 absorbance readings at or near blank level was 2×10^{-6} g/l using 50×10^{-6} l.

**The theoretical detection limit in crude oils is approximately 0.5 ppm petroleum sulfonate using 1 ml of undiluted oil.

***In a series of diluted solutions of benzenesulfonate at a constant ionic strength, the concentration starts to deviate from the Nernst linear response at 10^{-5} M using 10 ml solution.

TABLE XII

SUMMARY OF OBSERVATION ON METHODS OF DETERMINATION (CONTINUED)

Ref.	Method	Determination Effected	Advantages	Limitations
(59)	titrimetric	purity of sulfonate in a mixture	simple equipment	barium sulfonates must be soluble in the presence of $Ba(OH)_2$
(60)	titrimetric	industrial sulfonated products	the end point is visible	need to prevent access of CO_2 during the titration
(62) (63)	two-phase titrn. (methylene blue or cationic/ anionic dyes)	sulfonates in oil-soluble petroleum sulfonates	simple equipment	----------
(64)	two-phase titrn. (back titrn.)	trace amounts of LAS or ABS in fresh or sea water	better than (73)	not applicable in presence of relatively high potassium ion concentration
(66)	gravimetric	alkylarenesulfonates by precipitating with benzidine	--------	----------
(67)	gravimetric	petroleum sulfonic acids in acid sludges	simple equipment	----------
(68)	gravimetric	sulfonate in oil-soluble petroleum sulfonates	simple equipment	----------
(69) (70)	UV spectrometric	alkylarenesulfonate in detergents	--------	phenyl chromophores absorbing in 220-230 nm cause interference

TABLE XII (Continued)

Ref.	Method	Determination Effected	Advantages	Limitations
(71)(72)	UV spectrometric (multicomponent)	individual arenesulfonates in an isomeric mixture	--------	applicability depends on differences in shape of spectrum of each component
(73)	colorimetric (methylene blue)	alkylarenesulfonates in detergents	--------	SCN^- ions must be removed before extracting with chloroform
(74)	colorimetric (methylene blue plus polyurethane foam)	alkylbenzenesulfonate traces in river waters	the amount of methylene blue-sulfonate complex bonded on the foam is determined visually	----------
(76)	colorimetric (Azure A)	ABS or LAS in water	better than (73)	only applicable to determine the content of anionic sulfactants
(77)	colorimetric (diazosulfanilic acid)	sulfonates of low volatility after converting to the corresponding phenols	a complementary method for GC (84)	not suitable to determine sulfonates containing halogen groups
(81)	IR spectrometric	isomeric alkylarenesulfonates	--------	----------

TABLE XII (Continued)

Ref.	Method	Determination Effected	Advantages	Limitations
(82)	Gas chromatographic (sulfonyl chloride)	to separate and determine aliphatic or aromatic sulfonates or mixture of both	-----	not applicable to sulfonates containing -OH or $-NH_2$ groups
(83)	Gas chromatographic (hydrogenation and sulfonylization)	α-alkensulfonates and hydroxyalkanesulfonates (C_{14}-C_{18}) in synthetic detergents	-----	some side reactions may interfere with the determination
(84)	Gas chromatographic (alkali fusion	to determine homologous arenesulfonates	-----	not applicable to sulfonates containing halogen groups
(85)	Gas chromatographic (pyrolysis)	mono- and disfulfonates	applicable to nonvolatile sulfonates	----------
(86)	NMR	isomeric arenesulfonates	------	a well separated spectrum is needed
(87)	mass spectrometric	arenesulfonates (qualitative)	------	need access to spectra of enough reference compounds
(89)	atomic absorption spectrometric	anionic detergents in fresh or sea water at ppb levels	------	S^{2-} and Fe^{3+} give large interferences
(91)	radiometric	petroleum sulfonate in crude oils	better than (63)	only a linear calibration curve is used

TABLE XII (Continued)

Ref.	Method	Determination Effected	Advantages	Limitations
(94)	use of ion-selective membrane electrode	individual arenesulfonates	fast response	some anions may interfere

membrane electrode not only has been used in individual determination of arenesulfonates but also has potential for the individual determination of alkanesulfonates.

4. The applications, advantages, and limitations of the methods of determination are summarized and compared in Table XII.

5. From the viewpoint of accuracy, the methods of titrimetry (59) (60) and two-phase titration with two dyes (63) give an accuracy within ± 0.3%. In these two, the two-phase titration is faster than titrimetry.

D. Separation Methods

Separation methods for sulfonates are needed in industrial and analytical fields to purify petroleum sulfonates for use in lubricating oils and greases, to purify water by removing trace amounts of alkylarenesulfonates or analytically to investigate fast separation methods for aliphatic and aromatic sulfonates which are useful in industry or pharmacy.

Seven separation methods for analytical use are reviewed here: solvent extraction, continuous electrophoresis, gas chromatography, ion-exchange chromatography, paper chromatography, thin-layer chromatography, and liquid chromatography.

1. Solvent Extraction

Separation of petroleum sulfonic acids from oil in a mixture of water-alcohol (1:1) at 40-45^{o}C was reported by Myshkin, Lavrova, and Ivanova (96) in 1961. After the oil was separated and removed from a separatory funnel, the aqueous alcohol solution was treated with hydrochloric acid and then the sulfonic acids were extracted into an ether

layer, which was dried to a constant weight and used for determining the content of petroleum sulfonic acids. Only qualitative analysis was reported.

A removal of anionic detergents (mainly alkylarenesulfonate) in water by extraction with kerosene containing a liquid amine anion exchanger was reported by Dunning, Kreevoy, and White (58) in 1965. The extracted ammonium-sulfonate complex in the organic phase was washed with a basic solution and the sulfonate, which migrated to the aqueous phase, was determined while the organic solvent with the liquid amine was reused. This method depends mostly on the selectivity of the liquid amine anion exchanger, which must be insoluble in water and form ion pairs with the sulfonates. The solvent extraction technique is usually time-consuming.

2. Continuous Electrophoresis

A separation of 4-biphenylsulfonate and 4,4'-biphenyldisulfonate by use of continuous electrophoresis was studied by Skelly (97) in 1965. The mono- and di-sulfonates were separated on a Beckman/Spinco Model CP continuous-flow paper electrophoresis cell and were collected in separate volumetric flasks. Since these two sulfonates have the same absorptivity at 266 nm (shown in Figure 56), the concentration ratio of mono-/di- and the total concentration of sulfonates can be obtained by UV spectrophotometry. The accuracy was within 1.4% for 24.85 mg of monosulfonate and within 5% for 5 mg of disulfonate. The precision was ± 0.7%. Although the accuracy and precision are reliable in the range of 5-25 mg, this procedure takes about 12 hours per analysis. It is really a slow process.

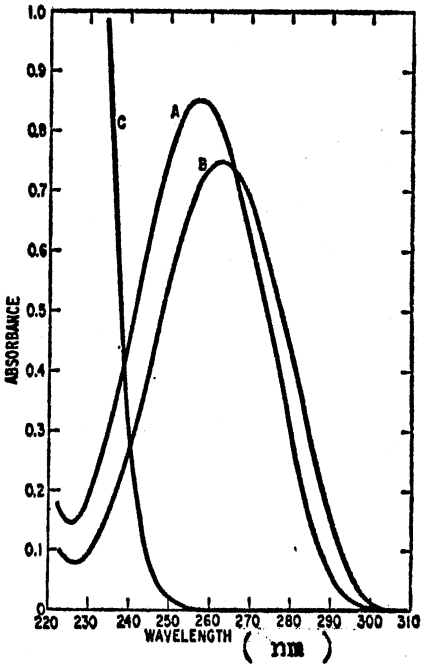

Figure 56. UV Spectra for Biphenyl Mono- and Disulfonates

A. 1.00 mg sodium biphenylsulfonate per 100 ml solution.

B. 1.00 mg disodium biphenyldisulfonate per 100 ml solution.

C. 2% acetic acid as an electrolyte

3. Gas Chromatography

a. Gas-Liquid Chromatography

Besides those methods previously mentioned (82) (83) (84) (85), a trace amount of linear alkylbenzenesulfonate (LAS) in waste water at ppm levels was estimated by Swisher (98) in 1966. After the water in a sample was evpoarted, the residue was desulfonated and the resultant phenyl-n-alkanes were detected by gas chromatography. Only semiquantitative results were reported.

In 1967, Parsons (99) qualitatively analyzed a mixture of naphthalene mono-, di-, and tri-sulfonic acids by converting the sulfonic acids to the corresponding sulfonyl fluorides. A chromatogram was obtained with good resolvable peaks in 3 minutes; it is represented in Figure 57. Since naphthalenetrisulfonyl fluoride is more volatile and thermally stable than the sulfonyl chloride, more reproducible peaks are obtained. However, it takes more time (1.5 hr) to prepare a fluoride derivative.

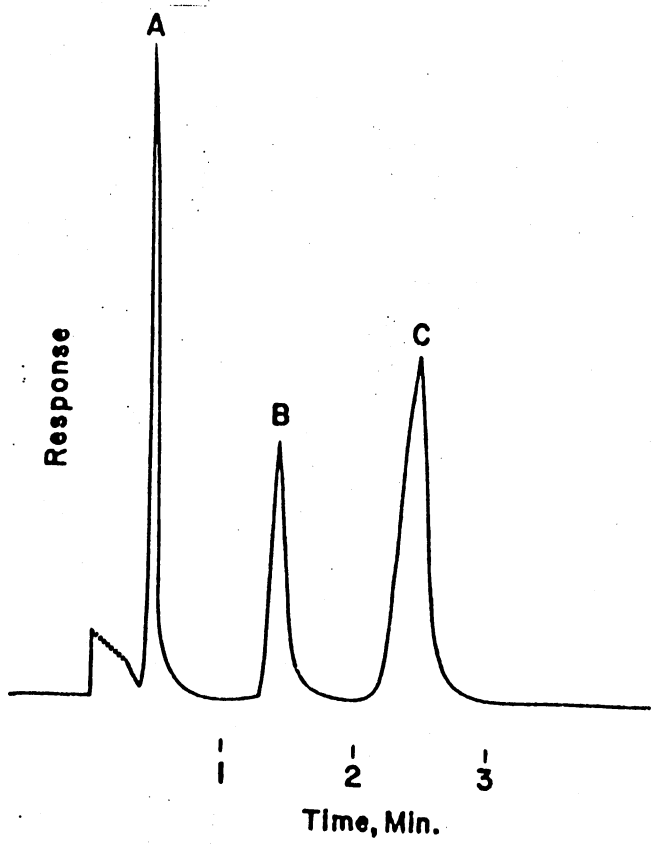

Figure 57. Chromatogram of Naphthalene Mono-, Di-, and Tri-sulfonyl Fluorides

A. 2-naphthalenesulfonyl fluoride
B. 2,6-naphthalenedisulfonyl fluoride
C. 1,3,6-naphthalenetrisulfonyl fluoride

b. Gas-Solid Chromatography

A separation of alkylbenzenesulfonic acids by converting to the corresponding sulfonyl fluorides and analyzing by gas adsorption chromatography was reported by Krylov (100) in 1976. A column of 3000 x 3 mm packed with silochrome-2 adsorbent, nitrogen carrier gas, and a hydrogen flame-ionization detector were used. The separation is based on the varying stability of hydrogen bonding between the hydroxyl-group protons of silochrome and the electron density of the aromatic sulfonyl fluorides. Ten aromatic sulfonic acids were separated and the chromatogram is represented in Figure 58.

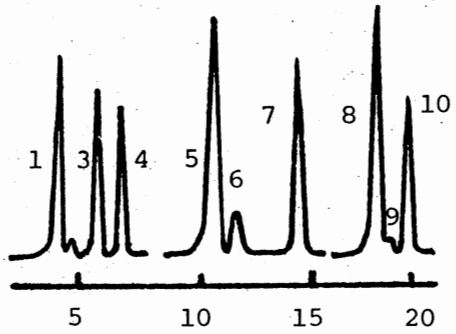

Figure 58. Chromatogram of 10 Aromatic Sulfonyl Fluorides

Chromatograms of aromatic sulfonyl fluorides obtained on Silochrome-2: 1, 2, 3) p-, m-, and o-toluenesulfonyl fluorides; 4) benzenesulfonyl fluoride; 5, 6, 7) p-, m-, and o-cumenesulfonyl fluoride: 8) m-xylene-

4-sulfonyl fluoride; 9) m-xylene-2-sulfonyl fluoride; 10) p-xylenesulfonyl fluoride.

4. Ion-Exchange Chromatography

A separation of binary mixtures of both aliphatic and aromatic monosulfonic/disulfonic acids by using an Amberlite XAD-2 resin was reported by Scoggins and Miller (101) in 1968. The disulfonates were eluted first with water or NaCl solution and then the monosulfonates were eluted with methanol, 10-ml fractions being collected. The alkanesulfonates were determined titrimetrically and arenesulfonates by UV spectrometry. The accuracy was within ± 5% but the process is relatively slow.

In 1970, a cross-linked polyalkyleneamine anion exchange resin, Bio-Rex 5-Cl^- (270/325 mesh), was used by Stehl (102) to separate some homologs of arenesulfonates. A mobile phase consisting of water : acetonitrile : methanol (1 : 1 : 1) and a salt gradient of 0 to 1.0 M LiCl as eluent were used. Mono- and di-sulfonates were separated within 30-45 minutes. There are two advantages of this method:

a. Some arenesulfonates containing -OH or $-NH_2$ groups, which are not suitably handled by GC (82), can be easily separated by this technique.

b. The gradient elution improves the efficiency of separation by lowering the height equivalent to a theoretical plate (HETP).

The separation of linear (LAS) and branched (ABS) alkylbenzenesulfonates by use of a weakly acidic cation-exchange resin, Amberlite CG-50 (100-200 mesh), was reported by Fudano and Konishi (103) in 1970. A column (500 x 26 mm) was slurry packed and washed with an eluent (0.5

M ammonium sulfate-43% methanol) for 1 hr before the sample was introduced. The bound sulfonates were eluted with the eluent in the order of LAS and then ABS, and these were measured with the aid of an UV detector. The accuracy was ± 6.6% for LAS and ± 1.1% for ABS, and the precision was within ± 0.7%. It took about 15 hours to obtain the separated peaks in the chromatogram.

Using the same technique in 1971, Fudano et al. (104) separated 3-hydroxypentadecanesulfonate and 2-pentadecenesulfonate by eluting with 0.5 M NaCl-30% 2-propanol. The amount of sulfonates was determined by the colorimetric methylene blue method (73). The accuracy was within ± 2.3% for 4 mg of each, but the time required for analysis was about 24 hours.

Another separation of four isomeric monosulfonic acids (derived from sulfonation of phenanthrene) by using a weak acid SG-1 cation-exchange resin was reported by Kachurin and Vasilenko (105) in 1975. The procedure used a gradient elution of potassium chloride solution (0.5-0.02 M) and a column of 500 x 10 mm. The mixture of 2-, 3-, 9-, and 1-phenanthrenesulfonate was separated and the composition was determined by UV multicomponent analysis in the region of 250-306 nm. The accuracy was within ± 7% for 0.3 g sample. Again, the process took more than 26 hours.

5. Paper Chromatography

In 1964, Coyne and Maw (106) studied the separation of several alkanesulfonic acids by conversion to the corresponding ammonium sulfonates and use of paper chromatography. Acetic-acid-washed Whatman No. 1 papers, and developing reagents of bromocresol green or silver fluores-

ceinate were used. Seven solvents systems investigated were as follows:

a. t-butyl alcohol-formic acid-water (16:1:4)

b. acetone-formic acid-water (16:1:3)

c. mesityl oxide-formic acid-water (25:25:12)

d. phenol-formic acid-water (75:1:25)

e. ethanol-aqueous ammonium acetate (5:2)

f. ethyl acetate-acetic acid-water (3:1:1)

g. ethanol-ammonium hydroxide-water (20:1:4)

The R_f values of seven alkanesulfonates (10 µg each) measured are tabulated in Table XIII. Among these, solvent system b is the most suitable to separate methane- and ethanesulfonates.

6. Thin-Layer Chromatography

A separation of alkanesulfonates and alkylbenzenesulfonates using thin-layer chromatography was reported by Takeshita, Jinnai, and Yoshida (107) in 1976. A stationary phase of a polyamide on cellulose and 2-propanol mixture and a developing solvent of 0.1-1.0 N aqueous ammonia-pyridine (15:1) were used. After developing, the layer was sprayed with pinacryptol yellow reagent and examined under UV light at 253.6 nm. R_f values were used for identifying constituents of sulfonates and the intensity of the yellow spots was used for quantitative measurement. The R_f values were higher for sulfonates with a shorter carbon chain than those with a longer carbon chain. The detection limit was 2 µg for C_4-C_{18} alkanesulfonates and C_1-C_{14} benzenesulfonates.

In the same year, Franc, Pikes, and Hajkova (108) separated a mixture of 1-naphthalenesulfonic acid and 2-naphthalenesulfonic acid using Silufol UV-254 as a stationary phase and t-butyl alcohol:ethanol (1:1)

TABLE XIII

R_f VALUES OF ALKANESULFONATES IN SEVEN SOLVENT SYSTEMS USING PAPER CHROMATOGRAPHY

Alkanesulfonate	R_f x 100						
	Solvent Systems						
	a	b	c	d	e	f	g
Methanesulfonate	34	35	69	41	68	17	61
Bromomethanesulfonate	59	53	70	44	72	37	64
Iodomethanesulfonate	57	56	71	48	70	39	63
Ethanesulfonate	64	42	68	56	73	20	67
2-Bromoethanesulfonate	70	65	77	54	77	34	72
Methanedisulfonate	10	7	61	7	32	5	22
Ethane-1,2-disulfonate	14	14	66	7	45	5	39

as a developing solvent. A stable brown-black color was developed after spraying with hydroxylamine solution and then cupric acetate solution. The chromatogram was evaluated on a densitometer at 480 nm. R_f values of 0.6 and 0.0 were obtained for 1-naphthalenesulfonic acid and 2-naphthalenesulfonic acid, respectively. A standard deviation of 3.5% and a detection limit of 10 μg were reported.

7. Liquid Chromatography

a. Conventional Liquid-Liquid Chromatography

Several binary mixtures of arenesulfonic acids were separated by Fritz and Gilletee (109) in 1968 by use of liquid-liquid chromatography. A solution of 5% Alamine 336 hydrochloride in toluene coated on Chromosorb W as a stationary phase, a dilute aqueous acid ($HCl/HClO_4$) as a mobile phase, a glass column (110 x 13 mm), and a Bausch and Lomb Spectronic 600 spectrophotometer were used. The binary systems studied were:

- 2-aminobenzenesulfonate and 2-amino-5-nitrobenzenesulfonate
- 2-aminobenzenesulfonate and 6,7-dihydroxy-2-naphthalenesulfonate
- benzenesulfonate and p-toluenesulfonate

The first component in the mixture was eluted with 0.5 M HCl and the second component with 1.0 M HCl plus 1.0 M $HClO_4$. The accuracy was within ± 5% at 0.050 mmole for each species. It took about 1.5 hr to separate each binary mixture.

A separation of alkanemonosulfonates (C_{10}-C_{20}) from the alkane di- or polysulfonates was reported by Ali and Laurence (110) in 1973; they used a moist cellulose in petroleum ether as the packing material. The monosulfonic acid was eluted with 5% 1-butanol in petroleum either and

di- and polysulfonic acids with water, 25 ml fractions being collected. The sulfonic acids were determined titrimetrically. The accuracy and precision were ± 1.8% and ± 0.8%, respectively, for 26 wt. % dodecanesulfonate, but the process is time-consuming.

b. High-Pressure Liquid-Liquid Chromatography (HPLLC)

A separation of eight arenesulfonates in 50 min and five arenesulfonates in 5 min using HPLLC (Siemens SP200) was reported by Kraak and Huber (111) in 1974. Flow rates of 0.30 ml/min and 0.64 ml/min were used; the chromatograms are shown in Figure 59 and Figure 60, respectively. In these systems, an aliphatic amine (tri-n-octylamine) coated on diatomite (5-10 μm) as a stationary phase, a dilute perchloric acid (pH = 1.5) solution as a mobile phase, a glass column (185 x 3.0 mm), and a stainless-steel pre-column (500 x 10 mm) were used. In 1977, Kraak et al. (112) used the same system to separate a mixture containing alkanesulfonic acids (C_6, C_7, and C_8) in 8 minutes. The chromatogram is represented in Figure 61. The separation of sulfonic acids depends on ion-pair formation ($R_3\overset{+}{N}H$, $O_3\overset{-}{S}$-R) on the stationary phase and can be adjusted by changing the pH, the anionic concentration of the mobile phase, and the temperature in order to obtain a good resolution.

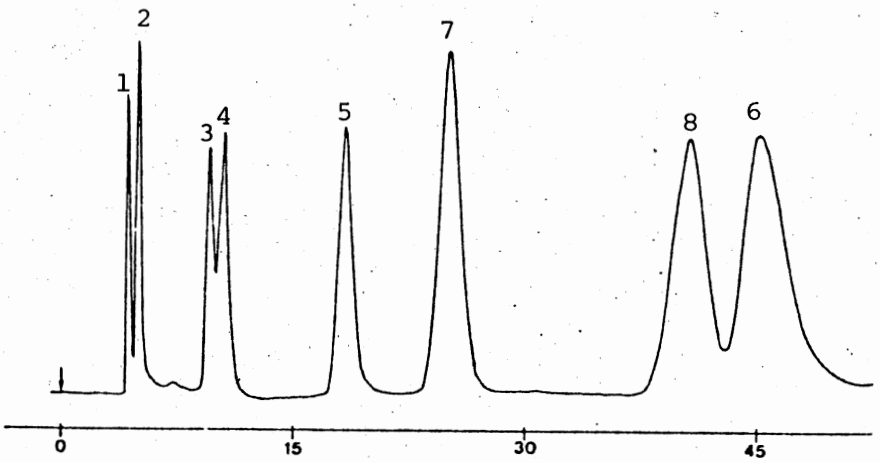

Figure 59. Separation of 8 Arenesulfonates by HPLLC

Sample: (1) 3-aminotoluenesulfonic acid; (2) 2-amino-benzenesulfonic acid; (3) benzenesulfonic acid; (4) 4,5-dihydroxy-2,7-naphthalenedisulfonic acid; (5) 4-nitrobezenesulfonic acid; (6) 2-naphthol-3,6-disulfonic acid; (7) 2-naphtholsulfonic acid; (8) 1-naphthol-5-sulfonic acid

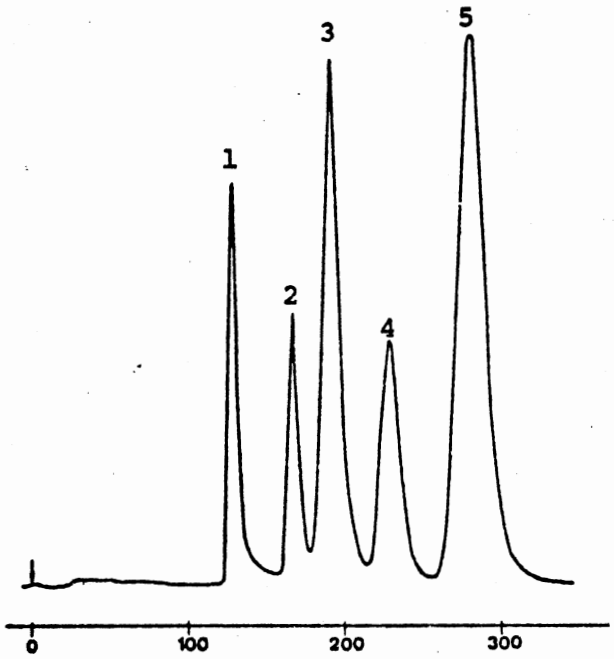

Figure 60. Separation of 5 Arenesulfonates by HPLLC

Sample: (1) 3-aminotoluenesulfonic acid; (2) benzenesulfonic acid;
(3) 4-nitrobenzenesulfonic acid;
(4) 2-naphthol-3,6-disulfonic acid;
(5) 2-naphthol-6-sulfonic acid

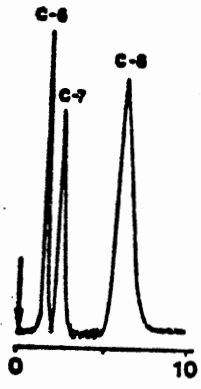

Figure 61. Separation of 3 Alkanesulfonates by HPLLC

C_6, C_7, and C_8 alkanesulfonic acids

Using reversed-phase high-pressure liquid-liquid chromatography in 1975, Wahlund (113) reported separating a mixture of benzenesulfonate and p-toluenesulfonate in 22 minutes. A stationary phase of 1-pentanol coated on silica supports, a mobile phase of aqueous tetrabutylammonium (TBA) salt with a flow rate of 0.72 ml/min, a stainless-steel column (300 x 2.7 mm), and a precolumn (150 x 4.5 mm) were used. The chromatogram is shown in Figure 62. As before, the separation of sulfonates is based on the partition of ion-pairs (R_4N^+, ^-O_3SR) between the stationary phase and the mobile phase. The concentration of R_4N^+ in the mobile phase can be adjusted in order to obtain well resolved peaks and relatively fast separation.

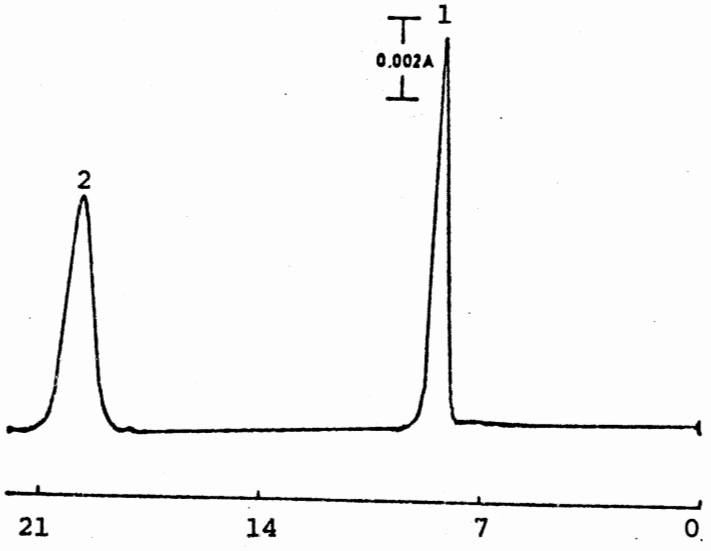

Figure 62. Separation of Benzenesulfonate and p-Toluenesulfonate by HPLLC

Sample: (1) benzenesulfonate; (2) p-Toluenesulfonate

In liquid-liquid chromatography, the stationary phase is usually slightly soluble in the mobile liquid. Therefore, a pre-column is provided for pre-saturation of the mobile liquid and the liquid stationary phase in order to avoid stripping the stationary liquid in the column.

c. High-Pressure Liquid-Solid Chromatography (HPLSC)

The possibility of using high-speed liquid-solid chromatography for the separation of arenesulfonates was investigated by Kirkland (114) in 1971. Zipax SAX (a strong anion exchanger made up of dense, spherical, porous-layer beads) was used to bind sulfonates and dilute aqueous perchloric acid was used as mobile phase with a volume flow rate of 0.54 ml/min at a column pressure of 370 psig. Five arenesulfonates were separated in 30 min; the chromatogram is shown in Figure 63. Although the mixture was not completely resolved, separation was reasonably fast.

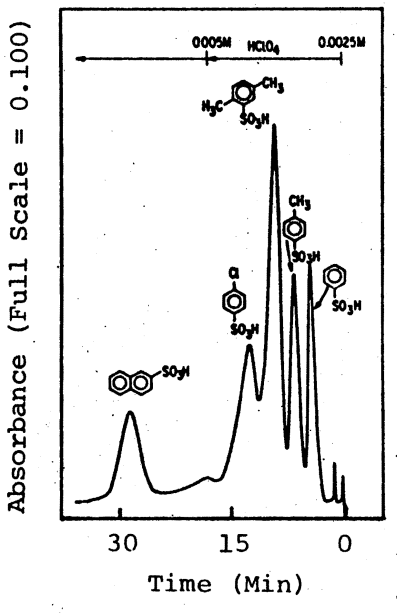

Figure 63. Separation of 5 Arenesulfonates by HPLSC

In 1976, Knox and Laird (115) used SAS silica, a reversed-phase material made of short-chain hydrocarbon groups bonded to the surface of spherical silica gel, as a stationary phase and a water-propanol (5:2) mixture containing 1% of cetyltrimethylammonium bromide as a mobile phase to separate four isomeric naphthylaminesulfonic acids. The separation is based on the distribution of cetyltrimethylammonium-sulfonate ion pairs between the water-rich eluent and adsorbed-layer rich in propanol. The chromatogram is represented in Figure 64.

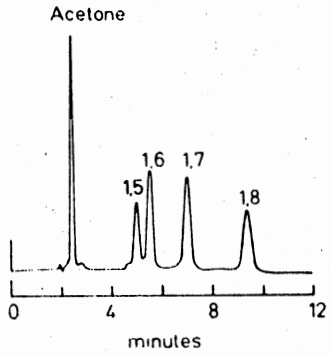

Figure 64. Separation of 4 Naphthylamine Sulfonic Acids by HPLSC

Column: 120 x 5 mm stainless steel

From the characteristics obtained in batch experiments (116), Pietrzyk and Chu (117) separated six benzenesulfonic acid derivatives by using reversed-phase HPLC in 1977. A stationary phase of nonpolar Amberlite XAD-4, which is a polystyrenedivinylbenzene copolymer, a mobile phase of 0.1 M NaCl in 40% MeOH, a pressure of 300-700 psi, and

a flow rate of 0.4 ml/min were used. The chromatogram is shown in Figure 65.

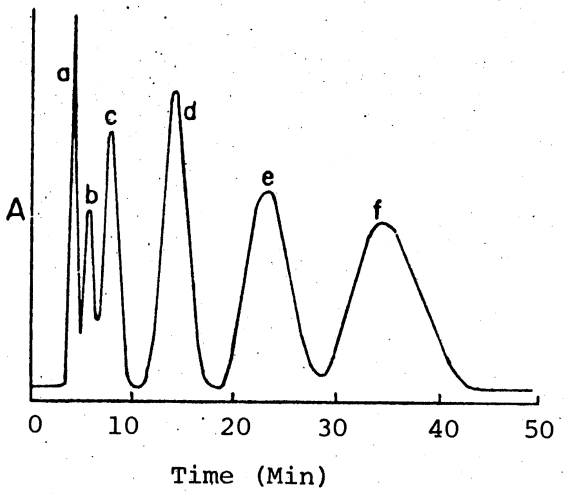

Figure 65. Separation of 6 Benzenesulfonic Acid Derivatives by HPLSC

Column: 450 x 2.36 nm
Sample: a. p-hydroxybenzenesulfonic acid; b. benzenesulfonic acid; c. p-methoxybenzenesulfonic acid; d. p-nitrobenzenesulfonic acid; e. 2,4-dinitrobenzenesulfonic acid; f. 2,4,6-trinitrobenzenesulfonic acid

In liquid-solid chromatography, the packing materials (114) (116) (117) usually tend to swell and therefore require maintenance of a constant level of water in the eluent (e.g. guard column) to ensure reproducible separations. In order to overcome this procedural disadvantage, stationary phases having short-chain hydrocarbon groups bonded on the surface of silica gel have been developed (115). Since glass with controlled pore size may have larger available volume and capacity than on

the surface of the silica gel, the results of separation by HPLSC may be improved by using such glass.

E. Summary of Observations on Methods of Separation

A summary of methods, type of sulfonates separated, speed of the separation process, applications, advantages, amounts of sample used, and methods of determination is presented in Table XIV.

F. Conclusions

Among the twelve determination methods for sulfonates, titrimetric, two-phase titration, and gravimetric methods need only simple equipment; the two-phase titration method is particularly reliable for the determination of sulfonate contents in oil-soluble petroleum sulfonates, and it is fast and provides good accuracy and precision. Ultraviolet absorption, colorimetric, infrared spectrometry, gas chromatographic, nuclear magnetic resonance, mass spectrometric, atomic absorption, and radiometric methods require more advanced instrumentation. Although the amount of sample used for each method is tabulated in Table XI, the suitable concentrations of samples are used (118) as follows: ultraviolet absorption, visible absorption, and atomic absorption methods are usually used for quantitative analysis at ppm, ppm, and ppb levels, respectively; infrared spectrometric, nuclear magnetic resonance, and mass spectrometric methods are largely used for qualitative or structural identification at the moderate concentration level (20-50%); gas chromatographic methods are widely used both for qualitative and quantitative analyses at the ppb level. The general time for analysis

TABLE XIV

SUMMARY OF OBSERVATION ON METHODS OF SEPARATION

Ref.	Method	Type of Sulfonates Separated	Speed of the Separation Process	Applications	Advantages	Amounts of Sample Used	Method of Determination
(58)	solvent extraction	aromatic	slow	to determine trace amounts of alkylarenesulfonates in sewage	simple equipment	2-20 ppm	-----
(96)	solvent extraction	aromatic	slow	to separate and determine the content of sulfonate in oil-soluble petroleum sulfonic acids	------	----	drying and weighing
(97)	continuous electrophoresis	aromatic	very slow (-- 12 hrs.)	to separate arenemono- and disulfonates	------	(2.5-5.0) x 10^{-2} g	UV
(99)	GC (sulfonyl fluoride)	aromatic	relatively slow	to separate arenesulfonates	better than (82) for naphthalenetrisulfonate	0.5 g	flame ionization detector
(100)	GC (sulfonyl fluoride)	aromatic	relatively slow	to separate alkylbenzenesulfonic acids	------	----	flame ionization detector
(101)	Ion-exchange (XAD-2 resin)	both	slow (1-8 hrs.)	to analyze alkane- and arene- mono- and disulfonates (until C_{14})	-----	0.66-1.0 g aliphatic, 0.1 g aromatic	titrimetry UV
(102)	ion-exchange (polyalkylenamine)	aromatic	relatively fast (30-45 min.)	to separate arenemono- and disulfonates	better than GC (80) for sulfonates containing -OH or $-NH_2$ groups	$1x10^{-5}$ g (each)	UV
(103)	ion-exchange (Amberlite CG-50)	aromatic	very slow (15 hrs.)	to separate linear and branched alkylbenzenesulfonates	-----	$9x10^{-3}$ g	UV
(104)	ion-exchange (amberlite CG-50)	aliphatic	very slow (24 hrs.)	to separate α-olefinsulfonates and hydroxysulfonates (C_{14}-C_{16})	-----	$4x10^{-3}$ g (each)	colorimetry (15) (methylene blue)

TABLE XIV (Continued)

Ref.	Method	Type of Sulfonates Separated	Speed of the Separation Process	Applications	Advantages	Amounts of Sample Used	Method of Determination
(105)	ion-exchange (SG-1 resin)	aromatic	very slow (26 hrs.)	to separate and determine isomeric monosulfonic acids	-----	0.3 g	UV (multicomponent)
(106)	paper chromatography	aliphatic	slow	to separate and determine methane- and ethanesulfonates	simple Whatman papers are used as absorbent of stationary phase	$(1-5)\times10^{-6}$ g	drying and spraying with bromocresol green or silver fluoresceinate
(107)	thin-layer chromatography	mixtures of aliphatic and aromatic	slow	to separate alkylalkanesulfonates (C_4-C_{18}) and alkylbenzenesulfonates (C_0-C_{14})	-----	$(3-10)\times10^{-6}$ g (each)	UV
(108)	thin-layer chromatography	aromatic	slow	to separate 1-naphthalenesulfonic acid and 2-naphthalenesulfonic acid	color developed is stable for several months	$(3-7)\times10^{-5}$ g	densitometry
(109)	LLC	aromatic	relatively slow	to separate arenesulfonates	-----	2×10^{-3} g (each)	UV
(110)	LLC	aliphatic	slow (4 hrs.)	to separate alkanemonosulfonates from alkane di- or polysulfonates (C_{10}-C_{20})	-----	$(2.1-3.5)\times10^{-2}$ g	titrimetry
(111)	HPLLC	aromatic	fast (5-45 min.)	to separate arenesulfonates	fast	-----	UV
(112)	HPLLC	aliphatic	very fast (8 min.)	to separate C_6-C_8 alkanesulfonates	fast	1×10^{-8} g	tensammetry
(113)	HPLLC (reversed phase)	aromatic	fast (22 min.)	to separate benzenesulfonate and p-toluenesulfonate	fast	$(3-4)\times10^{-6}$ g (each)	UV

TABLE XIV (Continued)

Ref.	Method	Type of Sulfonates Separated	Speed of the Separation Process	Applications	Advantages	Amounts of Sample Used	Method of Determination
(114)	HPLSC	aromatic	fast (30 min.)	to separate arenesulfonates	fast	$(5-150)\times10^{-4}$ g	UV
(115)	HPLSC	aromatic	very fast (10 min.)	to separate naphthylaminesulfonic acid isomers	fast	$(1-50)\times10^{-6}$ g	UV
(117)	HPLSC	aromatic	relatively fast	to separate benzenesulfonic acid derivatives	inexpensive Amberlite XAD-4 resin is used as a stationary phase	$(5-50)\times10^{-6}$ g	UV

with instrumental techniques is short but the time for preparing samples may be large. Mass spectrometry is usually combined with gas chromatography to quantitatively analyze mixtures. Although the radiometric methods are slow (30 min/each counting), they are not limited by the dark color of crude oils. The use of ion-selective membrane electrodes gives a fast response, generally within 1 minute. They have been used in the determination of individual aromatic sulfonates in the range of 10^{-5} M - 10^{-1} M. The application of ion-selective membrane electrodes to measure the concentration of alkanesulfonates, however, has not been reported as yet.

Among the seven separation methods for sulfonates reviewed here, solvent extraction, paper chromatography, and thin-layer chromatography need only simple equipment, while continuous elctrophoresis, gas chromatography, ion-exchange chromatography, and liquid chromatography require a fair degree of instrumentation. The speed of analysis for gas chromatography, high-pressure liquid-liquid chromatography, and high-pressure liquid-solid chromatography is good, but it may take several hours to prepare samples for gas chromatography. Solvent extraction, paper chromatography, and thin-layer chromatography are slow by nature. Continuous electrophoresis and ion-exchange chromatography (with cation-exchange resins) are very slow. From the papers reviewed, it can be concluded that high-pressure liquid-liquid chromatography and high-pressure liquid-solid chromatography are powerful techniques for the analysis of sulfonates. Since a pre-column is generally needed in liquid-liquid chromatography and a guard column is usually used in liquid-solid chromatography, an organic compound chemically bonded to an inert matrix, such as controlled-pore glass, used as stationary

phase, should offer advantages over the reviewed liquid-liquid chromatography and liquid-solid chromatography methods, although the capacity of the chemically bonded resin should be relatively large for successful application.

CHAPTER VI

CHROMATOGRAPHIC SEPARATION OF AROMATIC SULFONATES

From the values of distribution coefficients for aromatic sulfonates obtained in batch experiments (Figures 38 and 51), a study centered on the chromatographic separation of aromatic sulfonates by liquid-solid chromatography (LSC) was performed. The results are discussed in this chapter. The synthesized CPG-8HO$_x$ resin (either 125-177 microns or 37 - 74 microns) was used as a stationary phase and acid solutions (such as HCl or $HClO_4$) were used as mobile phases.

An elution profile for aromatic sulfonates in an open column was obtained and is presented in Part A. Details of a chromatographic separation for a mixture of aromatic sulfonates and some factors which affect the resolution are discussed in Part B. An EPA (Environmental Protection Agency) sample containing linear alkylate sulfonates (LAS) was qualitatively analyzed; tested results are reported in Part C, and a prediction of a chromatographic separation for the aliphatic sulfonates (methanesulfonate and ethanesulfonate) is discussed in Part D.

A. Elution Profile for Four Aromatic Sulfonates in an Open Column

1. Experimental

a. Materials

The synthesized CPG-8HO$_x$ resin (125 - 177 μ) as described in Chapter IV.D.1. was used. A. R. reagents of benzenesulfonic acid, p-toluenesulfonic acid, 2-mesitylenesulfonic acid, 1-naphthalenesulfonic acid, and hydrochloric acid have been described previously.

b. Apparatus

Baush and Lomb Spectronic 505 spectrophotometer and a matched pair of quartz cell (1.00 cm) were used for absorbance measurements in eluent fraction. A 10-ml glass buret with an internal diameter of 0.60 cm and a length of 49 cm packed with the synthesized CPG-8HO$_x$ resin was used as a column.

c. Procedure

The synthesized CPG-8HO$_x$ resin (about 3.0 g) was slurry packed into the glass column (49 x 0.60 cm) using deionized-distilled water. Glass wool plugs were used in the lower part and the top of the column to keep the resin in place. Since chloride ion has a lower K_d value (Figure 30) than PTS^-, hydrochloric acid solutions were used as eluting agents. The ionic strengths of sample solutions of sulfonates were adjusted to 0.10 M with addition of 1.0 M HCl.

After finishing the packing, the column was conditioned by washing with 40 ml of 0.10 M HCl. A sample of 0.20 ml of 0.0100 M benzenesul-

fonate solution was pipetted into the top of the column and allowed to sink in the column for 15 minutes. The sulfonate was then eluted with 0.10 M HCl at a flow rate of 0.20 ml/min, fractions being collected every 2.00 ml. Absorbances were measured at 260 nm using 0.10 M HCl as blank.

After benzenesulfonate ion was eluted, the column was washed with deionized-distilled water until absorbance equal to that of the blank was obtained. The column was re-conditioned with 0.10 M HCl and the next sulfonate species (p-toluenesulfonate, 2-mesitylenesulfonate, and 1-naphthalenesulfonate) was introduced and eluted as described above. Absorbances for PTS^-, $2\text{-}MS^-$, and $1\text{-}NS^-$ were measured at 259 nm, 271 nm, and 281 nm, respectively.

2. Data and Results

An elution profile for aromatic sulfonates (absorbance versus volume of effluent) is shown in Figure 66. Some results obtained from the elution profile are tabulated in Table XV.

3. Discussion

a. The results obtained and shown in the elution curve (Figure 66) indicate that the retention time (or the retention volume) increases in the order of $BS^- < PTS^- < 2\text{-}MS^- < 1\text{-}NS^-$ as predicted from distribution coefficients (Figure 51) obtained in batch experiments. The resolution between the two homologous species is also proportional to the difference in K_d between these two. For example, the resolution for BS^- and PTS^- is poor (0.31) because their K_d values are very close, while that for $2\text{-}MS^-$ and $1\text{-}NS^-$ is very good (> 1.5) because of the large

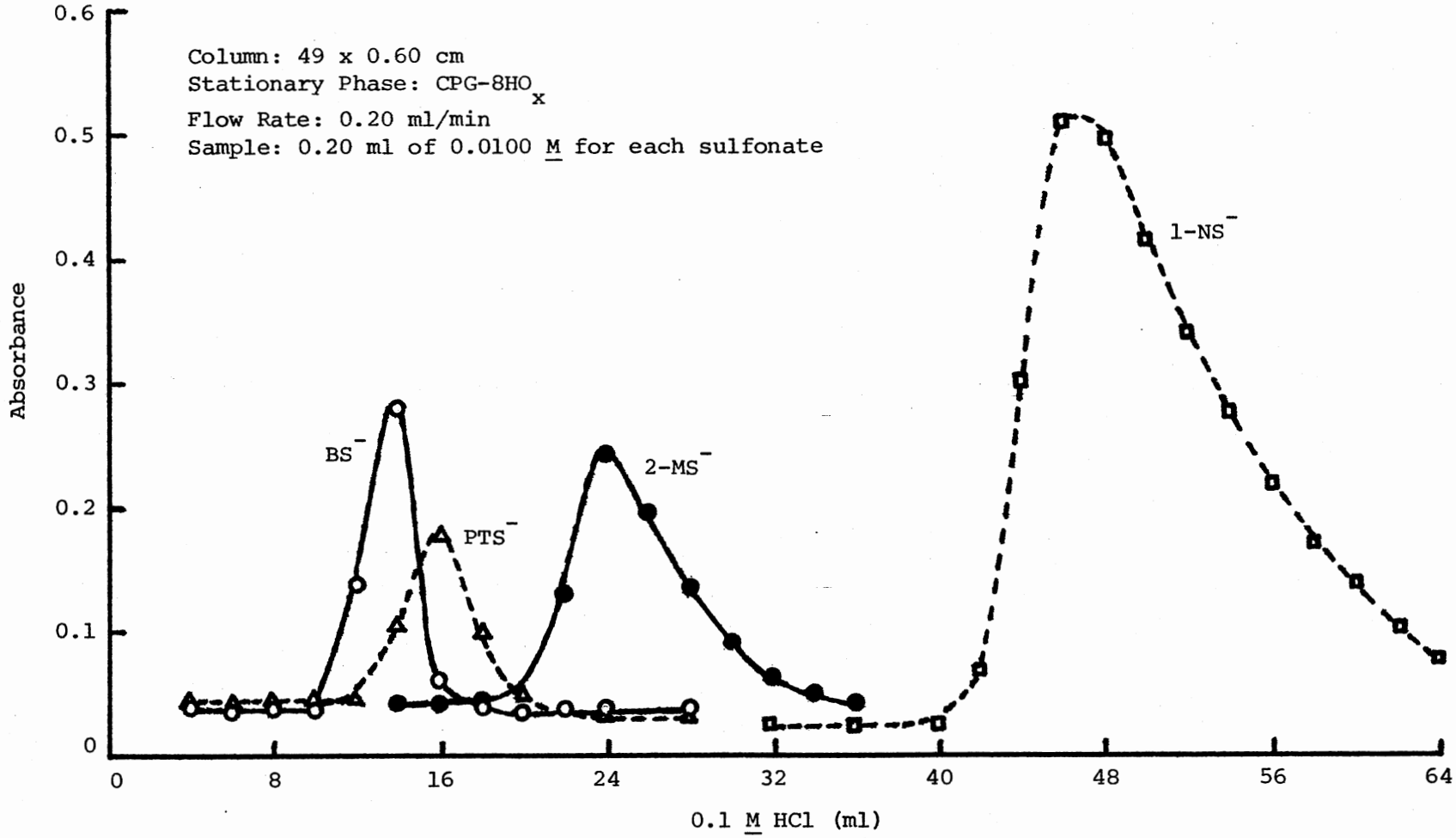

Figure 66. Elution Profile for Four Aromatic Sulfonates in an Open Column

TABLE XV

RESULTS OBTAINED FROM DATA COLLECTED IN THE SEPARATION OF SOME AROMATIC SULFONATES IN OPEN COLUMN

Sulfonate Species	BS^-	PTS^-	$2\text{-}MS^-$	$1\text{-}NS^-$
Elution Order, i	1	2	3	4
Retention Volume, V_R, (ml)	14.1	15.9	23.8	46.0
Flow Rate (ml/min)	0.20	0.20	0.20	0.20
Retention Time, T_R, (min)	70.5	79.5	119.	230.
Width at Base				
ω_b (ml)	5.4	6.2	10.1	17.7
ω_i (min)	27.0	31.0	50.5	88.5
Apparent Number of Theoretical Plates [45(a)][27(b)]				
$N = 16 \left(\frac{V_R}{\omega_b}\right)^2$	109	105	88.8	108
Height Equivalent to a Theoretical Plate				
$HEPT = \frac{L}{N}$ [=] $\frac{mm}{Plate}$	4.50	4.67	5.52	4.54
where L = 490 mm				
Resolution [45(a)][27(b)]				
$R_s = \frac{(t_R)_{i+1} - (t_R)_i}{\frac{1}{2}(\omega_{i+1} + \omega_i)}$	$R_{1,2} = 0.31$	$R_{2,3} = 0.97$	$R_{3,4} = 1.60$	

difference in K_d's. It is concluded that the distribution coefficients (K_d) obtained in batch experiments can be used to predict the elution order and at least qualitatively foresee the degree of separation in column experiments.

b. Since the resolution for BS^- and PTS^- was too poor and the retention time for $1\text{-}NS^-$ was too long, the following factors were considered.

(i) Mobile Phases. A component gradient elution may be performed using sulfuric acid (pH~1) to separate BS^- from PTS^- and then using perchloric acid (pH~1) to elute $2\text{-}MS^-$ and $1\text{-}NS^-$. Since distribution constants for the 8-hydroxyquinolinium-anion pair (in Chapter III) increase in the order of $(H_2O_x^+, HSO_4^-) < (H_2O_x^+, Cl^-) < (H_2O_x^+, ClO_4^-)$, it is predicted that the molar distribution coefficient, K_d, for anions would follow the same trend (in Chapter IV.A and IV.B) by forming $(CPG\text{-}8H_2O_x^+, A^-)$ on the resin. When Cl^- is used as an eluting agent, the sulfonate ions are replaced by chloride ion from the resin as shown in Equation (83) in the order $BS^- > PTS^- > 2\text{-}MS^- > 1\text{-}NS^-$.

$$(CPG\text{-}8H_2O_x^+, {}^-O_3S\text{-}R)_{resin} + Cl^- \rightleftharpoons (CPG\text{-}8H_2O_x^+, Cl^-)_{resin} + R\text{-}SO_3^- \quad (83)$$

If hydrochloric acid is replaced by sulfuric acid as a mobile phase, bisulfate ion will displace the sulfonates from the resin more slowly than chloride ion does. Hence, the separation for BS^- from PTS^- should be improved. On the other hand, if perchloric acid is used, perchlorate ion will displace the sulfonates from the resin faster than chloride ion does; therefore, the elution time for $2\text{-}MS^-$ and $1\text{-}NS^-$ should become shorter but a reasonable resolution value should be retained.

(ii) Parameters That Affect Resolution. Since the resolution for BS^- and PTS^- was only 0.31, some parameters (such as column length, internal diameter of the column, flow rate, and particle diameter of the CPG-8HO$_x$ resin) need to be varied in order to obtain better separations.

A formula relating resolution to the selectivity factor, the capacity factor, the column length, and the HETP has been reported by Huber and Van Urk-Schoen (119) and is shown below:

$$R_{1,2} = (\gamma_{12} - 1) \left(\frac{k'_2}{1 + k'_2}\right) \left(\frac{L}{H_2}\right)^{\frac{1}{2}} \quad (84)$$

where $R_{1,2}$ = resolution of components 1 and 2,

γ_{12} = selectivity factor = $\frac{(K_d)_2}{(K_d)_1}$,

K_d = molar distribution coefficient,

k'_i = capacity factor of ith component

= $(K_d)_i \times q$,

q = ratio between the ion-exchanger mass and the mobile phase volume,

L = column length,

H = HETP

A relationship between retention time, column length, the average velocity of flow, or volume flow rate, internal diameter, and capacity factor has been shown (119) in Equations (85) and (86).

$$t_{R_i} = \frac{L}{\langle v \rangle} (1 + k'_i) \quad (85)$$

or

$$I.D. = \left\{ \frac{4 \times v \times t_{R_i}}{3.14 \times L \times (1 + k'_i)} \right\}^{\frac{1}{2}} \quad (86)$$

where t_{R_i} = retention time for component i,

<v> = average velocity of flow,

v = volume flow rate,

I.D. = internal diameter of the column

Since K_d values are obtained from batch experiments, k_i' can be calculated from an estimated q; H is obtained from the elution profile; and L can be estimated from Equation (84) for a given $R_{1,2}$. The internal diameter (I.D.) can be estimated from Equation (86) for a given v and t_{R_i}, where t_{R_i} is estimated from Equation (85). Hence, the relationship among resolution, column length, and internal diameter can be calculated and is tabulated in Table XVI. From these data, it is evident that a column length of 100 cm with an internal diameter of 0.20 cm should provide reasonable separation. Results with a column of this characteristics are reported in Part B of this chapter.

In LSC, the HETP decreases with decrease in particle diameter as is mentioned in Chapter II.B.2.b.(iii) and as is shown in Equation (87) [27(b), 45(a)], and therefore the resolution is improved (Equation (84)). Hence, a smaller particle size (37-74 μ) was also used; results with this packing material are reported also in Part B of this chapter.

$$H = \frac{1}{(\frac{1}{A}) + \frac{1}{C_M\langle v\rangle}} + C_s\langle v\rangle \qquad (87)$$

where A = eddy diffusion coefficient = $\Lambda\, d_p$,

$C_M\langle v\rangle$ = diffusion effect due to convection from lateral mass transfer

$$= \frac{\Omega\, d_p^{\,2}\, \langle v\rangle}{D_M} ,$$

TABLE XVI

RELATIONSHIP AMONG RESOLUTION ($R_{1,2}$), COLUMN LENGTH (L) AND INTERNAL DIAMETER (I.D.)

$R_{1,2}$	L (cm)	I.D. (cm)
0.8	66	0.25
0.9	84	0.22
1.0	103	0.20
1.1	126	0.18
1.2	149	0.16_5

where $k_1' = 1.40$, $k_2' = 1.56$, $q = 0.4$, (estimated),

$K_{d_1} = 3.5$, $K_{d_2} = 3.9$, $r_{12} = 1.11$,

$H_1 = 0.45$ $(\frac{cm}{Plate})$, $H_2 = 0.46_7$ $(\frac{cm}{Plate})$,

$v = 0.20$ $(\frac{ml}{min})$, $t_{R_1} = 38$ (min) estimated by assuming L = 100 cm and I.D. = 0.20 cm in Eq. (85).

$c_s\langle v\rangle$ = mass transfer across the stagnant mobile phase for a porous column packing

$$= \frac{(1-\phi + k')^2 \, d_p^2 \, \langle v\rangle}{30\,(1-\phi)(1+k')^2 \, r \, D_M},$$

Λ and Ω = functions of the packing structure,

d_p = particle diameter,

D_M = diffusion coefficient of solute in the mobile phase,

$\langle v\rangle$ = average flow velocity,

ϕ = fraction of total mobile phase in the interparticle space,

r = tortuous factor inside the particle.

B. Chromatographic Separation of Aromatic Sulfonates

On the basis of the rationale presented as discussion in Chapter VI.A.3.b., 0.10 M H_2SO_4, 0.10 M HCl, and 0.10 M $HClO_4$ were used as mobile phases to compare elution peaks for a sample of 0.10 M benzenesulfonate ion. A glass tube (99 x 0.20 cm) packed with the synthesized CPG-8HO_x resin (125-177 μ) was used as a column. The flow rate was adjusted to 0.60 ml/min and a sample size of 8 μl was used. Since tailing was pronounced when solutions of H_2SO_4 and HCl were used as eluents, while it was much decreased when $HClO_4$ was used, $HClO_4$ was chosen as preferred eluting agent. Several sample sizes were also tested and the smallest one available with the devices at our disposal was found to be 8 μl. This sample size gave the least amount of tailing.

1. Experimental

a. Materials

Two different particle sizes (125-177 μ and 37-74 μ) of synthesized CPG-8HO$_x$ resin (as described in Chapter IV.D) were used as packing material (stationary phase).

b. Apparatus

An apparatus was set up as shown in Figure 67. A capillary glass tube (99 x 0.20 cm) slurry-packed with the synthesized CPG-8HO$_x$ resin (either 125-177 μ or 37-74 μ of particle diameters) was used as a column. A sintered glass disc (coarse frit) was glued on the bottom of the column with epoxy resin to keep the stationary phase in place. Two three-way (Teflon) Hamilton valves were connected to the top and the bottom of the column in order to get rid of air bubbles, if any. A mini-pump (Gilson Model Miniplus 2) of variable speed was used to deliver the mobile phases through the column. A rotary injection valve, as shown in Figure 68, was used to introduce a sample to the column. This valve is similar to the one described by Ruzicka and Hansen for flow injection analysis (120). The sample sizes can be varied by changing the length of the sample loop made from microbore Tygon tubing (Cole Parmer Instrumental Company) with I.D. = 0.51 mm and O.D. = 1.7 mm. A Bausch and Lomb Spectronic 505 spectrophotometer was used as detector for absorbance measurements. A chart speed of ~3.3 cm/min (the slowest available in the Spectronic 505) was used for recording of chromatograms. A far-transparent UV quartz flow cell (~185 μl total volume) with 10 mm path length (Markson Science Inc.), Model Type E-178-Q-10, was used as

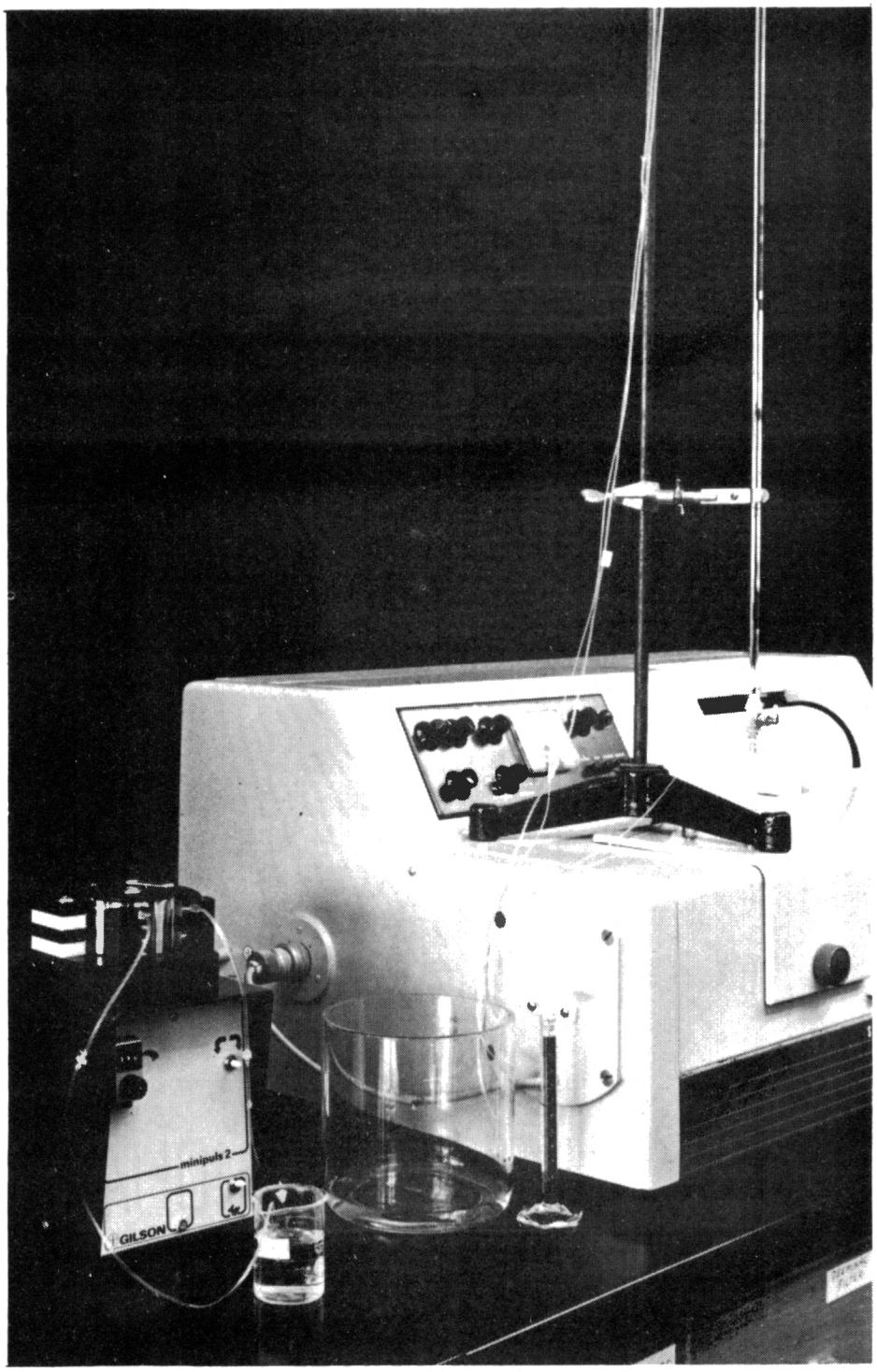

Figure 67. Instrumental Set-Up Used for Liquid-Solid Chromatographic Separations

*The column is connected to the sample rotary-injection valve (Figure 68)

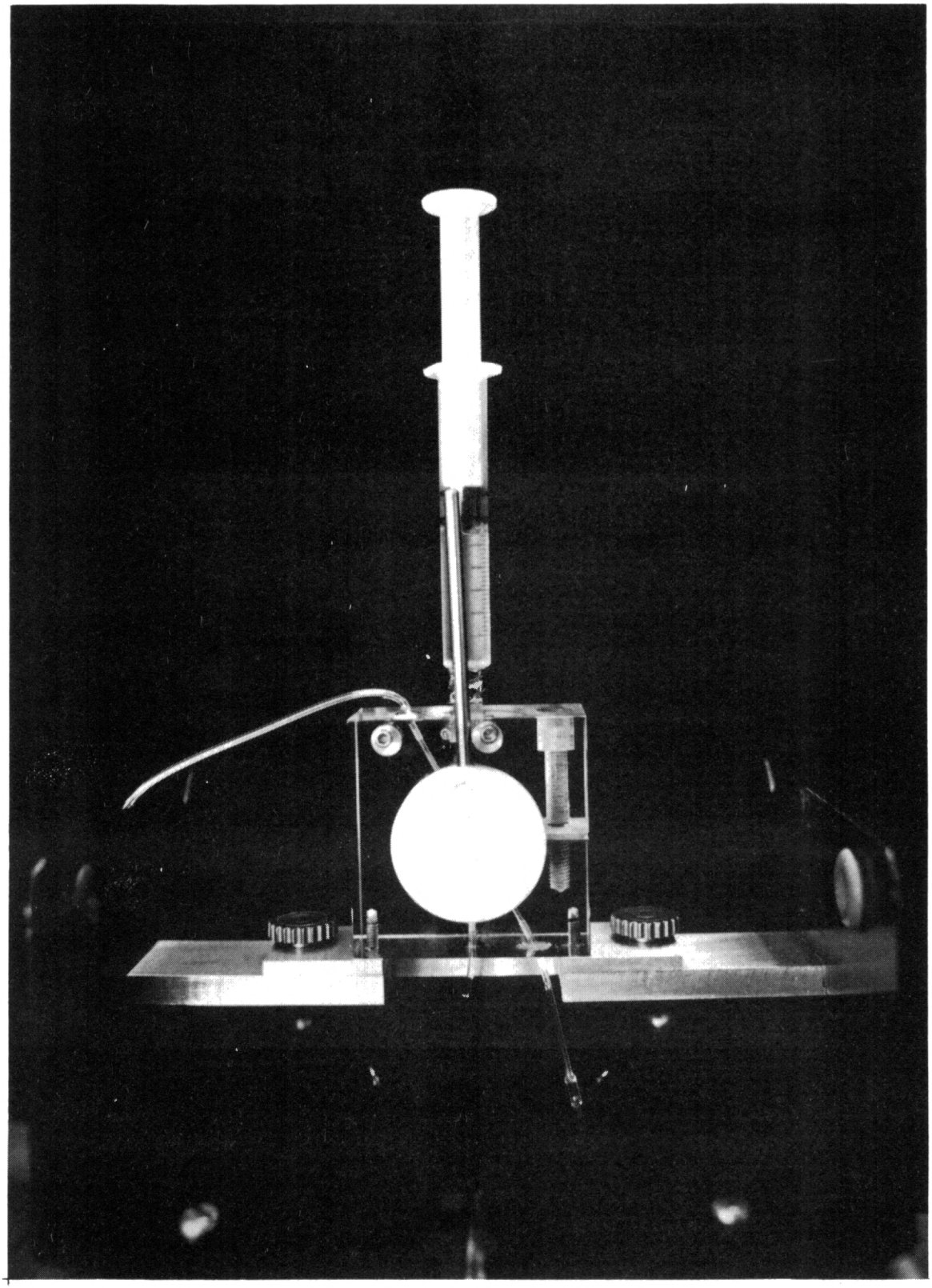

Figure 68. Details of Rotary-Injection Valve

sample cell. Another fixed quartz cell (3.5 ml) with 1.0 cm path length was used as reference cell.

Since the (slowest available) chart speed of the recorder was still too fast to contain the whole spectrum in one run and the elution peaks show tailings suggesting a Poisson distribution (121, 122) curves, the chromatograms were retraced and plotted using a plotter (Hewlett-Packard 9862 A) interfaced to a desk-top computer (Hewlett-Packard 9825 A).

c. Procedure

(i) Column Packed With Synthesized CPG-8HO_x Resin of Particle Size (125-177 μ). The aim of the work reported here was to find the maximum resolution for BS^- and PTS^- at various flow rates (0.15-0.61 ml/min). After packing, the column was pre-washed with 0.10 M HCl for about 30 minutes to ensure the Cl^- was on the resin as (CPG-8$H_2O_x^+$, Cl^-). Since Cl^- has a relatively small K_d value, it can be easily replaced by the anions in the sample. The sample loop was filled with a sample of a mixture of 0.050 M BS^- and 0.050 M PTS^- (pH = 1.0 by addition of 1.0 M $HClO_4$). After sliding the rotary valve to the left side, the 8-μl sample in the sample loop was injected into the top of the column along with the eluting agent (0.10 M $HClO_4$). The effluent from the column was connected to the flow cell. The absorbance was measured against 0.10 M $HClO_4$ as a reference solution at a wavelength of 260 nm and recorded on the chart paper. The flow was adjusted with aid of the knob which controls the pump speed and it was measured with a 10-ml graduated cylinder (± 0.01 ml) at the outlet of the flow cell.

(ii) Column (99 x 0.20 cm) Packed With Synthesized CPG-8HO_x Resin

(Particle Size of 37-74 μ). The first goal in designing this experiments was the same as c(i) above; that is, to find the optimum resolution for BS^- and PTS^- at various flow rates (0.166 - 0.27 ml/min) using a mixture of 0.0250 M BS^- and 0.0250 M PTS^- (pH = 1.0 by addition of 1.0 M $HClO_4$) as a sample.

After obtaining the "maximum possible" resolution ($R_{1,2}$ = 0.99) at a flow rate of 0.22 ml/min, a mixture of 0.0250 M BS^-, 0.0250 M PTS^-, 0.0250 M 2-MS^-, and 0.0125 M 1-NS^- at pH~1.0 was tested at this "optimum" flow rate. As before, the column was conditioned with 0.10 M HCl for 30 minutes and then the sample (the mixture of four aromatic sulfonates) was introduced and eluted with 0.10 M $HClO_4$. However, the retention times for 2-MS^- and 1-NS^- were relatively long (about 65 min. and 110 min., respectively). In order to elute 2-MS^- and 1-NS^- faster, both an increased concentration of $HClO_4^-$ (from 0.10 M to 0.44 M by adding 30 ml of 0.50 M $HClO_4$ to about 5 ml of 0.10 M $HClO_4$ remaining in a beaker with the original eluting agent in it) and an increased flow rate (from 0.22 ml/min to 0.35 ml/min) were used simultaneously after PTS^- was completely separated from BS^- in about 28 minutes. The absorbance values were recorded as before. The sample loop used was again 8 μl in volume.

2. Results

a. Effect of Flow Rate on Resolution ($R_{1,2}$) for BS^- and PTS^-

Data obtained for resolution at various flow rates, corresponding retention times (t_R), number of theoretical plates (N), and HETP are tabulated in Table XVII(a) and XVII(b) for packing material of particle

TABLE XVII

DATA OBTAINED FOR SEPARATING A MIXTURE OF BS^- AND PTS^-

Table	Flow Rate (Ml/Min)	$R_{1,2}$	t_{R_1} (Min)	t_{R_2} (Min)	t_{ω_1} (Min)	t_{ω_2} (Min)	N_1	N_2	H_1 ($\frac{mm}{Plate}$)	H_2 ($\frac{mm}{Plate}$)
	0.61	0.48	7.34	9.77	2.91	7.20	102	29.5	9.70	33.6
(a)	0.30	0.71	16.7	21.9	5.00	9.71	178	81.4	5.56	12.2
	0.15	0.74	32.4	42.3	9.57	17.1	183	98.0	5.41	10.1
	0.16_6	0.84	25.8	32.0	5.41	9.36	364	187	2.72	5.29
(b)	0.19	0.93	21.4	27.0	4.82	7.23	315	223	3.14	4.44
	0.20_5	0.93	20.0	25.2	4.37	6.83	335	218	2.96	4.54
	0.22	0.99	18.5	23.5	4.14	5.96	319	249	3.10	3.98
	0.23	0.91	18.2	23.0	4.24	6.36	294	209	3.37	4.73
	0.27	0.86	15.3	19.3	3.75	5.56	266	193	3.72	5.13

(a) A sample of 0.050 M BS^- and 0.050 M PTS^- at pH = 1.0 using 125-177 μ particle size of the synthesized CPG-8HO_x resin.

(b) A sample of 0.025 M BS^- and 0.025 M PTS^- at pH = 1.0 using 37-74 μ particle size of the synthesized CPG-8HO_x resin.

where $N = 16 \left(\frac{t_R}{t_\omega}\right)^2$ and $H = \frac{L}{N}$.

material of particle sizes 125-177 μ and 37-74 μ, respectively. A plot of resolution ($R_{1,2}$) versus volume flow rate for the packing with smaller particle sizes (37-74 μ) is shown in Figure 69. A plot of theoretical number of plates (N) for BS^- and PTS^- versus flow rate is shown in Figure 70 and a plot of HETP versus flow rate is presented in Figure 71.

b. Effect of Particle Size on Resolution ($R_{1,2}$) for BS^- and PTS^-

The resolution is compared using two different particle sizes at approximately the same flow rate and is shown in Figure 72.

c. Separation of Four Aromatic Sulfonates

A chromatogram for the separation of four aromatic sulfonates (BS^-, PTS^-, $2\text{-}MS^-$, and $1\text{-}NS^-$) using the computer retracing is presented in Figure 73. Both increasing concentration gradient and flow programming were used after 28 minutes. Since the concentration of $HClO_4$ (eluting agent) changes, the baseline is slightly shifted to a higher absorbance reading. The baseline shown in Figure 73 was thus corrected and an absorbance of 0.02 was presented. In order to simulate the original chromatogram obtained in the recorder, a correction factor of 1.8 and 0.9 was used for BS^- and PTS^- species, respectively. Details of computerized retracing program used are listed in Appendix C, which is similar to that reported by Janssens (123) but uses different computer languages.

3. Discussion

a. The results obtained in Figure 69 show that there is an optimum

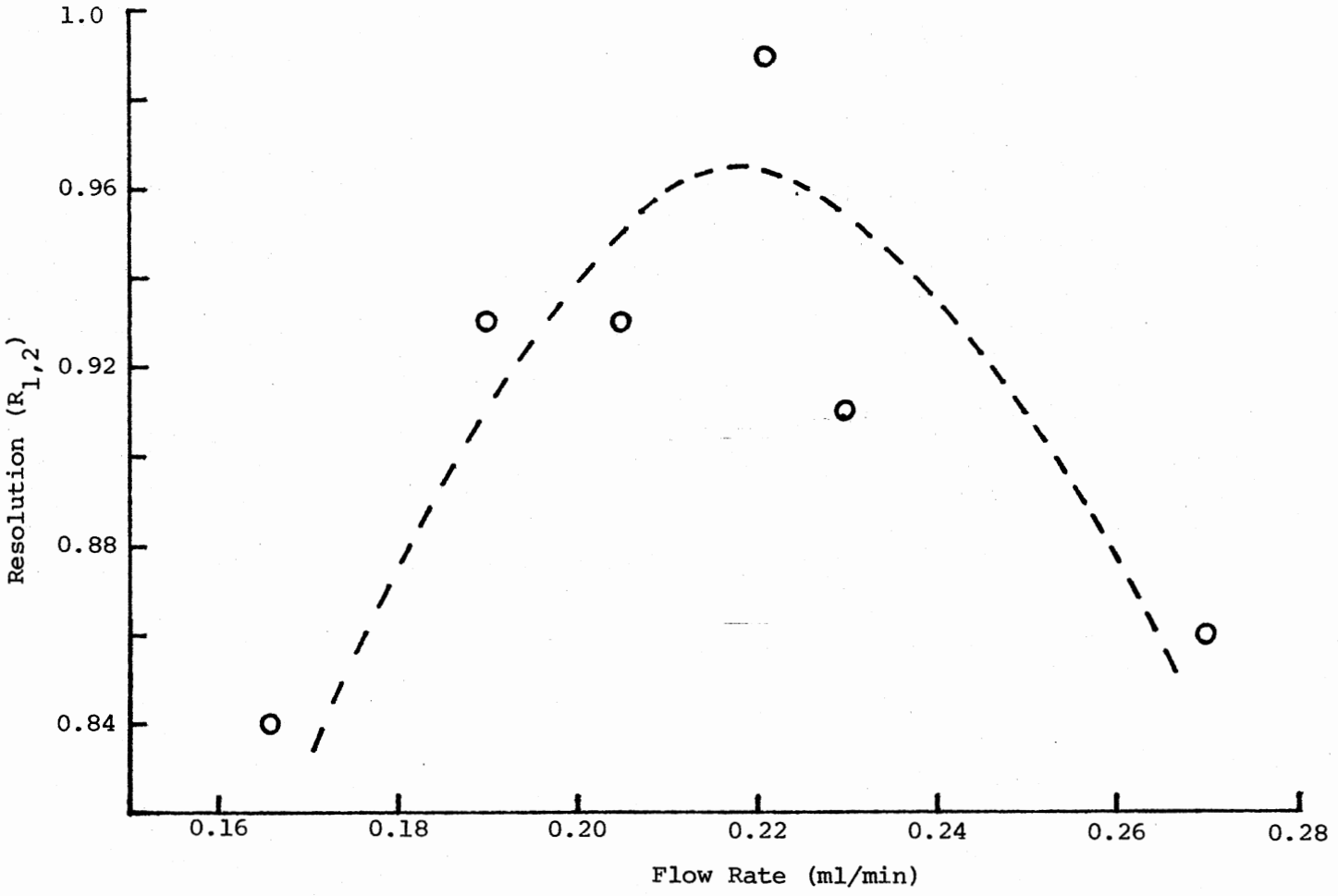

Figure 69. Resolution for BS^- and PTS^- at Various Flow Rates

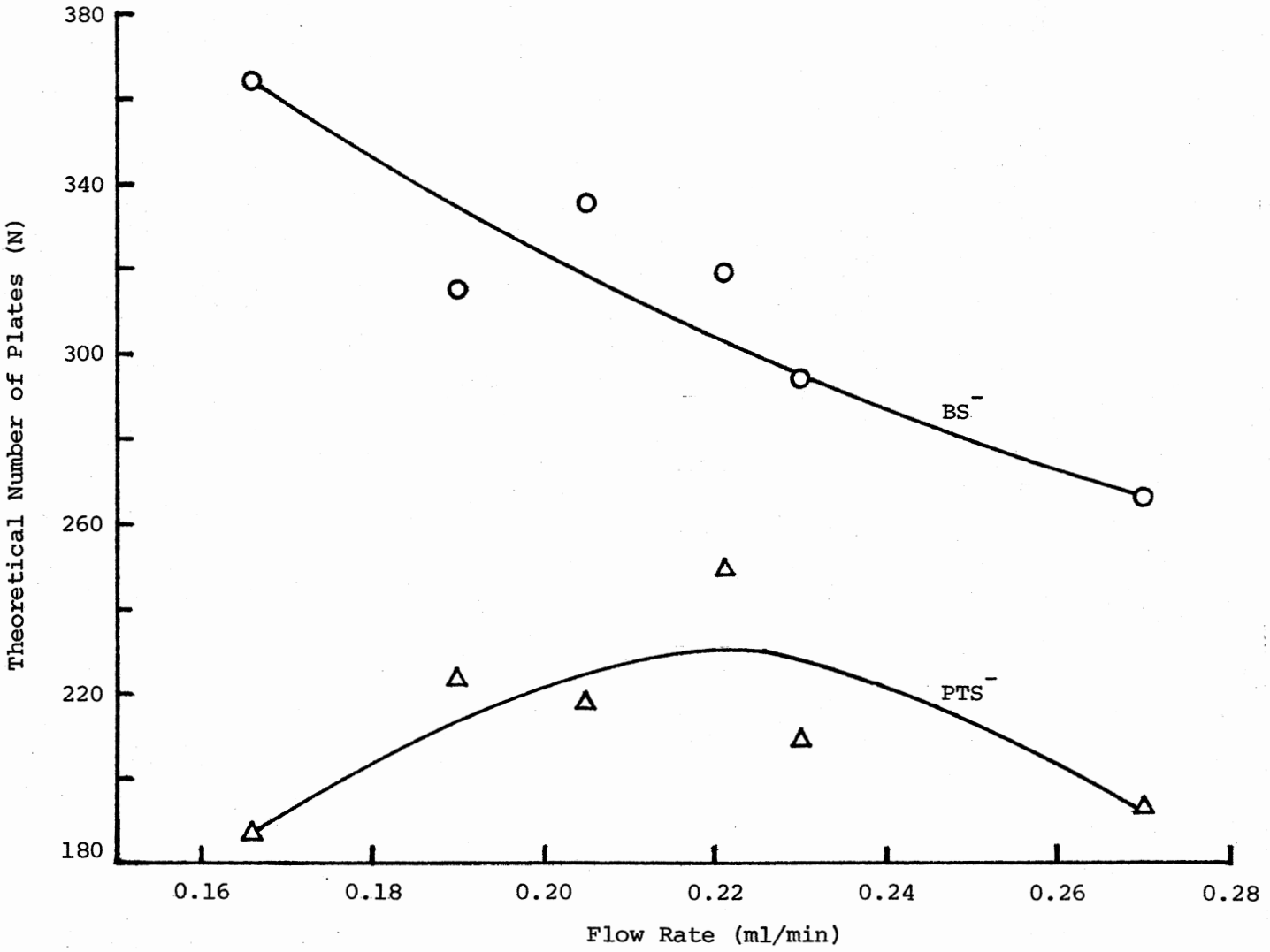

Figure 70. Theoretical Number of Plates for BS^- and PTS^- at Various Flow Rates

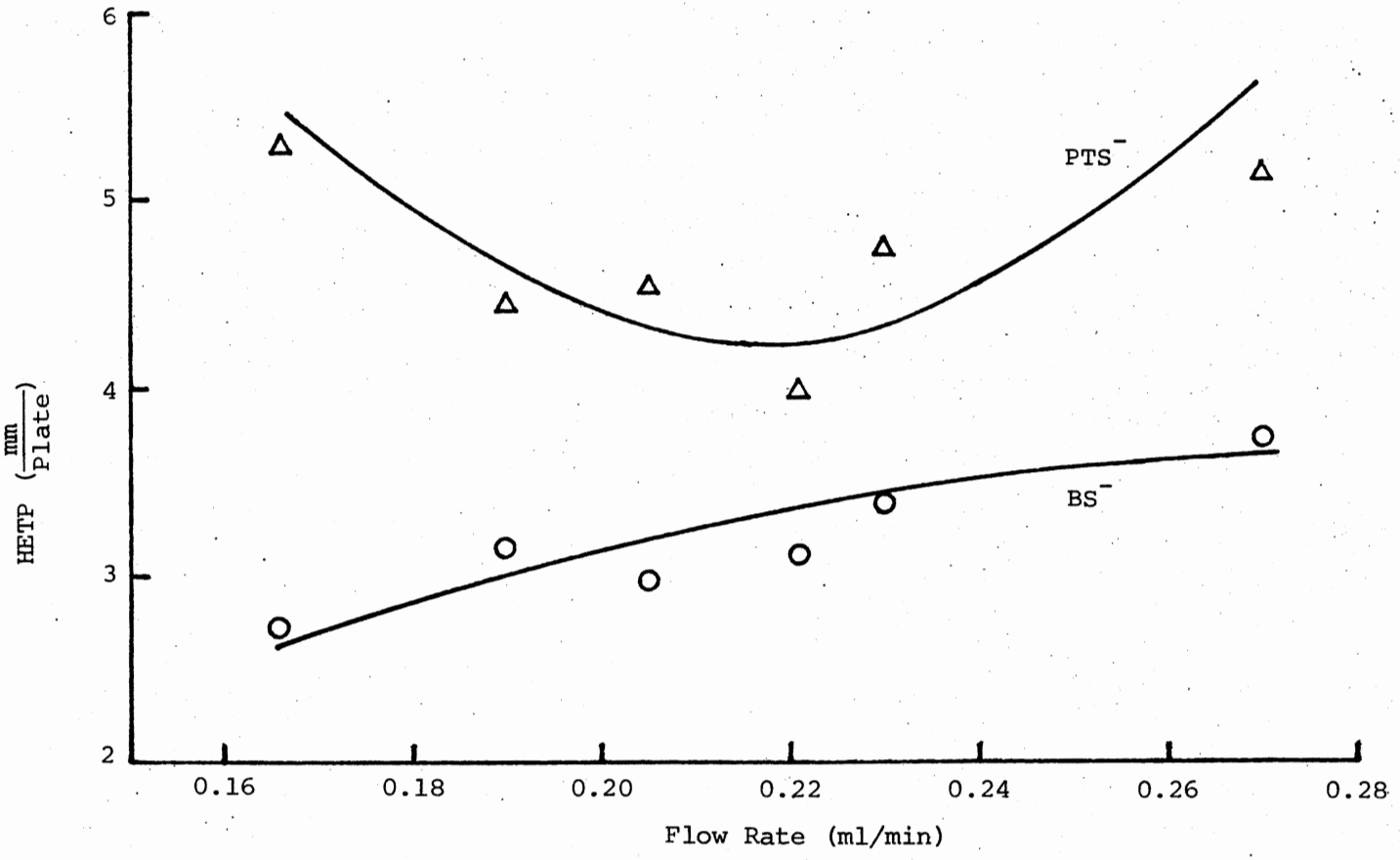

Figure 71. HETP Versus Flow Rate for BS^- and PTS^-

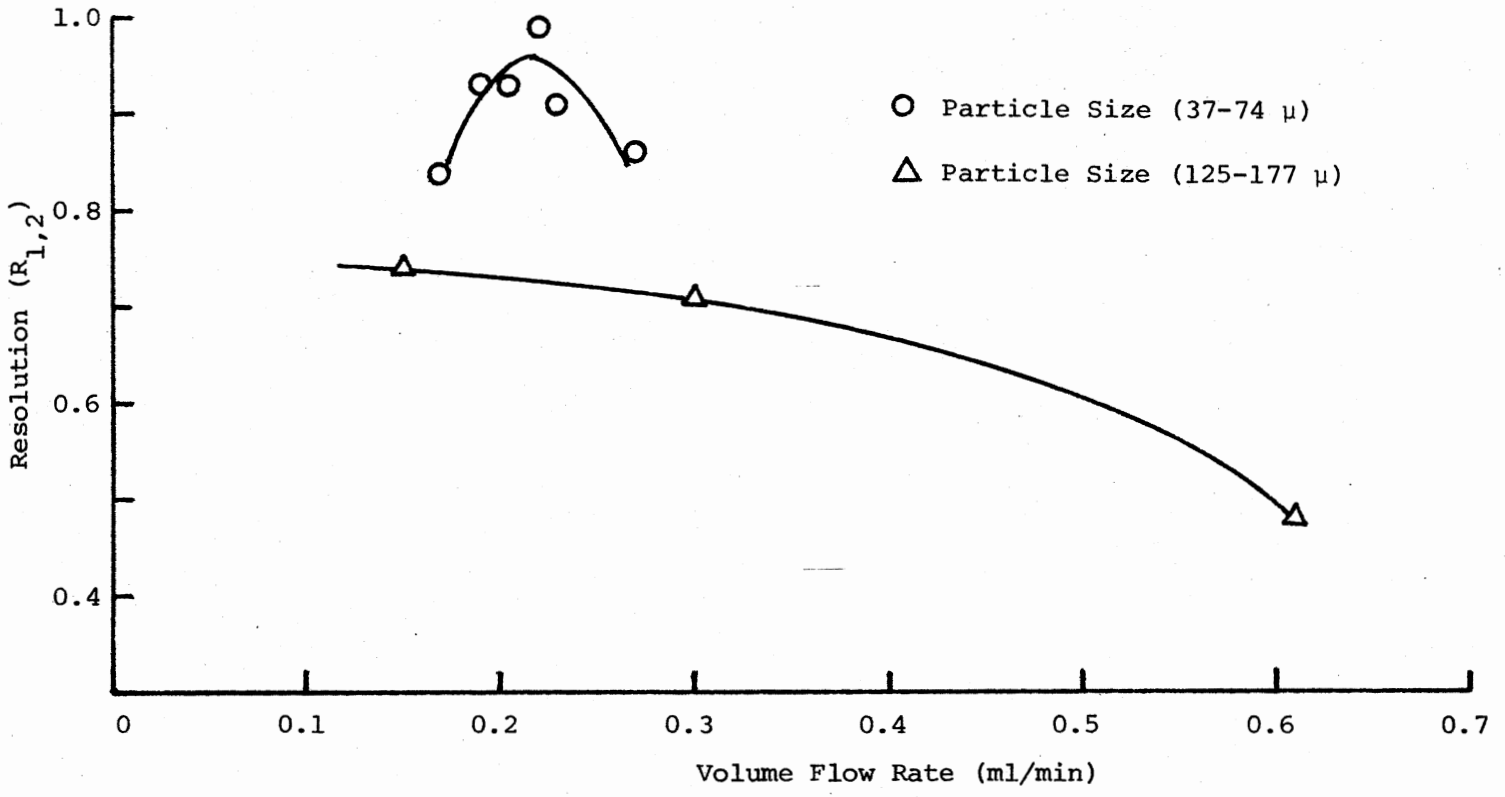

Figure 72. Effect of Particle Size on Resolution ($R_{1,2}$)

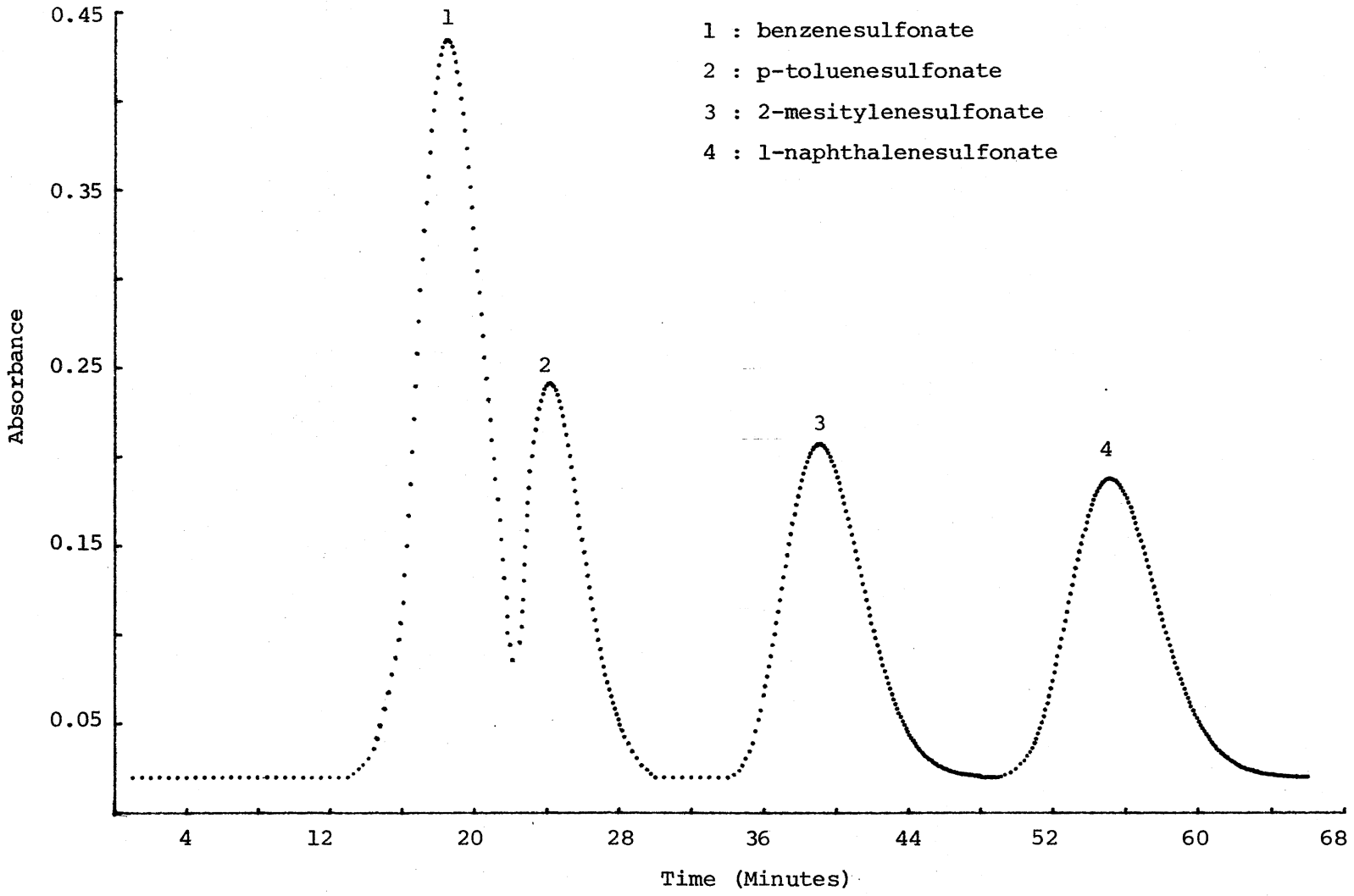

Figure 73. Chromatogram for the Separation of Four Aromatic Sulfonates

flow rate (0.22 ml/min) which gives the best possible resolution (0.99) for BS^- and PTS^-. When the flow rate is larger than the optimum, the mass transfer of solute across the stagnant mobile phase becomes more non-equilibrium; the term $C_s\langle v\rangle$ in Equation 87 increases and H also increases (Figure 71). Hence, the resolution ($R_{1,2}$) in Equation (84) decreases. Since N = L/H, the number of theoretical plates (N) also has to decrease as shown in Figure 70. When the flow rate is smaller than the optimum, the <v> term in Equation (87) becomes smaller, and band broadenings due to $C_M\langle v\rangle$ and $C_s\langle v\rangle$ are smaller. Hence H_1 becomes smaller for BS^- (Figure 71) and N_1 becomes larger for BS^- (Figure 70). However, N_2 for PTS^- becomes smaller. This indicates that the column efficiency for PTS^- is also low at the relatively slow flow rate. The separation using CPG-8HO$_x$ resin may depend on a combination of ion-pair partition (Equation 52) and surface adsorption (Equation 56) on the glass beads. Since BS^- has a smaller K_d value than that of PTS^-, the surface adsorption effect may be smaller for BS^- and the ion-pair partition may be more favored than surface adsorption. While the surface adsorption effect for PTS^- may be very large, especially at slow flow rate, and more favored than ion-pair partition. Because of too slow desorption for PTS^- from the resin, a pronounced band broadening on the base (t_{ω_2}) would occur. Although the retention time (t_R) increases at a lower flow rate, the increase of t_{ω_2} exceeds that of t_{R_2}, as shown in Equation (88). Hence, N_2 becomes

$$N_2 = 16\left(\frac{t_{R_2}}{t_{\omega_2}}\right)^2 \qquad (88)$$

smaller (Figure 70) and H_2 becomes larger (Figure 71) for PTS^- at a smaller flow rate. The resolution ($R_{1,2}$) can also be calculated from Equation (89).

$$R_{1,2} = \frac{t_{R_2} - t_{R_1}}{\frac{1}{2}(t_{\omega_2} + t_{\omega_1})} \qquad (89)$$

Although ($t_{R_2} - t_{R_1}$) becomes larger at a smaller flow rate, the sum of ($t_{\omega_2} + t_{\omega_1}$) is even larger; hence, the resolution ($R_{1,2}$) becomes smaller (Figure 69).

b. The results obtained in Figure 72 show that the resolution for BS^- and PTS^- is improved, as expected, when the smaller particle size packing is used. It was reported by Snyder (49) that H was proportional to $d_p^{(1.4-1.8)}$ when d_p values of 20-70 μ were used in liquid chromatography. If the resolution ($R_{1,2}$) is proportional to $(H)^{-\frac{1}{2}}$ in Equation (84), then the resolution is estimated to be proportional to $(d_p^{0.7-0.9})^{-1}$. However, the results calculated from Figure 72 show that the resolution ($R_{1,2}$) is proportional to $(d_p^{0.13-0.30})^{-1}$ when the average particle size is used. This may be because the exponent of d_p depends on the capacity ratio, k', of the sample (45(a)) and because more than a mechanism for partition is in operation in our case.

c. The chromatogram of Figure 73 shows that the molar distribution coefficients obtained in batch experiments (Figure 51) and the elution profile (Figure 66) obtained with the open column are very helpful in predicting some parameters needed in liquid chromatography. Although the resolution obtained for BS^- and PTS^- is 0.99, two distinct peaks are observed. If a resolution of 1.0 (2% overlap of each band) or 1.5 (base-

line separation) is needed, the column length may be increased to 101 cm or 227 cm, respectively, on the assumption that the resolution is proportional to $(L)^{\frac{1}{2}}$ as shown in Equation (84).

d. After the first two components were eluted (Figure 73), an increasing concentration of $HClO_4$ and an increasing flow rate were used to rapidly elute the other two species. The base line was shifted to a higher absorbance reading (about 0.05 absorbance unit). This may be because the refractive index of the solution in the sample cell changes owing to the concentration programming from 0.10 M to 0.44 M of $HClO_4$.

C. Qualitative Analysis of a Linear Alkylate Sulfonate (LAS) EPA Standard Sample

1. Experimental

a. Material

The stock LAS solution, which contains 5.55% active LAS of an average molecular weight of 318, was prepared by EPA (Environmental Monitoring and Support Laboratory-Cincinnati in cooperation with the Soap and Detergent Association). Hydrochloric acid and perchloric acid have been described previously. Deionized-distilled water was used to dilute samples as necessary.

b. Apparatus

The apparatus set-up (Figure 67) with the column (99 x 0.20 cm) packed with the synthesized CPG-$8HO_x$ resin (37-74 μ) was used. A sample loop of 20 μl was used instead of 8 μl in order to have enough sample (or large enough concentration) in the effluent to be detected by the UV

detector. The Bausch and Lomb Spectronic 505 spectrophotometer was also used for absorbance measurements. A pair of matched quartz cells (1.00 cm path length) and the flow cell, as described in Chapter VI.B.1.b were used.

c. Procedure

The sample was preliminarily tested in the UV region (200-400 nm) using the spectrophotometer. Since the absorbance of the stock LAS solution obtained was larger than 1.0 in the region of 200-332 nm, solutions of successive dilution (1:1 with deionized-distilled water) were prepared and measured.

After obtaining the relative maximum absorbances at wavelengths of 222 nm, 253 nm, and 258 nm, the stock LAS sample solution (20 µl) was injected into the column and analyzed similarly to that described for the separation of aromatic sulfonate mixtures. The wavelengths of 222 nm and 253 nm were used for detection.

2. Results

Spectra scanning from 200 nm to 350 nm for diluted LAS solutions were obtained and are shown in Figure 74. The results of chromatographic separation with detection at 222 nm and 253 nm, respectively, are plotted and shown in Figures 75 and 76, respectively.

3. Discussion

a. The spectra obtained in Figure 62 show that the LAS sample contains some components that absorb at 222 nm, 253 nm, and 258 nm. These components were qualitatively analyzed according to the following rules

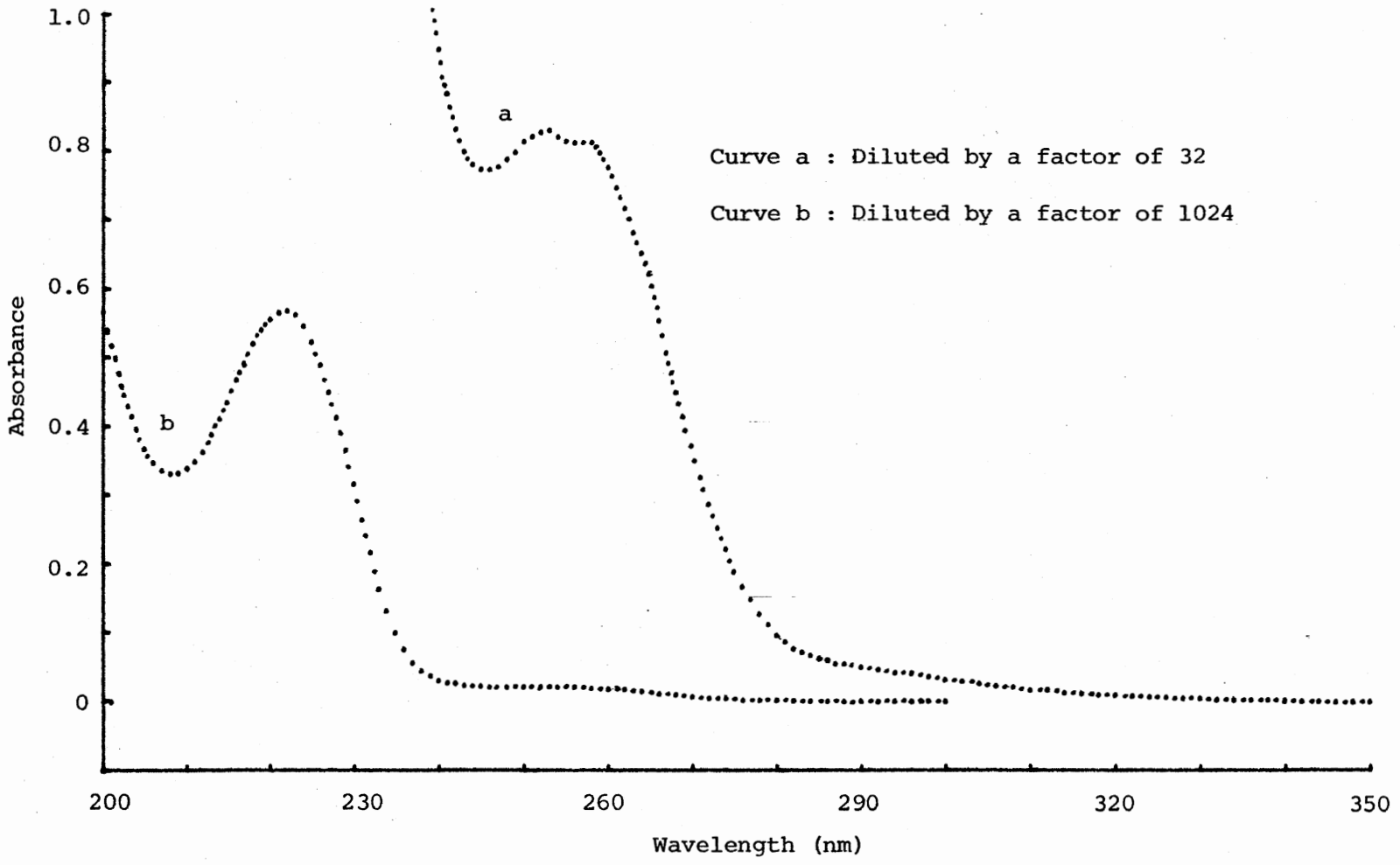

Figure 74. Spectra of Linear Alkylate Sulfonate

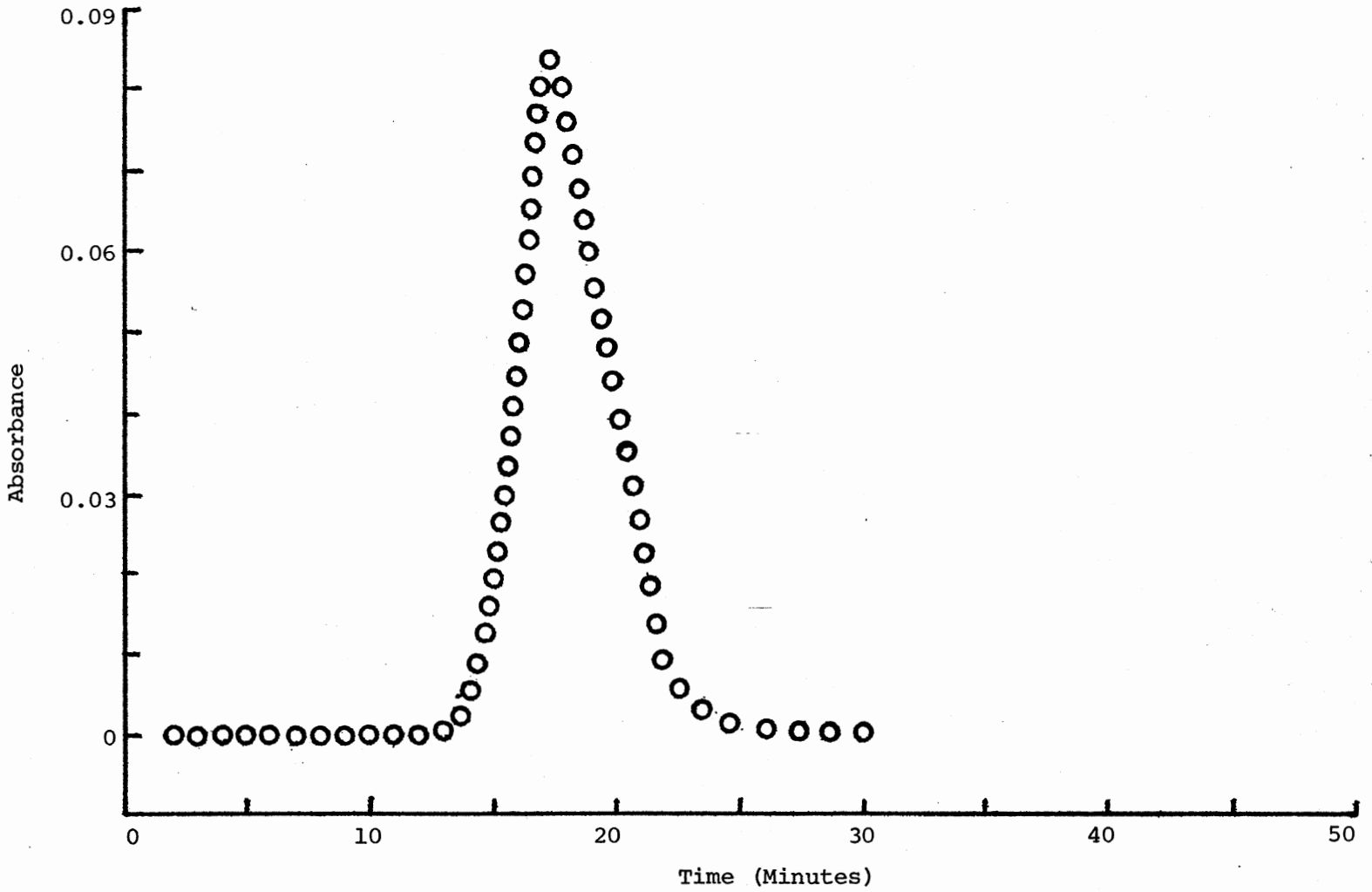

Figure 75. Chromatogram for the LAS Sample at λ = 222 nm

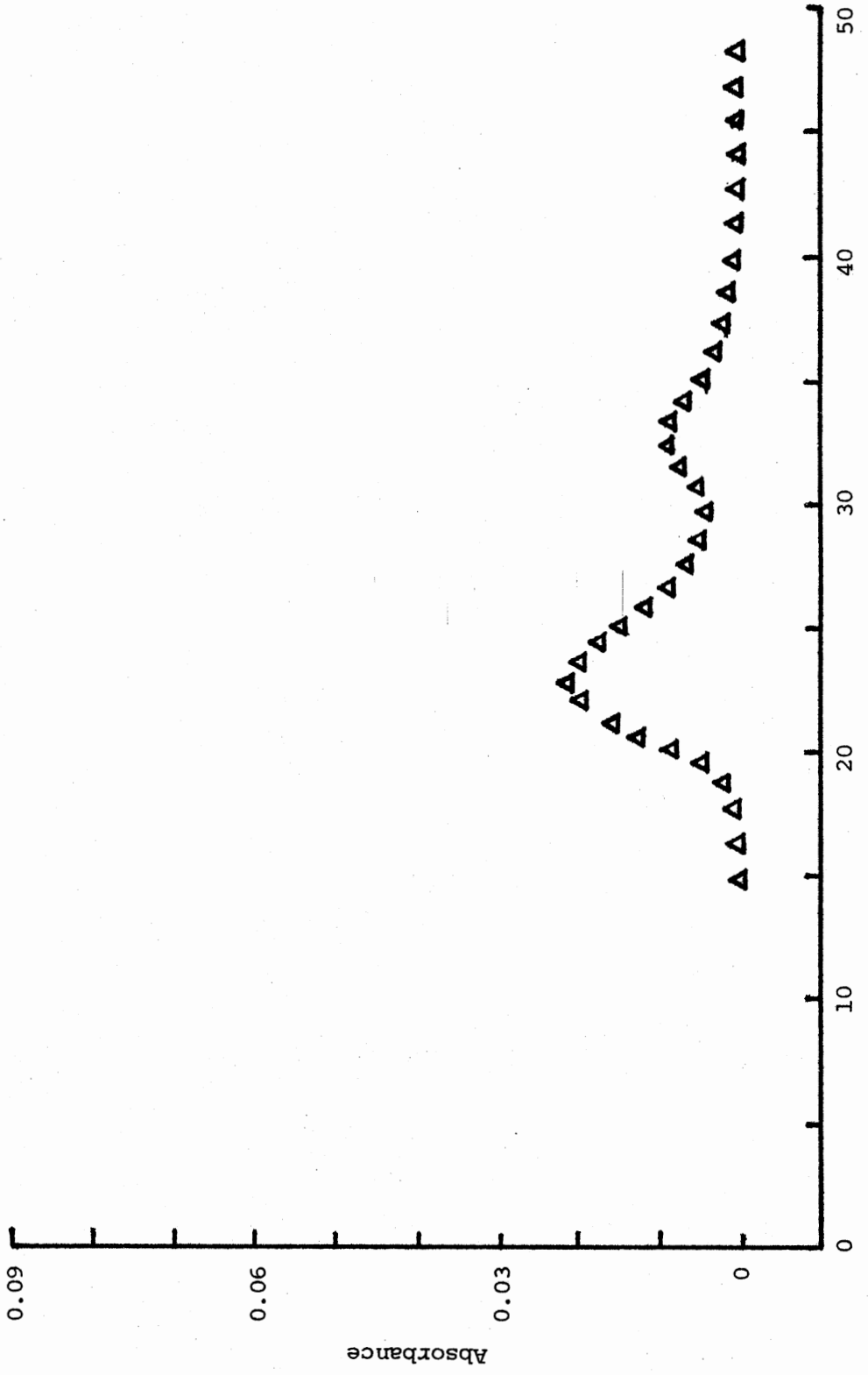

Figure 76. Chromatogram for the LAS Sample at 253 nm

(124):

(i) Unsubstituted 1,3-butadiene 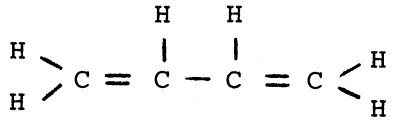 has a λ_{max} at 217 nm.

(ii) For each alkyl group attached to a carbon of the conjugated system, the λ_{max} increases by 5 nm.

(iii) For each double bond which extends the conjugated system, λ_{max} increases by 30 nm. However, if the diene system is within a ring, λ_{max} increases by 36 nm.

The absorbance at 222 nm may be due to the combination of (i) and (ii) above; that at 253 nm may be due to the combination of (i) and (iii); and that at 258 nm may be due to the combination of (i), (ii), and (iii) above. Hence, it may be concluded that the LAS sample contains primarily components such as the following:

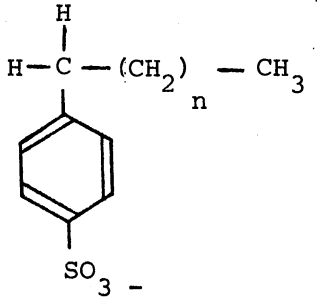

Since the average molecular weight is given as 318, n may be estimated to be about 9 or 10.

b. The retention time obtained from the chromatogram of Figure 75 shows that it is comparable with that of benzenesulfonate (17.3 min.) when the wavelength of 222 nm was used. While the retention time of the first peak in Figure 76 is comparable with that of p-toluenesulfonate (23 min.). The second peak in Figure 76 may be due to a minor component or impurity. From the above discussion, it can be inferred that the LAS

sample is composed in its major part of a p-toluenesulfonate (or mixture).

D. A Prediction of Chromatograms for Some Aliphatic Sulfonates

Since the aliphatic sulfonates can not be determined by UV spectroscopy and no means for their continuous monitoring was at our disposal, it was considered of interest to predict a chromatogram based on the experimental results obtained for aromatic sulfonates (such as, Figures 51 and 73) and the molar distribution coefficients for aliphatic sulfonates (Figure 52) at pH around 2.8. Since only methanesulfonates and ethanesulfonates were used, the separation of these two species was considered.

If a mixture of methanesulfonate and ethanesulfonate is injected into the column with at a volume flow rate of 0.35 ml/min, the retention times and resolution can be estimated as follows:

$$t_{R_i} = \frac{L}{\langle v \rangle} (1 + k'_i) \tag{85}$$

$$R_{5,6} = (r_{56} - 1) \left(\frac{k'_6}{1 + k'_6}\right) \left(\frac{L}{H_6}\right)^{\frac{1}{2}} \tag{90}$$

where 5 represents methanesulfonate and 6 represents ethanesulfonate. Since the capacity factor, k'_i, equals the product of $q \cdot (K_d)_i$, q can be estimated from t_R and K_d of 1-naphthalenesulfonate species, which is near to the aliphatic sulfonates. Let 4 represent 1-naphthalenesulfonate, L = 99 cm, v = 0.35 ml/min, I.D. = 0.20 cm, then

$$\frac{L}{\langle v \rangle} = \frac{L}{\frac{v}{\frac{\pi}{4}(I.D.)^2}} = \frac{99}{\frac{0.35}{\frac{\pi}{4}(0.20)^2}} = 8.81 \text{ (min.)} \quad (91)$$

If the volume flow rate is 0.35 ml/min, then

$$t_{R_4} = (28 \text{ min} \times \frac{0.22 \text{ ml/min}}{0.35 \text{ ml/min}}) + (55-28) = 44.7 \text{ min} \quad (92)$$

k'_4 can be obtained by incorporating Equations (91) and (92) into (85). Hence

$$k'_4 = 4.0_7 = q \cdot K_{d_4} \quad (93)$$

Since $K_{d_4} = 7.12$ at pH about 2.8 (Figure 51), q can be obtained from Equation (93) as follows:

$$q = \frac{4.07}{7.1_2} = 0.57_2 \quad (94)$$

Since $K_{d_5} = 27.8$ and $K_{d_6} = 30.2$ (Figure 52), k'_5 and k'_6 can be calculated as follows:

$$k'_5 = q \cdot K_{d_5} = 0.57_2 \times 27.8 = 15.9 \quad (95)$$

$$k'_6 = q \cdot K_{d_6} = 0.57_2 \times 30.2 = 17.3 \quad (96)$$

Then, the retention times (t_{R_5} and t_{R_6}) can be obtained by inserting Equations (91), (95), and (96), respectively, into Equation (85).

$$t_{R_5} = 8.81 (1 + 15.9) = 149 \text{ (min.)} \quad (97)$$

$$t_{R_6} = 8.8_1 (1 + 17.3) = 161 \text{ (min.)} \quad (98)$$

Since

$$\gamma_{56} = \frac{(K_d)_6}{(K_d)_5} = \frac{30.2}{27.8} = 1.09 \quad (99)$$

and

$$L = 99 \text{ cm},$$

the resolution ($R_{5,6}$) can be estimated from Equation (84) by assuming that $H_6 = 0.60 \frac{\text{cm}}{\text{Plate}}$, which is extrapolated from H_2 in Figure 71, as follows:

$$R_{5,6} = (1.09-1) \left(\frac{17.3}{1+17.3}\right) \left(\frac{99}{0.60}\right)^{\frac{1}{2}} = 1.09 \quad (100)$$

or, if $H_6 = 0.40 \frac{\text{cm}}{\text{Plate}}$, which is extrapolated from H_1 in Figure 71, then, the resolution becomes

$$R_{5,6} = (1.09-1) \left(\frac{17.3}{1+17.3}\right) \left(\frac{99}{0.40}\right)^{\frac{1}{2}} = 1.34 \quad (101)$$

A predicted chromatogram is simulated as shown in Figure 77 at pH of 2.8 and with a flow rate of 0.35 ml/min.

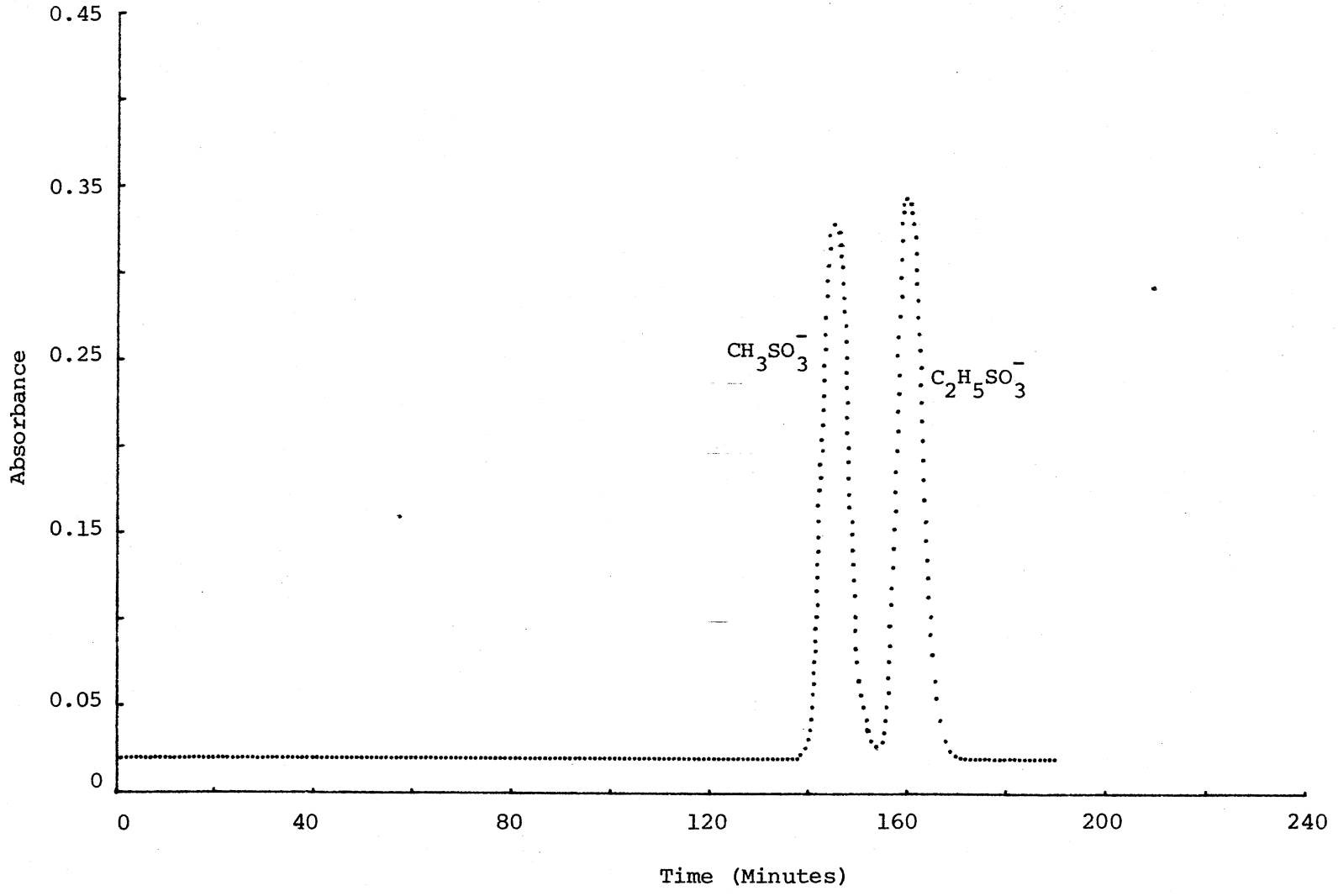

Figure 77. Predicted Chromatogram for Two Aliphatic Sulfonates at pH = 2.8 and Flow Rate = 0.35 ml/min

CHAPTER VII

SUMMARY

Chapter I is an introduction to the historical development of 8-hydroxyquinoline and its naming, structure, solubility, absorption spectra, and pKa_1 value of the protonated form. Chapter II reports some general studies on parameters that affect ion-pair formation. These parameters are concentrated on the nature of the anions, the nature of the organic solvent, and the protolysis side reaction.

Distribution constants for 8-hydroxyquinolinium-anion pairs in liquid-liquid systems were estimated, in Chapter III, using Dyrssen's equation (1). The results obtained in isopentyl alcohol and in 1-butanol system are tabulated in Tables II and IV, respectively. The trend of the $K_{D(H_2O_x^+,A^-)}$ value for anions studied can be qualitatively explained by the theory discussed in Chapter II. However, the $K_{D(HO_x)}$, distribution constant for 8-hydroxyquinoline, value obtained from the slope of Dyrssen's equation is not a constant, as expected, for a given organic solvent, as indicated in Table III and V. This indicates that the model used by Dyrssen is a simplified one. Some modified equations were tested but the results obtained were not satisfactory either, although the trend of $K_{D(H_2O_x^+,A^-)}$ was similar to that obtained from Dyrssen. This may be summarized that Dyrssen's model is only good for estimating $K_{D(H_2O_x^+,A^-)}$ but the real model must be very complicated,

especially for the slope term in Dyrssen's equation.

The 8-hydroxyquinolinium-anion pair studies in liquid-solid system were described in Chapter IV. The molar distribution coefficients, K_d, obtained in Chapter IV.A and IV.B show that the trend for the 8-hydroxyquinolinium-anion pair formation paralleled that in liquid-liquid systems. The K_d values (Figure 38) obtained in batch experiments in Chapter IV.C increase in the order of benzenesulfonate < p-toluenesulfonate < 2-mesitylenesulfonate < 1-naphthalenesulfonate at low pH. Thus it can be predicted that the elution order will be BS^- < PTS^- < $2\text{-}MS^-$ < $1\text{-}NS^-$ in a column chromatography. The degree of separation can also be qualitatively compared from the trend of K_d's. The relative larger K_d values obtained for aliphatic sulfonates compared to those of aromatic ones at pH around 2.8 suggest that a group separation for sulfonates may be possible. The synthesized CPG-$8HO_x$ resin, as described in Chapter IV.D, showed a larger capacity than that of Corning's by a factor of about 2.11. The distribution coefficients obtained in Chapter IV.E (Figures 51 and 52) show that a group separation for sulfonates will be better than that of Corning's, and a separation for aromatic sulfonates is also possible, especially for PTS^-, $2\text{-}MS^-$, and $1\text{-}NS^-$ species at pH around 1.

Chapter V is a literature review of analytical methods for separation and determination of aliphatic and aromatic sulfonates. It is concluded that liquid-liquid and liquid-solid chromatography are powerful techniques for the analysis of sulfonates. Among the determination methods, the use of ion-selective membrane electrodes gives a fast response (within 1 minute); however, the application of ion-selective membrane electrodes to measure the concentration of aliphatic sulfonates

has not been reported yet.

On the basis of the information gathered in Chapter III (liquid-liquid systems) and in Chapter IV (liquid-solid systems), a chromatographic separation of aromatic sulfonates was performed in Chapter VI. The synthesized CPG-8HO$_x$ resin was used as stationary phase and suitable acidic solutions (HCl or $HClO_4$) were used as mobile phases. Chapter VI.A gives an elution profile of aromatic sulfonates (BS^-, PTS^-, $2\text{-}MS^-$, and $1\text{-}NS^-$) in an open column (49 x 0.60 cm). The information obtained from this profile (Figure 66) is also helpful to select the parameters needed for liquid-solid chromatography which was carried out in Chapter VI.B. A "maximum possible" resolution of 0.99 was obtained for BS^- and PTS^- at the optimum flow rate of 0.22 ml/min in a column (99 x 0.20 cm) packed with the synthesized CPG-8HO$_x$ resin (37-74μ particle diameter). After PTS^- was separated from BS^-, an increasing concentration of eluting agent (from 0.10 M to 0.44 M $HClO_4$) and an increasing flow rate (from 0.22 ml/min to 0.35 ml/min) were used, simultaneously, in order to elute $2\text{-}MS^-$ and $1\text{-}NS^-$ faster. A retraced chromatogram using a computer (Hewlett-Packard 9825A) and a plotter (Hewlett-Packard 9862A) was obtained and is shown in Figure 73. The effect of particle size on resolution (Figure 72), and the effect of flow rate on HETP (Figure 71), on theoretical number of plates (Figure 70), and on resolution (Figure 69) for BS^- and PTS^- are also discussed in Chapter VI.B. A qualitative analysis of a Linear Alkylate Sulfonate (LAS) EPA standard sample was tested as recorded in Chapter VI.C. It is concluded that LAS sample is composed largely of p-toluenesulfonate.

An attempt to make an ion-selective membrane electrode sensitive

to ethanesulfonate was made; the results obtained are included in Appendix D. Since the electrode potential starts rising when the ethanesulfonate concentration is larger than 10^{-4} M and the largest change of potential per decade concentration obtained is only + 46 mV in the range of 10^{-2} M to 10^{-1} M, this membrane electrode is not sensitive enough to serve as a chromatographic detector. Hence, a prediction of expected chromatograms for methanesulfonate and ethanesulfonate was tried as discussed in Chapter VI.D. by using the information available from aromatic sulfontes and the molar distribution coefficients of aliphatic sulfonates.

The experiments done in this thesis have shown that 8-hydroxyquinolinium ion is a powerful ion-pairing cation (at low pH) that can be used or applied to separate several anions either by liquid-liquid extraction or liquid-solid chromatography with a relative inexpensive instrumental set-up.

A SELECTED BIBLIOGRAPHY

(1) G. Schill, "Isolation of Drugs and Related Organic Compounds by Ion-Pair Extraction", in Ion Exchange and Solvent Extraction, a series of advances, Chapter 1, Vol. 6, J. A. Marinsky and Y. Marcus (editors), Marcel Dekker (New York, 1974).

(2) Y. Marcus and A. S. Kertes, Ion-Exchange and Solvent Extraction of Metal Complexes, Wiley-Interscience (London, 1969).

(3) U. Mayer, Coord. Chem. Rev., 21, 159 (1976).

(4) G. Schill, K. O. Borg, R. Modin, and B. A. Persson, "Ion-Pair Extraction in the Analysis of Drugs and Related Compounds", in Essays on Analytical Chemistry, E. Wanninen (editor), Pergamon Press (New York, 1977), pp. 379-395.

(5) E. Eksborg and G. Schill, Anal. Chem., 45, 2092 (1973).

(6) G. J. Moody and J. D. R. Thomas, Selective Ion Sensitive Electrodes, Merrow Publishing Co., Ltd. (England, 1971).

(7) J. Koryta, Ion-Selective Electrodes, Cambridge University Press (New York, 1975).

(8) R. Berg, Pharm. Ztg. Berl., 71, 1542 (1926); cited in R. G. W. Hollingshead, Oxine and Its Derivatives, The Butterworths Scientific Publications (London, 1954), Volume 1, p. 1.

(9) G. H. Morrison and H. Freiser, Solvent Extraction in Analytical Chemistry, John Wiley & Sons, Inc., (New York, N. Y., 1957), pp. 162-165.

(10) E. B. Sandell, Colorimetric Determination of Trace of Metals, 3rd. edn., Interscience, (New York, N. Y., 1959).

(11) Q. Fernando and J. P. Phillips, J. Am. Chem. Soc., 74, 3103 (1952).

(12) J. J. Fox, J. Chem. Soc., 1119 (1910).

(13) I. M. Kolthoff, Chem. Weekbl., 24, 606 (1927).

(14) K. G. Stone and L. Friedman, J. Am. Chem. Soc., 69, 209 (1947).

(15) S. Lacroix, Anal. Chim. Acta, 1, 260 (1947).

(16) H. Irving, J. A. D. Ewart, and J. T. Wilson, J. Chem. Soc., 2672 (1949).

(17) J. P. Phillips, R. L. Elbinger, and L. L. Merritt, J. Am. Chem. Soc., 71, 3987 (1949).

(18) E. B. Sandell and D. C. Spindler, J. Am. Chem. Soc., 71, 3806 (1949).

(19) R. Nasanen, P. Lumme, and A. L. Mukula, Acta Chem. Scand., 5, 1199 (1951).

(20) D. Dyrssen, Svensk. Kem. Tidskr., 64, 213 (1952).

(21) H. A. Mottola and H. Freiser, Talanta, 13, 55 (1966).

(22) G. H. Morrison and H. Freiser, Solvent Extraction in Analytical Chemistry, John Wiley and Sons, Inc., New York, 1957, p. 249.

(23) H. Goto, Sci. Rep. Tohoku Univ., 26, 391 (1937-8) and 26, 418 (1938).

(24) H. R. Fleck and A. M. Ward, Analyst, 58, 388 (1933).

(25) H. R. Fleck, Analyst, 62, 378 (1937).

(26) M. Borrel and R. A. Paris, Anal. Chim. Acta, 6, 394 (1952).

(27) (a) H. Freiser, "Solvent Extraction", An Introduction to Separation Science, B. L. Karger, L. R. Snyder, and C. Horvath (editors), John Wiley and Sons, Inc. (New York, 1973), Chapter 9.

(b) The same book as described in Ref. (27)(a), Chapter 5.

(28) T. Moeller, Ind. Eng. Chem. (Anal. Ed.), 15, 270, 346 (1943).

(29) L. D. Pennington and M. B. Williams, Ind. Eng. Chem., 51, 759 (1959).

(30) F. Vernon and H. Eccles, Anal. Chim. Acta, 63, 403 (1973).

(31) F. Vernon, Chem. Ind., 634 (1977).

(32) F. Vernon and K. M. Nyo, Separation Sci. Technol., 13, 263 (1978).

(33) Idem., J. Inorg. Nucl. Chem., 40, 887 (1978).

(34) E. D. Moorhead and P. H. Davis, Anal. Chem., 46, 1879 (1974).

(35) General Catalog, Pierce Chemical Company, P.O. Box 177, Rockford, Illinois, 61105, 1976-1977, pp. 274-296.

(36) J. R. Jezorek and H. Freiser, Anal. Chem., 51, 366 (1979).

(37) S. Siekierski, J. Radioanal. Chem., 31, 335 (1976).

(38) E. Sekido, Y. Yoshimura and Y. Masuda, J. Inorg. Nucl. Chem., 38, 1183 (1976).

(39) R. M. Diamond and D. G. Tuck, Prog. Inorg. Chem., 2, 109 (1960).

(40) J. J. Bucher and R. M. Diamond, J. Phys. Chem., 69, 1565 (1965).

(41) J. H. Hildebrand and R. L. Scott, The Solubility of Non-electrolytes, 3rd. ed., Dover Publications (New York, 1964).

(42) J. H. Hildebrand, J. M. Prausnitz, and R. L. Scott, Regular and Related Solutions, Van Nostrand Reinhold Company (New York, 1970).

(43) C. Hansen, Ind. Eng. Chem., Prod. Res. Dev., 8, 2 (1969).

(44) A. Ringbom, Complexation in Analytical Chemistry, Wiley (New York, 1963).

(45) (a) B. L. Karger, in Modern Practice of Liquid Chromatography, J. J. Kirkland (editor), Interscience, (New York, 1971), Chapter 1.

(b) The same book as described in Ref. (45)(a), p. 226.

(46) N. A. Parris, J. Chromatogr. Library, Vol. 5, "Instrumental Liquid Chromatography", Elsevier Scientific Publishing Co., (New York, 1976), p. 96.

(47) S. Przeszlakowski and R. Kocjan, Chromatographia, 10, 358 (1977).

(48) J. A. Dean, Chemical Separation Methods, Van Nostrand Reinhold Company, (New York, 1969), p. 96.

(49) L. R. Snyder, J. Chromatog. Sci., 7, 352 (1969).

(50) Y. Marcus, Introduction to Liquid State Chemistry, John Wiley and Sons, (New York, 1977), pp. 250-251.

(51) H. H. Willard, L. L. Merritt, and J. A. Dean, Instrumental Methods of Analysis, 4th ed., Van Nostrand Reinhold Company, (New York, 1965), pp. 764-765.

(52) M. Windholz, S. Budavari, L. Y. Stroumtsos, and M. N. Fertig (editors), The Merck Index, 9th ed., Merck and Co., Inc., Rahway, (New Jersey, 1976), pp. 150-151.

(53) R. T. Morrison and R. N. Boyd, Organic Chemistry, 2nd ed., Allyn and Bacon, Inc., (Boston, 1966), p. 701.

(54) A. F. M. Barton, Chem. Rev., 75, 731 (1975).

(55) H. H. Weetal, Biochim. Biophys. Acta, 212, 1 (1970).

(56) K. F. Sugawara, et al., A Handout of Corning Glass Works on Synthesizing of 8-Hydroxyquinoline as Immobilized Chelating Compound on Controlled Pore Glass (550Å).

(57) "Sonneborn Petroleum Sulfonates, Standard of the Industry for More Than 70 Years." Handout of Witco Chemical Sonneborn Division, New York, N. Y., 10017. (The year is not recorded on the Handout.)

(58) H. N. Dunning, M. M. Kreevoy, and J. M. White, U.S. Patent 3,215,622 (1965); C.A. 64, 436 (1966).

(59) W. H. Houff, D. R. Christie, and R. H. Beaumont, Anal. Chem., 29, 1866 (1957).

(60) E. A. Gribova, Zavodskaya Lab., 27, 154 (1961); translated to Eng. in Industrial Lab., 27, 155 (1961).

(61) S. R. Epton, Trans. Faraday Soc., 44, 226 (1948).

(62) D. J. Fenwick, Ind. Lubr. Tribol. 23, 201 (1971).

(63) P. I. Brewer, J. Inst. Petrol. (London), 58, 41 (1972).

(64) L. K. Wang, J. Y. Yang, and M. H. Wang, Eng. Bull. Purdue Univ., Eng. Ext. Ser., 142, 76 (1973).

(65) L. K. Wang, J. Y. Yang, R. G. Ross, and M. H. Wang, Water Resour. Bull., 11, 267 (1975).

(66) R. K. Maurmeyer and M. Rafalowitz, Mikrochim. Acta, 561 (1964).

(67) S. K. Chhibber, O. N. Anad, and V. P. Malik, Indian J. Technol., 14, 355 (1976).

(68) R. R. Parmar and B. N. Sahukar, Ind. Lubr. Tribol., 28, 192 (1976).

(69) R. M. Kelley, E. W. Blank, W. E. Thompson, and R. Fine, ASTM Bull., 237, 70 (1959).

(70) E. H. Brandli and R. M. Kelley, J. Am. Oil Chem. Soc., 47, 200 (1970).

(71) H. Cerfontain, H. G. J. Duin, and L. Vollbracht, Anal. Chem., 35, 1005 (1963).

(72) J. M. Arends, H. Cerfontain, I. S. Herschberg, A. J. Prinsen, and A. C. M. Wanders, Anal. Chem., 36, 1802 (1964).

(73) J. Longwell and W. D. Maniece, Analyst. 80, 167 (1955).

(74) T. Tanaka, K. Hiiro, and A. Kawahara, Japan Anal., 24, 320 (1973); cited in Anal. Chim. Acta, 99, 11 (1978).

(75) L. K. Wang, U.S. Patent 3,992,149 (1976); C.A. 86, 110878 (1977).

(76) L. K. Wang and R. G. Ross, Int. J. Environ. Anal. Chem., 4, 285 (1976).

(77) L. R. Whitlock, S. Siggia, and J. E. Smola, Anal. Chem., 44, 532 (1972).

(78) K. C. Schreiber, Anal. Chem., 21, 1168 (1949).

(79) D. Barnard, J. M. Fabian, and H. P. Koch, J. Chem. Soc., 2442 (1949).

(80) H. Alter and M. Bit-Alkhas, Text. Res. J., 39, 479 (1969).

(81) S. D. Kullbom and H. F. Smith, Anal. Chem., 35, 912 (1963).

(82) J. J. Kirkland, Anal. Chem., 32, 1388 (1960).

(83) T. Nagai, S. Hashimoto, I. Yamane, and A. Mori, J. Am. Oil Chem. Soc., 47, 505 (1970).

(84) S. Siggia, L. R. Whitlock, and J. C. Tao, Anal. Chem., 41, 1387 (1969).

(85) S. Siggia and L. R. Whitlock, Anal. Chem., 42, 1719 (1970).

(86) H. Cerfontain, A. Koeberg-Telder, C. Kruk, and C. Ris, Anal. Chem., 46, 72 (1974).

(87) A. Heywood, A. Mathias, and A. E. Williams, Anal. Chem., 42, 1272 (1970).

(88) P. T. Crisp, J. M. Eckert, and N. A. Gibson, Anal. Chim. Acta, 78, 391 (1975).

(89) P. T. Crisp, J. M. Eckert, N. A. Gibson, G. F. Kirkbright, and T. S. West, Anal. Chim. Acta, 87, 97 (1976).

(90) C. G. Taylor and J. Watters, Analyst, 97, 533 (1972).

(91) D. M. Clementz, Anal. Chem., 49, 1148 (1977).

(92) C. J. Coetzee and H. Freiser, Anal. Chem., 40, 2071 (1968).

(93) N. Ishibashi and H. Kohara, Bunseki Kagaku, 21, 100 (1972); C.A. 76, 107667 (1972).

(94) N. Ishibashi, H. Kohara, and K. Horinouchi, Talanta, 20, 867 (1973).

(95) N. Ishibashi and H. Kohara, Anal. Letters, 4, 787 (1971).

(96) E. A. Myshkin, N. N. Lavrova, and Z. M. Ivanova, Zavodskaya Lab., 27, 163 (1961); translated to Eng. in Industrial Lab., 27, 164 (1961).

(97) N. E. Skelly, Anal. Chem., 37, 1526 (1965).

(98) R. D. Swisher, J. Am. Oil Chemists' Soc., 43, 137 (1966).

(99) J. S. Parsons, J. Gas Chromatog., 5, 254 (1967).

(100) E. N. Krylov, Zavodskaya Lab., 42, 778 (1976); translated to Eng. in Industrial Lab., 42, 1023 (1976).

(101) M. W. Scoggins and J. W. Miller, Anal. Chem., 40, 1155 (1968).

(102) R. H. Stehl, Anal. Chem., 42, 1802 (1970).

(103) S. Fudano and K. Konishi, J. Chromatogr., 51, 211 (1970).

(104) Idem., J. Chromatogr., 62, 467 (1971).

(105) O. I. Kachurin and V. Y. Vasilenko, Zh. Anal. Khim., 30, 585 (1975); translated to Eng. in J. Anal. Chem. USSR, 30, 493 (1975).

(106) C. M. Coyne and G. A. Maw, J. Chromatogr., 14, 552 (1964).

(107) R. Takeshita, N. Jinnai, and H. Yoshida, J. Chromatogr., 123, 301 (1976).

(108) J. Franc, V. Pikes, and M. Hajkova, J. Chromatogr., 119, 661 (1976).

(109) J. S. Fritz and R. K. Gillette, Anal. Chem., 40, 1777 (1968).

(110) W. R. Ali and P. T. Laurence, Anal. Chem., 45, 2426 (1973).

(111) J. C. Kraak and J. F. K. Huber, J. Chromatogr., 102, 333 (1974).

(112) C. P. Terweij-Groen and J. C. Kraak, J. Chromatogr., 138, 245 (1977).

(113) K. G. Wahlund, J. Chromatogr., 115, 411 (1975).

(114) J. J. Kirkland, Anal. Chem., 43, (12), 37A (1971); cited in J. Chromatogr. Libr., 3, 934 (1975) by J. Churacek.

(115) J. H. Knox and G. R. Laird, J. Chromatogr., 122, 17 (1976).

(116) D. J. Pietrzyk and C. H. Chu, Anal. Chem., 49, 757 (1977).

(117) Idem., Anal. Chem., 49, 860 (1977).

(118) S. Siggia, Survey of Analytical Chemistry, McGraw-Hill Book Co. (N. Y., 1968).

(119) J. F. K. Huber and A. M. Van Urk-Schoen, Anal. Chim. Acta, 58, 395 (1972).

(120) J. Ruzicka, E. H. Hansen, H. Mosbaek, and F. J. Krug, Anal. Chem., 49, 1858 (1977).

(121) S. L. Meyer, Data Analysis for Scientists and Engineers, John Wiley and Sons, Inc. (New York, 1975), Chapter 24.

(122) P. R. Bevington, Data Reduction and Error Analysis for the Physical Science, McGraw-Hall Book Co., (New York, 1969), Chapter 3.

(123) G. Janssens, J. High Resol. Chromatogr. Chromatogr. Commun., #10069, p. 84, Feb. (1979).

(124) C. J. Creswell and O. Rungquist, Spectral Analysis of Organic Compounds, Burgess Publishing Company (Minnesota, 1970), p. 41.

(125) A. Craggs, G. J. Moody, and J. D. R. Thomas, J. Chem. Educ., 51, 541 (1974); cited in Analysis with Ion-Selective Electrodes, by P. L. Bailey, Heyden and Son, Ltd., (Great Britain, 1976), p. 221.

(126) G. J. Moody, R. B. Oke, and J. D. R. Thomas, Analyst, 95, 910 (1970).

(127) J. Ruzicka, E. H. Hansen, and J. C. Tjell, Anal. Chim. Acta, 67, 155 (1973).

(128) Newsletter of Orion Research Incorporated, Vol. 1, No. 5, Oct. 1969.

(129) Handbook of Mathematical Functions With Formulas, Graphs, and Mathematic Tables, U.S. Department of Commerce National Bureau of Standards, Applied Math Series 55 (1965).

APPENDIX A

DERIVATION OF DYRSSEN'S MODEL (REFERENCE (20))

It is assumed that 8-hydroxyquinolinium-anion pair is formed as shown in Figure 78.

Where $\underline{o}$ refers to an organic phase; $\underline{\omega}$ refers to an aqueous phase; $K_{D(HO_x)}$ and $K_{D(H_2O_x^+,A^-)}$ are partition constants of 8-hydroxyquinoline and 8-hydroxyquinolinium-anion pair between the organic phase and the aqueous phase, respectively; K_f is the formation constant for the 8-hydroxyquinolinium-anion pair in the aqueous phase; and Ka is the acid dissociation constant of the HA.

The dissociation constants of protonated and neutral 8-hydroxyquinoline, Ka_1 and Ka_2, respectively, can be expressed as follows:

$$H_2O_x^+ \overset{Ka_1}{\rightleftharpoons} H^+ + HO_x \qquad \text{(A1)}$$

$$HO_x \overset{Ka_2}{\rightleftharpoons} H^+ + O_x^- \qquad \text{(A2)}$$

where

$$Ka_1 = \frac{[H^+][HO_x]}{[H_2O_x^+]} \qquad \text{(A3)}$$

$$Ka_2 = \frac{[H^+][O_x^-]}{[HO_x]} \qquad \text{(A4)}$$

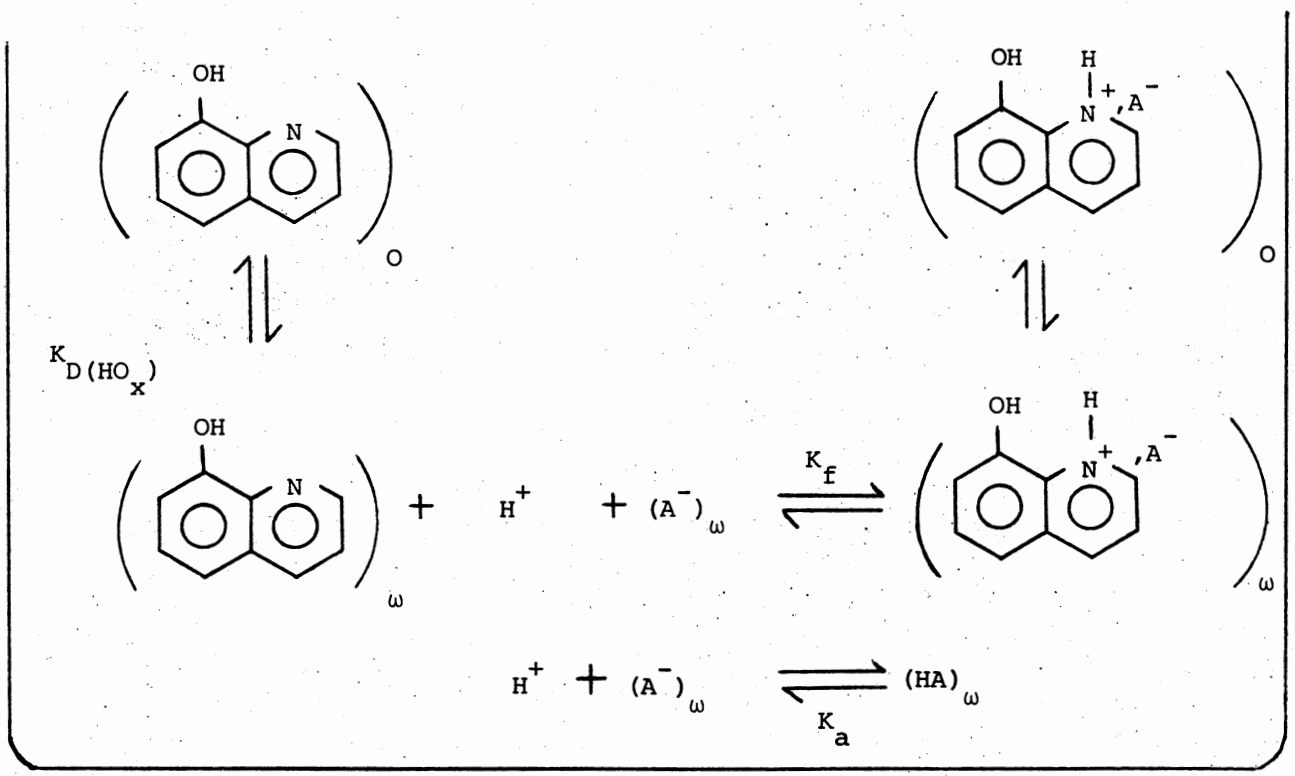

Figure 78. A Sketch for the 8-Hydroxyquinolinium-Anion Pair Formation and Extraction

The partition constants of $K_{D(H_2O_x^+,A^-)}$ and $K_{D(HO_x)}$ are shown as follows:

$$K_{D(H_2O_x^+,A^-)} = \frac{[H_2O_x^+,A^-]_o}{[H_2O_x^+,A^-]_\omega} \quad \text{(A5)}$$

$$K_{D(HO_x)} = \frac{[HO_x]_o}{[HO_x]_\omega} \quad \text{(A6)}$$

The distribution ratio, D, for 8-hydroxyquinoline is defined as a ratio of equilibrium concentration of total species of 8-hydroxyquinoline in an organic phase to that in an aqueous phase and is expressed in Eq. (A7)

$$D = \frac{\Sigma[HO_x]_o}{\Sigma[HO_x]_\omega} = \frac{[H_2O_x^+,A^-]_o + [HO_x]_o}{[H_2O_x^+]_\omega + [HO_x]_\omega + [O_x^-]_\omega} \quad \text{(A7)}$$

Assuming that the concentration of $(A^-)_\omega$ is much larger than that of $[H_2O_x^+]_\omega$ and that Ka is very large, so that $[H_2O_x^+,A^-]_\omega$ is predominant and equivalent to that of $[H_2O_x^+]_\omega$. Equation (A7) can be rewritten as follows:

$$D = \frac{[H_2O_x^+,A^-]_o + [HO_x]_o}{[H_2O_x^+,A^-]_\omega + [HO_x]_\omega + [O_x^-]_\omega} \quad \text{(A8)}$$

Since pKa_1 (20) is approximately 5, $[HO_x]_\omega$ and $[O_x^-]_\omega$ are small and negligible by comparing with $[H_2O_x^+]_\omega$ at a low pH of 1-2. Hence, Equation (A8) is simplified as

$$D = \frac{[H_2O_x^+,A^-]_o + [HO_x]_o}{[H_2O_x^+,A^-]_\omega} \quad \text{(A9)}$$

Incorporating Equations (A5) and (A6) into (A9) gives

$$D = K_{D(H_2O_x^+,A^-)} + \frac{K_{D(HO_x)}\ [HO_x]_\omega}{[H_2O_x^+,A^-]_\omega} \qquad \text{(A10)}$$

Since $[H_2O_x^+,A^-]_\omega$ formed is equivalent to $[H_2O_x^+]_\omega$ according to the assumption, Equation (A10) can be rewritten as follows:

$$D = K_{D(H_2O_x^+,A^-)} + \frac{K_{D(HO_x)}\ [HO_x]_\omega}{[H_2O_x^+]} \qquad \text{(A11)}$$

A substitution of $\frac{Ka_1}{[H^+]}$ for $\frac{[HO_x]_\omega}{[H_2O_x^+]_\omega}$, from Equation (A3) into Equation (A11) results Equation (A12) which was first used by Dyrssen in 1952.

$$D = K_{D(H_2O_x^+,A^-)} + \frac{Ka_1\ K_{D(HO_x)}}{[H^+]} \qquad \text{(A12)}$$

APPENDIX B

ADDITIONAL PAPERS OF INTEREST NOT INCLUDED IN THE REVIEW

B1. D. R. Zornes, G. P. Willhite, and M. J. Michnick, "An Experimental Investigation into the Use of High-Pressure Liquid Chromatography for the Determination of Petroleum Sulfonates." Soc. Pet. Eng. J., 18, 207 (1978); C.A. 89, 148993 (1978).

B2. C. E. Kind, "Extractive Separation of Non-Surface Active Components From a Mixture Containing These Components, Water, and Sulfated and/or Sulfonated Organic Components." Ger. Offen. 2,753,024; C.A. 89, 45376 (1978).

B3. I. B. Bronfin, L. F. Veselovskaya, and R. A. Vinnikova, "Method for Determination of the Chemical Composition of Raw Materials in the Production of Sulfonate Additives." Neftepererab. Neftekhim. (Moscow), 11, 43 (1977); C.A. 88, 91886 (1978).

B4. S. Miwa, Y. Ohno, and S. Sato, "Separation of Metallic Sulfonates for Detergent-Dispersants and Base Oil by Gel Permeation Chromatography." Kanzei Chuo Bunsekishoho, 17, 95 (1977); C.A. 87, 70582 (1977).

B5. D. P. Stognushko, G. A. Tember, L. Y. Glukhova, I. A. Volkov, V. N. Ivanov, A. T. Perikova, and Y. I. Usatenko, "Determination of Alkylbenzene Sulfonates, Toluenesulfonate and Sodium Sulfate in Pastes." Neftepererab. Neftekhim. (Moscow), 2, 34 (1977); C.A. 87, 70649 (1977).

B6. I. Bargenda, S. Lettau, J. Sommer, R. Sowada, H. Leue, F. Rose, and W. Werner, "Extraction of Sulfonates From Diluted Aqueous Solutions." Ger. (East), 121,779; C.A. 87, 22398 (1977).

B7. I. G. Dagaeva, D. B. Boguslavets, V. A. Kuznetsov, and O. L. Glavati, "Determination of Oil-Soluble Sulfonates by Two-Phase Titration." Sb. Tr. Vses. Ob'edin Neftekhim, 11, 75 (1976); C.A. 87, 87474 (1977).

B8. L. A. Pobortseva, N. D. Sorokina, N. Y. Udovichenko, and A. S. Savrasov, "Method for Rapid Determination of Active Substances in Products of Sulfonation of Organic Compounds With Sulfur Trioxide and Its Hydrates." Neftepererab. Neftekhim. (Moscow), 7, 34 (1977); C.A. 87, 119650 (1977).

B9. V. N. Ivanov, N. I. Gorina, D. P. Stognushko, G. A. Tember, and I. A. Volkov, "Analysis of Sodium Alkylbenzenesulfonates by Nephelometric Titration." Maslo-Zhir. Prom-St., 9, 24 (1977); C.A. 87, 153699 (1977).

B10. L. Neubauer, "New Detection Method in Thin-Layer Chromatography of α-Olefinsulfonates." Chem. Prum., 27, 196 (1977); C.A. 87, 62150 (1977).

B11. S. Hashimoto, K. Asano and T. Nagai, "The Use of NMR Shift Reagents for the Analysis of Surface-Active Agents Containing Sulfonic Groups. Determination of Sodium Alkanesulfonates by an NMR Method." Bunseki Kagaku, 26, 5 (1977); C.A. 86, 157409 (1977).

B12. H. Berthold, P. Fulde, H. Guenther, H. Leue, F. Rose, and W. Werner, "Separation of Paraffin and Alkane Sulfonate Containing Mixtures." Ger. (East) 11608 (1975); C.A. 86, 7064 (1977).

B13. N. A. Ovesnove, O. A. Efremenko, and F. M. Shemyakin, "Extraction-Photometric Analysis of Organic Compounds Containing the Sulfo Group Using Basic Antipyrine Dyes." V. sb., Atomno-absorbtsion. Analiz Prom. Materialov i Syr'ya, 196 (1976); C.A. 85, 153555 (1976).

B14. A. Nakae, K. Furuya, T. Mikata, and M. Yamanaka, "Analysis of Ingredients in Detergents by High-Speed Liquid Chromatography. (I) Determination of Lower Alkylbenzenesulfonates in Detergents by High-Speed Liquid Chromatography." Nippon Kagaku Kaishi, 9, 1426 (1976); C.A. 85, 179400 (1976).

B15. A. Utsunomiya, S. Setsuda, S. Itoh, and S. Naito, "Anionic Surfactants. I. Determination of LAS with Infrared Spectroscopy." Kanagawa-Ken Eisei Kenkyusho Nempo, 24, 118 (1974); C.A. 85, 130087 (1976).

B16. Z. Przybylski and M. Nowak, "Analysis of Sulfonic Acids by IR Spectroscopy." Nafta (Katowice, Pol.), 31, 436 (1975); C.A. 85, 35308 (1976).

B17. S. Eksborg and G. Schill, "Ion Pair Chromatography of Organic Compounds." Proc. Int. Solvent Extr. Conf., 3, 2149 (1974); C.A. 84, 12090 (1976).

B18. M. G. Kazakova and V. G. Zizin, "Determination of the Fractional Composition of Hydrocarbon Radicals in Alkanesulfonates."

Prom-st' Sintetich. Kauchuka. Ref. Sb., 7, 13 (1975); C.A. 84, 123074 (1976).

B19. V. A. Kremer, L. T. Andreeva, A. M. Borovskikh, and N. A. Benedis, "Determination of Aromatic Mono- and Disulfonic Acids by Nonaqueous Titration." Otkrytiya, Izobret., Prom. Obraztsy, Tovarnye Znaki, 51, 114 (1974); C.A. 83, P22081 (1975).

B20. M. Schroder-Nielsen, "Quantitative Determinations by Ion Pair Extraction. II. Extraction of Carboxylates and Sulfonates as Ion Pairs and Adducts With Dibenzo-18-Crown-6 and Other Adduct-Forming Agents." Acta Pharm. Suec., 11, 541 (1974); C.A. 83, 103328 (1975).

B31. H. Puschmann, "Analysis of Olefinsulfonates." Fette, Seifen, Anstrichm., 75, 434 (1973); C.A. 80, 28736 (1974).

B32. S. Hashimoto, H. Tokuwaka, and T. Nagai, "Analysis of α-Olefinsulfonic Acids by NMR Spectroscopy." Nippon Kagaku Kaishi, 12, 2384 (1973); C.A. 80, 59084 (1974).

B33. J. Pirkl, "Reagents for Detection of Aromatic Sulfonic Acids on Paper Chromatograms." Czech. 150,017 (1973); C.A. 80, 78199 (1974).

B34. V. A. Peristyi, A. A. Semenov, G. M. Gaevoi, and Z. I. Bukhshtab, "Determination of Alkenesulfonates." Neftepererab. Neftekhim., 10, 30 (1972); C.A. 78, 99472 (1973).

B35. A. S. Drozdov and Z. V. Didenko, "Determination of Sulfonic Acids and Sulfuric Acid in Products of Hydrocarbon Sulfoxidation." Neftepererab. Neftekhim. (Moscow), 1, 36 (1973); C.A. 78, 138205 (1973).

B36. O. Y. Velitskaya and S. K. Kondrashova, "Determination of Sulfonic Acids in Petroleum Residues." Neftepererab. Neftekhim., 9, 40 (1972); C.A. 78, 86858 (1973).

B37. Y. Kasai, Y. Uda, W. Yano, and W. Kimura, "Analysis of Sulfonate- and Sulfate-type Surfactants." Nippon Kagaku Kaishi, 12, 2394 (1972); C.A. 78, 60032 (1973).

B38. H. Berthold, P. Fulde, H. Guenther, H. Leue, F. Rose, and W. Werner, "Separation of Paraffin- and Alkanesulfonate-containing Mixtures." Ger. (East) 83,761 (1971); C.A. 78, 149370 (1973).

B39. W. Kupfer and K. Kuenzler, "Analysis of Petroleum Sulfonates by Column Chromatography." Fette, Seifen, Anstrichm, 74, 287 (1972); C.A. 77, 90930 (1972).

B40. V. A. Kozlov, V. V. Kharitonov, V. P. Leshchev, and A. A. Spryskov, "Sulfonation. 83. Determination of the Isomeric Composition of Nonvolatile Sulfonic Acids by Gas-Liquid Chromatography."

Izv. Vyssh. Ucheb. Zaved., Khim. Khim. Tekhnol., 14, 1850 (1971); C.A. 76, 94314 (1972).

B41. I. D. Leonov, N. A. Gafarova, E. A. Drizo, L. A. Gnusareva, and V. A. Benkovskii, "Separation of Alkylbenzenesulfonate Isomers." Tr. Inst. Khim. Nefti. Prir. Solei. Akad. Nauk Kaz., 1, 116 (1970); C.A. 75, 65869 (1971).

B42. K. Yasuda, "Thin-Layer Chromatography of Aromatic Sulfonic Acids." Bunseki Kagaku, 20, 796 (1971); C.A. 75, 136826 (1971).

B43. D. Lojodice and B. M. Colombo, "Colorimetric Method for the Analysis of Sulfonates." Farmaco, Ed. Prat., 25, 763 (1970); C.A. 74, R 130409 (1971).

B21. J. Dukovic and M. Vranes, "Gas Chromatographic Determination of Sulfonic Acids." Arh. Rud. Tehnol., 12, 3 (1974); C.A. 83, 52951 (1975).

B22. Z. I. Bukhshtab, L. V. Gasyuk, and V. A. Peristyi, "Quantitative Determination of Alkenesulfonates by Titration in Organic-Aqueous Solvent System." Vestn. Khark. Politekh. Inst., 92, 47 (1974); C.A. 83, 30305 (1975).

B23. V. A. Zakupra, S. V. Timoshenko, O. L. Glavati, T. V. Medvedeva, R. V. Fialkovskii, and N. F. Mitrofanova, "Analysis of Oil-Soluble Sulfonates and Sulfonic Acids by Liquid Chromatography." Neftepererab. Neftekhim. (Moscow), 6, 34 (1975); C.A. 83, 134673 (1975).

B24. T. Ishii, K. Yamane, H. Kato, and K. Kunihiro, "Gas Chromatographic Analysis of Alkanesulfonates by Forming Mercapto Derivatives." Yakugaku, 24, 229 (1975); C.A. 83, 45140 (1975).

B25. L. T. Andreeva, V. A. Kremer, A. I. Levchenko, and A. M. Borovskii, "Determination of Sulfonic Acids and Sulfonates in Waste Waters by Potentiometric Titration in Nonaqueous Media." Obrabotka Suspenzii, Emulsii i Prom. Stochn Vod, 101 (1974); C.A. 83, 47808 (1975).

B26. V. A. Kozlov, V. V. Zelov, and A. A. Spryskov, "Sulfonation Reaction. Analysis of Aromatic Sulfonic Acids by Gas-Liquid Chromatography and Reaction Gas-Liquid Chromatography." Tr. Ivanov. Khim.-Tekhnol. in-ta, 16, 126 (1973); C.A. 83, 52983 (1975).

B27. V. A. Zakupra, S. V. Timoshenko, O. L. Glavati, T. V. Medvedeva, R. V. Fialkovskii, and N. F. Mitrofanova, "Analysis of Oil-Soluble Sulfonates and Sulfonic Acids by Liquid Chromatography." Neftepererab. Neftekhim., 6, 34 (1975); C.A. 83, 134673 (1975).

B28. L. T. Andreeva, V. A. Kremer, A. M. Borovskikh, and A. I. Levchenko, "Determinaton of Condensed Ring Aromatic Sulfonic Acids by Nonaqueous Potentiometric Titration." Tr. III Vses. Konf. po analit. Khimii nevod. rastvorov i ikh fiz.-khim, svoistvam., 1974, (ch. 1), 50-4; C.A. 83, 201655 (1975).

B29. S. Hashimoto, H. Tokuwaka, and T. Nagai, "Rapid Determination of Sodium Hydroxyalkanesulfonates in α-Olefinsulfonates by NMR Spectroscopy." Bunseki Kagaku, 23, 210 (1974); C.A. 81, 57989 (1974).

B30. G. I. Shilov, "Determination of Sodium Alkanemonosulfonates in Emulsion Poly-(vinyl chloride) by a Colorimetric Method." Plast. Massy, 4, 75 (1974); C.A. 81, 136695 (1974).

B44. A. Saus, F. Asinger, and L. Loh, "Quantitative Determination of Sulfoxidation Products of High Molecular Paraffin Hydrocarbons." Tenside, 7, 3 (1970).

B45. A. A. Spryskov and V. A. Kozlov, "Sulfonation Reactions. LXIII. Quantitative Determination of Isomeric Sulfonic Acids and Their Derivatives With the Aid of Gas-Liquid Chromatography." Izv. Vyssh. Ucheb. Zaved., Khim. Khim. Tekhnol, 11, 785 (1968); C.A. 69, 95576 (1968).

B46. J. Hay, "Separation of Alkane Sulfonic Acids From Mixtures Containing Sulfuric Acid." Brit. 1,099,784; C.A. 69, 18611 (1968).

B47. S. Nishi, "Simple Identification of Alkylarene Sulfonates by Alkali Fusion Combined With Gas Chromatography." Bunseki Kagaku, 14, 917 (1965); C.A. 64, 3858 (1966).

B48. J. C. Espector, "A Simple and Rapid Analytical Method for True Sulfonates, Particularly Dodecylsulfonates, in the Presence of Alkyl Sulfonates, and (or) Sulfonate Oils." Vortraege Originalfassung Intern. Kongr. Grenzflaechenaktive Stoffe, 3, Cologne, Ger., 3, 68 (1960); C.A. 57, 8681 (1962).

B49. O. Ruzicka and L. Vilim, "Continuous Determination of Alkylarylsulfonates in Waste Water." Vodni Hospodarstvi, 10, 348 (1960); C.A. 55, 6745 (1961).

B50. M. P. Bespyatov, E. A. Preobrazhenskaya, O. V. Rits, V. E. Orcharenko, and L. I. Slominskii, "The p-Toluidine Method for Determining Petroleum Sulfonic Acids." Masloboino-Zhirovaya Prom., 25, 18 (1959); C.A. 54, 16803 (1960).

B51. V. Cerchez and O. Popescu, "Determinaton of Sulfonic Acids in Presence of Sulfuric Acid. Application to the Analysis of Sulfonic Acids." Acad. Rep. Populare Romine, Filiala (luj) Studii Cercetari Chim., 7, 155 (1956); C.A. 52, 8851 (1958).

B52. I. V. Furne and L. A. Karinova, "Determination of Sulfonic Acids in Mixtures With Sulfuric Acid by Titrimetric Method." Zavod. Lab., 42, 26 (1976); translated to Eng. in Industrial Lab., 42, 40 (1976). The results of the determination for the sulfonic acids are not detailed enough to compare.

B53. T. Okumura, T. Kadono, and A. Isoo, "Sintered Thin-Layer Chromatography With Flame Ionization Detector Scanning." J. Chromatogr., 108, 329 (1975); C.A. 83, 93211 (1975). This is a rapid TLC for qualitative and quantitative analysis for various organic compounds. However, only one species of p-aminobenzenesulfonic acid was mentioned in one of the figures.

B54. W. O. Ranky and G. T. Battaglini, "A Study of Analytical Methods for Alpha Olefin Sulfonates." Chem. Spec. Mfr. Ass., Proc. Annu. Meet., 54, 83 (1967); C.A. 69, 68484 (1968). This paper relates to the methods of determination for sulfonation of alpha olefins. Among the products, hydroxysulfonates are determined by a titrimetric method; the active olefinsulfonates by p-toluidine HCl method; and cumenesulfonates by UV method.

B55. R. Amos, "Use of Thin-Layer Chromatography in the Analysis of Lubricating Oils." Fresenius Z. Anal. Chem., 236, 350 (1968); C.A. 69, 20875 (1968). The separation of five synthetic sulfonates and three petroleum sulfonates were investigated by thin-layer chromatography using Silica Gel F 254 as an adsorbent, a mixture of methyl acetate/ethanol/ammonia (70:20:10) as a developing solvent and Pinacryptol Yellow as revealing reagent. However, the names of sulfonates were not mentioned.

B56. R. E. Barden and D. A. Jaeger, "Gel Filtration Chromatography of Petroleum Sulfonates." J. Chromatogr., 109, 377 (1975); C.A. 83, 100524 (1975). It only gives some information about qualitative analysis of the composition of petroleum sulfonates. Although three samples of petroleum sulfonate were tested, their names were not mentioned.

B57. V. P. Malik and L. Lewicki, "Studies on Acid Sludge: Part I-Separation, Analysis, and Fractionation of Petroleum Sulfonic Acids (Green Acids) From Acid Sludge." Indian J. Technol. 11, 30 (1973); C.A. 79, 96567 (1973). It is unclassified because the procedure of analyzing petroleum sulfonic acids involves extraction of acetone, titration with NaOH, and a series extraction with ethyl ether and isoamyl alcohol.

B58. E. E. Smissman and C. F. Barfknecht, "Polarographic Analysis of Some Sulfonic Acids." J. Pharm. Sci., 53, 1404 (1964); C.A. 62, 2243 (1965). This paper reported only gave an information that alkanesulfonic and most arenesulfonic acids have a half-wave potential at -1.6 V by using a dropping mercury electrode as a cathode and Ag/AgCl as an anode. No quantitative results were mentioned.

B59. B. M. Milwidsky, "Continuous Liquid/Liquid Extraction in Detergent Analysis." Soap. Chem. Spec., 45, 79 (1969). This paper gives some information about qualitative separation for monosulfonic acids from disulfonic acids in detergents. The separation is based on the fact that the disulfonic acids are not soluble in ethyl ether but are soluble in alcohols.

APPENDIX C

A PROGRAM TO RETRACE THE CHROMATOGRAMS USING THE HEWLETT-PACKARD 9825 A COMPUTER AND THE HEWLETT-PACKARD 9862 A PLOTTER

This program is to retrace a chromatogram which belongs to the Poisson distribution curve where the gamma function is used to compute any fractional factorials. The range of each peak (or number of observations) and the mean of the Poisson distribution curve should be given. In order to simulate the true picture of the chromatogram, some multiplication factors may be needed.

C.1. The Poisson Distribution (121,122)

The Poisson distribution curve may be represented as shown in Figure 79. In our case, X refers to elution time and probability refers to absorbance readings. The Poisson distribution formula used is expressed as follows:

$$P = \frac{C\, A^{X}\, e^{-A}}{X!} \qquad (C1)$$

where P = absorbance,

A = the mean,

X = elution time,

e = exponential

C = a multiplication factor

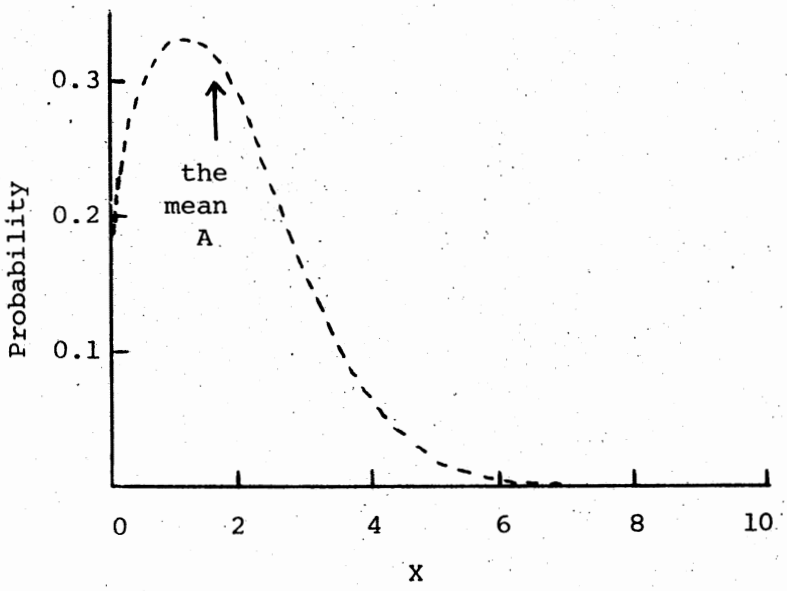

Figure 79. Typical Poisson Distribution Curve

C.2. The Gamma Function

When the increment of data point on X is not an integer, the gamma function is used and is approached by Equation (C2)(129).

$$P(X+1) = X! = 1 + a_1 x + a_2 x^2 + a_3 x^3 + a_4 x^4 + a_5 x^5 + \varepsilon(x) \qquad (C2)$$

where $0 \leq x \leq 1$

and $a_1 = -0.5748646,$

$a_2 = 0.9512363,$

$a_3 = -0.6998588,$

$a_4 = 0.4245549,$

$a_5 = -0.1010678,$

$|\varepsilon(x)| \leq 5 \times 10^{-5}$

C.3. The Important Symbols Used in the Program

x = time

A = the mean

C = the multiplication factor

S = X!

P = absorbance

C.4. Program Used

```
0:  scl  0,68,0, .45   (The scale of x and y)
1:  axe  0, 0,4, .05   (the intercept of x and y; the unit scale
                        on x and y)
2:  fxd  8             (8 figures after the decimal)
3:  0 → X
4:  "start": X + 1 → X (an increment of 1 on x)
5:  if X > 16; gto "one"
6:  plt X, .02         (plot x,y)
7:  csiz  0, .00000001, .00000001, 0
8:  lbl "."
9:  gto "start"
10: "one": if X > 22; gto "two"
11: X-16 → Z
12: 3.07 → A; 1.8 → C
13: gsb "sub 1"        (go to subroutine labeled "sub 1")
14: gto "start"
15: "two":  if X > 28; gto "three"
16: X - 22 → Z
17: 2.70 → A; 0.9 → C
```

```
18:  gsb "sub 1"
19:  gto "start"
20:  "three": if X > 35; gto "four"
21:  plt X, .02
22:  gto "start"
23:  "four": if X > 48; gto "five"
24:  X - 35 → Z
25:  4.6 → A; 1 → C
26:  gsb "sub 1"
27:  gto "start"
28:  "five": if X > 50; gto "six"
29:  plt X, .02
30:  gto "start"
31:  "six": if X > 64; gto "seven"
32:  X - 50 → Z
33:  5.7 → A; 1 → C
34:  gsb "sub 1"
35:  gto "start"
36:  "seven": if X > 66; gto "eight"
37:  plt X, .02
38:  gto "start"
39:  "eight": pen
40:  stp
41:  end
42:  "sub 1": if Z > 1; gto "ten"
43:  1-.5748646*Z+.9512363*Z↑2
     -.6998588*Z↑3 → U
```

```
44:  .4245549*Z↑4 -.1010678*Z↑5 → V
45:  U + V → S
46:  A↑Z/S * EXP(-A) → P
47:  P * C → P
48:  P + .02 → P
49:  plt X, P
50:  ret
51:  "ten": Z → G
52:  Z → N
53:  1 → S
54:  S*G → S
55:  if G > 2; G-1 → G; gto 54
56:  G - 1 → Z
57:  1-.5748646* Z + .9512363 * Z↑2
     -.6998588*Z↑3 → K
58:  .4245549*Z↑4 - .1010678*Z↑5 → T
59:  K + T → J
60:  S*J → S
61:  N → Z
62:  gto 46
```

APPENDIX D

SOME EXPLORATORY WORK DIRECTED TOWARD THE PREPARATION OF AN ION-SELECTIVE MEMBRANE FOR ALIPHATIC SULFONATES

A limited attempt to make ion-selective membrane electrodes for aliphatic sulfonates was undertaken and is described in this Appendix. Details of preparing the membrane and the responses obtained for ethanesulfonate ion were illustrated.

D.1. Preparation of a Membrane Sensitive to Ethanesulfonate

D.1.a. Materials

A. R. grade poly(vinyl chloride), PVC, (Alrich Chemical Co.), tetrahydrofuran (Mallinckrodt), potassium chloride (Mallinckrodt), and A. R. grade sodium chloride, ethanesulfonic acid, and sodium hydroxide, which have been described previously, were used without further purification. The synthesized CPG-8HO$_x$ resin (125-177 μ), as described in Chapter IV.D.1, was used. Poly(vinyl chloride) tubing (15.5 mm internal diameter) was used as body for the electrochemical sensor.

D.1.b. Apparatus

A glass ring and a smooth glass plate was used as a container to

prepare membrane discs as shown in Figure 80 (125). The glass ring had an internal diameter of 35 mm and a height of 30 mm.

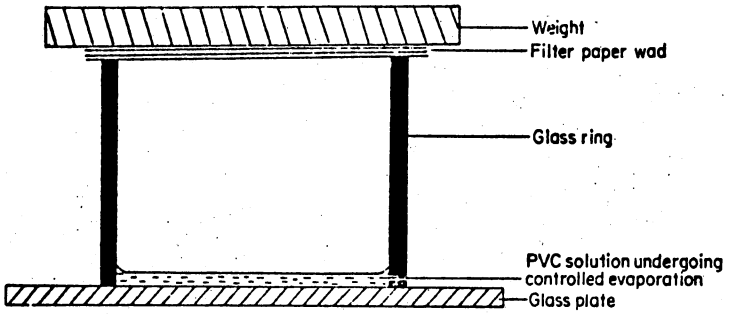

Figure 80. Experimental Arrangement for Casting PVC Membranes

D.1.c. Procedure

The procedure used is similar to that of Thomas, et al. (126). A suitable amount (~0.4 g) of the synthesized CPG-8HO$_x$ resin was weighed out in a 20-ml beaker. The resin was slowly added to an organic mixture containing 0.17 g of PVC in 6.0 ml of tetrahydrofuran. The mixture was stirred and then poured into the glass ring, which was sealed on a glass plate with Dow Corning silicone lubricant. The top of the glass ring was covered with a pad of filter paper (Schleicher and Schuell filter paper No. 589) on which a heavy lead weight was placed (Figure 80). The assembly was left for about 48 hours to allow the tetrahydrofuran to evaporate. The thickness of the film was about 1.0 mm after drying.

After the membrane was dry, the film was peeled away from the glass with a razor blade. Individual membrane discs were cut from the film with a cork borer of the same diameter as the internal diameter of the PVC tubing. The tubing was about 10 to 12 cm long. The disc was then glued on to a flat end of the PVC tube with a solution (4% w/w) of PVC in tetrahydrofuran as adhesive. After mounting and drying, the membrane electrode was conditioned with an inner reference solution of 0.10 M NaCl and 0.10 M $NaC_2H_5SO_3$ and an outer solution of 0.10 M $NaC_2H_5SO_3$ for 24 hours before use.

D.2. Testing the Response of the Ethanesulfonate Membrane Electrode

D.2.a. Experimental

(i) Reagents

Analytical reagents of ethanesulfonic acid, NaCl, KCl, NaOH, Orion 90-00-02 inner filling solution and Orion 90-00-03 (10% KNO_3) outer filling solution were used.

(ii) Apparatus

The electrode set up for potentiometric measurements is shown in Figure 81. The membrane electrode and an Orion double-junction electrode (described in Chapter IV.B.1.b) were connected to a potentiometer (Orion Research Model 801 A digital MV meter) which could be read to ± 0.1 MV.

(iii) Procedure

A series of solutions of known concentration (10^{-7} M - 10^{-1} M) of

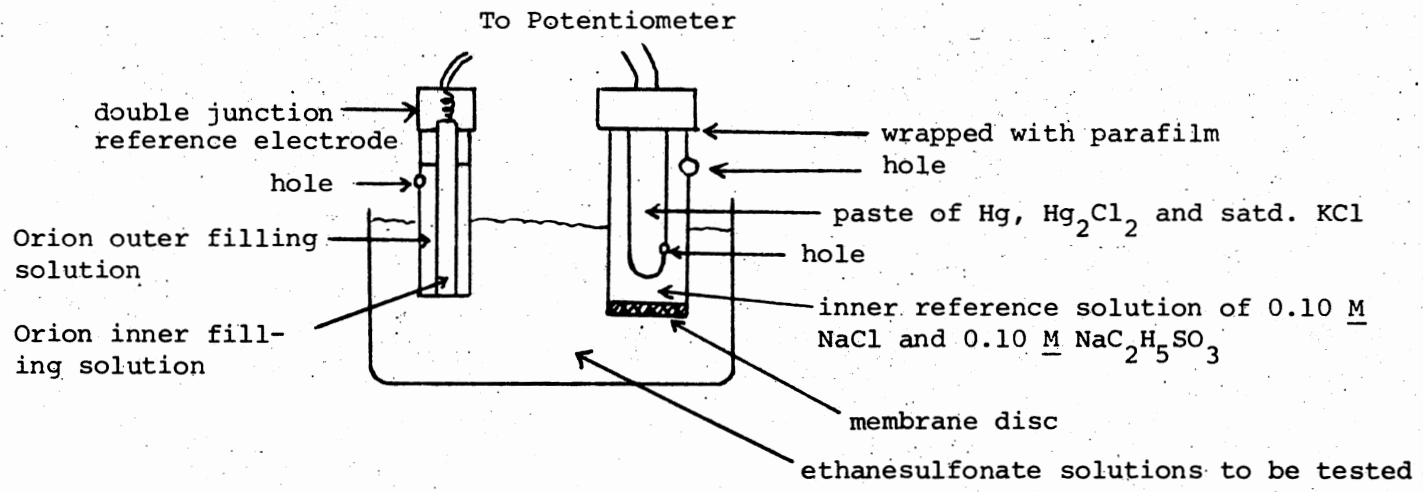

Figure 81. Electrode Set Up for Potentiometric Measurements

ethanesulfonate were prepared. Their ionic strengths were adjusted to 0.10 M by addition of 1.0 M NaCl. Each solution to be measured was put in a 100-ml beaker equipped with a magnetic stirrer. The voltages were recorded when readings on the MV meter became stable (within ± 0.3 MV) i.e., in about 5 minutes. Between each pair of measurements, the electrodes were rinsed with deionized-distilled water and blotted dry with "kimwipes". A solution of 0.10 M NaCl was also tested as a blank.

D.2.b. Results

The electrode potentials measured at various concentrations of ethanesulfonate are tabulated in Table XVIII. The pH of the sample solutions were measured with a Zeromatic pH meter and are also listed in Table XVIII. A plot of electrode potential versus ethanesulfonate concentration is shown in Figure 82.

D.2.c. Discussion

The experimental cell can be represented as follows:

$$\text{Ref(1)//0.10 M } Na^+,Cl^-,\ \underbrace{\text{0.10 M } Na^+,\ C_2H_5SO_3^-}_{\text{inner reference solution}}/\text{Membrane}/\underbrace{C_2H_5SO_3^-,Na^+,Cl^-}_{\text{sample solution to be tested}}\text{//Ref(2)}$$

ISE

where Ref (1) is a saturated calomel electrode containing $Hg/Hg_2Cl_2/KCl$(satd.),

Ref (2) is the Orion double-junction reference electrode containing 10% or 1 M KNO_3.

The electrode potential, E, (127) can be expressed as shown in Equation (D1).

TABLE XVIII

DATA OF ELECTRODE POTENTIAL COLLECTED AT VARIOUS ETHANESULFONATE SOLUTIONS WHICH IONIC STRENGTHS ARE KEPT AT 0.10 M WITH NaCl

Concentration of Ethanesulfonate (M)	pH of Sample Solution	EMF Versus a Double Junction Reference Electrode (MV)	Concentration of NaCl in the Sample (M)
Blank (0.10 M NaCl)	4.75	+23.0	0.10
10^{-7}	3.65	+23.0	0.10
10^{-6}	3.65	+23.0	0.10
10^{-5}	3.65	+23.0	0.10
10^{-4}	3.54	+23.0	0.10
10^{-3}	2.97	+27.0	0.10
10^{-2}	1.95	+45.0	0.090
10^{-1}	1.00	+91.0	0.0

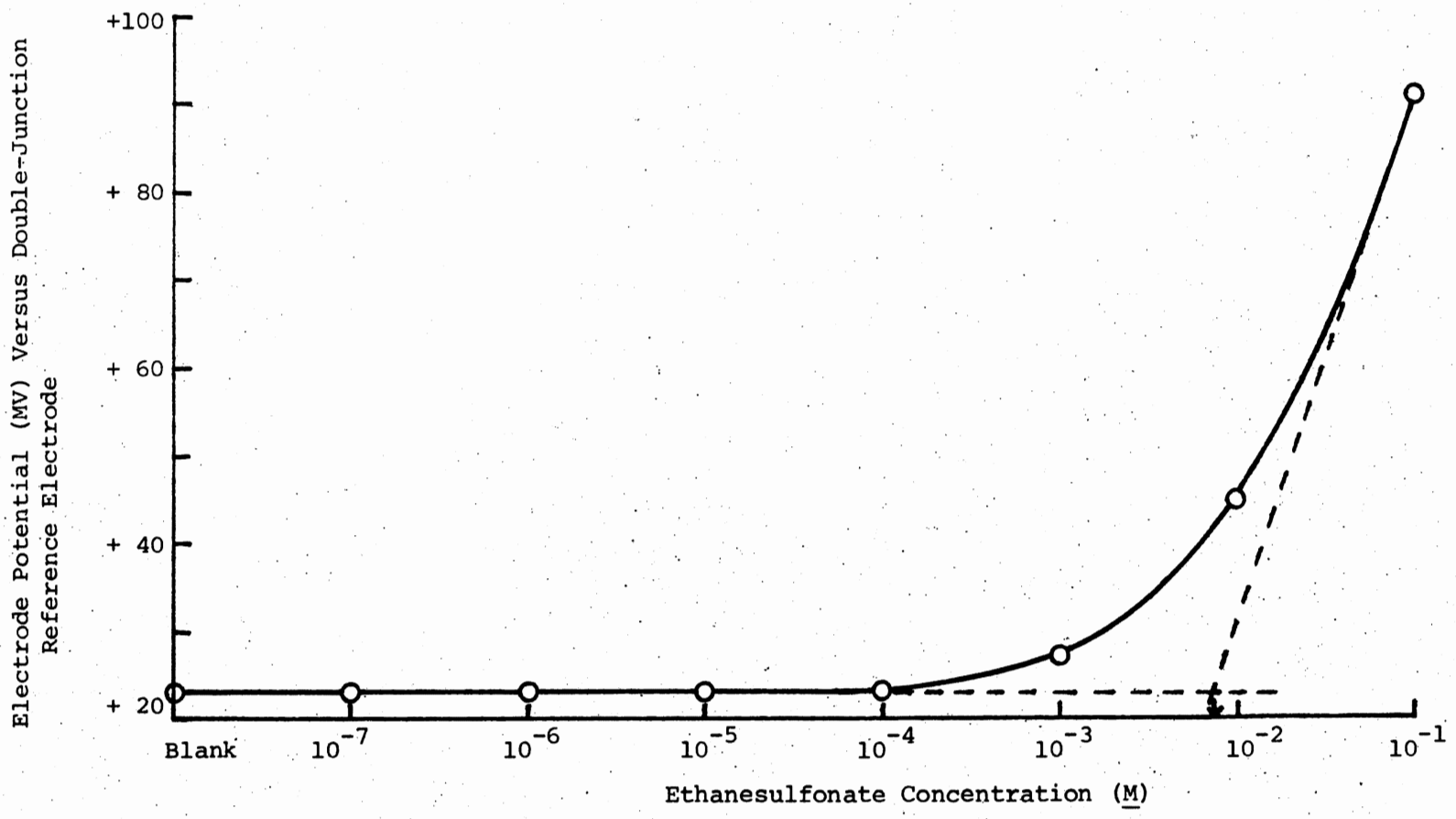

Figure 82. Response of a Membrane Electrode to Ethanesulfonate Ion at Ionic Strength of 0.10 M Adjusted With 1.0 M NaCl

$$E = E^{o}_{ISE} + \frac{2.303\ RT}{Z_i F} \log a_{C_2H_5SO_3^-} \qquad (D1)$$

where E^{o}_{ISE} is a constant whose value depends on the phase boundary potentials and the potential of the double junction reference electrode; Z_i is the charge on the ion being measured; $\frac{2.303\ RT}{F}$ is the Nernst factor which equals 59.16 mV at 25°C ; and $a_{C_2H_5SO_3^-}$ is the activity of $C_2H_5SO_3^-$ being measured in the sample solutions.

Since the solutions to be tested were kept at the same ionic strength (0.10 M), the activities ($a_{C_2H_5SO_3^-}$) in the sample solutions were directly proportional to the concentration of ethanesulfonate ions. The results obtained in Figure 82 show that the electrode potential starts rising when the ethanesulfonate concentration is larger than 10^{-4} M. Especially, a change of potential per decade concentration is +46 mV in the range of 10^{-2} M to 10^{-1} M. However, the response has not completely reached the Nernstian's (59.16 mV) response. This may be because the capacity of the CPG-8HO$_x$ resin in the membrane is not large enough to allow to reach the Nernst response.

When the ethanesulfonate concentration is lower than 10^{-4} M, the readings of electrode potential reach a constant value which is the same as that of the blank solution. This may be because the concentration of chloride ion in the sample is large enough to interfere with the measurements of ethanesulfonate ions. The electrode potential, E, may be expressed as shown in Equation (D2).

$$E = E^{o}_{ISE} + \frac{2.303\ RT}{Z_i F} \log \left(a_{C_2H_5SO_3^-} + K_{i,j}\ a_j^{\frac{Z_i}{Z_j}}\right) \qquad (D2)$$

where i = the species which is of interest = $C_2H_5SO_3^-$ in this case,

j = the interferent species = Cl^- in this case,

$K_{i,j}$ = the selectivity coefficient of $C_2H_5SO_3^-$ in the presence of Cl^- in this case,

a_j = the activity of Cl^- in the sample in this case.

The selectivity coefficient, $K_{i,j}$, can be estimated from Figure 82. After extending the horizontal line and the steep slope, as shown in Figure 82, an intercept is obtained. Let the value obtained in the horizontal axis equal to $K_{i,j}\, a_j^{\frac{Z_i}{Z_j}}$ (128). Since $a_j \sim 0.10$ M, $Z_i = 1$, $Z_j = 1$, and the intercept = 7.7×10^{-3}, the $K_{i,j}$ can be obtained as 7.7×10^{-2}.

The pH of the sample solution (Table XVIII) may also affect the potential readings. Since at lower pH and higher concentration of ethanesulfonate ion, larger potential readings are obtained. This may be because the ion pair of (CPG-$8H_2O_x^+$, $C_2H_5SO_3^-$) is favored on the membrane disc.

VITA[2]

Mao-Sung Kuo

Candidate for the Degree of

Doctor of Philosophy

Thesis: LIQUID-LIQUID AND LIQUID-SOLID DISTRIBUTION STUDIES OF 8-HYDROXYQUINOLINIUM-ANION PAIR SYSTEMS: APPLICATION TO THE CHROMATOGRAPHIC SEPARATION OF ALIPHATIC AND AROMATIC SULFONATES

Major Field: Chemistry

Biographical:

Personal Data: Born in Taiwan, Republic of China, January 8, 1948, the son of Mr. and Mrs. Tung-Shu Kuo.

Education: Received the Bachelor of Science degree in Chemical Engineering from Tunghai University, Taichung, Taiwan, Republic of China, in June, 1969; received the Master of Science degree in Chemistry from Ohio State University, Columbus, Ohio, in June, 1975; completed the requirements for the Doctor of Philosophy degree from Oklahoma State University in December, 1979.

Professional Experience: Teaching Assistant, Department of Chemistry, Tunghai University, Taichung, Taiwan, Republic of China, 1970-1972; Graduate Teaching Associate, Department of Chemistry, Ohio State University, Columbus, Ohio, 1972-1975; Graduate Teaching Assistant, Department of Chemistry, Oklahoma State University, Stillwater, Oklahoma, 1975-present.